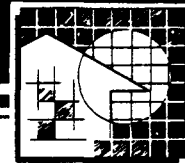


Contract Report



Theoretical and Computational Investigation of Algorithms for Simultaneous Heat and Moisture Transport in Buildings

Task 2 Final Report

Milestone #218 and 220 (combined)
FSEC-CR-191-88

Solar Cooling Research Project
Cooperative Agreement
No. DE-FC03-86SF16305

Prepared for
U.S. Department of Energy
Assistant Secretary of
Conservation and Renewable Energy
Office of Solar Heat Technologies

Gas Research Institute
Florida Power & Light Company

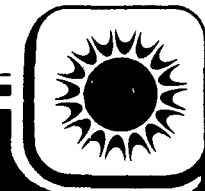
October 1988

Alp Kerestecioglu
Muthusamy Swami
Rajiv Dabir
Navaid Razzaq
Philip Fairey

Florida Solar Energy Center
300 State Road 401
Cape Canaveral, Florida 32920

For Reference

Not to be taken from this room



Unclassified

Distribution - Unlimited

DOE/SF/16305-2
UC-59

Theoretical and Computational Investigation
of Algorithms for Simultaneous Heat and
Moisture Transport in Buildings

Task 2 Final Report
Milestone #218 and 220 (combined)

Solar Cooling Research Project
Cooperative Agreement
No. DE-FC03-86SF16305

Prepared for
U.S. Department of Energy
Assistant Secretary of
Conservation and Renewable Energy
Office of Solar Heat Technologies
Gas Research Institute
Florida Power & Light Company

October 1988

Alp Kerestecioglu
Muthusamy Swami
Rajiv Dabir
Navaid Razaq
Philip Fairey

Florida Solar Energy Center
300 State Road 401
Cape Canaveral, Florida 32920

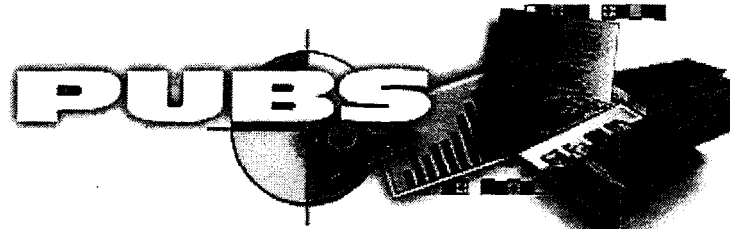


Energy Citations Database
ADOPT-A-DOC?

Bibliographic Citation

Document	<p>For copies of Journal Articles, please contact the Publisher or your local public or university library and refer to the information in the Resource Relation field.</p> <p>For copies of other documents, please see the Availability, Publisher, Research Organization, Resource Relation and/or Author (affiliation information) fields and/or Document Availability.</p>
Title	Theoretical and computational investigation of algorithms for simultaneous heat and moisture transport in buildings: Task 2 final report
Creator/Author	Kerestecioglu, A. ; Swami, M. ; Dabir, R. ; Razzaq, N. ; Fairey, P.
Publication Date	1988 Oct 01
OSTI Identifier	OSTI ID: 6668426; Legacy ID: DE89002082
Report Number(s)	DOE/SF/16305-2; FSEC-CR-191-88
DOE Contract Number	FC03-86SF16305
Other Number(s)	Other: ON: DE89002082
Resource Type	Technical Report
Resource Relation	Other Information: Portions of this document are illegible in microfiche products
Research Org	Florida Solar Energy Center, Cape Canaveral (USA)
Subject	32 ENERGY CONSERVATION, CONSUMPTION, AND UTILIZATION; 14 SOLAR ENERGY; SOLAR COOLING SYSTEMS; MATHEMATICAL MODELS; BUILDINGS; COMPUTER ARCHITECTURE; DEHUMIDIFICATION; DEHUMIDIFIERS; ENERGY CONSERVATION; FLORIDA; HEAT TRANSFER; MOISTURE; NUMERICAL DATA; PROGRESS REPORT; RESEARCH PROGRAMS; SOLAR ENERGY; DATA; DOCUMENT TYPES; ENERGY; ENERGY SOURCES; ENERGY TRANSFER; EQUIPMENT; FEDERAL REGION IV; INFORMATION; NORTH AMERICA; RENEWABLE ENERGY SOURCES; SOLAR EQUIPMENT; USA
Description/Abstract	This report covers the first year of a multiyear effort designed to develop mathematical modeling capabilities for simultaneous heat and moisture transport in buildings. This effort represents only one task of a cooperative research project with five major initial year elements: moisture research; analytical methods; radiant barrier systems; enthalpy exchange systems; and integrated systems research. The objective of the overall project is to develop research capabilities needed for the development and analysis of building integrated solar cooling and dehumidification alternatives suitable for hot, humid climates prevalent in the southeastern United States.
Country of Publication	United States
Language	English
Format	Medium: X; Size: Pages: 281
Availability	NTIS, PC A13/MF A01; 1.
System Entry Date	2008 Feb 08

National Renewable Energy Laboratory
PUBLICATIONS DATABASE



- Help
- Search
- New Pubs

Welcome to NREL's Information Clearinghouse (NICH) Publications Database. This database contains references to documents written and/or edited by staff and subcontractors of NREL.

Covering subjects related to sustainable energy technologies from 1977 to the present, our bibliographic database includes NREL technical reports, fact sheets, brochures, videos, books, journal articles, conference papers, patents, and exhibits.



Selected publications are available in full text online and can be located by searching the database or the DOE Information Bridge at www.osti.gov/bridge/. If the publication you want is not yet online, documents are available, unless otherwise noted, in limited quantities from the NREL Document Distribution Service: (303) 275-4363; fax: (303) 275-4053, email: sally_evans@nrel.gov

[HOME](#) | [Disclaimer](#) | [Questions or comments: Publications Webmaster](#) | [Security & Privacy](#)

NOTICE

This report was prepared as an account of work sponsored by an agency of the United States Government. Neither the United States nor any agency thereof, nor any of their employees, makes any legal warranty, expressed or implied, or assumes any liability or responsibility for any third party's use of the results or such use of any information, apparatus, product, or process disclosed in this report, or represents that its use by such third party would not infringe privately owned rights.

The work has been supported by the Solar Heating and Cooling Research and Development Branch, Office of Conservation and Solar Applications, U.S. Department of Energy.

SOLAR BUILDINGS RESEARCH AND DEVELOPMENT PROGRAM CONTEXT STATEMENT

In keeping with the national energy policy goal of fostering an adequate supply of energy at a reasonable cost, the United States Department of Energy (DOE) supports a variety of programs to promote a balanced and mixed energy resource system. The mission of the DOE Solar Buildings Research and Development Program is to support this goal, by providing for the development of solar technology alternatives for the buildings sector. It is the goal of the Program to establish a proven technology base to allow industry to develop solar products and designs for buildings that are economically competitive and can contribute significantly to building energy supplies nationally. Toward this end, the program sponsors research activities related to increasing the efficiency, reducing the cost, and improving the long term durability of passive and active solar systems for building water and space heating, cooling, and daylighting applications. These activities are conducted in four major areas: Advanced Passive Solar Materials Research, Collector Technology Research, Cooling Systems Research, and Systems Analysis and Applications Research.

Advanced Passive Solar materials Research -- This activity area includes work on new aperture materials for controlling solar heat gains, and for enhancing the use of daylight for building interior lighting purposes. It also encompasses work on low-cost thermal storage materials that have high thermal storage capacity and can be integrated with conventional building elements, and work on materials and methods to transport thermal energy efficiently between any building exterior surface and the building interior by non-mechanical means.

Collector Technology Research -- This activity area encompasses work on advanced low to medium temperature (up to 180°F useful operating temperature) flat plate collectors for water and space heating applications, and medium to high temperature (up to 400°F useful operating temperature) evacuated tube/concentrating collectors for space heating and cooling applications. The focus is on design innovations using new materials and fabrication techniques.

Cooling Systems Research -- This activity area involves research on high performance dehumidifiers and chillers that can operate efficiently with the variable thermal outputs and delivery temperatures associated with solar collectors. It also includes work on advanced passive cooling techniques.

Systems Analysis and Applications Research -- This activity area encompasses experimental testing analysis, and evaluation of solar heating, cooling, and daylighting systems for residential and nonresidential buildings. This involves system integration studies, the development of design and analysis tools, and the establishment of overall cost, performance, and durability targets for various technology or system options.

This report is an account of research conducted in the DOE Solar Cooling Program concerning whole-building moisture capacitance.

ACKNOWLEDGEMENT

The authors gratefully acknowledge the support of the U.S. Department of Energy (DOE), the Gas Research Institute (GRI), and the Florida Power and Light Company (FPL) for their cooperative support of this research. This work is specifically funded under DOE cooperative agreement #DE-FC03-86SF16305 and GRI contract #5087-243-1515. We are especially grateful to Mr. Fred Morse, Mr. David Pellish and Mr. Robert Hughey of DOE and Mr. Doug Kosar of GRI for their continued moral support of this important work.

The work reported here has been a team effort on the part of numerous people whose names do not appear on the title page. We would like to express special thanks to Dr. Subrato Chandra, the project manager of this project, for his insight, encouragement and assistance throughout the entire course of the work. We also have received help and advice from many others. It is not possible to acknowledge each of them but special thanks go to Dr. Arthur Shavit of the Technion in Isreal and Dr. Kirk Collier for the technical guidance and criticism they have provided.

DISTRIBUTION LIST

Thomas B. Romine, Jr.
Chairman TC, 4.1
300 Greenleaf
Fort Worth, TX 76107

Doug Burch
National Bureau of Standards
Bldg. 226
Gaithersburg, MD 20899

Edward F. Sowell
Chairman, TC 4.7
California State University
Dept. of Computer Science
Fullerton, CA 92634

Erv Bales
School of Arch.
New Jersey Inst. of Tech.
323 King Blvd.
Newark, NJ 07102

Martha Van Geem
Construction Technology Lab.
5420 Old Orchard Rd.
Skokie, IL 60077

Jack Verschoor
Verschoor Associates
179 Gail Lane
Bailey, CO 80421

Sam Tagore
U.S. Dept. of Energy, CE 111.1
1000 Independence Ave.
Washington, DC 20585

Larry Spielvogel
Wyncate House
Wyncate, PA 19095

Adrian Tuluca
Steven Winter Associates
6100 Empire State Bldg.
New York, NY 10001

Roy Sterling
Underground Space Center
Univ. of Minnesota
Minneapolis, MN 55455

Thomas H. Kuehn
Univ. of Minnesota
125 Mechanical Engineering
111 Church St., S.E.
Minneapolis, MN 55455

Anton TenWolde
Forest Products Lab
One Gifford Pinchot Dr.
Madison, WI 53705

Heinz Trechsel
H.R. Trechsel Assoc.
P.O. Box 211
Germantown, MD 20874

Mark Bomberg
National Research Council
Institute of Res. in Construction
Ottawa, Ontario K1A OR6
CANADA

Charles Hedlin
National Research Council
Division of Bldg. Research
Saskatoon Sask S7N OW9
CANADA

Thomas Miller
T.J. Miller Res. & Tech., Inc.
Box 268
Delphos, OH 45833

D. Herrone
716 S. Elm Blvd.
Champaign, IL 61820

Tamami Kusuda
7700 Dew Wood Dr.
Rockville, MD 20875

Dr. M.K. Kumaran
Research Officer
Building Services Section
Inst. of Res. in Construction
Ottawa, Ontario K1A OR6
CANADA

Dr. David Claridge
Texas A&M University
Mechanical Engineering Dept.
College Station, TX 77843-3123

GP. Mitalas
National Research Council
Institute of Res. in Construction
Ottawa (Ontario) K1A OR6
CANADA

Jim H. White
CMHC National Office
682 Montreal Rd.
Ottawa, Ontario K1A OP7
CANADA

Kenneth Wilkes
106 Inn Lake Apt. 0
Oak Ridge, TN 37830

David G. Ober
2290 S. Humboldt
Denver, CO 80210

William P. Goss
Univeristy of Mass.
Mechanical Engineering Dept.
Amherst, MA 01003

Bion D. Howard
NAHB
15th & M St. N.W.
Washington, DC 20005

James K. Lischkoff
Trow Ltd.
1595 Clark Blvd.
Brampton ONT CANADA
L6T 4V1

William R. Strezepek
DOW Chemical
P.O. Box 515
Granville, OH 43023

Ron P. Tye
Holometrix, Inc.
99 Erie Street
Cambridge, MA 02139

S.A. Barakat
National Research Council
Ottawa Ontario K1A OR6
CANADA

George E. Courville
ORNL, Bldg. 4508
P.O. Box X
Oak Ridge, TN 37831

Gustav O.P. Handegord
84 Old Mill Rd.
Etobicoke ONT MBX 1G9
CANADA

David T. Harrje
Center for Energy & Env. Studies
Engineering Quadrangle
Princeton University
Princeton, NJ 08540

Gren Yuill
G.K. Yuill & Associates
1441 Pembrina Hwy.
Winnipeg, Manitoba R3T 2C4
CANADA

Samuel J. Taylor
DOE, Buildings Division
M/S GF-253
1000 Independence Ave., SW
Washington, DC 20585

Joe Lstiburek
Trow Ltd.
1595 Clark Blvd.
Brampton ONT L6T 4V1
CANADA

Don Onysko
Forinlek Canada Corp.
800 Montreal Rd.
Ottawa Ontario K1G 375
CANADA

Reijo Kohonen, Dr Tech
Technical Res. Center of Finland
Lab. of Heating & Ventilation
Lämpömiehenkuja 3, SF-0215 Espoo
FINLAND

Harold A. Trethowen
Bldg. Research Assn NZ
Private Bag
Porirua
NEW ZEALAND

Franz C. Bauer
Ortech International
2395 Speakman Drive
Mississauga, Ontario L5K 1B3
CANADA

Dr. Greg A. Spolek
Mechanical Engineering Dept.
Portland State University
P.O. Box 751
Portland, OR 97207

Wayne Tobiason
Cold Regions Research
& Engineering Lab.
72 Lyme Road
P.O. Box 282
Hanover, NH 03755

Per I. Sandberg
National Testing Institute
Box 857
S50115, Boras
SWEDEN

Catherine Langalais
CRIR
BP 19
60290, Rantigny
FRANCE

TABLE OF CONTENTS

CHAPTER 1	INTRODUCTION AND SUMMARY	
CHAPTER 2	THEORETICAL APPROACH	
2.1	COMBINED HEAT AND MASS TRANSFER IN SOLIDS	2-1
2.2	MOISTURE TRANSPORT MECHANISMS	2-6
2.3	HISTORICAL SURVEY AND DISCUSSION OF THE MOISTURE THEORIES	2-10
2.4	HEAT AND MASS TRANSFER AND BUILDINGS	2-12
2.5	SAMPLE APPLICATION OF HEAT AND MASS TRANSFER TO A BUILDING	2-16
2.6	NUMERICAL SOLUTION TECHNIQUES	2-22
2.7	NATURE OF THE GOVERNING EQUATIONS	2-23
2.8	SOLUTION TYPES	2-24
2.9	CAPABILITIES OF FEMALP 2.1	2-26
CHAPTER 3	EXAMPLE SIMULATIONS	
3.1	HEAT AND MOISTURE TRANSFER IN COMPOSITE WALLS	3-2
3.2	WALL HEAT AND MASS TRANSFER COUPLED BUILDING ZONE	3-12
3.3	HEAT AND MASS TRANSFER IN A REAL ATTIC	3-16
3.4	HEAT AND MOISTURE TRANSFER IN COLD STORAGE FOUNDATIONS	3-23
3.5	HEAT MASS AND MOMENTUM TRANSFER IN A VENTED STORAGE WALL	3-31
REFERENCES		
APPENDIX A	DIFFERENT THEORIES ON COMBINED HEAT AND MASS TRANSFER	
A.1	LIQUID DIFFUSION THEORY	A-1
A.2	CAPILLARY THEORY	A-2
A.3	EVAPORATION-CONDENSATION THEORY	A-3
A.4	LUIKOV'S THEORY	A-4
A.5	PHILIP AND DE VRIES' THEORY	A-8
A.6	KRISCHER'S AND BERGER AND PEI'S THEORIES	A-10
A.7	LOW-INTENSITY HEAT AND MOISTURE TRANSFER IN MOIST SOILS	A-13
A.8	HEAT AND MASS TRANSFER EQUATIONS AND IRREVERSIBLE THERMODYNAMICS	A-17
APPENDIX B	FINITE ELEMENT SOLUTIONS	
B.1	ON THE THEORY OF FINITE ELEMENT FORMULATIONS	B-2
B.1.1	SUBDIVISION AND DISCRETIZATION	B-2
B.1.2	PROCESS OF LOCALIZATION	B-3

B.1.3	METHOD OF FORMULATION	B-3
B.1.4	GOVERNING TRANSIENT FINITE ELEMENT EQUATION	B-4
B.2	LIQUID DIFFUSION THEORY	B-7
B.3	CAPILLARY THEORY	B-8
B.4	EVAPORATION CONDENSATION THEORY	B-9
B.5	LUIKOV'S THEORY	B-10
B.6	PHILIP AND DE VRIES THEORY	B-11
B.7	KRISCHER AND BERGER-PEI'S THEORY	B-13
B.8	MOIST SOILS MODELS	B-14
B.9	IRREVERSIBLE THERMODYNAMICS	B-15
B.10	SHAPE FUNCTIONS	B-17
B.11	ISOPARAMETRIC FORMULATIONS	B-19
B.12	NUMERICAL INTEGRATION	B-21
B.13	ACTIVE ZONE EQUATION SOLVER	B-23
B.13.1	TRIANGULAR DECOMPOSITION	B-23
B.13.2	FORWARD ELIMINATION AND BACKWARD SUBSTITUTION	B-25
B.13.3	STORAGE CONSIDERATIONS	B-26
B.14	SOLUTION PROCEDURES	B-28
B.14.1	FIXED-POINT ITERATION	B-29
B.14.2	NEWTON-TYPE METHODS	B-30

APPENDIX C MATERIAL PROPERTIES NEEDED FOR VARIOUS THEORIES

APPENDIX D LITERATURE COMPILED MATERIAL PROPERTIES

APPENDIX E ZONE ENERGY AND MASS BALANCE EQUATIONS

E.1	ZONE ENERGY BALANCE EQUATION	E-1
E.2	ZONE MASS BALANCE EQUATION	E-4
E.3	LUMPED ANALYSIS ("EFFECTIVE PENETRATION DEPTH" CONCEPT)	E-7
E.4	"EFFECTIVE AIR MASS MULTIPLIER" CONCEPT	E-11
E.5	SOLUTION PROCEDURES	E-12
E.5.1	LUMPED ZONE THERMAL AND MASS EQUATIONS	E-12
E.5.2	LUMPED INTERNAL MASS EQUATIONS AND ZONE INTERACTIONS	E-13
E.5.3	EXACT SOLUTION FOR LUMPED MASS TRANSFER AND ZONE EQUATIONS	E-18

APPENDIX F INTERFACE EQUATIONS AND HEAT AND MASS TRANSFER COEFFICIENTS

F.1	HEAT AND MASS TRANSFER COEFFICIENT RELATIONS	F-1
F.1.1	REYNOLDS ANALOGY	F-1
F.1.2	J-FACTOR ANALOGY	F-2
F.1.3	GILLILAND'S ANALOGY	F-2
F.1.4	LEWIS RELATION	F-2
F.2	HEAT AND MASS INTERFACE EQUATIONS	F-3
F.2.1	THE BETA CONCEPT	F-4
F.2.2	NUMERICAL SOLUTION	F-6

APPENDIX G PSYCHROMETRIC AND EQUILIBRIUM FUNCTIONS

APPENDIX H THERMAL RADIATION MODELING

H.1	RADIATIVE BOUNDARY CONDITIONS AND FINITE ELEMENT FORMULATIONS	H-2
H.2	VIEW FACTOR CALCULATIONS	H-3
H.2.1	HOTTEL'S CROSSED-STRING METHOD	H-3
H.2.2	INTEGRAL METHOD	H-4
H.3	SCRIPT-F CALCULATIONS	H-5
H.4	SHADOW CHECKING	H-7
H.4.1	TWO-DIMENSIONAL SHADOW CHECKING	H-8
H.4.1.1	SIMPLE SHADOW CHECKING	H-8
H.4.1.2	DETAILED SHADOW CHECKING	H-9
H.4.2	THREE-DIMENSIONAL SHADOW CHECKING	H-10

APPENDIX I VALIDATIONS

I.1	TEST CASE NUMBER I	I-3
I.2	TEST CASE NUMBER II	I-6
I.3	TEST CASE NUMBER III	I-10
I.4	TEST CASE NUMBER IV	I-13
I.5	TEST CASE NUMBER V	I-15
I.6	TEST CASE NUMBER VI	I-17
I.7	TEST CASE NUMBER VII	I-20
I.8	TEST CASE NUMBER VIII	I-28

LIST OF FIGURES

No	TITLE	Page
2-1	Typical adsorption and desorption isotherms showing hysteresis	2-4
2-2	Water vapor transport mechanisms	2-8
2-3	Liquid water transport mechanisms	2-9
2-4	Building domains	2-13
2-5	Schematic of a simple building used in the example derivations	2-17
3-1.a	Composite wall without vapor retarder (Wall # 1)	3-2
3-1.b	Composite wall with vapor retarder (Wall # 2)	3-2
3-2.a	Finite element discretization of composite wall number 1	3-3
3-2.b	Finite element discretization of composite wall number 2	3-3
3-3.a	Ambient temperatures used as external boundary conditions for periodic analysis runs	3-4
3-3.b	Ambient mass transfer potential and water vapor density used as external boundary conditions for periodic analysis runs	3-5
3-4.a	Effect of combined heat and moisture transport on the surface temperature of composite wall # 1	3-7
3-4.b	Effects of combined heat and moisture transport on the interior surface fluxes of wall # 1 (no vapor retarder)	3-8
3-4.c	Effects of combined heat and moisture transport on the interior surface fluxes of wall # 2 (with vapor retarder)	3-9
3-4.d	Effect of a vapor retarder on the moisture content near the interior surface of the wall	3-10
3-4.e	Effect of a vapor retarder on the moisture content near the exterior surface of the wall	3-11
3-5	Wall construct used in the evaporation condensation model	3-12
3-6	Finite element discretization	3-13
3-7.a	Zone temperature histories with and without moisture effects and no internal gains for both simulations	3-14
3-7.b	Effects of combined heat and moisture transport on wall interior surface fluxes without internal gains	3-15

3-8	Layout of PCL attic cell 2	3-17
3-9.a	Comparison of predicted and measured temperature at insulation top without including moisture effects	3-19
3-9.b	Comparison of predicted and measured temperature at insulation top with moisture effects	3-20
3-9.c	Comparison of insulation top temperature prediction errors and measured vent air moisture removal rates	3-21
3-9.d	Comparison of predicted and measured outlet humidity ratios ..	3-22
3-10.a	Mesh used, materials and boundary conditions for the foundation basement of a cold store with vapor barriers in wall and floor	3-25
3-10.b	Mesh used, materials and boundary conditions for the foundation basement of a cold store with vapor barriers in wall only	3-26
3-11.a	Temperature ($^{\circ}\text{C}$) distribution in the foundation basement of a cold store with vapor barriers in wall and floor	3-27
3-11.b	Mass transfer potential ($^{\circ}\text{M}$) distribution in the foundation basement of a cold store with vapor barriers in wall and floor	3-28
3-11.c	Temperature ($^{\circ}\text{C}$) distribution in the foundation basement of a cold store with vapor barriers in wall only	3-29
3-11.d	Mass transfer potential ($^{\circ}\text{M}$) distribution in the foundation basement of a cold store with vapor barriers in wall only	3-30
3-12	Core vented storage system	3-31
3-13.a	Moisture isotherm for red brick	3-33
3-13.b	Moisture isotherm for concrete hw	3-34
3-14.a	Velocity vector in the vicinity of left bend	3-35
3-14.b	Velocity vector in the vicinity of right bend	3-35
3-15.a	History of averaged temperature of vent air at outlet	3-36
3-15.b	History of averaged vapor density of vent air at outlet	3-37
3-15.c	History of averaged relative humidity of vent air at outlet ..	3-38
B-1	One-dimensional linear line element and local normalized co-ordinates	B-18

B-2	Two-dimensional linear rectangular element and local normalized co-ordinates	B-18
B-3	Three-dimensional linear brick element and local normalized co-ordinates	B-18
B-4	Skyline storage method for K-matrix	B-27
E-1	Thermodynamic surface equilibrium	E-8
E-2	Schematics of lumped analysis concept	
	(a) Real moisture content profile	E-9
	(b) Lumped moisture content profile	E-9
H-1	Schematic of energy balance at a boundary	H-2
H-2	Hottel's crossed-string method for view factor determination .	H-3
H-3	Calculation of radiation view factors with integral method ..	H-5
H-4	Two-dimensional simple shadow checking configuration	H-8
H-5	Two-dimensional detailed shadow checking configuration	H-9
H-6	Three-dimensional shadow checking layout	H-11
H-7	Three-dimensional shadow checking layout	H-12
I-1	Problem description for test case I	I-3
I-2.a	FEMALP 2.1 validation case (I) for mid-mass	I-4
I-2.b	FEMALP 2.1 validation case (I) for high-mass	I-5
I-3	Problem description for test case II	I-6
I-4.a	FEMALP 2.1 validation case (II) for low-mass	I-7
I-4.b	FEMALP 2.1 validation case (II) for mid-mass	I-8
I-4.c	FEMALP 2.1 validation case (II) for high-mass	I-9
I-5	Problem description for test case III	I-10
I-6.a	FEMALP 2.1 validation case (III) for mid-mass	I-11
I-6.b	FEMALP 2.1 validation case (III) for high-mass	I-12
I-7	Problem description for test case IV	I-13
I-8	FEMALP 2.1 validation case (IV) for high-mass	I-14
I-9	Problem description for test case V	I-15
I-10	FEMALP 2.1 validation case (V) for high-mass	I-16

I-11	A composite plane wall suddenly exposed to convection on both sides	I-17
I-12	ASHRAE transfer function calculations versus FEMALP 2.1 predictions	I-19
I-13	FEMALP 2.1 validation case (VII) for $T_r=294.26$ K	I-22
I-14.a	FEMALP 2.1 validation case (VII) for $Q_T=0$	I-23
I-14.b	FEMALP 2.1 validation case (VII) for $Q_T=1465.5$ K	I-24
I-14.c	FEMALP 2.1 validation case (VII) for $Q_T=1465.5$ K	I-25
I-15.a	FEMALP 2.1 validation case (VII) for $Q_T=1465.5$ K	I-26
I-15.b	FEMALP 2.1 validation case (VII) for $Q_T=1465.5$ K	I-27
I-16	Schematic layout of the PCL attic	I-30
I-17.a	Comparison of predicted and measured ceiling heat fluxes without moisture effects	I-31
I-17.b	Comparison of deck bottom temperature prediction error and measured vent air moisture removal rate	I-32

LIST OF TABLES

No	TITLE	Page
2-1	Brief description of moisture modeling techniques	2-14
3-1	Material properties used in Luikov's model	3-3
3-2	Boundary and initial conditions	3-3
3-3	Thermal properties	3-12
3-4	Material description and property source for combined heat and moisture transfer in an attic	3-18
3-5	Boundary condition description for combined heat and moisture transfer in an attic	3-18
3-6	Material properties used in Luikov's model	3-23
B-1	Numerical time integration constants	B-5
B-2	Integrand for different dimensions	B-21
B-3	Sampling point values and weights for Gauss-Legendre quadrature	B-22
C-1	Thermophysical properties required for various heat and mass transfer theories	C-2
D-1	Equilibrium isotherms for various building materials	D-3
D-2	Water vapour diffusivity values of various building materials	D-14
D-3	Water vapour diffusivity value ranges for various building materials	D-23
D-4	Coefficients of moisture transfer	D-26
D-5	Coefficients of water diffusion at 20 °C	D-28
D-6	Moisture permeability for various building materials	D-29
F-1	Mass transfer coefficient conversions	F-3
F-2	Mass transfer variables	F-4
F-3	Interface equations	F-5
F-4	Betas for different models	F-6
I-1	Material properties used in validation test cases I through	

V	I-2
I-2	Description of ASHRAE constructs used for comparison	I-17
I-3	Material properties used in test case VII	I-20
I-4	Scheduled ambient temperature used in test case VII	I-20
I-5	Zone operating conditions used in test case in test case VII	I-21
I-6	Material description for test case VII	I-28
I-7	Boundary condition description for test case VII	I-29

NOMENCLATURE

A	Area [m ²]
a	Constant used to define the equilibrium sorption curve [dimensionless]
A _f	Furniture surface area [m ²]
A _w	Wall surface area [m ²]
b	Constant used to define the equilibrium sorption curve [dimensionless]
c	Constant used to define the equilibrium sorption curve [dimensionless]
C _S	Specific heat of the solid wall material [W.h/kg.K]
C _p	Specific heat [W.h/kg.K]
d ^p	Constant used to define the equilibrium sorption curve [dimensionless]
D _A	Molecular diffusivity of water vapor in air [m ² /h]
h _M	Convective mass transfer coefficient
h _T	Convective heat transfer coefficient [W/m ² .K]
J _W	Liquid water flux [kg/m ² .h]
k _T	Thermal conductivity [W/m.K]
P _b	Barometric pressure [Pa]
P _V	Partial water vapor pressure [Pa]
P _{V,sat}	Partial water vapor pressure at saturation [Pa]
P1	Summation of all coefficients of terms containing the zone temperature.
P2	Summation of all coefficients of terms containing the zone humidity ratio.
Q _{fur-l}	Convective moisture gain from furniture [kg/h]
Q _{fur-s}	Convective sensible heat gain from furniture [kW]
q _M	Imposed mass flux (such as rain) [kg/m ² .h]
q _T	Imposed heat flux (such as solar radiation) [W/m ²]
Q _{sor-l}	Moisture gain due to functionally defined source term(s) [kg/h]
Q _{sor-s}	Sensible heat gain due to functionally defined source term(s) [kW]
Q _{wal-l}	Convective moisture flow rate from building surface into the zone [kg/h]
Q _{wal-s}	Convective heat gain from building surface into the zone [kW]
Q1	Summation of all terms not containing the zone temperature.
Q2	Summation of all terms not containing the zone humidity ratio.
R _V	Ideal gas constant [J/kg.K]
RH	Relative humidity [percentage]
T	Temperature [K]
T _f	Temperature of the furniture [K]
T _r	Temperature of room air [K]
T _{r0}	Initial room air temperature [K]
T _{w0}	Wall surface temperature [K]
T _{wα}	Ambient temperature [K]
U ^α	Moisture content on dry basis [kg/kg]
V _r	Volume of the room [m ³]
V _f	Furniture volume [m ³]
W	Humidity ratio [kg/kg]
W _f	Humidity ratio of the furniture [kg/kg]
W _r	Humidity ratio of room air [kg/kg]
W _{r0}	Initial room air humidity ratio [kg/kg]
W _w	Wall surface Humidity ratio [kg/kg]

GREEK LETTERS

δ _M	Effective penetration depth for lumped moisture equation [m]
δ _T	Effective penetration depth for lumped energy equation [m]
ε	Porosity [m ³ /m ³]
θ	Volumetric moisture content [m ³ /m ³]

λ Heat of vaporization [W.h/kg]
 μ Chemical potential of water [J/kg]
 ρ_F Density of furniture [kg/m³]
 ρ_L Density of liquid water [kg/m³]
 ρ_r Density of room air [kg/m³]
 ρ_S Density of the solid [kg/m³]
 ρ_V Water vapor density [kg/m³]
 $\rho_{V,\alpha}$ Ambient water vapor density [kg/m³]
 ϕ Relative humidity [0 to 1]
 τ Time [h]
 Φ Thermodynamic activity of water [0 to 1]
 τ_0 Tortuosity [dimensionless]

CHAPTER 1

INTRODUCTION AND SUMMARY

This report covers the first year of a multiyear effort designed to develop mathematical modeling capabilities for simultaneous heat and moisture transport in buildings. This effort represents only one task of a cooperative research project with five major initial year elements:

1. Moisture research
2. Analytical methods
3. Radiant barrier systems
4. Enthalpy exchange systems
5. Integrated systems research

The objective of the overall project is to develop research capabilities needed for the development and analysis of building integrated solar cooling and dehumidification alternatives suitable for hot, humid climates prevalent in the southeastern United States.

Only the analytical methods task is reported here. The goal of this task during the initial year has been to develop detailed and simplified computer algorithms that describe the behavior of simultaneous heat and moisture transport in buildings. The reader will see that this is a very important and difficult task.

Because of the complexity of the subject matter, it has been difficult to organize this report in a way that allows both a clear understanding of the problem and a detailed technical explanation of the proposed solution schemes. We have chosen to place the majority of the detailed technical information and data in a set of appendices that are organized by specific subject matter. We provide a general understanding of the phenomena in the main body of the report. We believe that such an organization will provide a better understanding of combined heat and mass transfer phenomena to a wider audience. At the same time, the appendices provide detailed state-of-the-art information to those with a strong background in specific disciplines.

Some important points must be clearly stated at the outset. The reader should understand that the work is not complete. This is true for a number of reasons; chief among them is the lack of detailed experimental data on the spatially

distributed behavior of moisture in materials. Some of the theory that is presented here and in the literature rests on only limited experimental data. The complexity of the phenomena often forces researchers to concentrate their effort in one specific area of the subject. As a result, the theoretical hypothesis is confirmed only for a limited portion of the potential range of combined heat and mass transport phenomena. Thus the theoretical hypothesis used to develop a specific analytical method often will not hold outside of the experimental range from which that theory was developed.

Notwithstanding these cautionary statements, the work reported here is considered vitally important to the continued development of an understanding of heat and moisture transport phenomena in buildings. This is particularly true for buildings in hot humid climates. In humid climates one of the major loads in air conditioned buildings is the moisture load. If alternative energy solutions are to be sought for the supply of cooling and dehumidification in these buildings, it is imperative that we be able to understand and model moisture transport.

Moisture has little effect on heating system performance but a profound effect on the performance of air conditioning systems. In order to accurately describe building performance during periods when cooling is needed it is very important to know the moisture conditions of the building. If one assumes that all building moisture is contained by the room air, then one is ignoring the fact that the materials which bound the room (e.g. wall surfaces, furnishings, linens, etc.) have the capability to store and release moisture. Thus, to assume that the only moisture that effects cooling system performance is contained in the room air is a false assumption that can lead to significant error in the prediction of room moisture conditions and cooling system loads.

In addition, the study of innovative cooling and dehumidification systems requires that analytical assessments of proposed concepts be performed if research is to be cost effective. Without an accurate tool such studies simply cannot be performed. Many innovative systems require that the building be fully integrated in the design. Excellent examples of this are the passive heating concepts that have been developed in recent years. Without the aid of detailed modeling capabilities the development of these concepts would not have been feasible.

It is possible to conceive of analogous solar cooling and dehumidification concepts that take advantage of natural diurnal cycles to cool and dehumidify buildings at much reduced energy costs. The development of such concepts is one of the major goals of this research. The cost effective study of these cycles, however, requires that accurate models of combined heat and moisture transport in buildings be made available to the researcher.

To that end, a detailed finite element computer code called FEMALP 2.1 has been developed. To the extent that exact analytical solutions and quality experimental data exist, the code has been well validated (see Appendix I).

FEMALP 2.1 is further development of FEMALP, the Finite Element Method Application Language Program, developed by the prime author of this report during his PhD dissertation work (Kerestecioglu, 1986). FEMALP has been used in previous sponsored research (Fairey, et al., 1986) to determine characteristic moisture transfer coefficients for use in a "lumped" moisture algorithm that was incorporated in the NBS TARP (Thermal Analysis Research Program) computer code.

This program, called MADTARP (Moisture Adsorption and Desorption Thermal Analysis Research Program) was subsequently used to determine the potential extent of moisture effects in buildings. Results from the work indicated that moisture plays a much more significant role in buildings than previously supposed.

FEMALP 2.1 is significantly advanced over its predecessor. A significant study of the world literature on moisture transport has been conducted and the program has been updated to provide highly advanced simulation capabilities. It is currently being used as graduate level teaching tool as well as for research. As a result, the program is under vigorous scrutiny resulting in constant improvement of its numerical solution and modeling techniques by a cadre of researchers and graduate students. It is appropriate to point out that FEMALP 2.1 is significantly more than a building simulation program. It is a highly advanced general simulation tool that can easily be used for building applications but it is by no means limited to buildings or building technology.

The literature contains a number of potentially valuable theoretical approaches to the solution of combined heat and mass transfer. The theoretical hypotheses, their origin, mathematics, and background are discussed in detail in Appendix A. FEMALP 2.1 has been developed to support six of these theories. Of the six, two seem particularly promising; Luikov's theory because it has very attractive governing equations and evaporation condensation theory because it is accompanied by numerous property data. Nonetheless, all six theories will be maintained until sufficient experimental data can be gathered to warrant abandoning them.

There are three good reasons to do this. First, we do not know a priori which theory or theories are the most appropriate or the most accurate for the task at hand. We must have more and better experimental data to determine this. Second, the nature of the governing equations for each theory are somewhat different. This results in some of them being significantly more computationally efficient and stable than others. For example, the same problem takes approximately six times less computer time using Luikov's theory than it does using evaporation condensation theory. For large scale building simulation problems this can have a pronounced effect on computer run times. For obvious reason this consideration cannot be ignored.

Third, and perhaps most important at the current stage, some of the theories are accompanied by relatively large amounts of material property data (e.g. evaporation condensation theory). These data are not transferable to the other theories and are difficult to obtain. The theories they support cannot be summarily discarded without very good reason. The property data requirements of each theory are listed in Appendix C and the property data that have been collected are given in Appendix D. Wherever possible the data have been reduced to functional relationships so as to be immediately usable by computer codes. More property data are available but they have not yet been reduced to this format. The reader is also cautioned that the property data have not been fully checked and cross checked against the source data. Therefore, some typographical and transpositional errors in the data set are possible.

The remainder of the body of this report is divided into two main sections. Chapter 2 provides a discussion of the phenomena and Chapter 3 gives illustrative examples some of the simulation capabilities FEMALP 2.1. The reader will gain an understanding of the complexity of the problem in the second

chapter and will be carried step-by-step through the thought processes that lead to our understanding of the physical phenomena of combined heat and moisture transport. Hypothetical examples are often used to illustrate and emphasize key points and the solution to a common but previously unsolved heat and moisture transport problem in buildings is fully developed for the reader. The available theories of combined heat and mass transfer are briefly discussed and the numerical and theoretical appropriateness of the solution techniques are critically compared.

The final chapter of the report provides insight into the importance of combined heat and moisture transport phenomena in buildings. A wide range of fairly routine but difficult building problems are not addressable without this capability. Results of the simulations described in Chapter 3 vividly illustrate the potential for simulation error when only heat transfer is modeled. These results additionally illustrate the wide range of capabilities provided by FEMALP 2.1.

CHAPTER 2

THEORETICAL APPROACH

This chapter is intended to summarize the phenomena of combined heat and mass transfer in buildings. The problem is rather complex, hence the mathematical derivations and details of the solution techniques have been purposely moved to the appendices. Where appropriate the appendices are referred.

A basic understanding of combined heat and mass transfer phenomena in solids is given in this chapter. The fundamental moisture transport mechanisms, driving forces (potentials), fluxes and the parameters effecting them are detailed. The available mass transfer theories and with their criteria are critically compared. The different combined heat and moisture transfer simulation techniques that can be applied to buildings are discussed in detail and solution approaches from the very simple to the very detailed are provided. The theoretical and mathematical development of a sample application of combined heat and mass transfer to a building problem is fully described and the numerical simulation techniques used in the solution of the governing equations are discussed. Last, the overall program capabilities of the developed model, FEMALP 2.1, are described.

2.1 COMBINED HEAT AND MASS TRANSFER IN SOLIDS

One of the major purposes of this chapter is to introduce the concept of combined heat and mass transfer. We wish to emphasize the words mass transfer. In this report the words mass transfer are used to define the transfer of moisture. And by moisture transfer we mean the transfer of water in its all phases (vapor, liquid, solid and all combinations of phase).

Mass transfer is very difficult to understand compared to heat transfer. It is equally difficult to conceptually visualize. In the last three decades several researchers have attempted to mathematically formulate and explain combined heat and mass transfer in solids. However, there is still no single theory or explanation that defines the problem. The literature is full of hypothesis. The difficulty of the problem will become quite apparent in the succeeding discussions.

The word solid is key to this discussion. Mass transfer in a gas or liquid medium is relatively easy to understand and the theory is well advanced. Real solids, however, are usually very different from the conceptual solids that are given in text books. Conceptual solids can be classified as follows (Brakel 1980).

CAPILLARY-POROUS MATERIALS -- Possible examples are crushed minerals, packed sand, polymer particles, non-hygroscopic crystals, some ceramics. The defining criteria are:

1. There is a clearly recognizable pore space. This pore space is filled with liquid if the capillary-porous medium is completely saturated, and filled with air when the medium is completely dry.
2. The amount of physically bound water is negligible (i.e., the medium is non-hygroscopic).
3. The medium does not shrink during drying.

HYGROSCOPIC-POROUS MATERIAL -- Possible examples are silica gel, alumina, zeolites, clay, molecular sieves, wood, and textiles. The defining criteria are:

1. There is a clearly recognizable pore space.
2. There is a large amount of physically bound liquid.
3. Shrinkage and swelling often occur in the initial stages of drying and wetting.

This class can be further subdivided into (1) hygroscopic, capillary-porous media (micro-pores and macro-pores; for example, wood, clays, and textiles), and (2) strictly hygroscopic media (only micro-pores; for example, silica gel, alumina, zeolites).

COLLOIDAL (NON-POROUS) MATERIALS -- Possible examples are soap, glue, and some polymers (e.g., nylon). The defining criteria are:

1. There is no internal pore structure.
2. All liquid is physically bound.

In the discussion of mass transfer we will attempt to give conceptual examples and compare mass transfer to heat transfer. We use heat transfer as an analogy because the theory is well established and the concepts are universally accepted.

EXAMPLE 1 -- Let us start with a very simple hypothetical case. There is an infinitely large test chamber where the temperature, T , and the humidity ratio, W , of the chamber air can be set to any desired value. Let us place a hypothetical material into the chamber set at $T=25^{\circ}\text{C}$ and $W=0.004$ kg/kg and wait for a long time and ask the question -- What are the conditions of the material? One will immediately say, "its temperature is 25°C , but I don't know what its moisture content is". Now elevate the temperature of the chamber to 50°C without changing its humidity ratio. Wait for a long time and ask the same question. The temperature of the hypothetical material will be 50°C . Its

moisture condition will still be undetermined but will be lower than in the first case because the material will dry when it is heated.

At this point one realizes that mass transfer is not that well defined and some clarification is needed. This is indeed true and at this point three additional concepts must be introduced.

1. **MOISTURE CONTENT** -- In mass transfer one needs to know the amount of water that is present in the solid material. The answer to the above question would be that the material contains X kg of water. Moisture content represents the total amount of water (in all phases) in the solid material. However, there are several different ways of defining moisture content. The most common is the moisture content on a dry weight basis. Usually it is denoted as Φ and is defined as follows:

$$U = \frac{\text{mass of the total water in the solid}}{\text{mass of the solid in the absence of water}}$$

The other one is the volumetric moisture content. It is denoted by H and is defined as follows (Roques and Cornish 1980):

$$\theta = \frac{U \rho_S (1 - \epsilon)}{\rho_L}$$

2. **RELATIVE HUMIDITY** -- From the above example one realizes that a rise in temperature dries the material. Thus, neither the temperature nor the humidity ratio alone can be used to define moisture transfer. In mass transfer operations a reference point that includes both the temperature and the humidity ratio is needed. The most commonly used reference point is the relative humidity. It is defined as follows:

$$RH = \frac{P_V}{P_{V,sat}} 100$$

3. **EQUILIBRIUM MOISTURE ISOTHERM** -- The equilibrium isotherm is a curve relating the equilibrium moisture content of a material to the relative humidity of the air it is in equilibrium with.

Figure 2-1 shows the adsorption and desorption isotherms of a typical hypothetical material. In region I, water is tightly bound at individual sorption sites and is unavailable for reaction. In this region, the curve is concave to the water activity (relative humidity) axis and represents the adsorption of the first layer (mono layer) of water vapor onto the surface of the adsorbing material. The bonding energy of this layer depends strongly on the chemical construction of the surface.

In region II, water is more loosely bound and corresponds to the second and following layers of sorbed water. The total pressure of the system is depressed by the presence of small capillaries. The sorption energy involved is predominantly that of condensation.

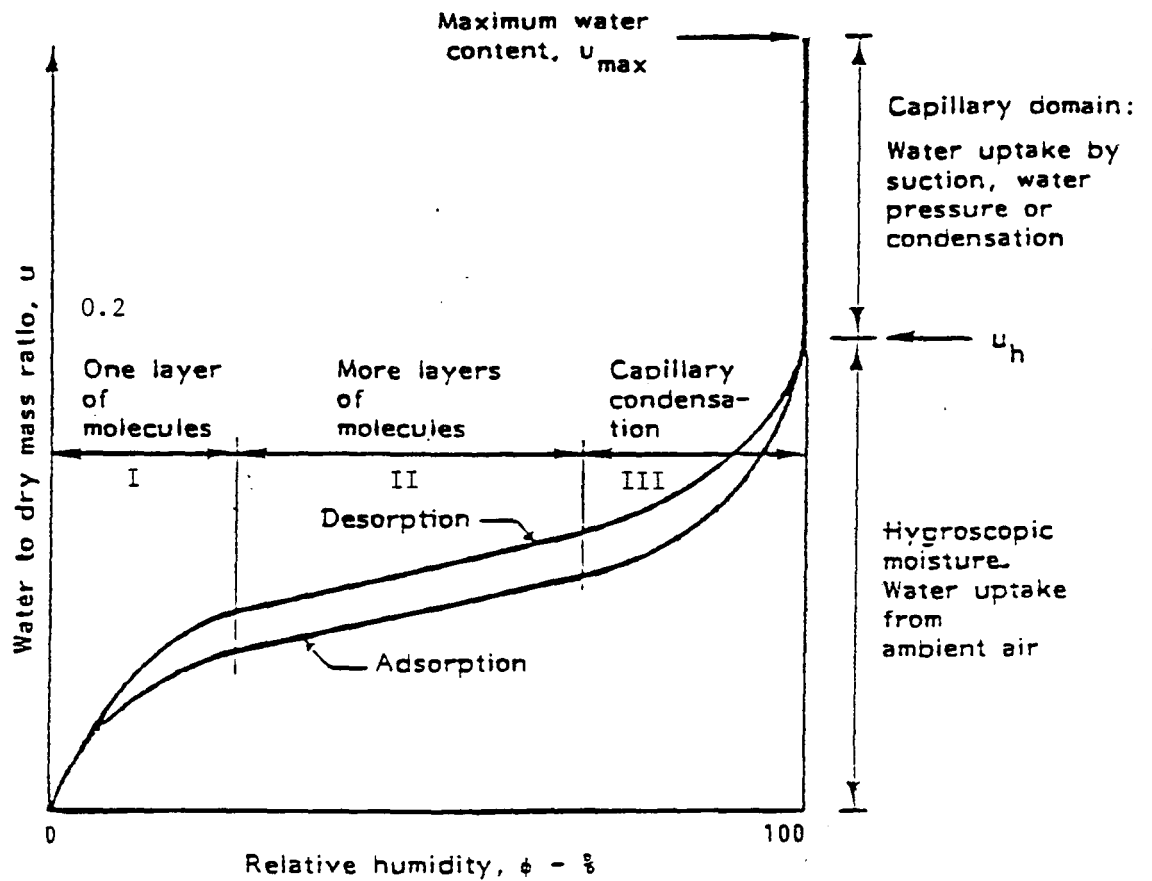


Figure 2-1 Typical adsorption and desorption isotherms showing hysteresis. The curves show connected values of RH of the ambient air and water content of the material at equilibrium at a constant temperature.

In region III water is present in the large capillaries, is relatively free for chemical reaction, and is capable of acting as a solvent. This region corresponds to many layers of water and is characterized by capillary condensation. At this point the vapor pressure of the system is influenced only moderately by preceding layers of sorbed water.

Note that there are two isotherms shown in Figure 2-1. The displacement between the adsorption and desorption curves is termed hysteresis. No conclusive explanation for this phenomenon is found in the literature. Cohan 1944 discusses some of the early hypotheses. One of these, the "ink-bottle" theory, has been proven to work for certain materials (Labuza 1968). More complicated hypotheses can be found in Young and Nelson 1967.

Now let us try to answer the question that we asked earlier. The relative humidity at $T=25^{\circ}\text{C}$ and $W=0.004\text{ kg/kg}$ is $\text{RH}=20$ percent. At $T=50^{\circ}\text{C}$ and $W=0.004\text{ kg/kg}$ the relative humidity is $\text{RH}=5$ percent. From Figure 2-1 we can say that under the first experiment the moisture content of the hypothetical material was 0.075 kg/kg and under the second it was 0.02 kg/kg . If one knows the dry weight of the hypothetical material (assume 2 kg) the answer is 0.15 kg of water for the first condition and 0.04 kg of water for the second.

There is still a problem associated with the example. One must answer the following question. From which curve do I read the value of the moisture content? The answer to this question seems simple at first. If the experiment started at 0 percent relative humidity, and the relative humidity is continuously increased the adsorption isotherm is used and if the experiment starts at 100 percent relative humidity and the relative humidity is continuously dropped then the desorption isotherm is used. But, what happens if the experiments start at 50 percent relative humidity then goes to 40 percent relative humidity and later to 60 percent relative humidity? Can I draw the state points? Unfortunately, the answer to this question is no. Further knowledge and experimental data are needed to draw the state point diagram for this problem. Unfortunately for some building materials hysteresis can be rather pronounced (10 to 15 percent). The phenomena are further complicated by the fact that, different sorption isotherms are obtained at different temperatures (see Table D-1 for details). Thus, the moisture storage capability and behavior between discrete equilibrium conditions may not be accurately known for many materials. The reader realizes that we are not able to obtain conclusive answers even though we are working with a steady-state problem.

Before we proceed further we must mention the effect of mass transfer on heat transfer. Suppose example 1 is restated as follows: in the initial stage the chamber condition is $T=25^{\circ}\text{C}$ and $W=0.004\text{ kg/kg}$. After a long period of time the chamber condition is changed to $T=25^{\circ}\text{C}$ and $W=0.008\text{ kg/kg}$. Again, we ask the same question -- What are the material's temperature and moisture content at the end of each set of conditions. The answer would be 25°C and 0.055 kg/kg of moisture at the end of the first stage, and 25°C and 0.065 kg/kg of moisture at the end of the second stage. From this we may conclude that the environment's moisture condition does not effect the steady-state temperature of the material, however, the temperature of the environment does effect the steady-state moisture content of the material. Restated, we say that we may change the steady-state moisture content of the material by changing either the temperature or humidity ratio of the chamber. However, we can only change the material's steady-state temperature by changing the temperature of the chamber.

2.2 MOISTURE TRANSPORT MECHANISMS

So far we have confined our discussion to steady-state heat and mass transfer phenomena. Our main objective, however, is to study combined heat and mass transfer under dynamic conditions. At this point the problem becomes much more complex and many additional hypotheses are introduced. We are using the word hypotheses because none of the theories are completely proven and universally adapted. The reason that they are not proven or universally adapted is due primarily to a lack of equipment that will measure the quantity of water within the solid material as a function of space (x, y and z coordinate) and time. In addition, the state of the water must also be measured. In other words, when we say the moisture content is 0.02 kg/kg, we must also know that 0.015 kg/kg is liquid moisture, 0.004 kg/kg is ice and 0.001 kg/kg is vapor. One can argue that the amount of water vapor within the solid compared to the amount of liquid present in the solid is negligible. That is true, but the point that must be considered is that the magnitude of the water vapor represents one of the major driving forces of mass transfer. The message we are trying to convey is that even though the water vapor contribution to the total water in the solid is negligible, the effect of that water vapor on the mass transfer rate is substantial. Consequently, in addition to the gross weight of water, the phase distribution must also be known.

EXAMPLE 2 -- Reconsider the same test chamber and the same specimen. In this experiment, we also place a weight measuring device in the chamber in order to measure any weight change in the hypothetical material. Initially, the chamber conditions are set to $T=25^{\circ}\text{C}$ and $W=0.004$ kg/kg, and the material is kept there for a long time, later the conditions are suddenly changed to $T=50^{\circ}\text{C}$ and $W=0.02$ kg/kg. Now we ask a very difficult question. Can we predict the temperature and moisture content of the hypothetical material as a function of time and spatial coordinates? What will it take to answer this question? Most probably, any person who is familiar with heat and mass transfer operations will say "yes we can predict them if you give us such and such material parameters". Now, these parameters, especially the ones that are related to mass transfer will probably be different for everyone. In other words everyone will require different parameters to perform this task.

However, if the above problem is posed in the absence of mass transfer, and the same question is asked. Then the simple answer would be as follows: "We will need the thermal conductivity, the density and the specific heat of the material and we will need the convective heat transfer coefficient at the surface". And the more sophisticated analyst will include "we will need these properties as a function of temperature". In the absence of mass transfer this is sufficient information to fully define and solve the problem. So, why are we unable to answer the same question in the presence of mass transfer? Why does everyone use different theories and property parameters? Before we answer these questions some background on mass transport mechanisms must be given.

The transport of water can be attributed to one or more of the following mechanism (Bruin and Luyben 1980, Fortes and Okos 1980):

1. Molecular vapor diffusion
2. Molecular liquid diffusion

3. Capillary flow
4. Knudsen diffusion
5. Surface diffusion
6. Stefan diffusion
7. Evaporation condensation
8. Poiseuille flow
9. Movement due to gravity

Figures 2-2 and 2-3 graphically display these mechanisms of moisture transport.

MOLECULAR DIFFUSION (Vapor) -- Diffusion of water vapor due to partial pressure gradients. These partial pressure gradients are caused by the affects of temperature gradients on sorption isotherms.

MOLECULAR DIFFUSION (Liquid) -- Diffusion in liquid-filled pores occurs by essentially the same mechanism as in gaseous systems. However, methods of correlation and prediction are less accurate because the fundamental theory of diffusion in liquid phase is less well developed than the theory of molecular diffusion in the vapor phase.

CAPILLARY FLOW (Liquid) -- Movement of liquid water due to capillary suction pressure.

KNUDSEN DIFFUSION (Vapor) -- In molecular diffusion the resistance to flow arises from collisions between diffusing molecules. The effect of pores is to reduce this vapor diffusion by imposing geometric constraints which are accounted for by a material property called the tortuosity factor. Molecular diffusion will be the dominant transport mechanism whenever the mean free path of the gas (i.e., the average distance traveled between molecular collisions) is small relative to the pore diameter. However, in small pores and at low pressures the mean free path is greater than the pore diameter and collisions of molecules with the pore walls occur more frequently than collisions among diffusing molecules. Under these conditions the collisions between molecules and pore walls provide the main diffusion resistance. This is known as Knudsen diffusion or Knudsen flow.

When a water molecule strikes the pore wall it does not bounce like a tennis ball. Rather the water molecule is adsorbed and re-emitted in a random direction. The direction in which the water molecule is emitted bears no relation to its original direction before the collision. It is this randomness that provides the characteristic feature of Knudsen diffusion.

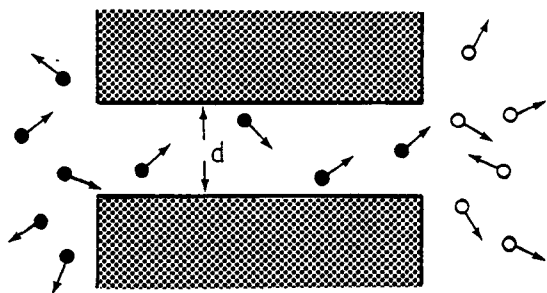
SURFACE DIFFUSION (Liquid) -- There is a direct contribution to the liquid flux from the transport through the physically adsorbed layer on the surface of the macro-pore, and this is referred to as surface diffusion. Although the mobility of the adsorbed phase will generally be much smaller than that of the gas phase, the concentration is very much higher; so, under conditions such that the thickness of the adsorbed layer is appreciable, a significant contribution to

TYPE

ILLUSTRATION

EQUATION

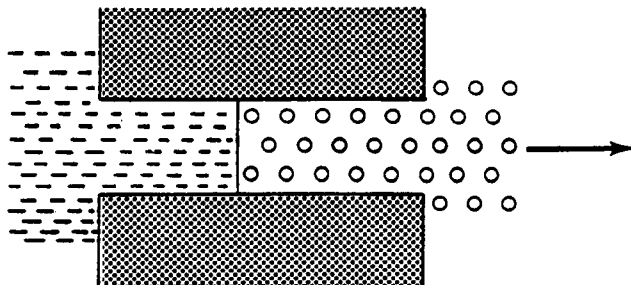
Knudsen diffusion



$$J_V = -\epsilon \tau_0 \beta D_k \nabla \rho_V$$

$$D_k = \frac{2}{3} d \left(\frac{2}{\pi} \frac{RT}{Mw} \right)^{0.5}$$

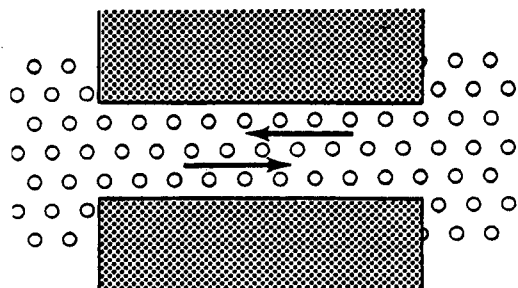
Stefan diffusion



$$J_V = -\epsilon \tau_0 D_a \frac{P}{P - P_V} \frac{Mw}{RT} \nabla P_V$$

$$D_a = \frac{830}{P_b} \left(\frac{T}{273} \right)^{1.81}$$

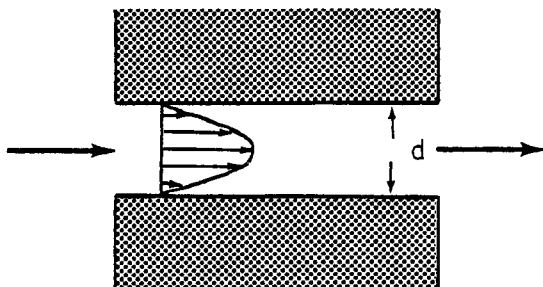
Mutual diffusion



$$J_V = -\epsilon \tau_0 D_a \nabla \rho_V$$

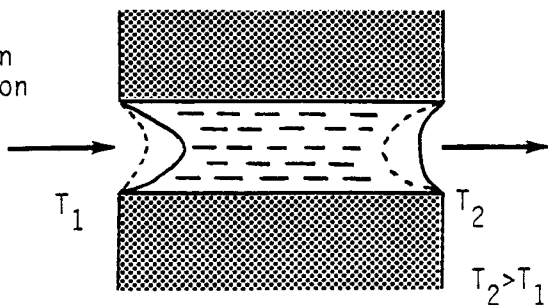
$$D_a = \frac{830}{P_b} \left(\frac{T}{273} \right)^{1.81}$$

Poiseuille flow



$$J_V = -\epsilon \tau_0 \frac{d_o^2}{32\mu} \nabla P$$

Evaporation condensation



$$J_V = J_V(\nabla T, \dots)$$

Figure 2-2. Water vapor transport mechanisms.

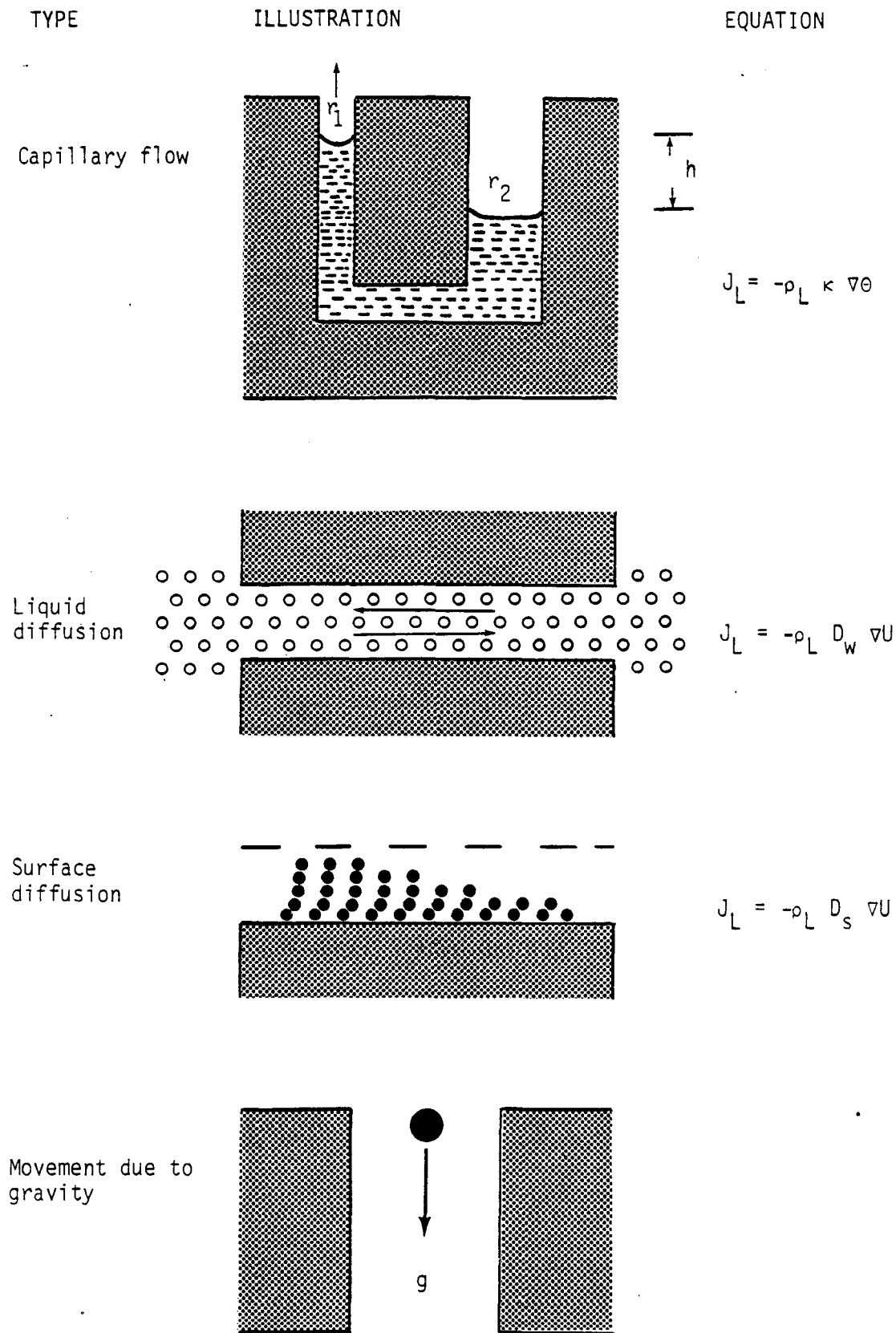


Figure 2-3. Liquid water transport mechanisms.

the flux is possible. Physical adsorption is thus seen as a prerequisite for the contribution from surface diffusion to be noticeable, and this requires temperatures not too far above the boiling point of the species considered. At high temperatures the thickness of the adsorbed layer decreases and any surface flux becomes small compared with the flux through the gas phase.

Surface diffusion is significant only in small diameter pores in which the flux through the gas phase can generally be attributed entirely to Knudsen diffusion. The surface diffusivity is a strong function of the moisture content.

STEFAN DIFFUSION (Vapor) -- Exploration of the consequences of allowing the fluid to have more than one component is undertaken by examining a two-component (binary) convection problem refers to as Stefan's diffusion problem. In Stefan's problem a container partially filled with a volatile liquid is exposed to an atmosphere of free of the vapor. The rate of evaporation is to be related to the saturation vapor pressure specified by the liquid temperature. Further details are given by Burmeister 1983.

EVAPORATION CONDENSATION (Vapor) -- Concurrent with heat transfer this process evaporates moisture in one location and recondenses it in another in a fashion analogous to the operation of a heat pipe.

POISEUILLE FLOW (Vapor) -- If there is a difference in total pressure across a particle, then there will be a direct contribution to the vapor flux from forced laminar flow through the macro-pores. This effect is generally negligible in a packed bed since the pressure drop over an individual particle is very small. The effect may be of greater significance in direct laboratory measurement of uptake rates in a vacuum system.

MOVEMENT DUE TO GRAVITY (Liquid) -- Movement of liquid water due to gravity. If the pore dimensions are extremely small then this component will be negligible.

2.3 HISTORICAL SURVEY AND DISCUSSION OF THE MOISTURE THEORIES

The combined heat and moisture transport in materials is very difficult to describe mathematically. In addition to liquid molecular diffusion, water transport by vapor diffusion, surface diffusion, Knudsen diffusion, capillary flow, purely hydrodynamic flow, and internal evaporation and condensation effects further complicate the problem. The traditional approach in the work of Krischer 1957 and the earlier work of Luikov 1964, and of Philip and De Vries 1957 and De Vries 1958 has been essentially to add the various contributions to the total flow of water. This results in the defining of an apparent (effective) water-diffusion coefficient D_W and an apparent thermal diffusion coefficient D_T to relate the total water flux (vapor+liquid) to the moisture and temperature gradients ∇U and ∇T , as indicated in the following equation:

$$J_W = - \rho_S D_W \nabla U - D_T \nabla T$$

We should realize that D_T is not related to the Soret effect, but is strictly dependent on the sorption isotherm, the evaporation and condensation mechanism of transport, and the temperature dependence of the capillary suction pressure (see Philip and De Vries 1957). Special mention must be made of the work of Harmathy 1969, who devised a theory for water transport in porous bodies

assuming that all movement of water takes place in the vapor phase, but with porous structure permeability that is dependent on the moisture content, and of Berger and Pei 1973 and 1975, who separately account for vapor and liquid transfer using constant permeabilities. Rotstein and Cornish, 1978 presented a model for combined heat and moisture transport in cellular tissues in which water transport is controlled by the flow through the gas-filled pores between cells.

During the 1960s it became fashionable to use flux equations that were claimed to be based on the phenomenological theory of irreversible thermodynamics as developed by Onsager 1931, Meixner 1943, Prigogine 1961, De Groot and Mazur 1962 and Fitts 1962. Examples of such studies are those of Luikov 1964, 1966 and 1975, soil-science applications by Cary and Taylor 1962 and Taylor and Cary 1964, and those of Roques and Cornish 1980, Valchar 1972, and, recently, Fortes and Okos 1978. Most notably Luikov et al. 1964, 1966 and 1975 pursued this direction, but the analysis is not fully rigorous. The assumptions of local thermodynamic equilibrium among all phases (gas, liquid, solid) and the failure to realize that an averaging procedure over a characteristic volume element containing all three phases is necessary before one can arrive at a constitutive equation for fluxes remain unresolved.

So far we have pointed out the salient aspects of the commonly quoted mass transfer models or, in general terms, heat and moisture transfer in hygroscopic capillary-porous bodies. At this point further limitations and restrictions of these models will be discussed.

From the thermodynamics of irreversible processes, it can be shown (De Groot 1951 and Prigogine 1961) that the actual driving forces for the moisture transport are chemical potentials and temperature gradients. The chemical potential of water in a material may be expressed, in terms of the difference between the chemical potential of water at a point in question in the material and the water in its reference state, by

$$\nabla\mu = \nabla\mu_s + \nabla\mu_p + \nabla\mu_o + \nabla\mu_f$$

where $\nabla\mu_s$ denotes the component of the chemical potential due to surface tension and radius of curvature of the water-air interface; $\nabla\mu_p$, that component due to the hydrostatic pressure of the moisture adjacent to the solid particle surface caused by the adsorptive forces surrounding the solid particle (excluding those forces due to surface tension and the radius of curvature of the water-air interface), and any pressure transmitted from external sources. $\nabla\mu_o$, that component due to osmotic pressure of the dissolved materials; and $\nabla\mu_f$, that component due to the chemical potential of water arising from its position in the adsorptive field surrounding the interstitial particles as well as the gravitational field.

In the view of the above expression, accepted fact that water can migrate in either liquid or vapor phase or both, it can be ascertained that the liquid-diffusion, capillary, or evaporation-condensation theory lacks a physical meaning when applied to a whole drying process. These theories are complementary to each other and should be taken as such. Philip and De Vries 1957 assumed the modified Kelvin equation (Equation A-5.10) to cover the whole range of moisture contents. However, readers with sufficient background will recall that Kelvin's equation is applicable only to the capillary condensation region. Luikov 1966 lumped together all the components of the total chemical

potential and created a new driving force for mass transfer (moisture transfer potential). Luikov's original equations (Equations A-4.15 and A-4.16) are very similar to Philip and De Vries, and both models should give similar result. Berger and Pei's approach, an extended version of Krischer's basic ideas, does not offer much innovation over Luikov's and Philip and De Vries' models, except for the fact that Berger and Pei take into consideration the isotherm equation (empirically obtained) as a coupling equation between liquid, vapor and heat transfer.

2.4 HEAT AND MASS TRANSFER AND BUILDINGS

Building science is interested in understanding buildings at a number of levels of detail. For one level the representation of phenomena by some type of artifact is sufficient. At another level, extensive and detailed information about specific behavior is desired and the analysis must be rigorous and highly accurate phenomenologically. For the most part this report concerns its discussion with the development of the latter level of capability but the development of alternative, more simplified levels of analysis are included in the discussion.

In building simulations the main interests are to predict the indoor conditions and the associated loads. In order to accomplish this the transport equations must be solved for each building component. In general a transport equation can be written in either lumped or distributed form. If the field variable (temperature or concentration) is not a function of space then lumped, but if the field variable is a function of space then distributed equations should be used. Both of these equations can be written as steady-state or transient.

If the whole building is represented with distributed equations then the problem can be solved as a continuum, and only one domain is needed. However, if some building components are defined by lumped equations and some are defined by distributed equations then the problem is not continuous and separate domains must be considered. A building can be easily divided into two domains: 1) the solid domain (envelope, internal mass, e.g.), and 2) the air domain ("zone"). Figure 2-4 is given to clarify these descriptions. In this case, the combined heat and moisture transfer taking place in the walls is formulated using distributed equations, but the energy and mass balance equations used for the air domain are lumped equations.

The chief concern of this report is the modeling of combined heat and moisture transport. Moisture transport occurs in both the solid and air domains of the problem. In the air domain moisture exists as a vapor. In the solid domains of the problem the moisture may occur in any or all of its three phases. Depending on the level of information that is required by a given problem, different analytical approaches may be used to define moisture behavior in a building. As one might expect, the more simplified the solution scheme the less informative the results. To be fair, however, one must also say that the more detailed the solution scheme the more costly the analysis.

Three distinct levels of complexity are presented here. Their advantages, disadvantages and data requirements are briefly described in Table 2-1. The analyst is encouraged to use good judgement in matching analysis methods with problem requirements.

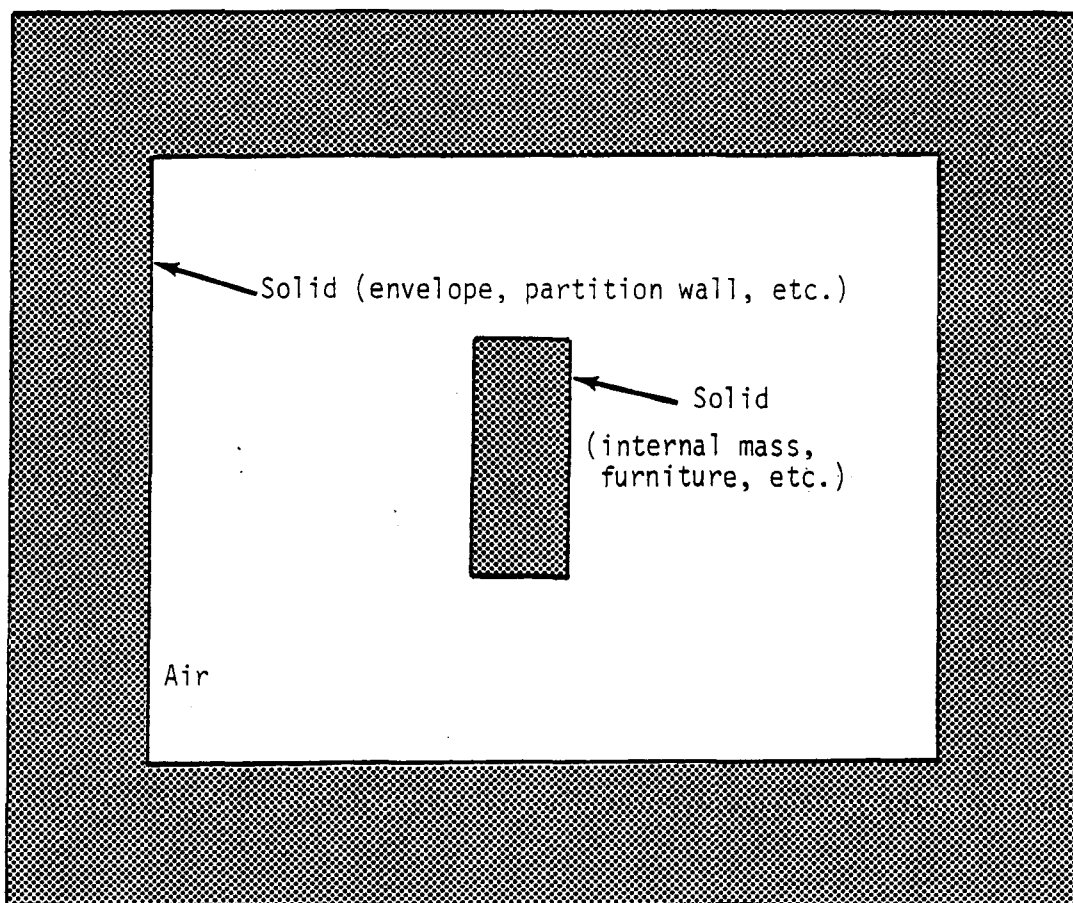


Figure 2-4. Building domains.

Table 2-1

Brief Description of Moisture Modeling Techniques

Whole-building moisture capacitance model

Advantages:

- Very simple
- Can be quickly implemented

Disadvantages:

- Cannot accurately account for h_{ig}
- Cannot accurately account for diffusion in solids
- Cannot accurately account for storage
- There may be no single appropriate value for E_m

Lumped model approach

Advantages:

- Accurately models h_{ig}
- Can be implemented in most existing programs (but not DOE 2.1)

Disadvantages:

- Requires artificial material thickness or h_m
- Geometries/materials not interchangeable
- Long-term storage cannot be modeled
- Different initial and operating conditions require different artificial M_d values

Distributed model approach

Advantages:

- Very accurate mathematically
- Allows variable property relations
- Phenomenologically correct
- Can obtain detailed, distributed data
- No case limitations

Disadvantages:

- Computation time may be long
- Only limited detailed property data available (GIGO)
- Requires FEM/FDM

Experimental data requirements

Whole-building capacitance (E_m) model

- Whole-building dynamic data over the range of likely conditions

Lumped model

- Equilibrium data over the range of likely conditions
- Mass transfer rate data over the range of likely conditions

Distributed model:

- Effective diffusivity data developed from lumped model data

OR

- Surface equilibrium plus
- Simultaneous temperature distributions and
- Simultaneous moisture content distributions (by phase)

1. The "effective air mass multiplier" concept.

The most simplified artifact one might employ for building moisture capacity would artificially magnify the moisture storage capacity of the room air (increase the weight of the dry air in the room) to represent the effects of moisture storage by the materials. This technique moves the moisture storage effects from the solid to the air domain of the problem. Even short term storage effects may be compromised by this. Additionally, this degree of simplification makes inclusion of moisture phase change effects virtually impossible because sorption requires a surface (solid) in physical reality. Nonetheless, such simplified analysis has a place and is discussed in significant detail in Appendix E, Section E.4.

2. The "effective penetration depth" concept.

The various elements of the solid domain may be treated differently. For instance, a lumped equation is often used to describe the thermal storage capacity of the house furnishings. A lumped equation may also be used to describe the moisture storage capacity of the furnishings if reasonable material property parameters can be ascertained. These properties, however, can only be obtained from experimental data or detailed modeling results. With good experimental data it is possible to aggregate all of the building's moisture storage capacity into a single lump and obtain reasonable predictions of zone thermal and moisture conditions:

In lumped moisture models there a number of parameters that can be effectively "adjusted" by the analyst. Many analyst chose to determine an "effective" convective mass transfer coefficient from experimental results and use actual thicknesses, surface areas, and moisture isotherms in the solution schemes. Because building energy transport is so dynamic, we have chosen to use "actual" convective mass transfer coefficients that are determined via existing functional relationships (e.g. the Lewis relation -- see Appendix F, Section F.1). Preferring to use actual surface areas and moisture isotherms, we determine an "effective penetration depth" from experimental data and represent the moisture capacity of the problem using a "lump" of this thickness. A full and detailed discussion of this approach is given in Appendix E, Section E.3.

Substantial work in lumped analysis has been done by Cunningham 1983(a), 1983(b) and 1984. Cunningham developed a model of moisture concentration in a building cavity containing hygroscopic material which would allow for fluctuating external climatic conditions. Very similar models with identical assumptions were also used by Cleary and Sonderegger 1984, Burch 1985, Cleary 1985, Cleary and Sherman 1985 for predicting the performance of attics. Kusuda 1983 and Kusuda and Miki 1985 again used a similar model for estimating the indoor humidity levels.

3. Distributed modeling concepts.

The most sophisticated numerical method of describing transport phenomena is through "distributed" modeling. Finite difference and finite element methods may be used. The methods and solution schemes reported here are for finite element modeling but many of the principles may apply equally to either.

In distributed modeling the problem domain is continuous, no "effective" parameters are required by the solution techniques and the "conditions" of the problem can be "known" at any point in space and time. Given accurate material properties and boundary conditions a good distributed model can "reproduce" physical phenomena with great confidence and in exquisite detail. In fact, one of the more valued uses of a distributed model is to develop and verify more simplified analysis methods. For example, we may have a material or system which we know will function within some limited range of periodic operating conditions (e.g. a building wall under natural environmental conditions). A distributed model of the wall may be exercised within the expected range of conditions and from the results an "effective moisture penetration depth" or other descriptive artifact may be developed for use in a "lumped" modeling approach.

Distributed finite element modeling of combined heat and moisture transport is covered in great detail in the appendices of this report. The details of the combined heat and moisture transport theories are given in Appendix A, and the finite element solution of each theory is also provided in Appendix B.

2.5 SAMPLE APPLICATION OF HEAT AND MASS TRANSFER TO A BUILDING

In this section the mathematical details of an application of a combined heat and mass transfer theory to a building is described. The geometry of interest is shown in Figure 2-5. For simplicity, except for one surface all the walls are assumed to be adiabatic and impermeable. Furniture is placed in the room and heat and moisture are internally generated. Here the objective is to write the governing equations for each of the domains (solid and air). After the equations and boundary conditions are properly cast in suitable forms the solutions strategies are explained.

The governing energy and moisture balance equations for the room are given as follows [see Appendix E Eqs. (E-1.1) and (E-2.1)]:

$$(\rho_r V_r C_p) \frac{dT_r}{dt} = Q_{fur-s} + Q_{sor-s} + Q_{wal-s} \quad (2-5.1)$$

$$(\rho_r V_r) \frac{dW_r}{dt} = Q_{fur-l} + Q_{sor-l} + Q_{wal-l} \quad (2-5.2)$$

In Equations (2-5.1) and (2-5.2) Q_{fur-s} and Q_{fur-l} represent the heat and moisture released or stored by the furniture, respectively. In this analysis the furniture are treated with lumped equations. Q_{sor-s} and Q_{sor-l} represent

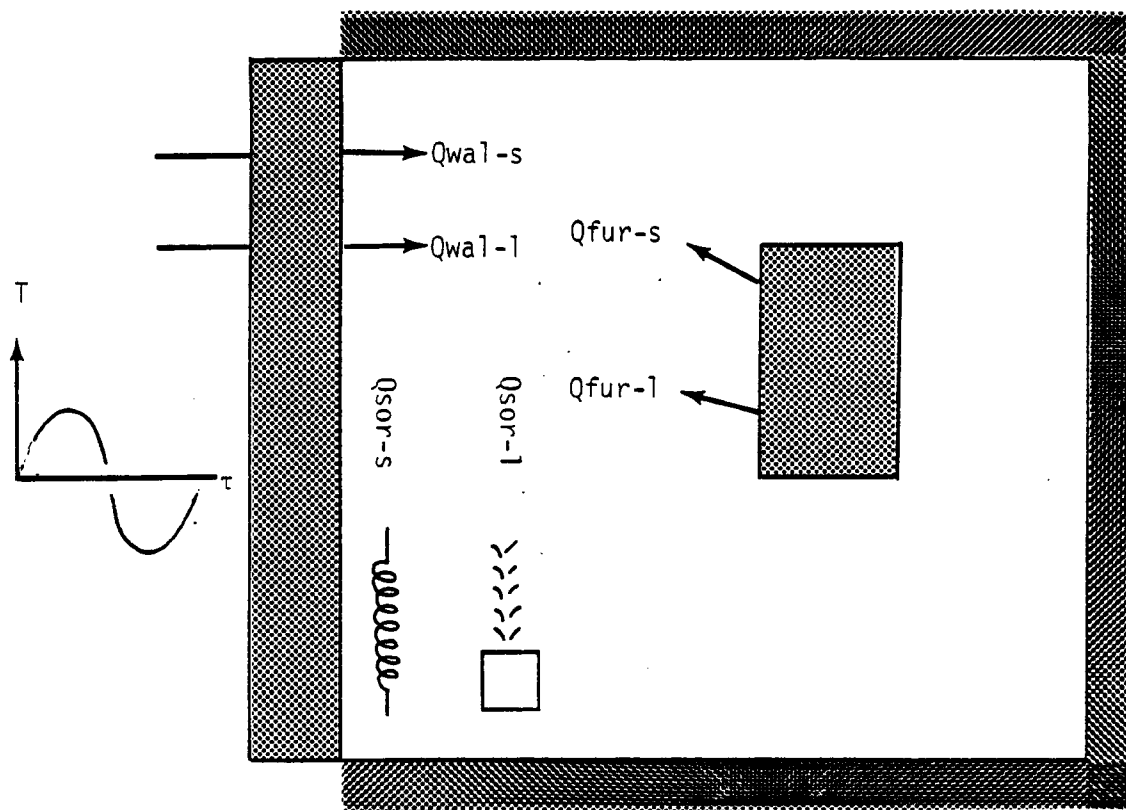


Figure 2-5. Schematic of a simple building used in the example derivations.

the amount of heat and moisture generated within the room, respectively, and they can be functions of time. $Q_{\text{wal-s}}$ and $Q_{\text{wal-l}}$ represent the amount heat and moisture crossing the envelope, respectively. The envelope is represented with detailed (distributed) heat and moisture transfer equations.

The furniture and wall terms are defined as follows for heat transfer [see Appendix E Eq. (E-1.11)]:

$$Q_{\text{fur-s}} = h_T A_f (T_f - T_r) \quad (2-5.3)$$

$$Q_{\text{wal-s}} = h_T A_w (T_w - T_r) \quad (2-5.4)$$

In Equations (2-5.3) and (2-5.4) T_f and T_w denote the temperature of the furniture and the temperature of the wall surface, respectively. Similarly, the furniture and wall terms for moisture transport are defined as follows [see Appendix E Eq. (E-2.11)]:

$$Q_{\text{fur-l}} = h_M A_f (W_f - W_r) \quad (2-5.5)$$

$$Q_{\text{wal-l}} = h_M A_w (W_w - W_r) \quad (2-5.6)$$

In Equations (2-5.5) and (2-5.6) W_f and W_w denote the humidity ratio of the air evaluated at the furniture's and wall's surface temperature and their material moisture contents, respectively.

If Equations (2-5.3) and (2-5.4) are substituted into Equation (2-5.1), and Equations (2-5.5) and (2-5.6) are substituted into Equation (2-5.2) then the governing energy and moisture balance equations can be written as follows [see Appendix E Eqs. (E-5.1) and (E-5.2)]:

$$\frac{dT_r}{dt} + P1(\tau) T_r = Q1(\tau) \quad (2-5.7)$$

$$\frac{dW_r}{dt} + P2(\tau) W_r = Q2(\tau) \quad (2-5.8)$$

Where

$$P1(\tau) = \frac{h_T (A_f + A_w)}{\rho_r V_r C_p} \quad ..$$

$$Q1(\tau) = \frac{1}{\rho_r V_r C_p} [h_T (A_f T_f + A_w T_w) + Q_{\text{sor-s}}]$$

$$P2(\tau) = \frac{h_M (A_f + A_w)}{\rho_r V_r}$$

$$Q2(\tau) = \frac{1}{\rho_r V_r} [h_M (A_f W_f + A_w W_w) + Q_{\text{sor-l}}]$$

Equations (2-5.7) and (2-5.8) are ordinary differential equations and in order for them to be considered complete, their initial conditions must be given. The initial conditions for Equations (2-5.7) and (2-5.8) can be written as:

$$@ r = 0 \quad Tr = Tr_o$$

and

$$@ r = 0 \quad Wr = Wr_o$$

If Equations (2-5.7) and (2-5.8) are closely examined then one realizes that there are six unknowns in the system of equations. Namely, the room temperature, Tr , the furniture temperature, T_f , the wall surface temperature, T_w , the room humidity ratio Wr , the furniture surface air humidity ratio, W_f , and the wall surface air humidity ratio, W_w .

As mentioned above the furniture is represented with lumped equations. The following equations can be used to represent the temperature, and the moisture content, of the furniture [see Appendix E Section E.3 Eqs. (E-3.4) and (E-3.5)].

$$(\rho_f A_f \delta_T C_p) \frac{dT_f}{d\tau} = h_{T A_f} (Tr - T_f) + \lambda h_{M A_f} (Wr - W_f) \quad (2-5.9)$$

$$(\rho_f A_f \delta_M) \frac{dU}{d\tau} = h_{M A_f} (Wr - W_f) \quad (2-5.10)$$

Where δ_T and δ_M are the empirically determined "effective penetration depth" for the thermal and moisture interactions. If Equations (2-5.9) and (2-5.10) are closely examined, one realizes that the system of equations does not close. The field variables for Eqs. (2-5.9) and (2-5.10) are the furniture temperature, the moisture content of the furniture, and the furniture surface air humidity ratio, [note that the zone temperature, and zone humidity ratio Wr are given by Eqs. (2-5.1) and (2-5.2)]. Consequently, a third relation is necessary.

This relation must be expressed in terms of the surface air humidity ratio and the moisture content of the furniture. The sorption isotherm may be used for this purpose by expressing the relative humidity axis of the isotherm in terms of T_f , W_f and P_b rather than relative humidity. For most building applications, however, the sorption isotherm of the furnishings is unknown. Conceivably one could be experimentally determined but that would require an almost infinite number of tests to characterize all potential building furnishings and combinations thereof.

We should point out that we do not require a sorption isotherm we only require a reasonably accurate relation between the surface air humidity ratio, and the moisture content of the furnishings. We can accomplish this with a fictitious isotherm if it is reasonable. Since the building furnishings are represented by a single lump in the governing zone balance equations the moisture diffusivity of the lump is not considered. Thus, a small error in the approximation of a sorption isotherm for the furnishings can be compensated by the "effective penetration depth" term if experimental data are available. Since this is the case we will use a hypothetical but reasonable equilibrium isotherm for the third equation. Thus the moisture content is defined as follows:

$$U = U(\phi, T_f) \quad (2-5.11.1)$$

$$\phi = \phi(T_f, W_f, P_b) \quad (2-5.11.2)$$

and from Equations (2-5.11.1) and (2-5.11.2)

$$U = U(T_f, W_f, P_b) \quad (2-5.11.3)$$

And the surface air relative humidity can be calculated by the following equation [see Appendix G Eq. (G-22)].

$$\phi_{n+1} = \phi_n - \frac{a \phi_n^b + c \phi_n^d - U}{a b \phi_n^{b-1} + c d \phi_n^{d-1}} \quad (2-5.12)$$

Equation (2-5.12) must be solved iteratively. The coefficients a, b, c and d can be obtained either from Table D-1 of Appendix D or from experiments. After the surface air relative humidity is calculated, and given a known furniture temperature and barometric pressure, the humidity ratio of the surface air can be calculated using the following equation [see Appendix G Eq. (G-22)].

$$W_f = \frac{0.62198 \phi}{\exp(-23.7093 + \frac{4111.0}{T_f - 35.45}) P_b - \phi} \quad (2-5.13)$$

If we did not want to simulate the wall in detail (with distributed equations) then our task is complete at this point. In other words, the wall surface temperature, T_w , and the wall surface humidity ratio, W_w , would not be calculated. An exact solution to this problem, with one lump, is given in Section E.5.3 of Appendix E.

If the walls are represented with detailed distributed equations and evaporation-condensation theory is used then the energy and mass transport equations for the entire thickness of the wall are given by the following equations [see Appendix A Eq. (A-3.1) and (A-3.2)].

$$\epsilon \frac{\partial \rho_V}{\partial \tau} + (1-\epsilon) \rho_S \frac{\partial U}{\partial \tau} = \nabla \cdot (\epsilon r_0 D_A \nabla \rho_V) \quad (2-5.14)$$

$$\epsilon \rho_S C_S \frac{\partial T}{\partial \tau} = \nabla \cdot (k_T \nabla T) + \lambda \rho_S \frac{\partial U}{\partial \tau} \quad (2-5.15)$$

where

- C_S Specific heat of the solid wall [W.h/kg.K]
- D_A Molecular diffusivity of water vapor in air [m^2/h]
- k_T Thermal conductivity of the solid wall [W/m.h]
- ϵ Porosity [m^3/m^3]
- λ Heat of vaporization [W.h/kg]
- ρ_S Density of the solid wall [kg/m^3]
- ρ_V Water vapor density [kg/m^3]
- r_0 Tortuosity factor [dimensionless]

As we see from Equations (2-5.14) and (2-5.15) we still do not have the desired parameters. The wall surface temperature, and surface air humidity ratio, come into play through the boundary conditions applied to Equations (2-5.14) and (2-5.15). The boundary conditions for Equations (2-5.14) and (2-5.15) are as follows [see Appendix A Eq. (A-3.3) and (A-3.3)]:

Room side:

$$-\epsilon\sigma D_A \nabla \rho_V = h_{M,\rho} (\rho_V - \rho_{V,r}) \quad (2-5.16)$$

and

$$-k_T \nabla T = h_T (T_w - T_r) \quad (2-5.17)$$

Ambient side:

$$-\epsilon\sigma D_A \nabla \rho_V = h_{M,\rho} (\rho_V - \rho_{V,\alpha}) - q_M \quad (2-5.18)$$

and

$$-k_T \nabla T = h_T (T - T_\alpha) - q_T \quad (2-5.19)$$

In Equations (2-5.18) and (2-5.19) q_M and q_T denote the imposed moisture and heat fluxes, respectively. Imposed moisture flux can be rain, and imposed heat flux can be solar radiation.

Closure of the equations described in this section again requires sorption isotherm data. The sorption isotherms can be represented with the following functional equation:

$$\rho_V = \rho_V(U, T) \quad (2-5.20)$$

Equation (2-5.20) can be derived through equations (G-15) and (G-22) of Appendix G. In this derivation the only input will be the material's equilibrium characteristics (a, b, c, and d coefficients that are defined in Table D-1 of Appendix D).

In Equation (2-5.16) the driving potentials are written in terms of water vapor densities, however, the zone moisture balance equation is written in terms of humidity ratio. Therefore, the following relation must be used to convert the water vapor density to humidity ratio [see Section F.2.1 of Appendix F, also see Eq. (F-2.1.1) and Table F-3].

$$\rho_{V,r} = \rho_r W_r \quad (2-5.21)$$

As can be seen from Equations (2-5.7), (2-5.8), (2-5.9), (2-5.10), (2-5.14) and (2-5.15) there are eight unknowns namely T_w , W_w , $\rho_{V,w}$, T_r , W_r , T_f , U and W_f . Considering equations (2-5.12), (2-5.13) and (2-5.21) reduces the whole system to six equations and six unknowns - T_w , $\rho_{V,w}$, T_r , W_r , T_f and W_f .

The system of equations considered in this problem are coupled, highly non-linear and therefore require an iterative solution procedure. Such an iterative procedure is described below.

Like all iteration procedures this iteration requires an initial approximation for all the unknowns. This approximation is usually the the initial condition. The first step is to solve the detailed wall heat and mass transport equations (2-5.14) and (2-5.15) using the finite element technique. The governing finite element transient equation employed for this purpose is Equation (B-1.7). A fixed point iteration scheme can be employed for solving the two heat and mass transport finite element equations. Such a scheme is completely described in Appendix B Section B.14.1. More details on the finite element formulation of the Evaporation-Condensation theory are given in Appendix B Section B.4. The boundary conditions for the detailed equations [Eqs. (2-5.16) through (2-5.19)] contain the $\rho_{V,r}$ term which is calculated using Equation (2-5.21). The solution of the detailed equations results in the temperature T_w and $\rho_{V,w}$ at the wall surface exposed to the room. Details on the solution procedure of heat and mass transport finite element equations interfaced to lumped equations for a room are given in Appendix F Section F.2.2. $\rho_{V,w}$ can be converted to W_w using the following relation:

$$W_w = \frac{\rho_{V,w}}{\rho_a} \quad (2-5.22)$$

The next step is to solve the lumped heat and mass transport equations for the room [Eqs. (2-5.9) and (2-5.10)] using the newly obtained W_w , T_w and the initial approximations for T_f and W_f . A closed form solution is available for the ordinary differential lumped equations which is given in Appendix E Section E.5.1. The solution of the room heat and mass transport equations would result in new values for T_r and W_r .

Finally, we solve the lumped heat and mass furniture equations [Eqs. (2-5.9) and (2-5.10)] using the newly obtained W_r , T_r and initial approximation for W_f . Once again the reader should refer to Section E.5.1 for closed form solutions for the lumped equations. The solution of the furniture heat and mass transport equations would result in new values for T_f and U . Next using the newly obtained values of T_f and U in Equations (2.5-12) and (2.5-13), a new value of W_f is obtained. It should be pointed out that the lumped equations for the room and the furniture can also be solved together using either a matrix inversion scheme or a Newton Raphson scheme (see Appendix E Section E.2).

This completes one iteration at the end of which we have new values for all the six unknowns. A convergence check is made at this point and if the results are within a tolerance limit, the iteration is stopped, otherwise the next iteration is started using the newly obtained values of the unknowns as the initial approximate. Many a times convergence is enhanced by using a relaxation technique before the next iteration is started. Details on relaxation techniques can be obtained from Appendix B Section B.14.1.

2.6 NUMERICAL SOLUTION TECHNIQUES

Once the governing equations and appropriate boundary conditions are specified for a problem, several techniques available for solution. Each has advantages and disadvantages over the other. The choice of the solution technique to be used involves several considerations, including but not limited to, accuracy, adaptability to a wide range of boundary conditions, computer storage and speed.

Two possible numerical approaches that may be taken for even a moderately complex problem are: 1) Finite difference method and 2) Finite element method.

In the simplest terms, the numerical methods are discretizations of analytical methods. Discretization of the problem significantly reduces the need for simplifying assumptions. Finite difference method is a process of local discretization of the differential formulation. Global formulation leads to finite element discretizations. Both methods lead to the solution of a system of linear algebraic equations. However, Finite element solutions are generally more accurate, are very well suited for problems with irregular geometry, and the formulations leading to it are mathematically sound.

Finite elements solutions, initially used in structural analysis, have gained significant attention in the areas of fluid flow and heat and mass transfer. The finite element method addresses the complexities of non-smooth solutions, geometric complications, non-separable boundary conditions and non-linearity, that normally plague other solution techniques, by what is known as a weak statement or variational statement. This statement is less restrictive on both the smoothness of the solution and the classes of functions from which solutions are sought. Any arbitrary weighting function may be used in the weak statement.

The Finite element method also easily lends itself well to the use of variable material properties, variable time steps in transient simulations, adaptive mesh strategies for error reduction, moving front problems and the modeling of inter-element thermal radiation to name only a few. For these reasons we have chosen the finite element method as our primary numerical simulation tool.

2.7 NATURE OF THE GOVERNING EQUATIONS

The governing equations used herein are non-homogenous and highly non-linear. The non-homogeneity arises from the fact that the equations are coupled to solve for the simultaneous diffusion of heat and moisture in capillary porous bodies. The non-linearity in the equations stems from the physical phenomena.

- o Transport properties vary rapidly with respect to the dependant variables, especially with respect to the moisture properties.
- o Boundary and inter-element radiation highly non-linear.
- o The advective terms in the transport equations are non linear.

The difficulty in the analysis of non-linear problems arises from the fact that no general theory is yet available for the solution of non-linear partial differential equations (PDEs). Each problem is treated individually and the solution is often ad hoc and approximate.

The combined heat and mass transfer equations [e.g. Eq. (A-3.1) and (A-3.2)] contain two time dependant terms, which further complicate the problem in finite element solution. The complete system consists of two PDEs and one algebraic equilibrium relation. Such a system may be treated in two different ways:

1. The equilibrium equation is substituted in the two governing PDEs, in place of one of the time dependent terms, using the product rule. This strategy is successful for the Luikov's theory but creates major stability problems for the evaporation-condensation theory.
2. The extra time dependant term is treated as an extra force term, F_2 , in the governing finite element Equations (B-14.1) and (B-14.2), thus making the moisture content a third nodal unknown defined only in the porous body domain. This strategy was successfully implemented in the evaporation-condensation theory. Instability was still problematic but was avoided through the use of small relaxation parameters in the fixed point iteration scheme (Appendix B Section B.14.1). The cause of this instability is attributable to the term responsible for phase change in the energy equation (See Eq. A-3.2 in Appendix A) The presence of this term leads to swings in the field variables beyond the regime of the psychrometric relations resulting in unacceptable oscillation and poor convergence of the solution.

Another major difficulty encountered was the scarcity of experimental data for different building materials. Even for the available data there exists the problem of finding an appropriate functional correlation for the equilibrium isotherm which would be valid for a wide range of materials and would cover a large temperature variation. After extensive investigation the appropriate functional correlations the one most valid for building materials was found to be Equation (G-9). It must be pointed out that although the moist soil model (See Appendix A, Section A.7) and the irreversible thermodynamics model (See Appendix A, Section A.8) are more advanced models for predicting the temperature and moisture in a porous body, these models are not practical because they require the use of many material properties which are not available. In this respect the evaporation condensation theory is the most practical because it requires only the porosity, tortuosity and the equilibrium relation of the porous body. Table C-1 lists the various material properties required for various heat and mass transfer theories.

2.8 SOLUTION TYPES

The solution phase of a transient heat and mass transfer FEM simulation is the most time consuming stage of the analysis. Medium to large problems could account for 80% of the total computer resources used. The highly coupled and non-linear nature of the equations calls for iterative solution, therefore the decision as to which solution algorithm to apply is a very crucial one.

The chosen algorithm should be convergent for a wide range of problems with minimal sensitivity to variations in initial conditions, flow parameters and geometry. The rate of convergence should also be reasonably high. Since no single iterative procedure satisfies all these conditions, a number of different solution procedures are used.

- o Successive substitution

- o Newton type methods
- o Newton-Raphson
- o Modified Newton
- o Quasi Newton

The method of successive substitution with relaxation is very simple to implement and is relatively insensitive to the initial iterate. But the convergence rate for this scheme is linear and therefore, very slow.

The Newton-Raphson method has a quadratic convergence rate and is self corrective in nature. However, this method is highly sensitive to the initial iterative and may fail to converge if the initial iterate does not lie within the radius of convergence. Also, this method needs the evaluation of one additional Jacobian matrix per iteration, resulting in $O(n^3)$ arithmetic operations per iteration, where n is the number of equations solved.

The modified Newton method requires the evaluation of the Jacobian only once. This reduces the number of arithmetic operations per iteration but at the price of a linear rather than a second order linear convergence rate.

The Quasi Newton methods strike a compromise between Newton-Raphson and modified Newton-Raphson methods by updating the Jacobian matrix at each iteration rather than leaving it unchanged (Modified Newton-Raphson) or recomputing it at each iteration Newton-Raphson.

Quasi Newton algorithm requires the storage and calculation of two vectors of dimension n and a scalar for each iteration (FIDAP, 1986). Each iteration would require $O(m \times n)$ operations where m is the mean bandwidth. This is substantial savings compared with $O(m^2 n)$ operations required for Newton-Raphson (Matthies and Strang, 1977). Once again, the price paid is reduction in convergence rate from quadratic to linear convergence (Dennis and More, 1965).

Sometimes a combination of two methods may yield better results as pointed out by Engleman (1981). Result of one iteration by successive substitution are used as the initial iterate for the Quasi Newton methods in a closed cavity. The reduction in execution time was almost 30% compared with results of Quasi Newton method alone.

It must be pointed out that although successive substitution has a slower convergence rate, it is more popular because of its smaller storage requirements. Since it solves one governing equation at a time, the savings in storage is tremendous compared to Newton type methods.

The finite element solution method is sensitive to the geometry of the problem and the mesh considered. A very coarse and 'unhealthy' mesh can lead to erroneous results. On the other hand a 'healthy' mesh can not only give better results but it can also result in convergence for limiting cases (e.g. duct flows for high Reynold's numbers). Unfortunately there presently exists no fixed or definite criterion for defining a 'healthy' mesh -- one has to rely on experience and judgement.

Mesh refinement in duct problems (starting with a finer mesh at the entrance region and having a coarser mesh at the exit) results in a quicker and more stable convergence. This is specially true for large length to width ratios for which 'wiggles' in the results are experienced for a normal (not refined) mesh. However, for certain fluid flow simulations using the vorticity-stream function concept, too fine a mesh at the boundaries can lead to instabilities in the vorticity boundary condition application. This is due to the fact that wall vorticities are calculated based on distance between the wall and adjacent fluid nodes (See Appendix J Section J.4). Thus very small distance leads to extremely large wall vorticity values that cause instability in the solution.

2.9 CAPABILITIES OF FEMALP 2.1

This section contains a listing of the present capabilities of FEMALP 2.1. It is important to point out that the the program is still under development and is not yet available to the general public. Under certain conditions the authors can release the program to researchers who have a defined need and are willing to serve as alpha level evaluators of the code.

A number of additional capabilities are anticipated for the program. Many of them address input and output friendliness and automated error checking and problem definition. These capabilities are simply premature at present. As a result the program requires extreme care and knowledge on the part of the user to assure that input requirements of the program are fully satisfied.

1. One-, two- and/or three-dimensional mixed simulation capabilities with
 - o One-dimensional linear line element
 - o Two-dimensional linear rectangular element
 - o Three-dimensional linear brick element
 - o One-, two- and/or three-dimensional higher order elements
 - o Distorted and/or undistorted element simulation
2. Steady-state and/or transient simulation modes with
 - o Variable simulation time step
 - o Variable time integration constant
 - o Lumped or consistent capacitance matrices
3. Simultaneous partial and/or ordinary differential equation solutions for
 - o Vorticity and stream function equations
 - o Energy equation
 - o X-momentum, Y-momentum and pressure equations
 - o Darcy flow equations (for flow in porous media)
 - o Turbulent kinetic energy and dissipation rate equations
 - o Algebraic turbulence models
 - o Combined heat and mass transfer equations for the following theories
 - Liquid diffusion theory
 - Luikov's theory
 - Berger and Pei's theory
 - Philip and De Vries theory
 - Evaporation-Condensation theory
 - Irreversible thermodynamics theory

- o Contaminant diffusion equation (in air only)
 - o User defined equation(s)
4. Thermal radiation modeling with
- o View factor calculations for irregular domains with shadow checking,
 - o Script-F calculations,
 - o Solid to solid and/or solid to gas radiation.
5. Material libraries with
- o Thermal properties
 - o Fluid flow properties
 - o Moisture properties (preliminary, see Appendix D)
6. Building zone simulation with
- o Lumped, and/or distributed modeling
 - o Multizone simulation
 - o Heat and mass generation
 - o Infiltration and ventilation with mixing efficiency factors
 - o Internal mass and furniture
 - o People and equipment
 - o User defined sinks or sources
 - o Mechanical system analysis (performance criteria supplied by user)
 - o Inter-zone airflow
 - o Sensible and latent load calculations
 - o Coupled envelope, system, plant and control interactions (criteria supplied by user)
 - o Ground heat and moisture simulations
7. Automatic and semi automatic mesh and boundary condition generation with band width minimization
8. Additional program features:
- o Variable Material properties
 - o Variable and/or controlled boundary conditions
 - o Advection problems
 - o Psychrometric algorithms
 - o User supplied data files for boundary condition input (weather, experimental, etc.)
 - o Multiple iteration schemes for non-linear equation solutions,
 - o Phase change materials
 - o Model size limited only by computer memory
 - o Interactive simulation control during execution with stop and restart capabilities.

CHAPTER 3

EXAMPLE SIMULATIONS

This chapter gives specific examples that demonstrate some of the capabilities of FEMALP 2.1. Heat and mass transfer simulations of composite walls using both Luikov's and evaporation condensation theories are presented. An attic model using evaporation condensation theory is presented and the results are compared to experimentally measured data. This simulation illustrates multiple zones with inter-zone airflow. Heat and mass transfer at the corner of a ground-foundation-wall intersection for cold storage building is also presented. Results from this analysis using Luikov's theory compare well with data from an identical problem found in the literature. The results of a heat, mass and momentum transfer simulation in a vented storage wall having forced air flow are also presented.

The simulations presented here are primarily for the purpose of demonstrating the capabilities of FEMALP 2.1. The examples used are sometimes hypothetical and the property data for some of the materials may not be entirely accurate due to differences in material nomenclature across data sets. Nevertheless, the capabilities demonstrated by the analyses represent a serious advancement in the state-of-the-art of building simulation capability.

3.1 HEAT AND MOISTURE TRANSFER IN COMPOSITE WALLS

The purpose of this example is to illustrate the application of Luikov's theory to study composite walls. The governing heat and mass transfer equations for Luikov's theory are given in Appendix A (Section A.4).

Two composite walls are considered; one without a vapor retarder and the other with a vapor retarder installed near the interior surface. Figures 3-1.(a) and 3-1.(b) illustrate the two walls. The finite element discretizations for these walls are shown in Figures 3-2.(a) and 3-2.(b). Material properties used in the simulation are given in Table 3-1. The physical definition and origin of these properties are given in Appendix A. Note that the thickness used for the vapor retarder is unusually large. This is one of ways to ensure an even mesh and consequently the stability of the finite element simulation. Both thermal and moisture conductivities were adjusted to counteract the effect of the use of the large thickness (See also Table 3-1.). Other methods to overcome the loss of stability when unusually small thickness are specified are currently being investigated, including but not limited to the use of double precision in the computer code. Both the thermal and moisture conductivities were adjusted to counteract the effect of the use of the large thickness. The walls are exposed to convective boundary conditions on both sides - one to the exterior ambient and the other to the interior room. For this simulation the room conditions are kept constant and the ambient conditions are varied periodically over a 24-hour cycle. The ambient temperature and mass transfer potential distribution over a two day period are shown in Figures 3-3.(a) and 3-3.(b), respectively. The boundary and initial conditions used in the simulations are tabulated in Table 3-2. Both walls were simulated for 10 days (240 h) in order to achieve periodic steady state.

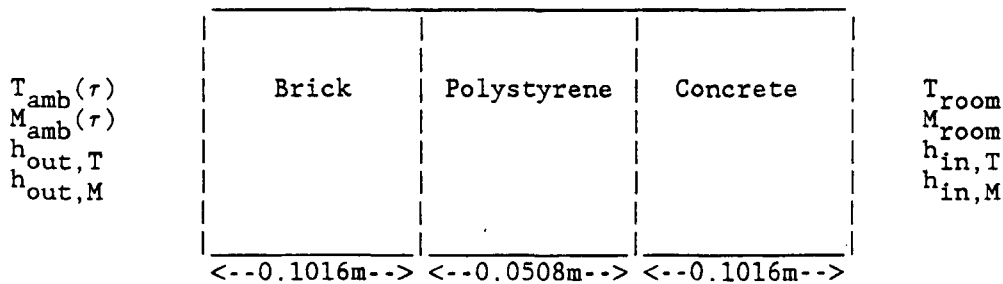


Figure 3-1.(a) Composite Wall without vapor retarder (Wall #1).

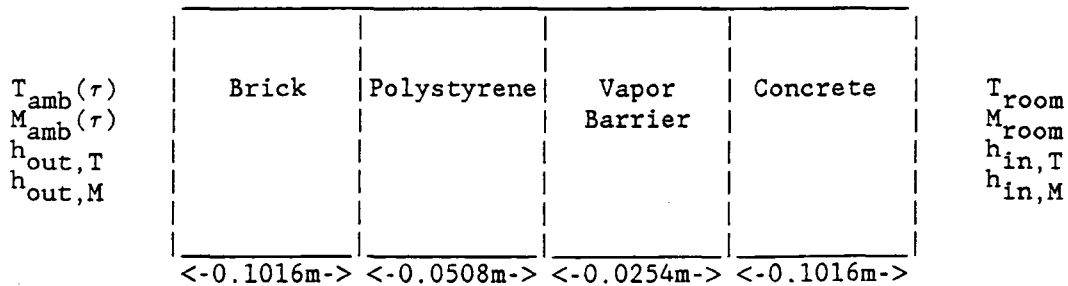


Figure 3-1.(b) Composite Wall with vapor retarder (Wall #2).

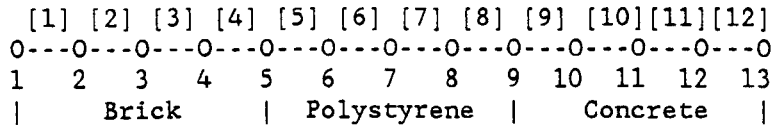


Figure 3-2.(a) Finite Element Discretization of composite wall number 1.

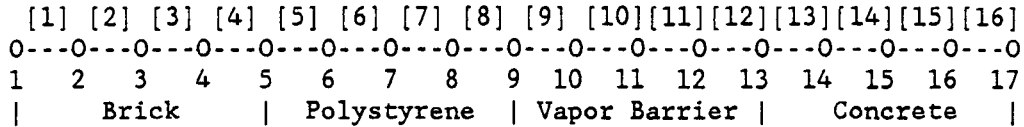


Figure 3-2.(b) Finite Element Discretization of composite wall number 2.

TABLE 3-1
 Material Properties Used in Luikov's Model

Material	k_T W/mK	ρ kg/m ³	C_p Wh/kgK	k_M kg/mh ^o M $\times 10^{-4}$	C_M kg/kg ^o M $\times 10^{-4}$	δ ^o M/K	γ	λ Wh/K
Brick	0.440	1200	0.244	2.174	18.0	0.56	0.3	694.4
Polystyrene	0.043	32	0.232	3.960	3.0	0.50	0.6	694.4
Concrete	1.750	2000	0.257	2.880	1.3	0.50	0.3	694.4
Vapor Barrier	100.0	1600	0.232	0.010	0.1	0.50	1.0	694.4

TABLE 3-2
 Boundary and Initial Conditions

$T_{initial}$	300.0 K
$M_{initial}$	50.0 ^o M
T_{room}	300.0 K
M_{room}	30.9 ^o M
$h_{in,T}$	3.0 W/m ² .K
$h_{in,M}$	0.0041 kg/m ² .h. ^o M
$h_{out,T}$	15.0 W/m ² K
$h_{out,M}$	0.0135 kg/m ² .h. ^o M

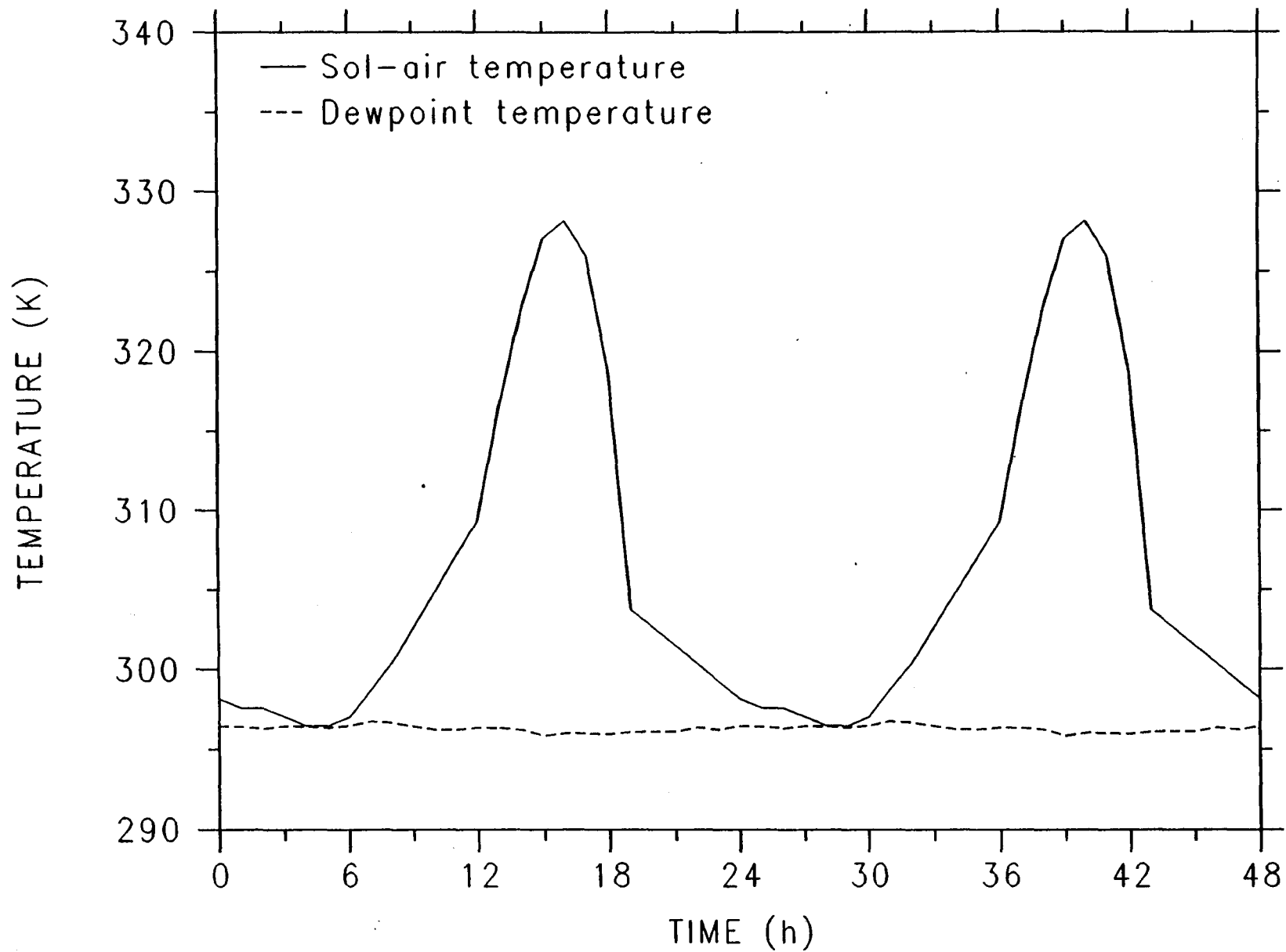


Figure 3-3a. Ambient temperatures used as external boundary conditions for periodic analysis runs.

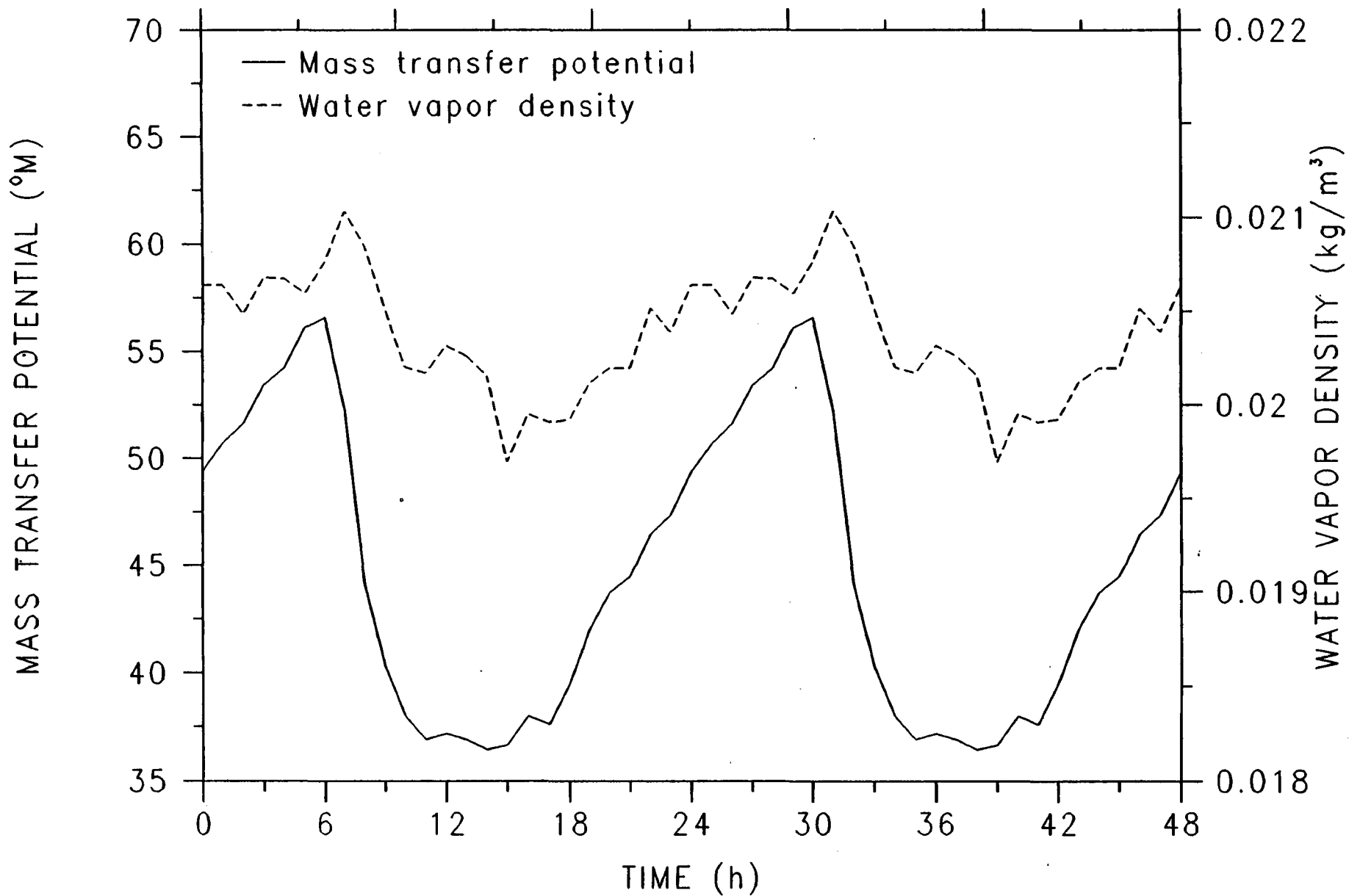


Figure 3-3b. Ambient mass transfer potential and water vapor density used as external boundary conditions for periodic analysis runs.

Figures 3-4.(a) thru 3-4.(e) show results from the simulations. Figure 3-4.(a) shows the exterior and interior surface temperatures with and without moisture effects for the wall without a vapor retarder. Note that the interior surface temperatures are always higher when moisture transport is ignored. This may have serious ramifications in the calculation of the heat flux through the wall and will ultimately lead to erroneous cooling load predictions. The amplitude of the temperature cycle is also larger when moisture effects are excluded. This is indicative of the fact that sorbed moisture stores thermal energy through a phase change resulting in a temperature effect that resembles a thermal capacitance effect.

The next example illustrates the use of the model to examine the effect of a vapor retarder on wall fluxes. Figure 3-4.(b) shows the fluxes for the wall without vapor retarder. Due to lower surface temperatures when moisture effects are modelled, the associated thermal flux is also lower. However, the moisture flux into the zone is substantially higher than the thermal flux. Figure 3-4.(c) shows similar results for the wall with a vapor retarder. The thermal fluxes with and without moisture effects are much closer to each other in this case because the vapor retarder significantly reduces the moisture transfer to the interior materials. The total energy flux for the case without vapor retarder is three times greater than for the case with the vapor retarder.

Figure 3-4.(d) shows predicted moisture contents close to the interior surface of the walls. For the wall with a vapor retarder, the moisture content at the interior surface as well as at the mid section of the concrete show little change with time. However, when the vapor retarder is absent, large cycling effects and significantly higher moisture contents are observed both at the surface and the mid section of the concrete. The presence or absence of a vapor retarder does not seem to have a significant effect on the moisture content at the exterior surface [Figure 3-4.(e)]. However, at the mid-brick section of the exterior, the moisture content for the case with a vapor retarder is much higher. This is due to the fact that moisture is unable to cross the vapor retarder to the interior surface resulting in a moisture buildup in the external portion of the wall.

Two important inferences may be drawn from the results. 1) Moisture transport in building materials is important and, if ignored, will lead to erroneous predictions. 2) The use of a vapor retarder can reduce the total energy flux into a zone.

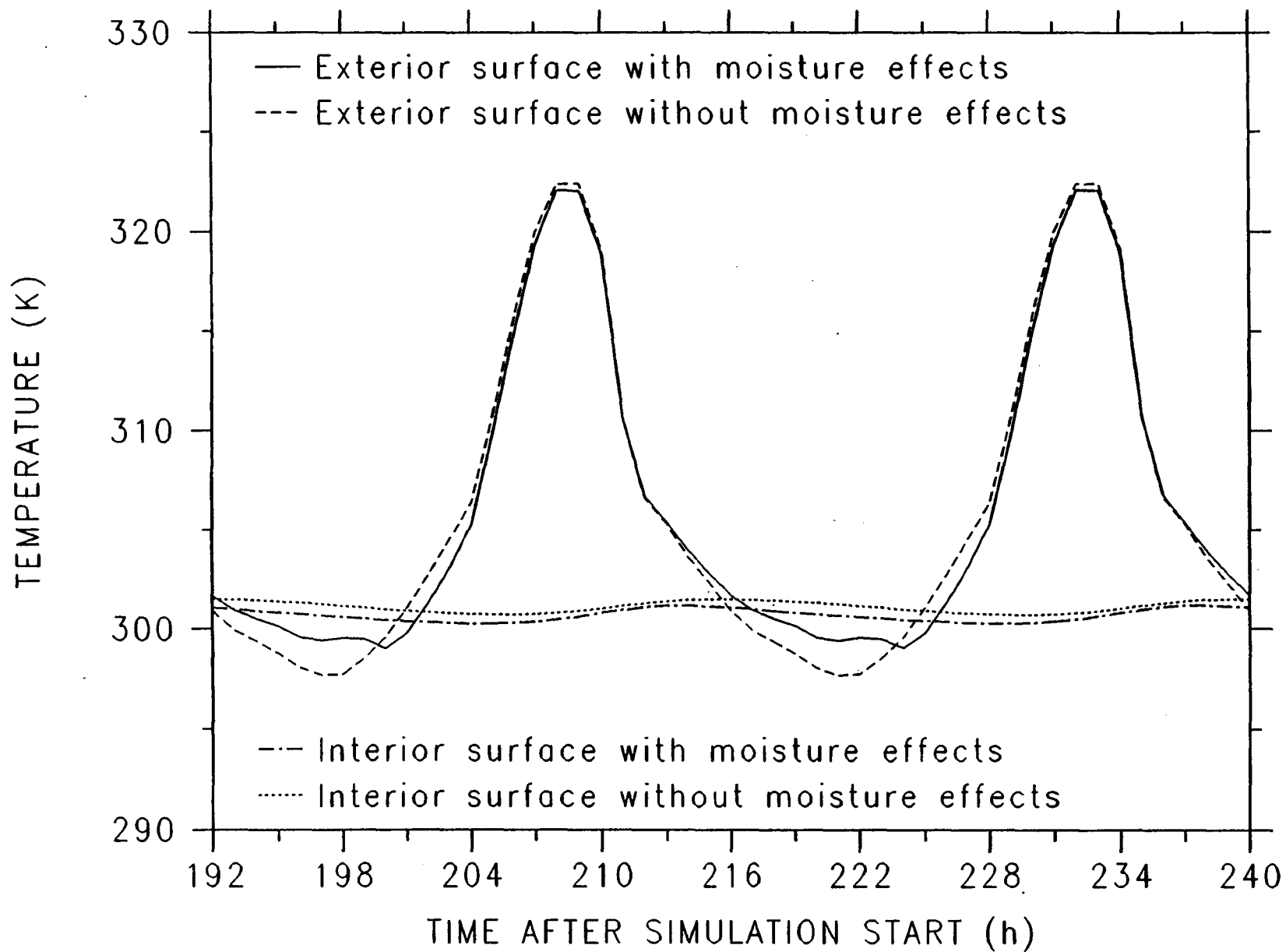


Figure 3-4a. Effects of combined heat and moisture transport on the surface temperatures of composit wall #1.

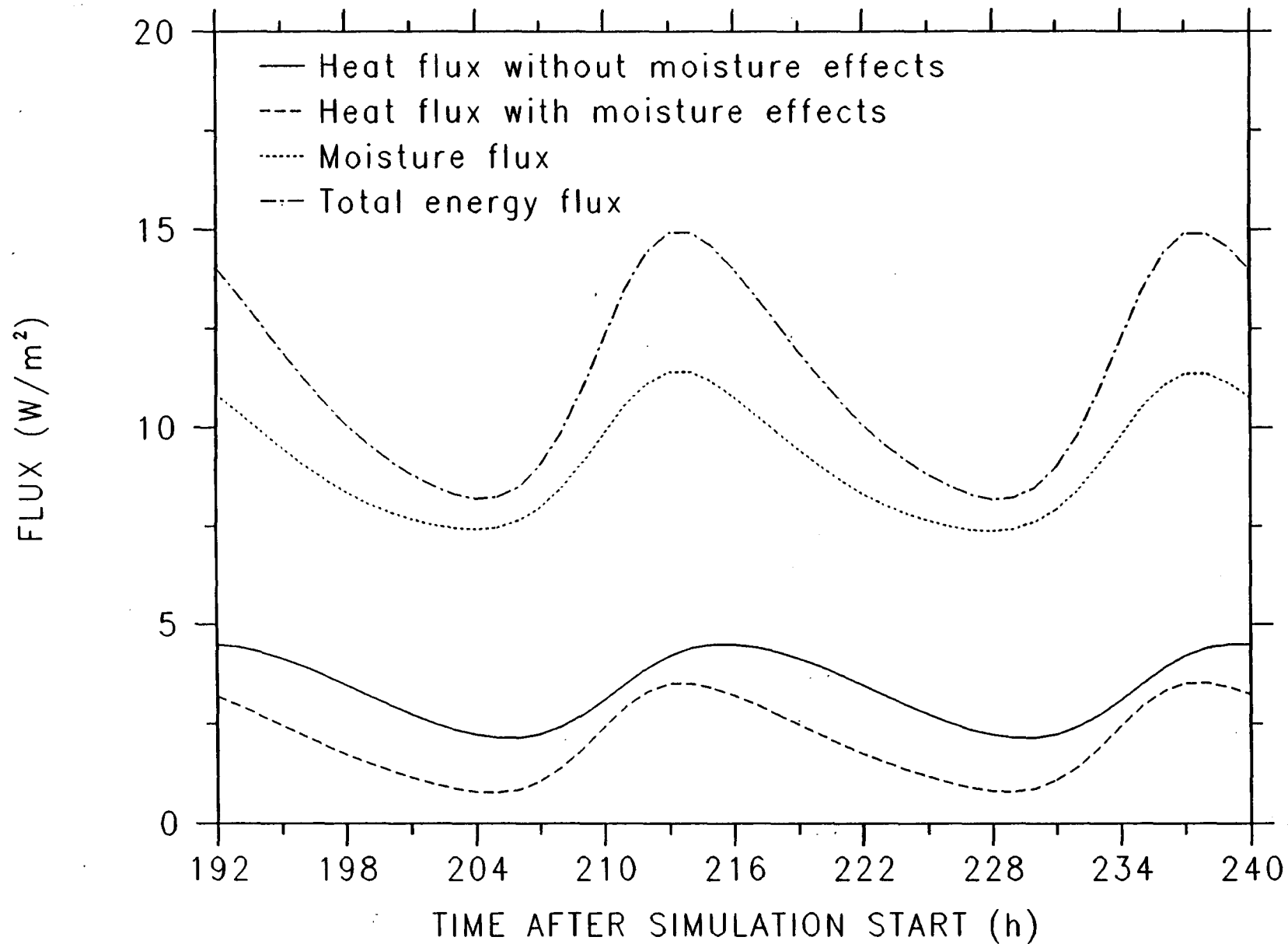


Figure 3-4b. Effects of combined heat and moisture transport on the interior surface fluxes of wall #1 (no vapor retarder).

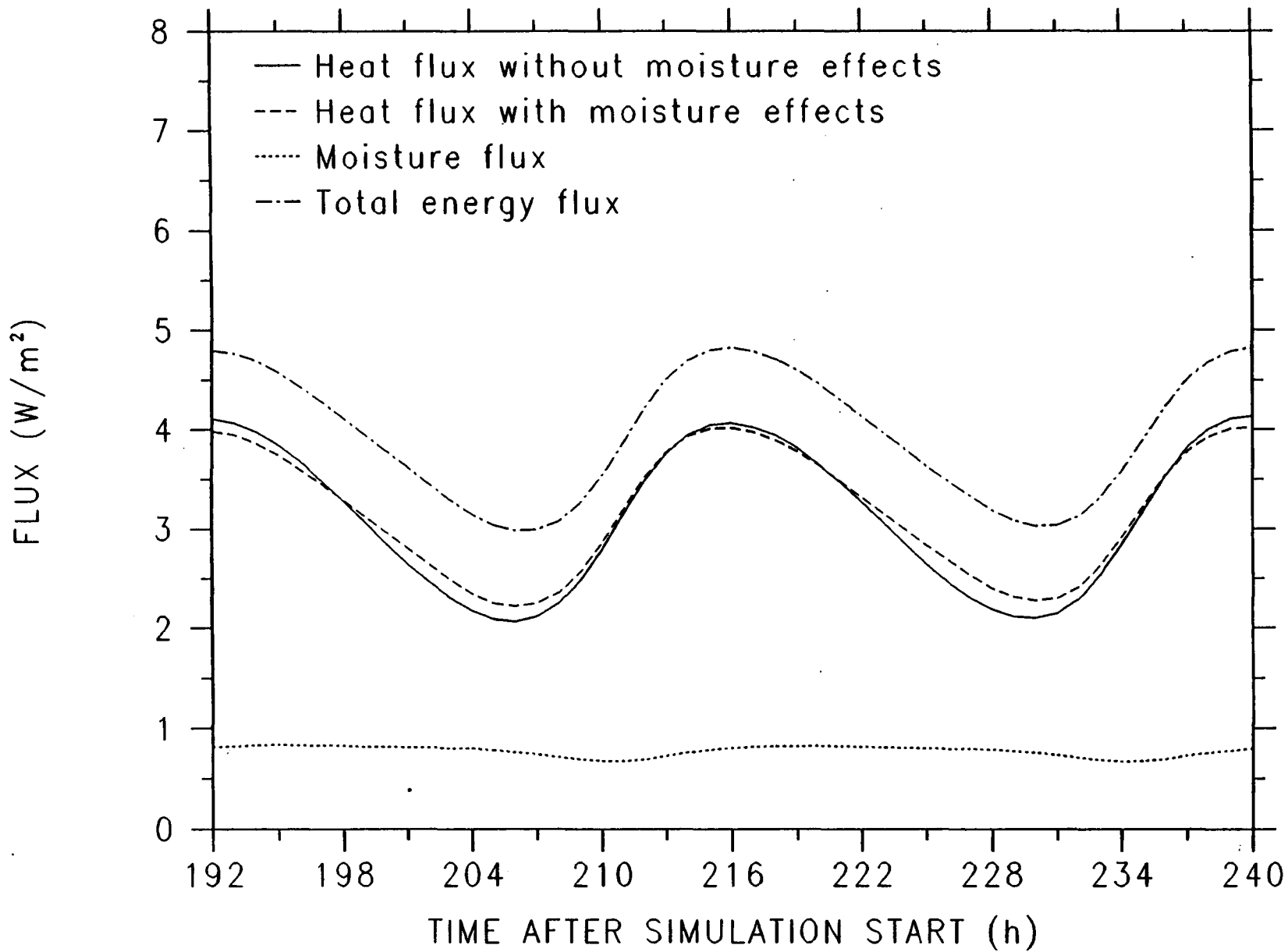


Figure 3-4c. Effects of combined heat and moisture transport on the interior surface fluxes of wall #2 (with vapor retarder).

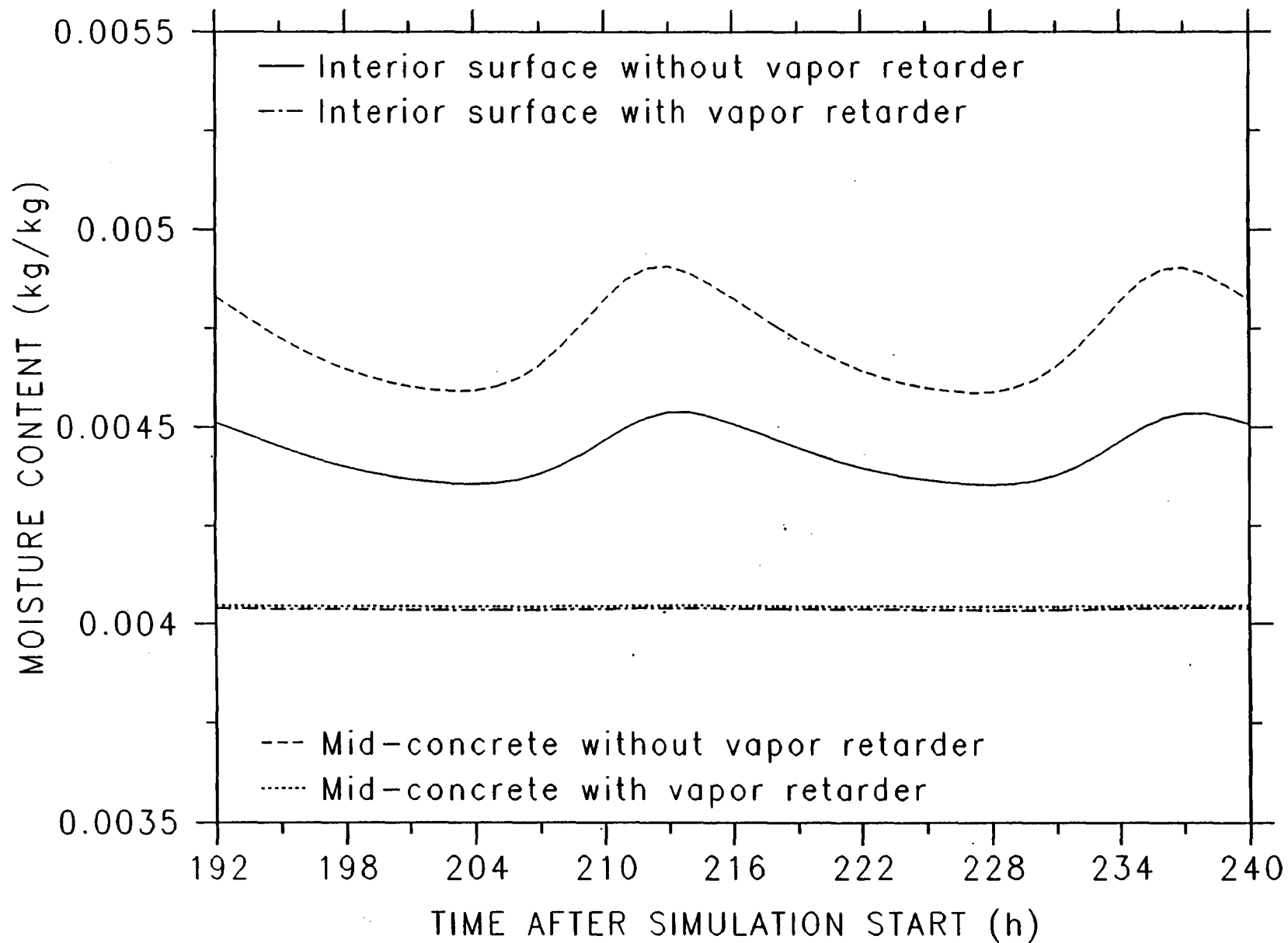


Figure 3-4d. Effect of a vapor retarder on the moisture content near the interior surface of the wall

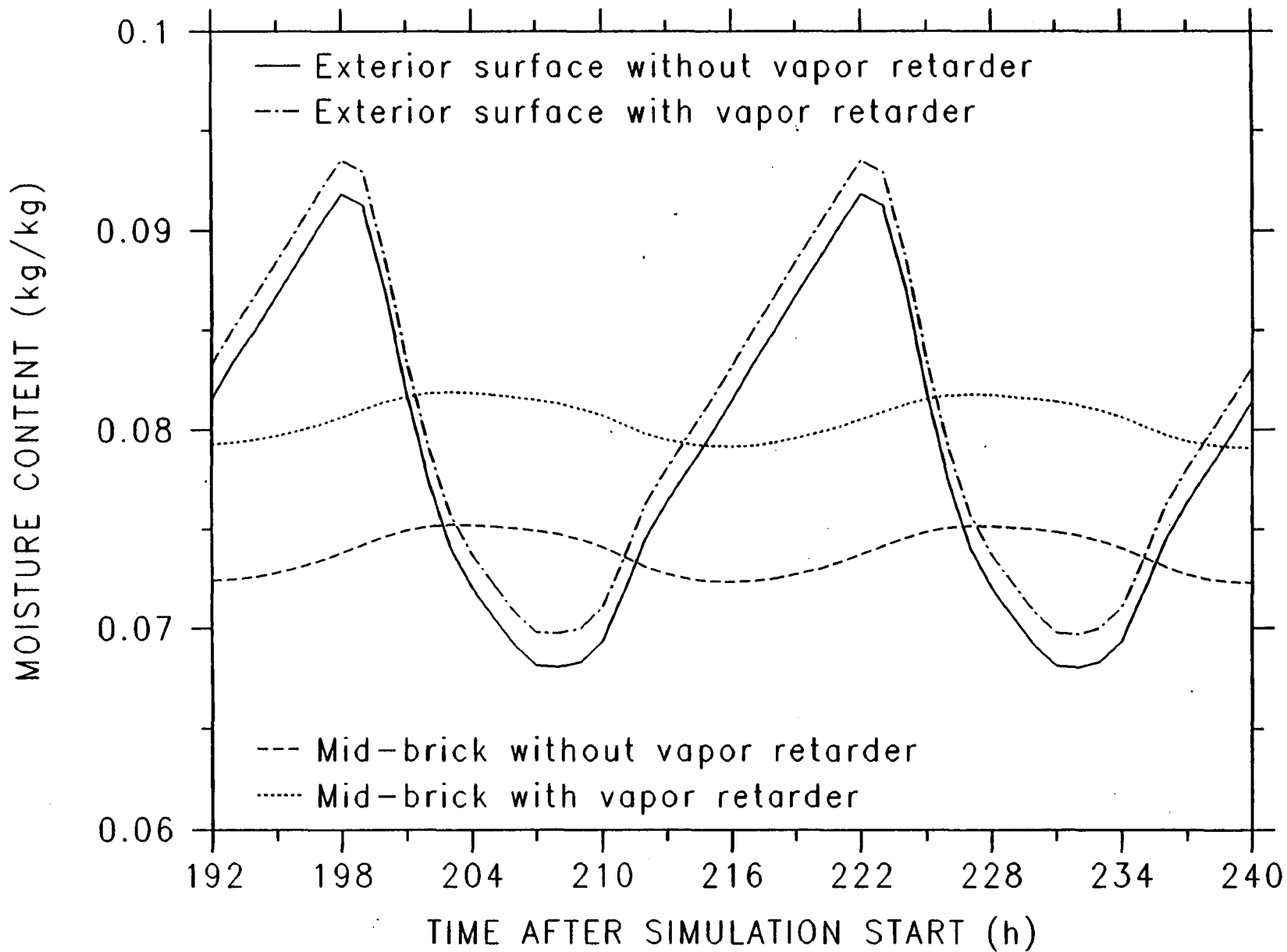


Figure 3-4e. Effect of a vapor retarder on the moisture content near the exterior surface of the wall

3.2 WALL HEAT AND MASS TRANSFER COUPLED BUILDING ZONE

In the previous example, the exterior surface of the wall was subjected to periodic convection and the interior surface was subjected to constant convection. The objective here is to demonstrate heat and mass transfer analysis capability when a wall is coupled to a zone. The conditions in the zone may either be floating or controlled. When a zone is coupled to a wall, the interface between the wall and zone poses additional complication because of the additional iterative loop involving heat and moisture balance for the zone. The mathematics as well as implementation strategies of heat and mass transfer for wall-zone coupled systems are discussed in detail in Appendix E. The heat and mass transfer phenomena occurring at the wall-zone interface is discussed in Appendix F. For the purpose of demonstration, a single composite wall coupled to a single zone is used. Extending this to multiple walls as well as multiple zones is fairly routine (See next example in Section 3.3). Although, the coupled heat and mass transfer equations for the Evaporation-Condensation theory (in Appendix A Section A.3) are employed for this analysis. Provided the appropriate material properties are known, a model based on any of the other heat and mass transport theories listed in Appendix A may be used.

Figure 3-5 shows the material names and associated thicknesses used in this analysis and Table 3-3 gives the associated thermal properties. Moisture properties were taken from Appendix D. Figure 3-6 shows the finite element discretization for this composite wall.

Ext	<-0.0920->	<-0.0127->	<-0.0159->	<-0.0889->	<-0.0102->	<-0.0127->	Int
	Face Brick	Air	Felt	Insulation	Vapor Barrier	Plaster	

Figure 3-5. Wall construct used in the evaporation condensation model.

TABLE 3-3
Thermal Properties

Material	Density (kg/m ³)	Ther. Cond. (W/m.K)	Specific Heat (W.h/Kg.K)
Air	1.2	0.0300	0.280
Face brick	2080.0	1.3000	0.256
Insulation fiber-glass	91.200	0.0430	0.232
Plaster finish	1600.0	0.727	0.232
Vapor Barrier	160.0	100.00	0.20
Felt	11.2	99.00	0.465

	0	...	0	...	0	...	0	...	0	...	0	...	0
Nodes ->	1		5		8		11		16		19		23
Material ->	Brick		Air		Felt		Insu		Vap Ret		Plast		

Figure 3-6. Finite element discretization.

On the exterior surface (node 1 in Figure 3-6) a time varying convective boundary condition for both moisture and temperature were applied. The sol-air temperature and the water vapor density, shown in Figures 3-3.(a) and 3-3.(b), respectively, were used as ambient boundary conditions. The sol-air temperature, rather than the actual ambient temperature and incident solar flux, is used here only for the sake of convenience and no simplification of the problem under study is implied. Use of actual ambient parameters, when available, such as actual ambient temperature, incident solar flux and sky temperature is fairly routine in the simulation. The zone temperature and humidity ratio were allowed to float.

Figure 3-7.(a) shows the zone temperature histories with and without moisture effects for the last 48-hour period of the simulation. The results show that the temperature cycle with and without moisture effects are different in amplitude as well phase. A much larger amplitude is observed when moisture effects are ignored. When moisture effects are included, the zone temperature cycle responds more slowly to the ambient pulse. The increase in phase lag is approximately two to three hours when moisture effects are included.

Figure 3-7.(b) shows the flux histories for the two runs described above. Due to smaller wall-zone temperature differentials, the magnitude of the thermal flux when moisture is modelled are lower. Note that the moisture flux is of the same order of magnitude as the thermal flux. It is therefore clear that the ignoring moisture effects over predicts zone temperatures.

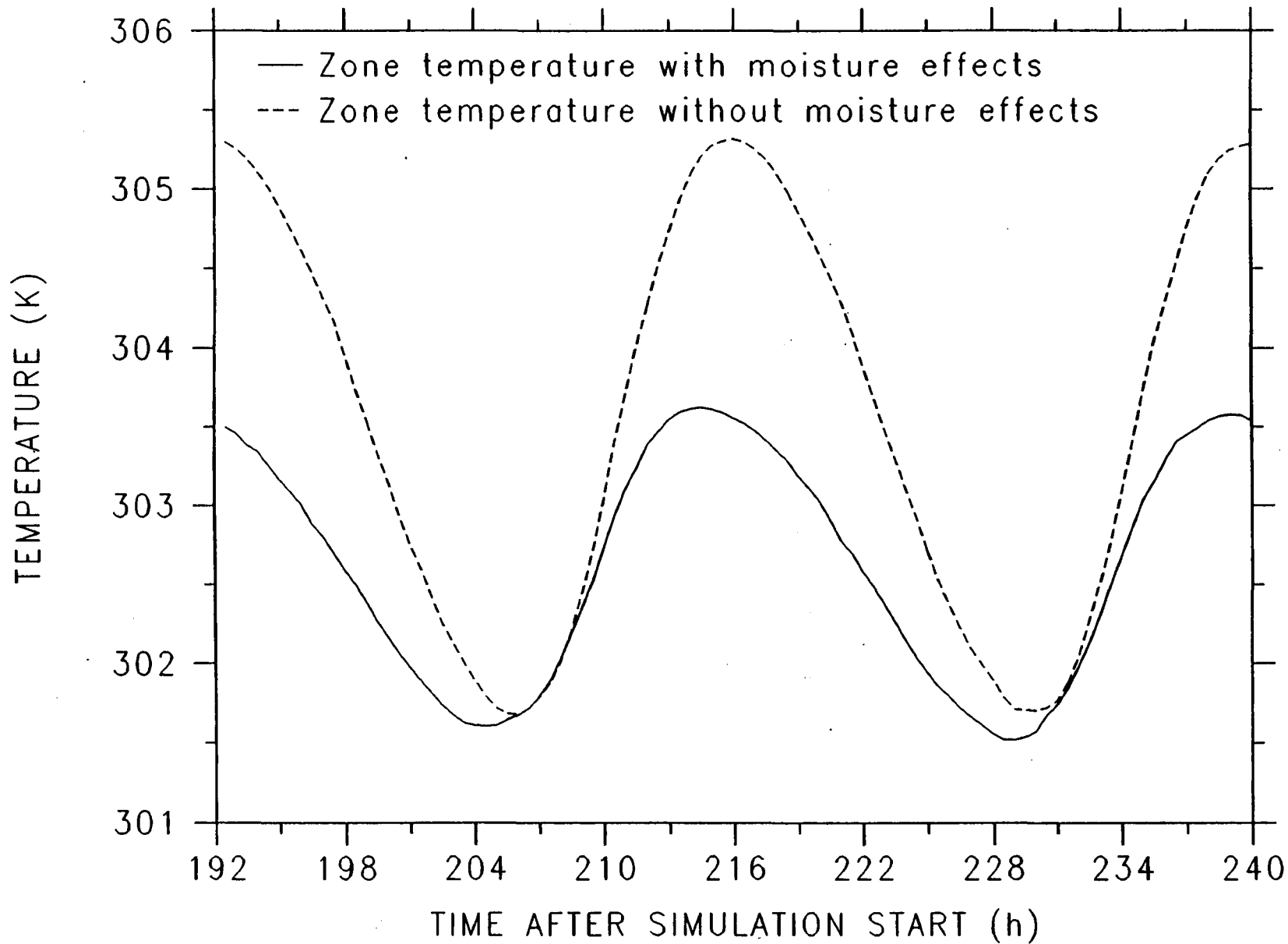


Figure 3-7a. Zone temperature histories with and without moisture effects and no internal gains for both simulations.

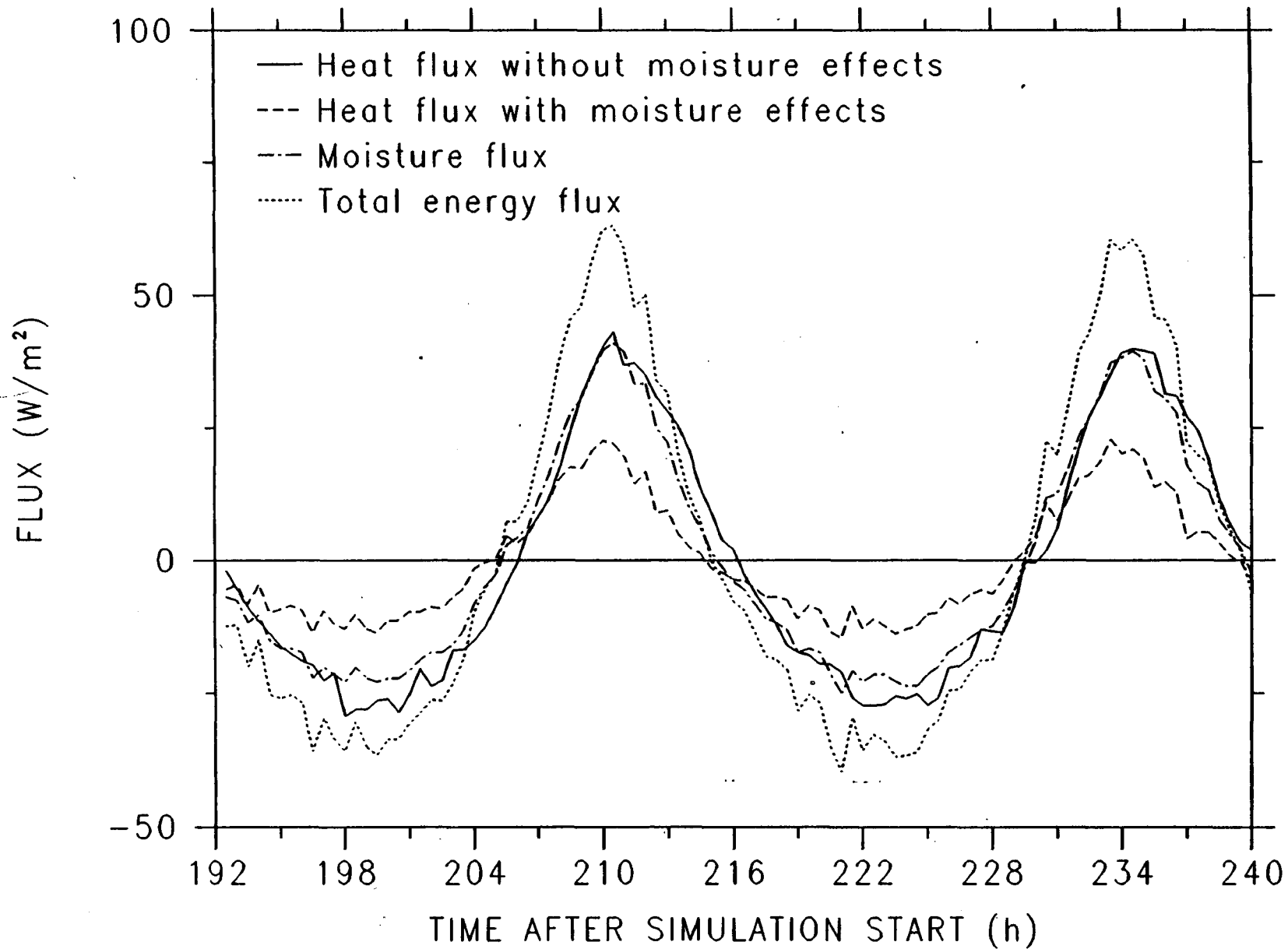


Figure 3-7b. Effects of combined heat and moisture transport on wall interior surface fluxes without internal gains.

3.3 HEAT AND MASS TRANSFER IN A REAL ATTIC

Heat and mass transfer occurring in the attic of the Florida Solar Energy Center's (FSEC) Passive Cooling Laboratory (PCL) was simulated and the results are compared to the measured data. The attic was instrumented in detail for temperature, heat flux and air moisture. A complete set of results using only heat transfer simulations are given in Appendix I.

Figure 3-8 shows the layout of cell 2 of the PCL attic. For the purposes of simulation, the attic air space is divided into seven lumped zones with ventilation air entering the first zone at C'-I' and leaving the seventh zone at C-I. The seven zones are coupled by interzone air flow. All air entering the attic moves progressively until it exits the attic. The dashed lines in Figure 3-8 indicate the zone partitions. The multi zone model, allows the temperature to vary from one zone to another. A seven zone model was chosen because it matched instrumentation divisions used in the actual attic.

Moisture transport was modelled using the evaporation-condensation theory discussed in detailed in Appendix A. One-dimensional linear elements were used to model the solid domains and a lumped model was used for zone air. The materials and boundary conditions used in the problem are given in Tables 3-4 and 3-5, respectively. Thermal properties for the attic components were taken from ASHRAE 1985. Moisture properties for the attic components were taken from the moisture properties compiled in Appendix D. The heat and mass transfer in the attic was simulated for a single 24-hour day.

Figures 3-9.(a) and 3-9.(b) show plots of predicted and measured insulation surface temperature histories simulated without and with the effects of moisture transport. The predicted temperatures when moisture is ignored are in general higher than measured values during attic heating periods and lower during cooling periods [Figure 3-9.(a)]. When moisture effects are included, the predicted temperatures are much closer during both periods [Figure 3-9.(b)].

Figure 3-9.(c) gives prediction errors (with and without moisture effects) and the measured attic vent air mass flux. Note in the figure that the prediction error for the case where moisture effects are ignored is qualitatively the same as the measured vent air mass flux. The maximum error in this case is about 3 K. However, when moisture effects are included the prediction errors are much lower with the maximum error of about 0.5 K.

Figure 3-9.(d) compares predicted and measured humidity ratios at the outlet of the attic. While an exact match was not obtained, it is clear that, the inclusion of moisture effects, has substantially reduced discrepancies between predictions and measured data. Uncertainties in moisture material property data and flow pattern in the attic air space are believed to be responsible for the disparities still existing between measurement and prediction.

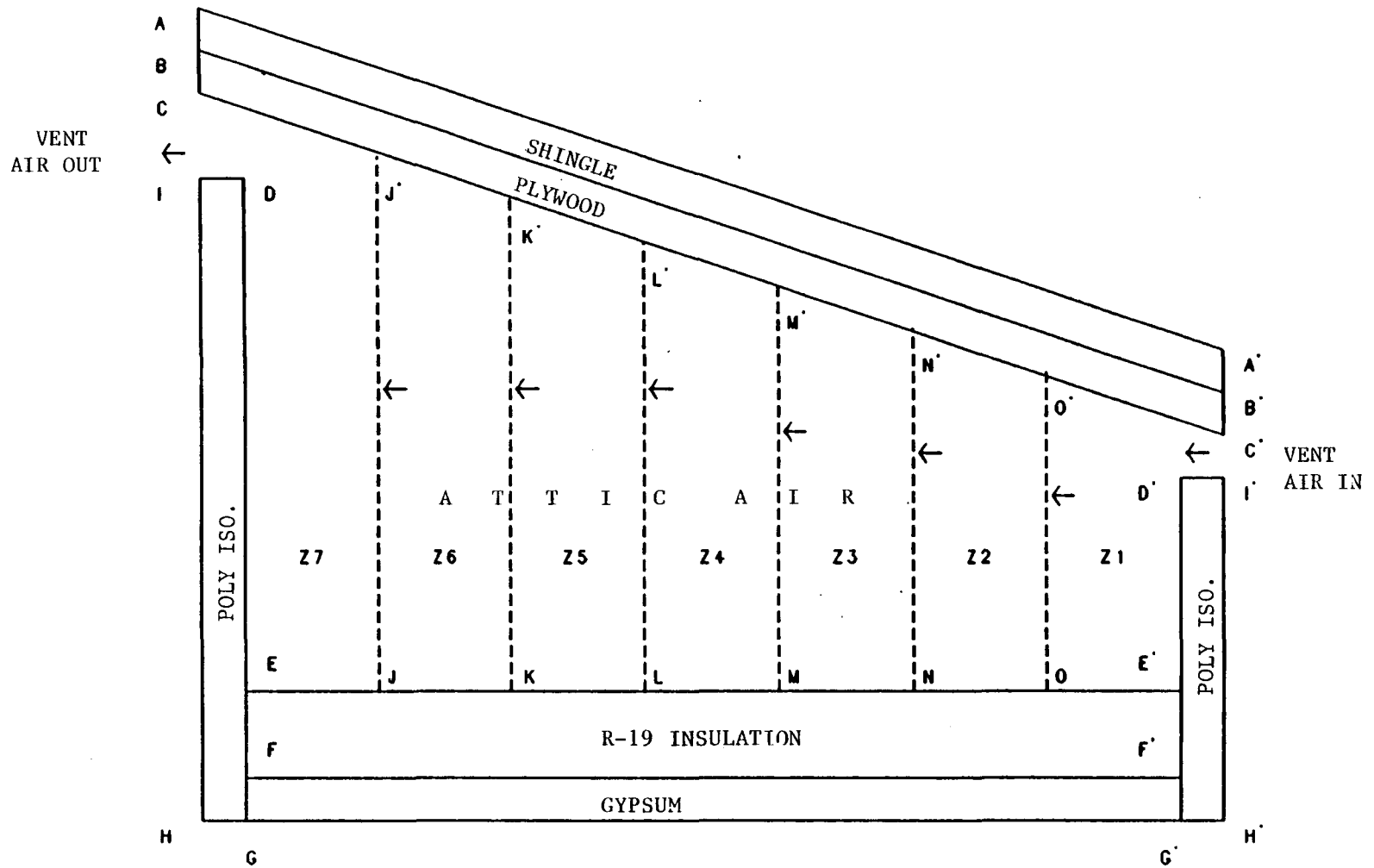


Figure 3-8. Layout of PCL attic cell 2.

TABLE 3-4
Material Description and Property Source for Combined Heat
and Moisture Transfer in an Attic

SURFACE	MATERIAL	COMPONENT	THERMAL PROPERTIES	EQUILIBRIUM DATA AND MOISTURE PROP
A-A'-B'-B	SHINGLE	ROOF	ASHRAE 1985	TABLES D-1 & D-2
B-B'-C'-C	PLYWOOD	ROOF	ASHRAE 1985	TABLES D-1 & D-2
E-E'-F'-F	INSULATION	CEILING	ASHRAE 1985	TABLES D-1 & D-2
F-F'-G'-G	GYPSUM	CEILING	ASHRAE 1985	TABLES D-1 & D-2
I-D-G-H	POLYISO	WEST WALL	ASHRAE 1985	TABLES D-1 & D-2
I'-D'-G'-H'	POLYISO	EAST WALL	ASHRAE 1985	TABLES D-1 & D-2
E-D-D'-E'	AIR	ZONE	ASHRAE 1985	TABLES D-1 & D-2

TABLE 3-5
Boundary Condition Description for Combined Heat and Moisture
Transfer in an Attic

BOUNDARY	HEAT TRANSFER			MOISTURE
	PRES. TEMP	CONVECTION TO	INTER-ELEMENT RADIATION	CONVECTION TO
A-A'	MEASURED INPUT			
B-B'				
C-J'		ZONE-7 AIR	YES	ZONE-7 AIR
J'-K'		ZONE-6 AIR	YES	ZONE-6 AIR
K'-L'		ZONE-5 AIR	YES	ZONE-5 AIR
L'-M'		ZONE-4 AIR	YES	ZONE-4 AIR
M'-N'		ZONE-3 AIR	YES	ZONE-3 AIR
N'-O'		ZONE-2 AIR	YES	ZONE-2 AIR
O'-C'		ZONE-1 AIR	YES	ZONE-1 AIR
E-J		ZONE-7 AIR	YES	ZONE-7 AIR
J-K	ZONE-6 AIR	YES	ZONE-6 AIR	
K-L	ZONE-5 AIR	YES	ZONE-5 AIR	
L-M	ZONE-4 AIR	YES	ZONE-4 AIR	
M-N	ZONE-3 AIR	YES	ZONE-3 AIR	
N-O	ZONE-2 AIR	YES	ZONE-2 AIR	
O-E'	ZONE-1 AIR	YES	ZONE-1 AIR	
G-G'	MEASURED INPUT			
D-E		ZONE-7 AIR	YES	
D'-E'		ZONE-1 AIR	YES	
I-H		AMBIENT		
I'-H'		AMBIENT		

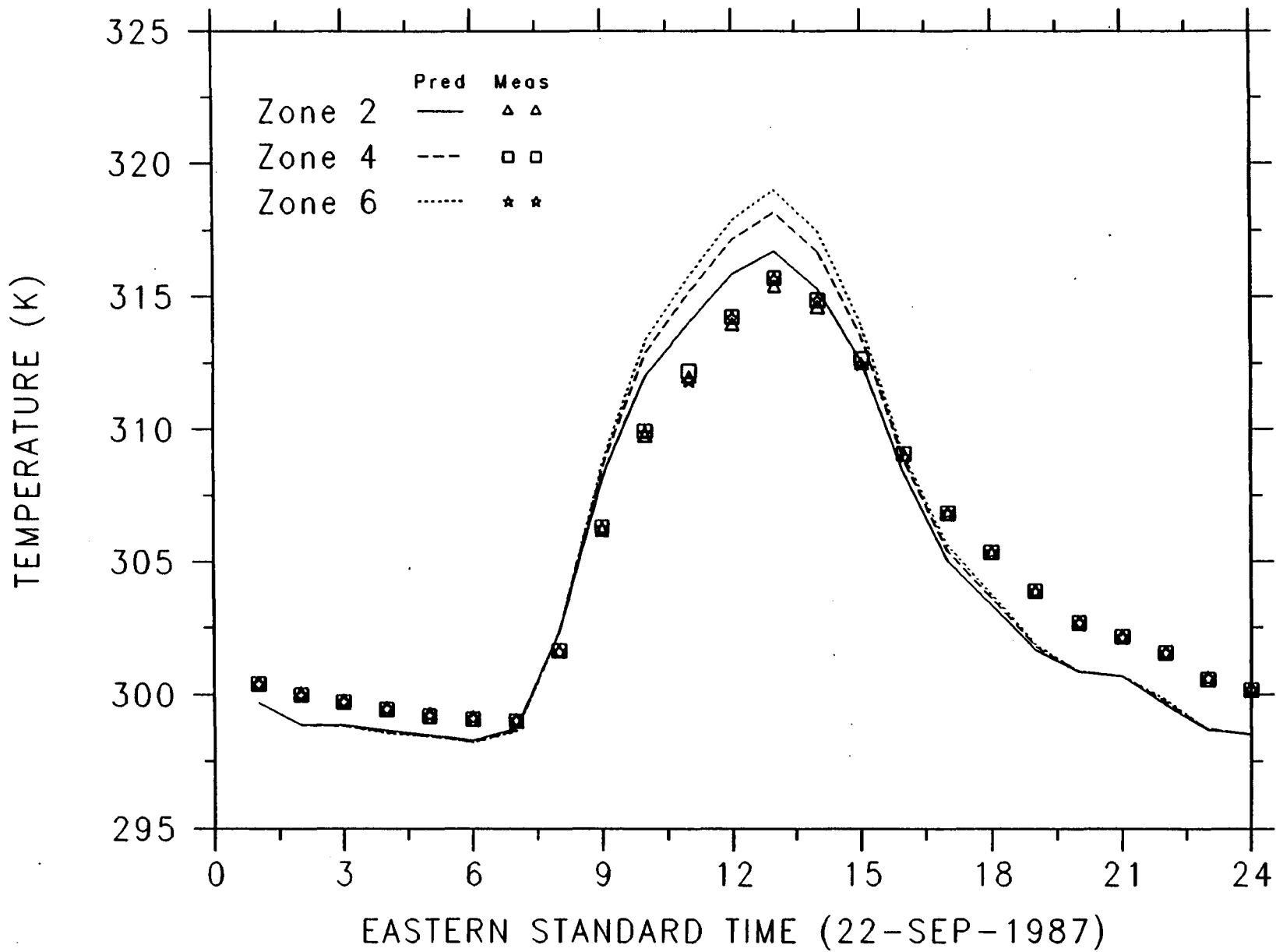


Figure 3-9a. Comparison of predicted and measured temperatures at insulation top without including moisture effects.

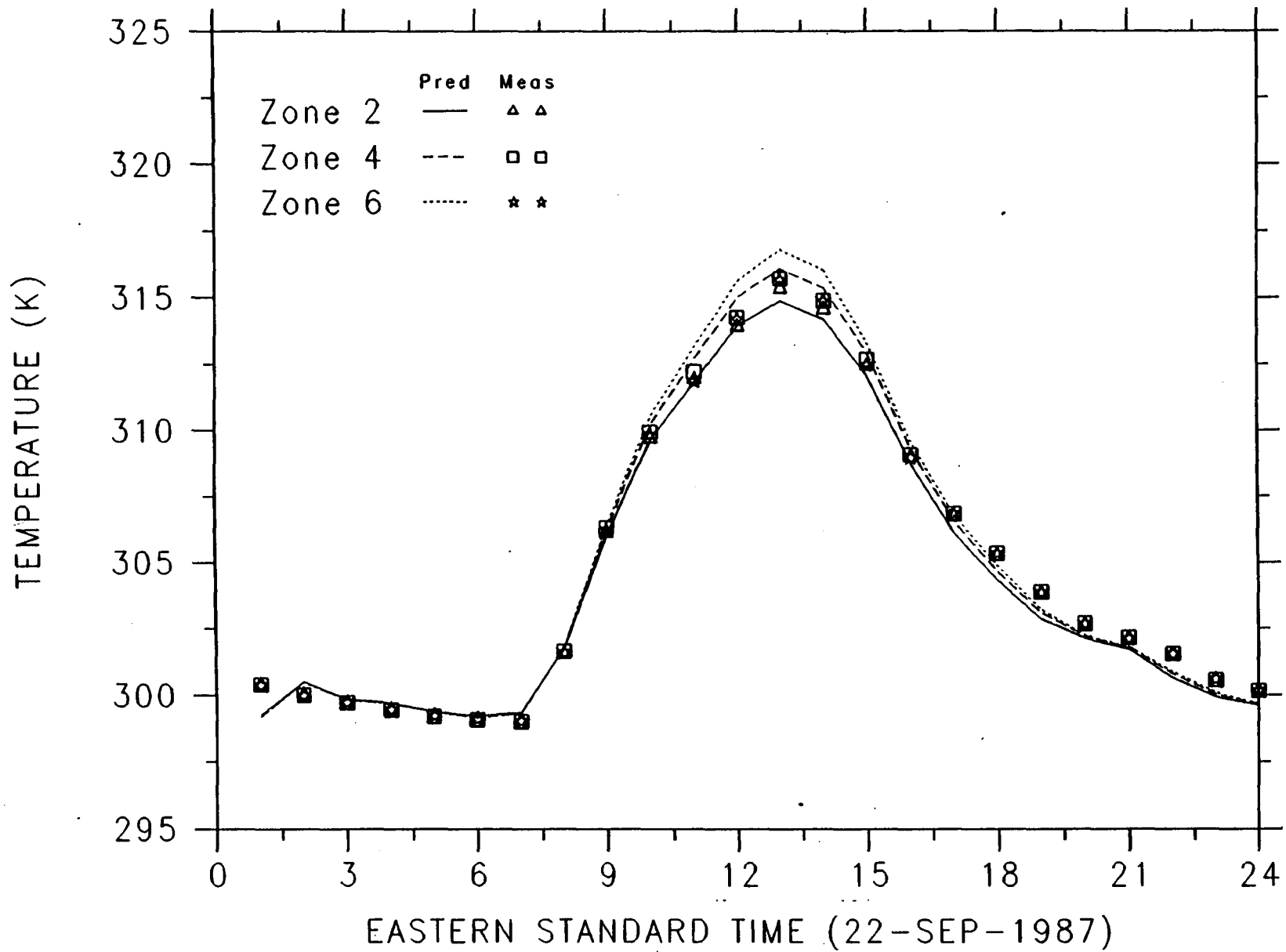


Figure 3-9b. Comparison of predicted and measured temperatures at insulation top with moisture effects.

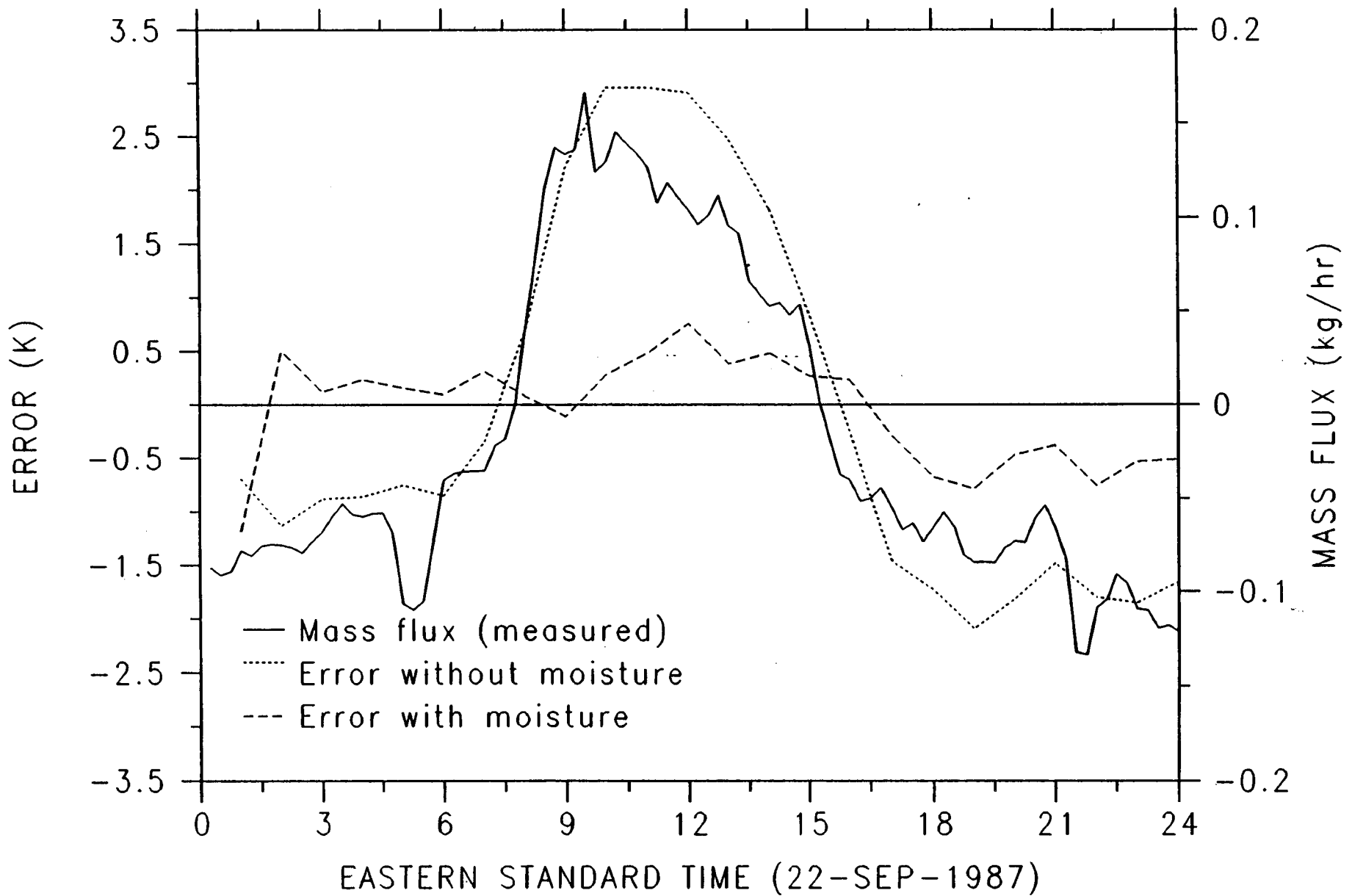


Figure 3-9c. Comparison of insulation top temperature prediction errors and measured vent air moisture removal rate.

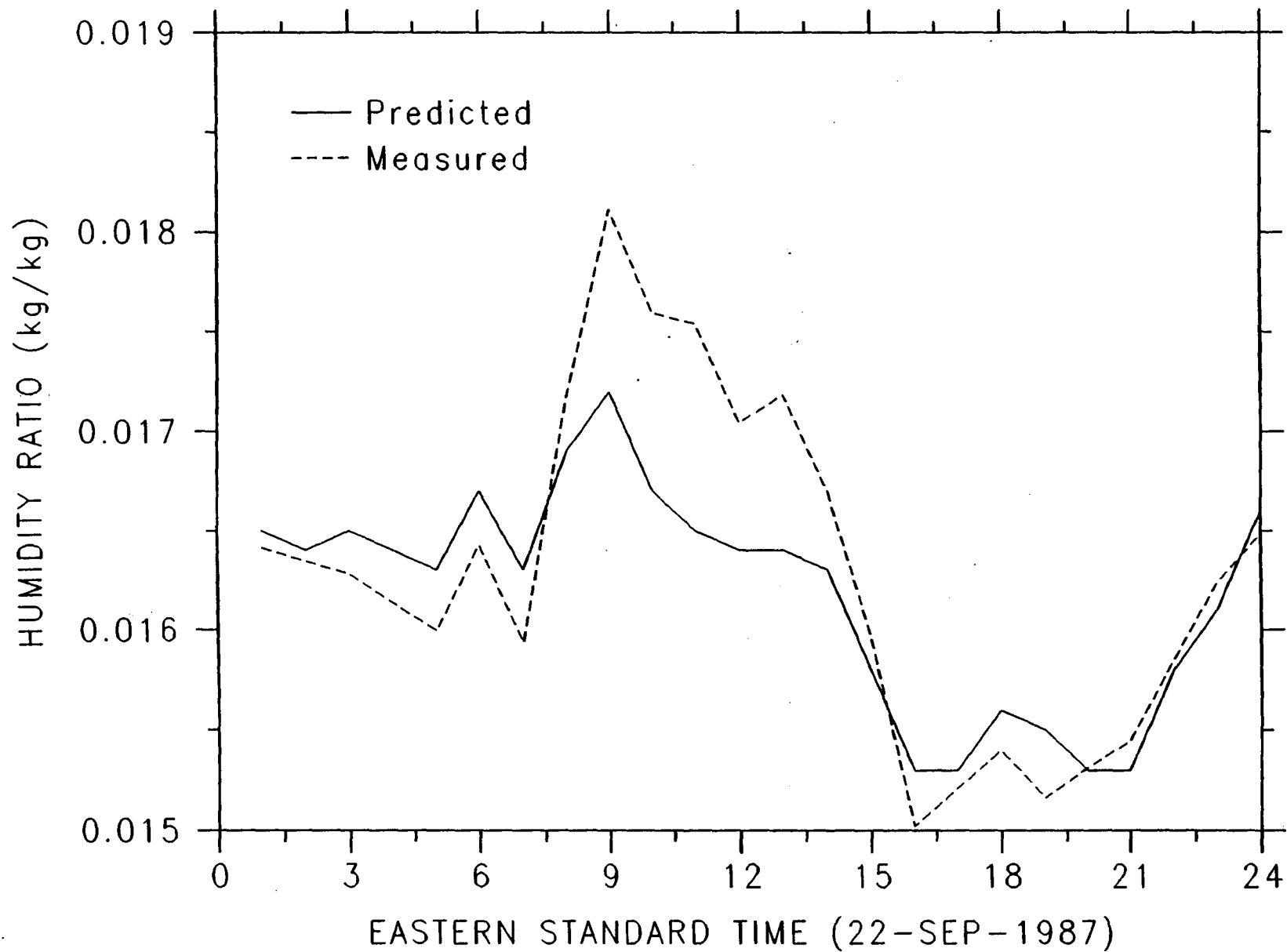


Figure 3-9d. Comparison of predicted and measured outlet humidity ratios.

3.4 HEAT AND MOISTURE TRANSFER IN COLD STORAGE FOUNDATIONS.

The objective of this study is to investigate the heat and moisture transfer in a foundation that is coupled to the ground using the theory proposed by Luikov. The governing heat and mass transfer equations for Luikov's theory are given in Appendix A (Section A.4). The geometry considered here is the foundation of a cold storage building [Figures 3-10.(a) and 3-10.(b)]. The geometry, boundary conditions and material properties were taken from Comini and Giudice 1978. Thus the study serves as a validation of the numerical solution procedure for Luikov's equations. Material properties used in the simulation are tabulated in Table 3-6. For the definition of these properties refer to Section A.4 of Appendix A.

Vapor retarders are usually employed in the walls of a cold storage building to reduce moisture migration. Otherwise serious damage to the thermal insulation may occur. However, a wrongly positioned vapor retarder may increase rather than decrease the moisture content in the thermal insulation. In order to investigate this phenomenon, two different arrangements of the vapor retarder are considered - one in which the vapor retarder is installed in the wall as well as the floor [Figure 3-10.(a)] and the other where it is absent in the floor [Figure 3-10.(b)]. The figures show the mesh as well as the boundary conditions for the problem.

Comini and Giudice 1978 analysed the above cases with identical boundary conditions but with a coarser mesh. The results presented here compare very favorably with the original results.

Table 3-6 Material Properties Used in Luikov's Model

Material	k_T W/mK	ρ kg/m ³	C_p Wh/kgK	k_M kg/mh ⁰ M x 10 ⁻⁴	C_M kg/kg ⁰ M x 10 ⁻⁴	δ °M/K	γ	λ Wh/K
Polystyrene	0.03	32	0.232	0.0378	3.0	0.50	1.0	694.4
Concrete	0.32	2000	0.257	0.504	1.3	0.50	1.0	694.4
Vapor Retarder	10.0	1600	0.232	0.0007	0.1	0.50	1.0	694.4
Clay	1.140	1000	0.256	3.960	27.0	0.50	1.0	694.4

Figures 3-11.(a) and 3-11.(b) show the temperature and Mass transfer potential distributions for the foundation with a vapor retarder in the floor. Figures 3-11.(c) and 3-11.(d) show the same information without the floor vapor retarder. Comparison of the isotherms for the two cases shows that the presence of the floor vapor retarder has a pronounced effect on the temperature distribution. In general, higher temperatures are observed close to the interior surface of the walls in the case where a floor vapor retarder is present [Figures 3-11.(a) and 3-11.(c)]. This will lead to higher temperature gradient near the interior surface and consequently to higher heat transfer to the storage room, indicating that the presence of vapor retarder limits moisture

transfer [Figures 3-11.(b) and 3-11.(d)] but increases heat transfer to the storage area.

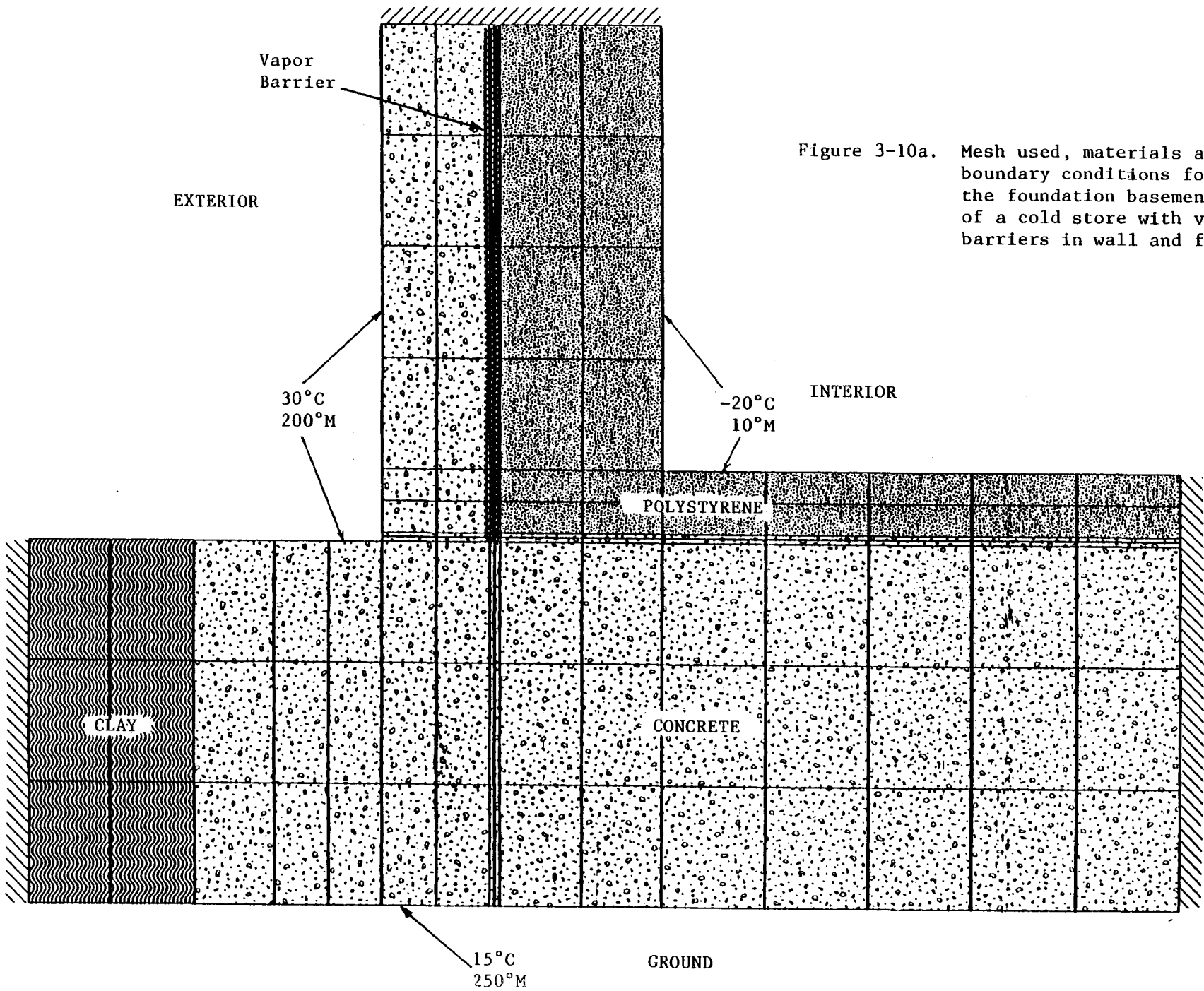


Figure 3-10a. Mesh used, materials and boundary conditions for the foundation basement of a cold store with vapor barriers in wall and floor.

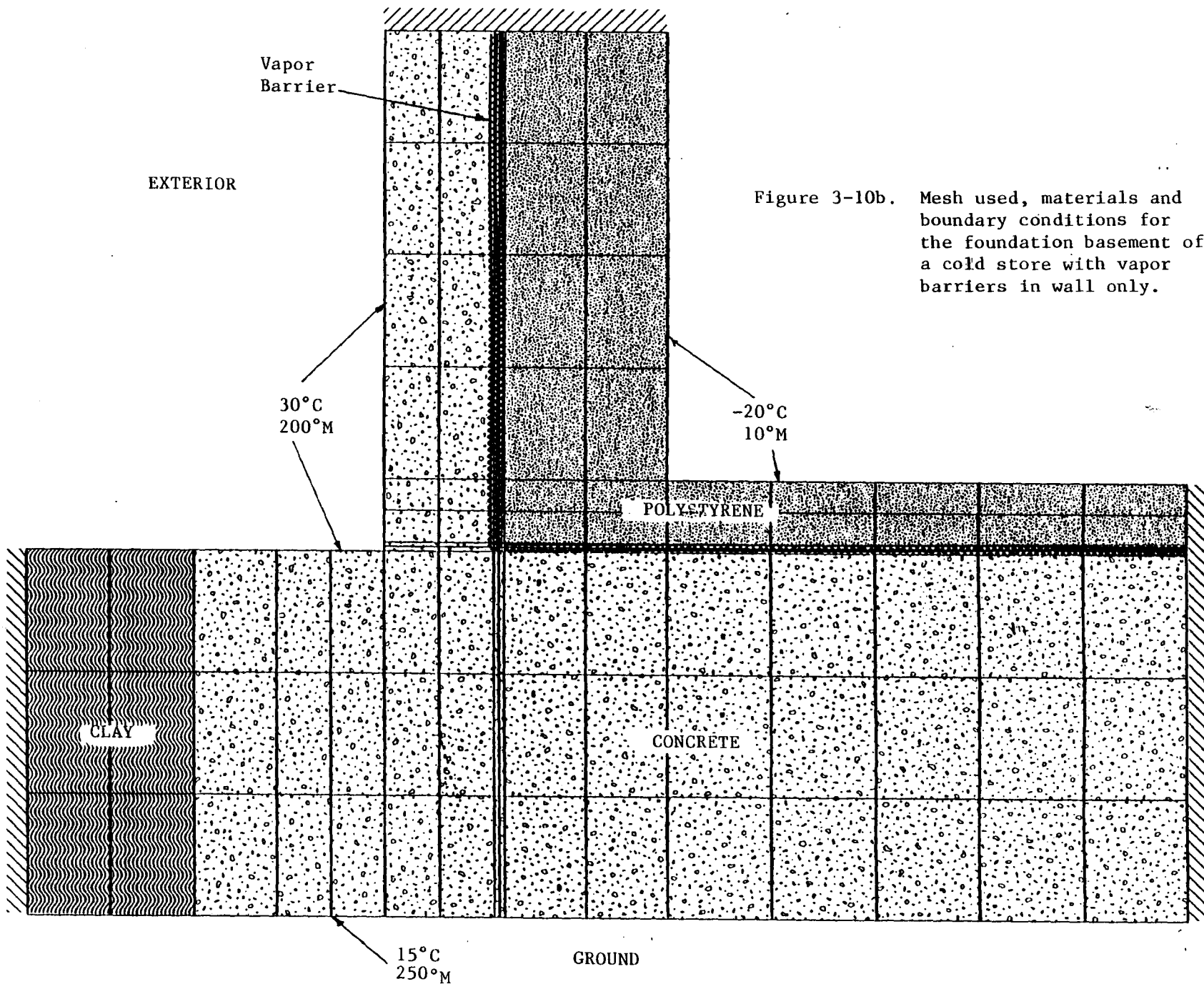


Figure 3-10b. Mesh used, materials and boundary conditions for the foundation basement of a cold store with vapor barriers in wall only.

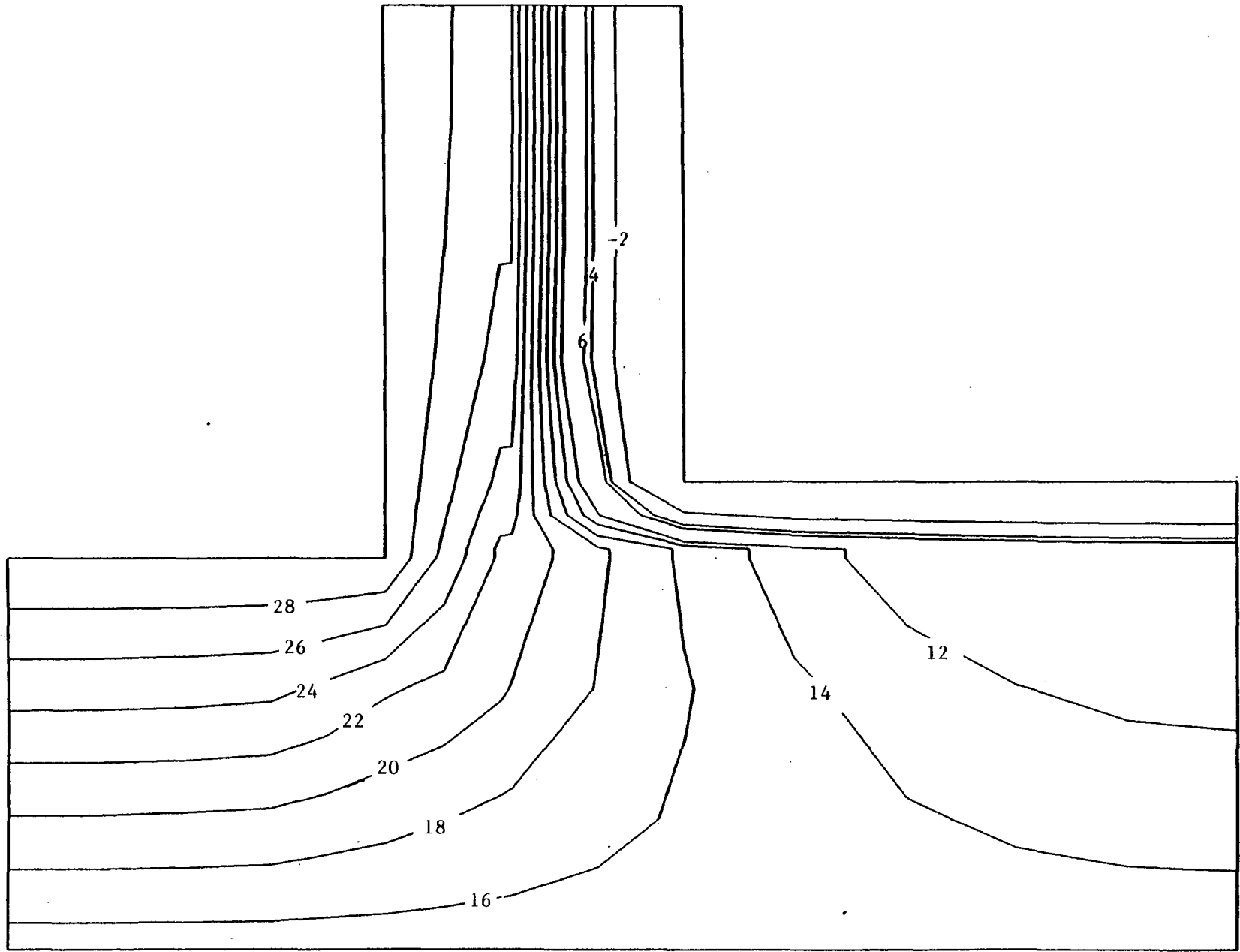


Figure 3-11a. Temperature ($^{\circ}\text{C}$) distribution in the foundation basement of a cold store with vapor barriers in wall and floor.

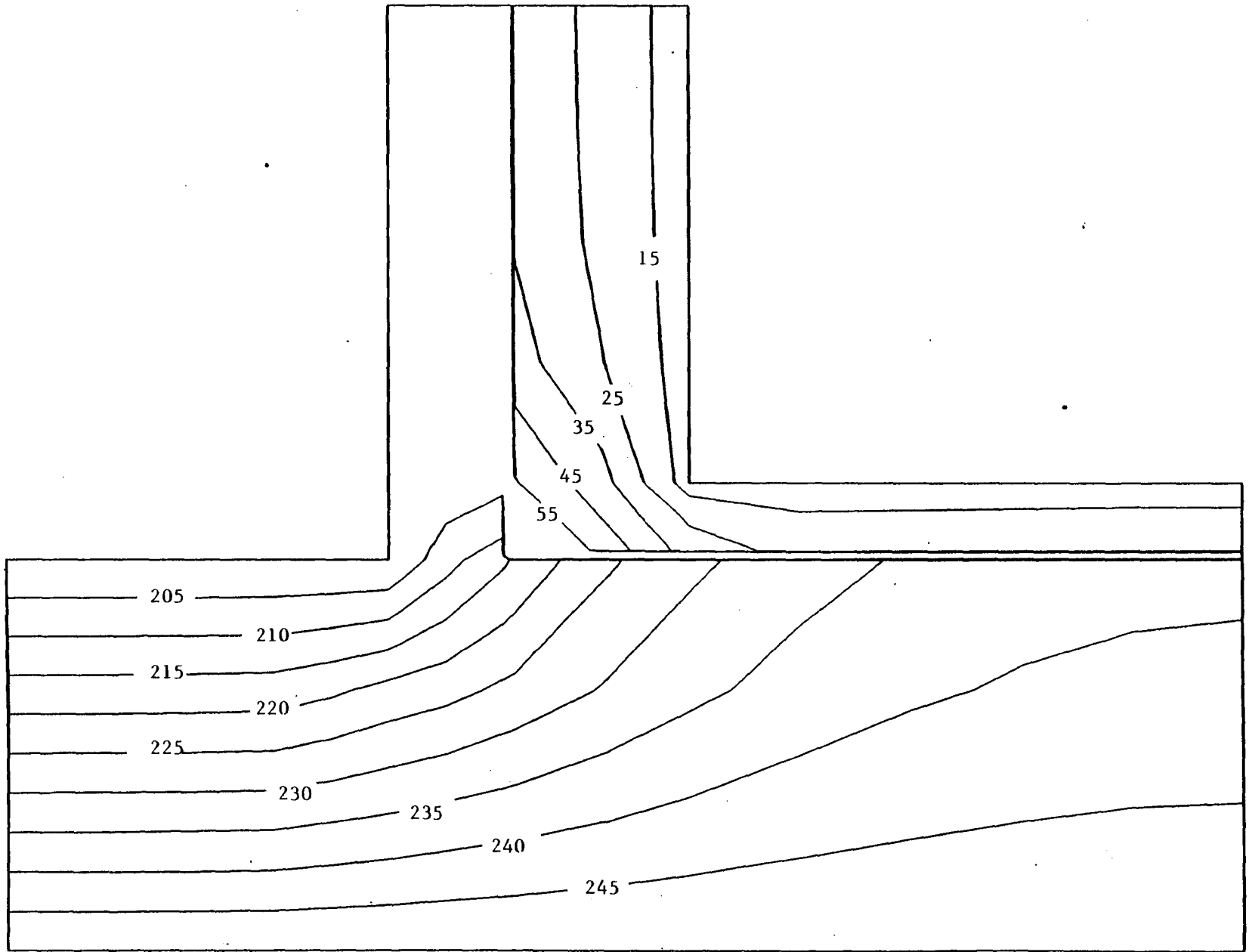


Figure 3-11b. Mass transfer potential ($^{\circ}M$) distribution in the foundation basement of a cold store with vapor barriers in wall and floor.

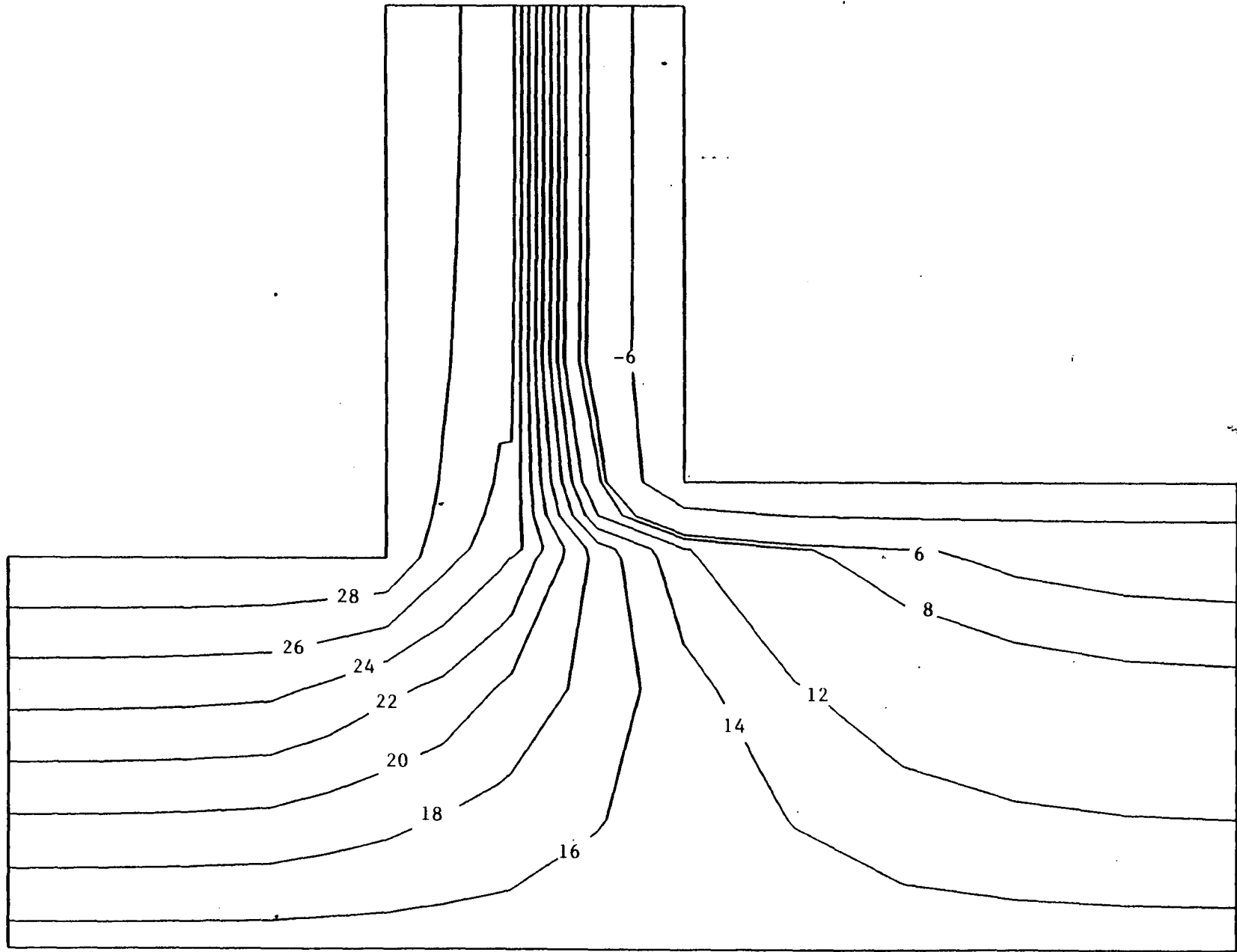


Figure 3-11c. Temperature ($^{\circ}\text{C}$) distribution in the foundation basement of a cold store with vapor barrier in wall only.

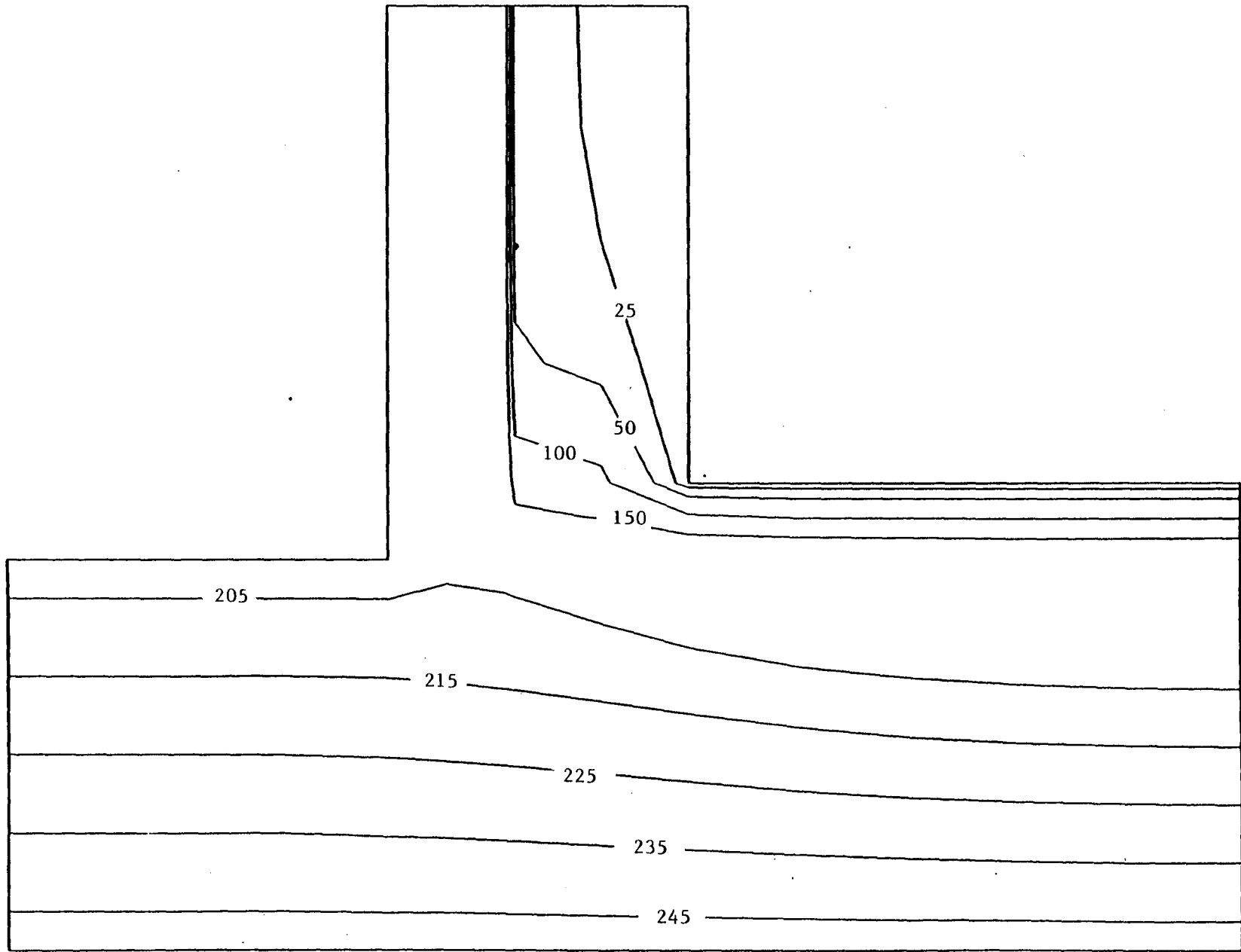


Figure 3-11d. Mass transfer potential ($^{\circ}M$) distribution in the foundation basement of a cold store with vapor barrier in wall only.

3.5 HEAT MASS AND MOMENTUM TRANSFER IN A VENTED STORAGE WALL

The purpose here is to study the heat, mass and momentum transport in a core-vented storage systems [Figure 3-12)]. Equations A-3.1 and A-3.2 have been solved simultaneously subject to the boundary conditions given by Equations A-3.3) and A-3.4 (see Appendix A). The finite element-formulation of these equations is given by Equations B-4.2 through B-4.12 (see Appendix B).

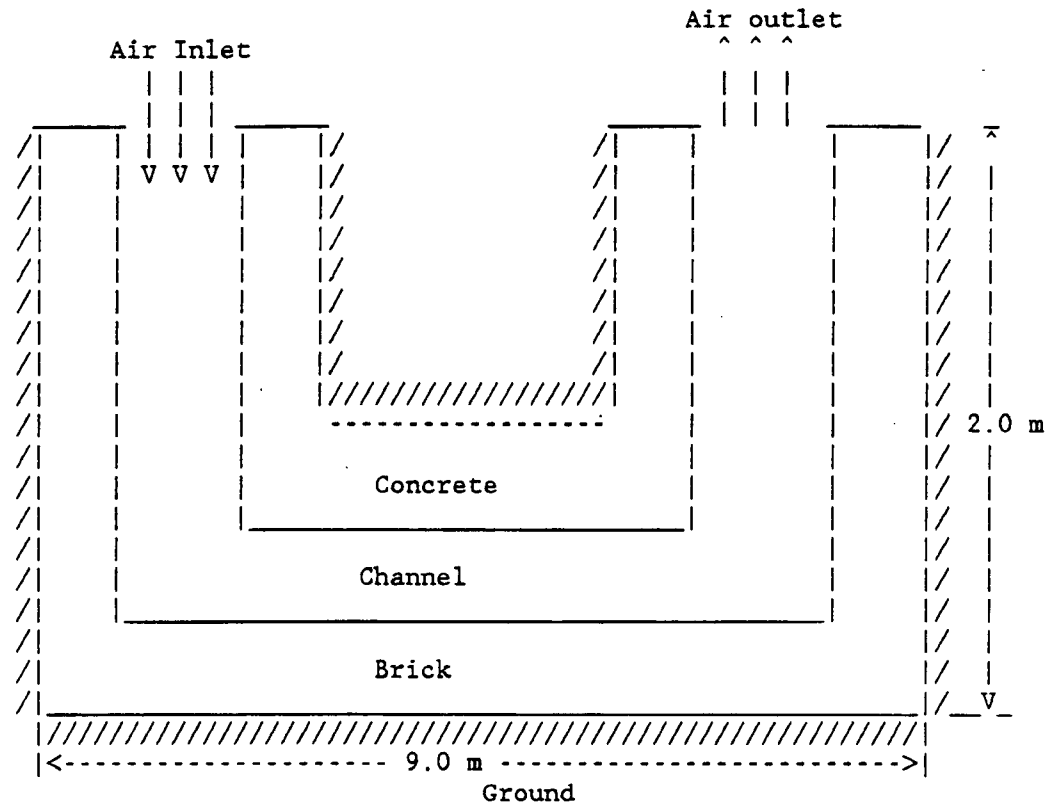


Figure 3-12. Schematic of a Core-vented storage system.

Referring to Figure 3-12, the outside walls are made of brick and the inside walls are made of high density concrete. The moisture isotherms for brick and concrete are shown in Figures 3-13.(a) and 3-13.(b) respectively. The storage wall has an insulated and impermeable boundary at the outer as well as the inner wall faces. The only way the system can undergo heat and moisture transfer is through core ventilation.

For the simulation presented here, the storage media were considered to be at the following initial conditions.

Initial temperature	- 293.15 K
Initial vapor density	- 0.00518 kg/m ³
Initial relative humidity	- 30%

and inlet conditions were held constant at:

Inlet temperature - 300.15 K
Inlet vapor density - 0.018 kg/m³
Inlet relative humidity - 70%

It is obvious that a case of moisture adsorption was simulated. The simulation was made for eight hours.

Figures 3-14.(a) and 3-14.(b) shows the velocity distribution in the ventilation channel at the bends. The inlet velocity was 150 m/h, corresponding to a Reynolds number of 250. The maximum velocity attained at the outlet was 172.47 m/h. As seen the Figures, the flow develops as it proceeds from inlet to outlet. Some recirculation resulting from the formation of vortex near the corners can be seen near the bends. Between the bends, the recirculation vanishes and the flow redevelops before reaching the final bend.

Figures 3-15.(a) through 3-15.(c) show the effective temperature, vapor density and relative humidity at the outlet of the channel as a function of time. In order to obtain the effective outlet conditions, nodal values were multiplied by the mass flow rate and averaged so as to yield a single mass flow weighted value. From the figures we see that all three parameters increase and asymptotically approach the inlet conditions. The example illustrates that fairly common building materials are capable of storing significant amounts of moisture and heat.

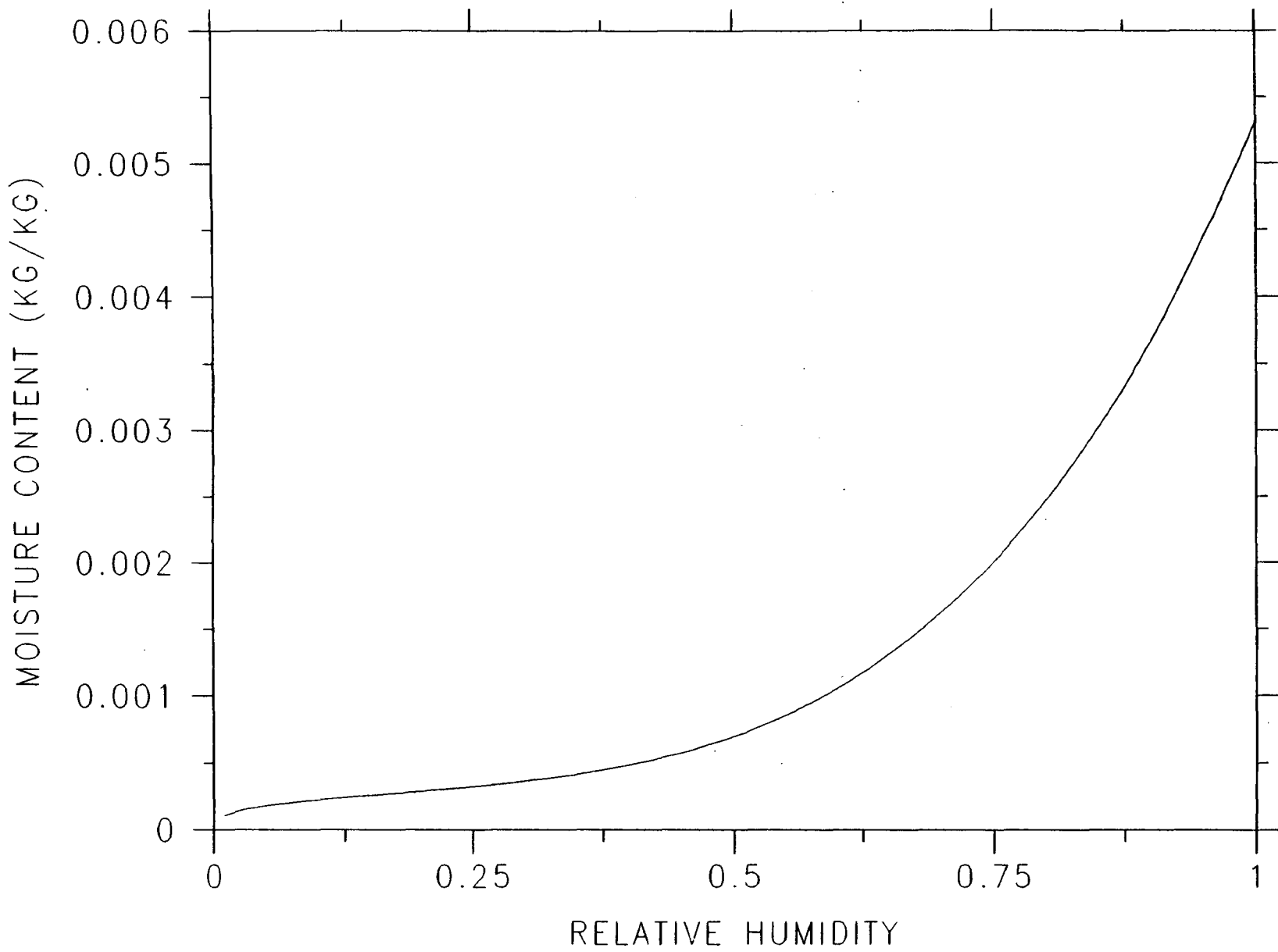


Figure 3-13a. MOISTURE ISOTHERM FOR RED BRICK.

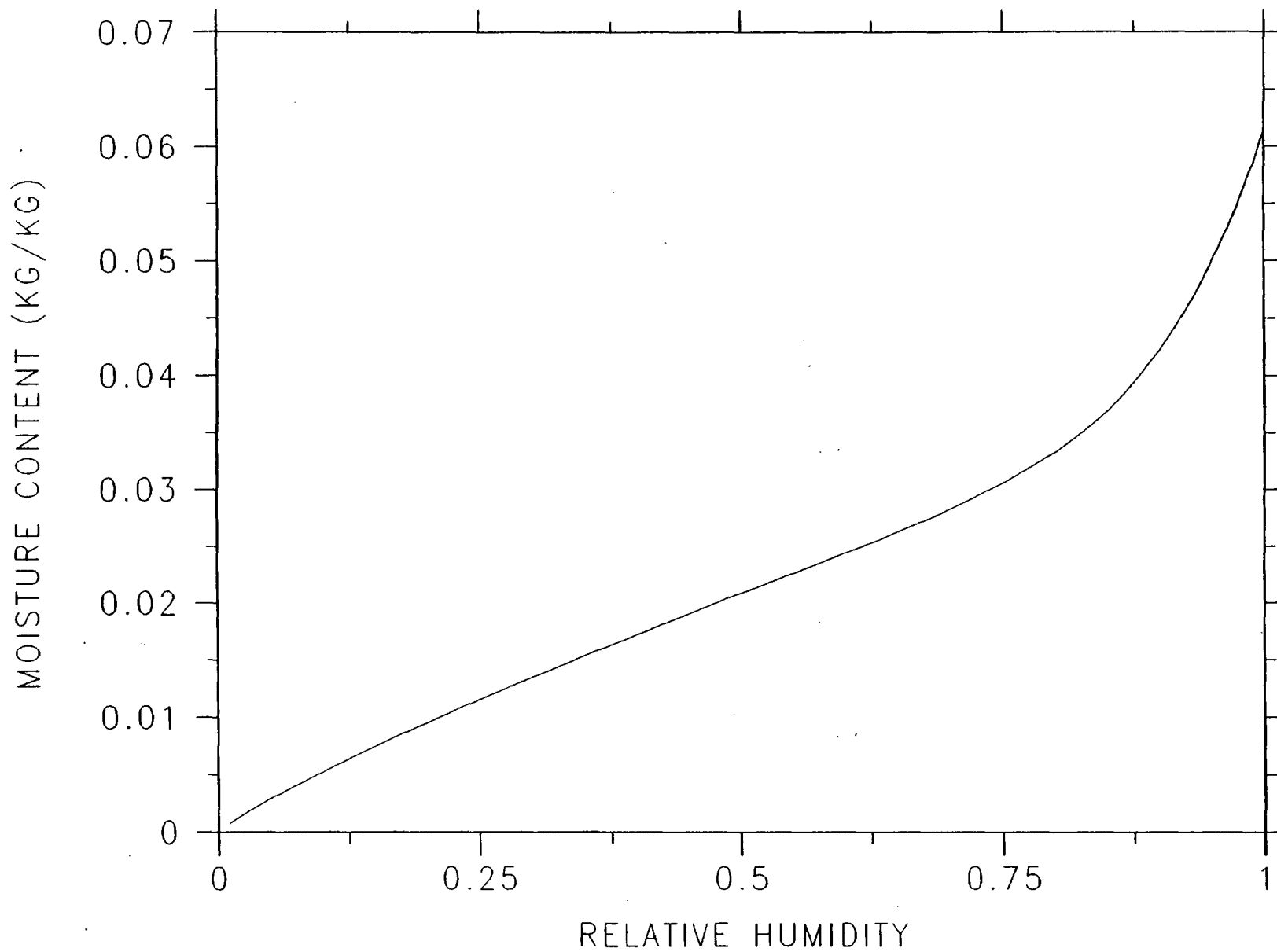
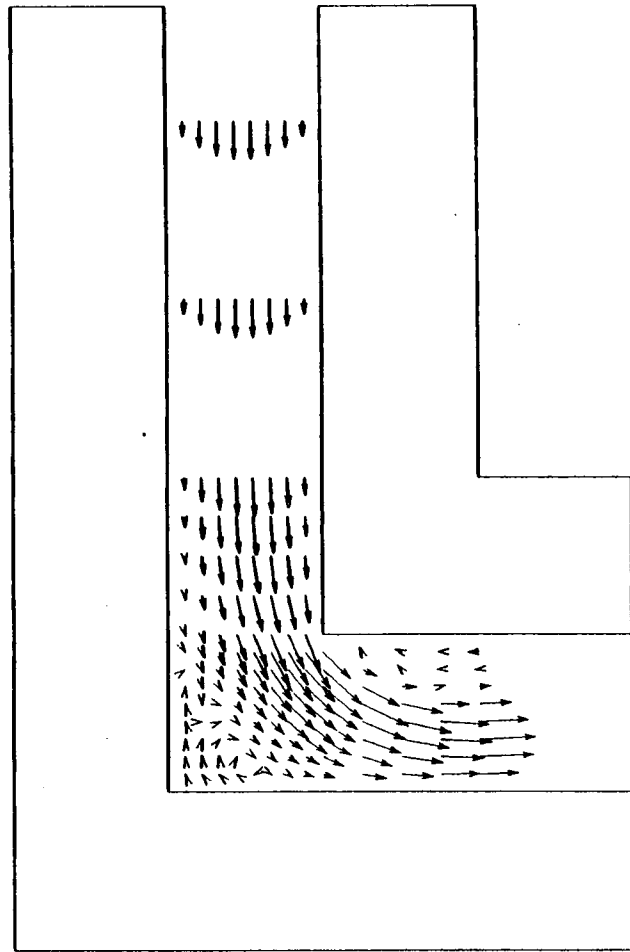


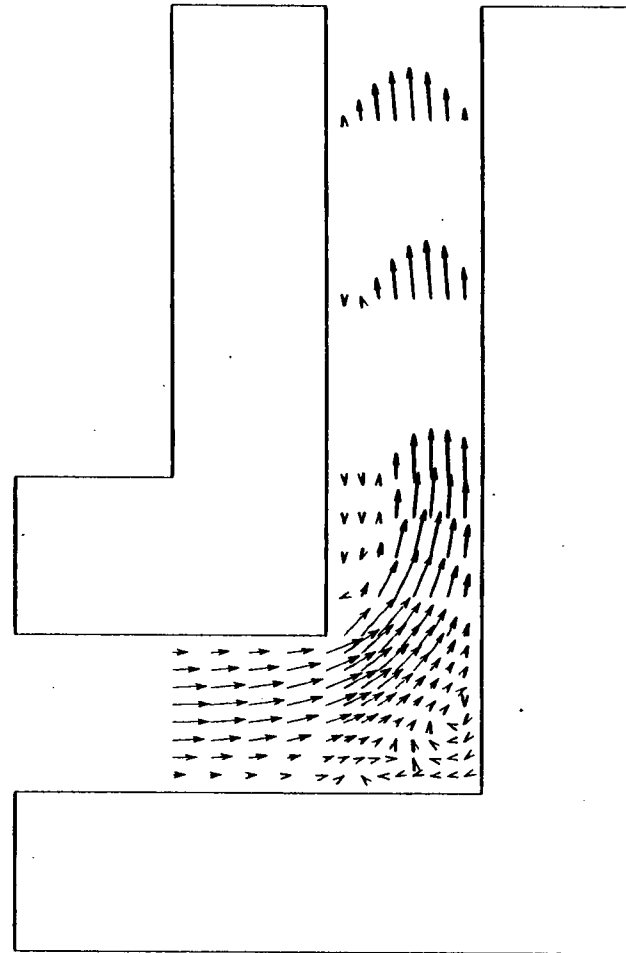
Figure 3-13b. MOISTURE ISOTHERM FOR CONCRETE HW.

VELOCITY PROFILE AT LEFT BEND FOR RE=250



BOUNDS = 0.00, 0.00, 0.40, 0.60,
 → VMAX = 322.4363
 (a)

VELOCITY PROFILE AT RIGHT BEND FOR RE=250



BOUNDS = 8.60, 0.00, 9.00, 0.60,
 → VMAX = 328.4896
 (b)

Figure 3-14.(a) and (b). Velocity fields in the vicinity of the left and right bends.

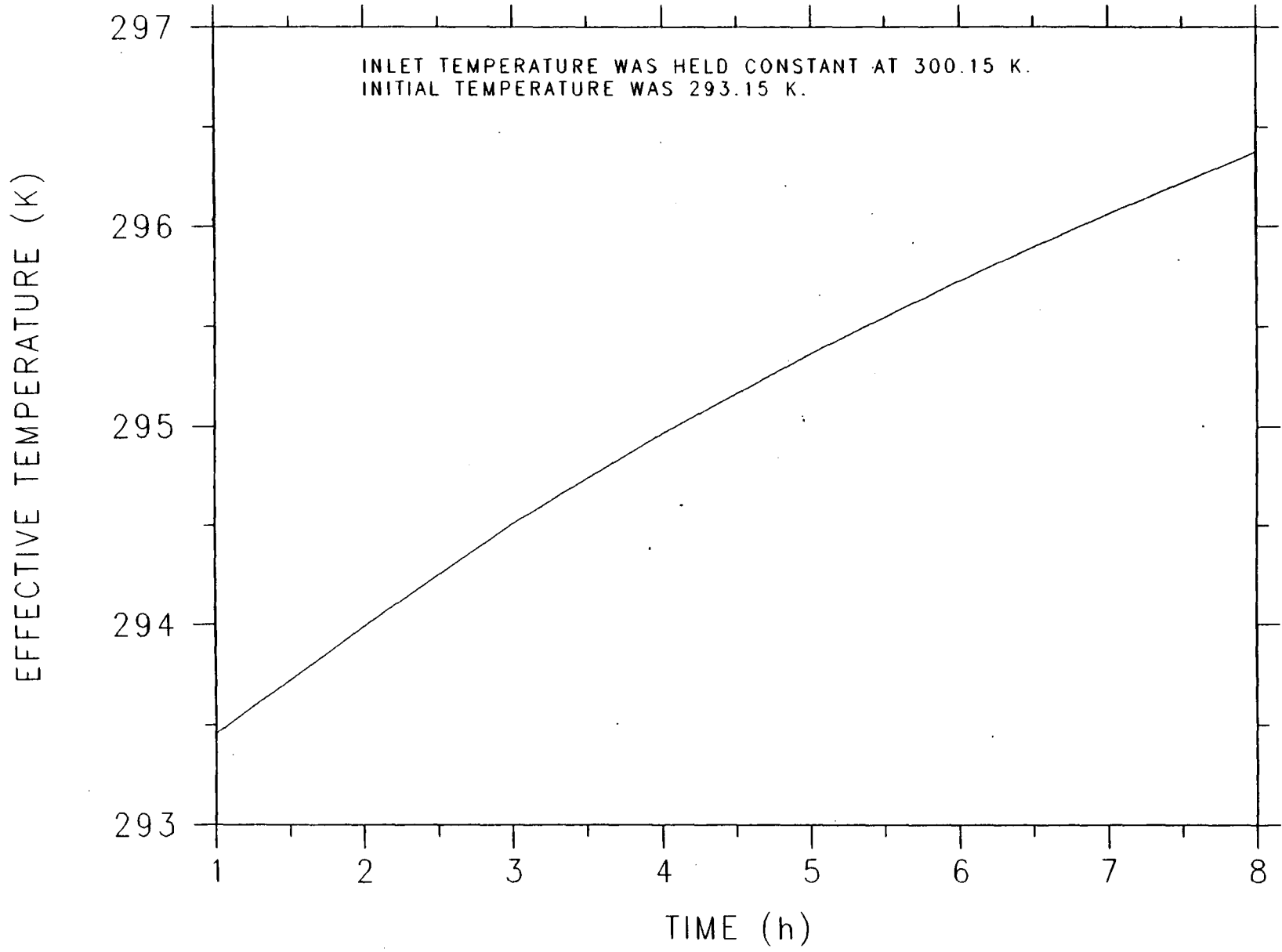


Figure 3-15a. History of averaged temperature of vent air at outlet.

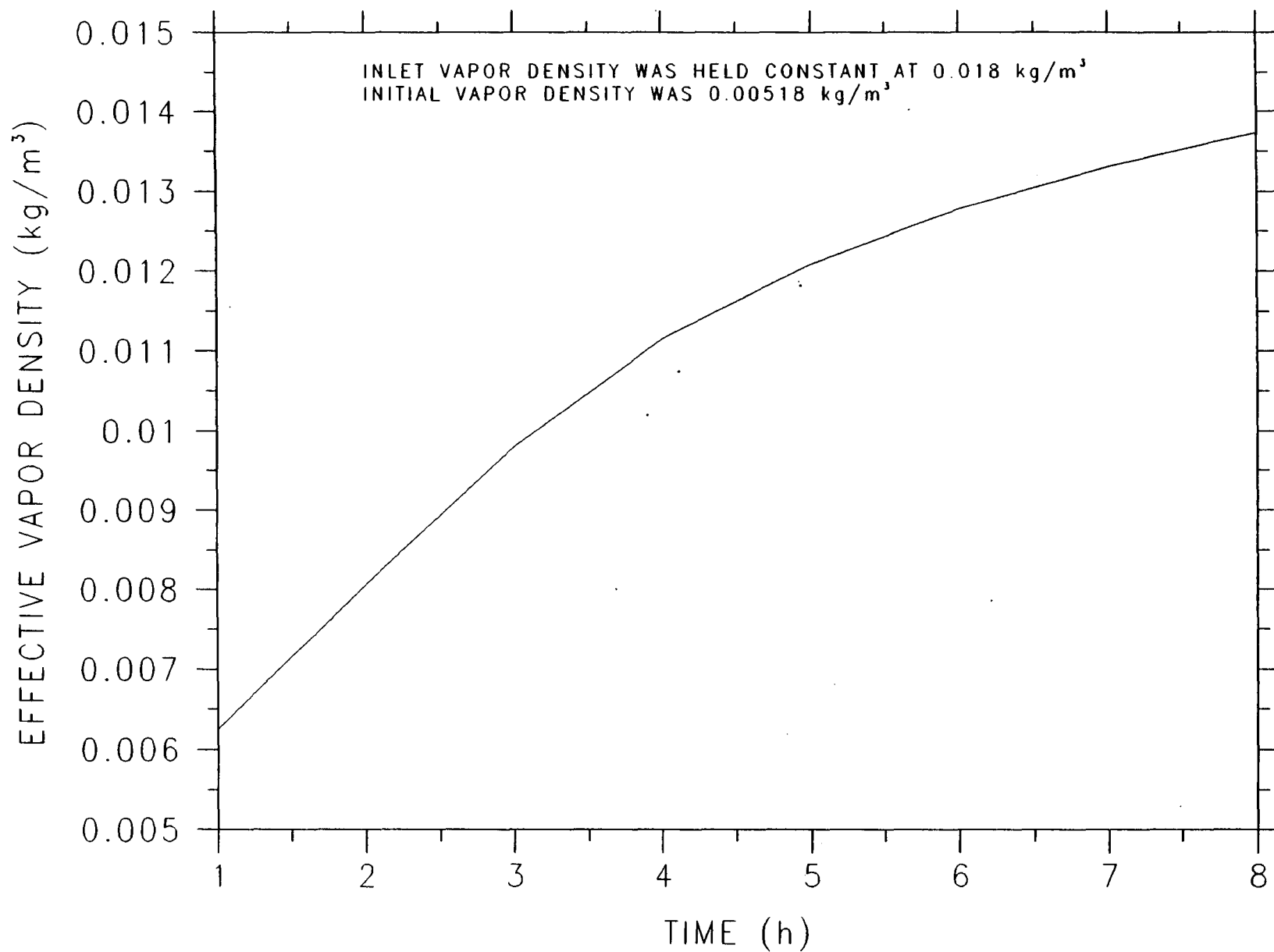


Figure 3-15b. History of averaged vapor density of vent air at outlet.

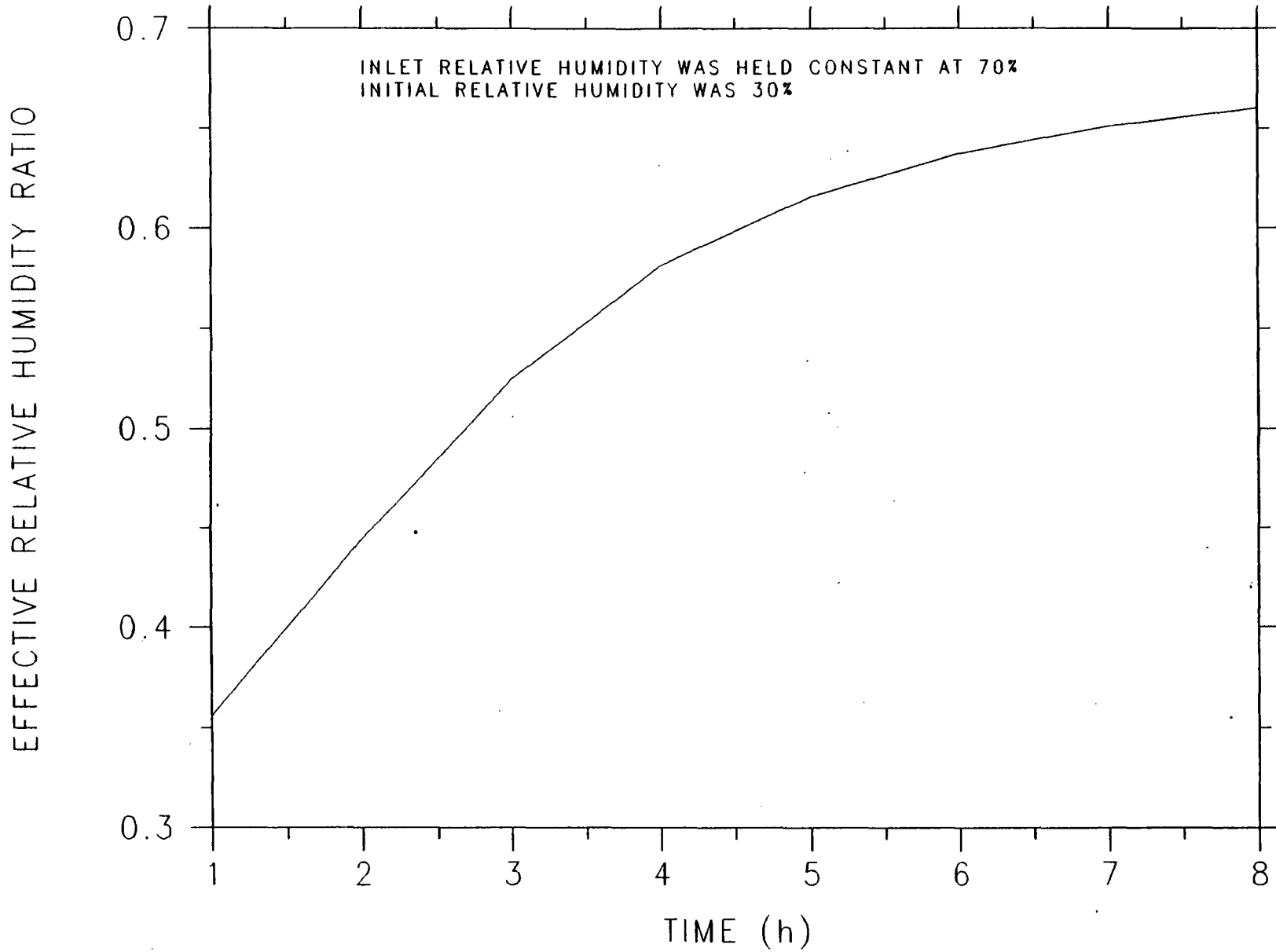


Figure 3-15c. History of averaged relative humidity of vent air at outlet.

REFERENCES

ASHRAE 1985, Handbook of fundamentals, Chapter 23, Atlanta: American Society of Heating, Refrigerating and Air-conditioning Engineers.

Babbit, J.D., "On the Differential Equations of Diffusion," Can. J. Res. A, Vol. 18, pp. 419-474, 1950.

Berger, D. and Pei, D.C.T., "Drying of Hygroscopic Capillary Porous Solids-A Theoretical Approach," Int. J. Heat Mass Transfer, Vol. 16, pp. 293-302, 1973.

Berger, D. and Pei, D.C.T., "The Effect of Different Modes of Operation on the Drying Process," Int. J. Heat Mass Transfer, Vol. 18, pp. 707-709, 1975.

Bomberg, M., Moisture Flow Through Porous Building Materials, Division of Building Technology, Lund Institute of Technology, (Lund Sweden) Report 52, 1974.

Brakel, J.V., "Mass Transfer in Convective Drying," in Advances in Drying, Vol. 1, Edited by Mujumdar, A.S., Hemisphere Publishing Co., N.Y., 1980.

Brooker, D.B., "Mathematical Model of the Psychrometric Chart," Trans. ASAE, Vol. 10, p. 558, 1967.

Bruin, S. and Luyben, K.Ch.A.M., "Drying of Food Materials a Review of Recent Developments," in Advances in Drying, Vol. 1, Edited by Mujumdar, A.S., Hemisphere Publishing Co., N.Y., 1980.

Buckingham, E.A., "Studies on the Movement of Soil Moisture," U.S. Dept. Agr. Bull. 38, 1907.

Burch, D., "Experimental Validation of a Mathematical Model for Predicting Moisture in Attics," in Moisture and Humidity, Measurement and Control in Science and Industry, Proceedings of the 1985 International Symposium on Moisture and Humidity, Washington, D.C., pp. 287-296, 1985.

Burmeister, L.C., Convective Heat Transfer, Wiley, New York, pp. 169-176, 1983.

Cary, J.W. and Taylor, S.A., "The Interaction of Simultaneous Diffusion of Heat and Water Vapor," Soil Sci., Am. Proc., Vol. 28, pp. 167-172, 1962

Ceaglske, N.H. and Hougen, O.A., "The Drying of Granular Solids," Trans. AIChE, Vol. 33, No. 3, pp. 283-312, 1937.

Cleary, P. and Sonderegger, R., "A Method to Predict the Hour by Hour Humidity Ratio in Attic Air," Presented at the ASTM Symposium on Thermal Insulation, Materials and Systems, Dallas, Texas, Dec. 2-6, 1984,

Cleary, P.G. "Moisture Control by Attic Ventilation - An In Situ Study" ASHRAE paper No. 2872 ASHRAE Winter Meeting, Chicago, January 1985.

Cleary, P. and Sherman, M., "Seasonal Storage of Moisture in Roof Sheathing," in Moisture and Humidity, Measurement and Control in Science and Industry,

Proceedings of the 1985 International Symposium on Moisture and Humidity, Washington, D.C., pp. 313-323, 1985.

Cohan, L.H., "Hysteresis and Capillary Theory of Adsorption of Vapor," J. Am. Chem. Soc., Vol. 66, pp. 98-105, 1944.

Comini, G., and Lewis, R.W., "A Numerical Solution of Two-Dimensional Problems Involving Heat and Mass Transfer," Int. J. Heat Mass Transfer, Vol. 19, pp. 1387-1392, 1975.

Comini, G., and Giudice, S.D., "Finite Element Analysis of Heat and Mass Transfer in Buildings," in Energy Conservation in Heating, Cooling, and Ventilating Buildings, Edited by Hoogendoorn C.J., and Afgan N.H., Vol. 1 pp. 26-36, Hemisphere Publishing Co., New York, 1978.

Cunningham, M.J., "A New Analytical Approach to the Longterm Behavior of Moisture Concentrations in Building Cavities - I. Non-Condensing Cavity," Building and Environment, Vol. 18, No. 3, pp. 109-116, 1983.

Cunningham, M.J., "A New Analytical Approach to the Longterm Behavior of Moisture Concentrations in Building Cavities - II. Condensing Cavity," Building and Environment, Vol. 18, No. 3, pp. 117-124, 1983.

Cunningham, M.J., "Further Analytical Studies of Building Cavity Moisture Concentrations," Building and Environment, Vol. 19, No. 1, pp. 21-29, 1984.

Cunningham, M.J., "Automatic Datalogging Timber Moisture Contents Over the Range 10% - 50% w/w," Moisture and Humidity 1985, Proceedings of the 1985 International Symposium on Moisture and Humidity, Washington, D.C., April 15-18, 1985.

De Vries, D.A., "Simultaneous Transfer of Heat and Moisture in Porous Media," Trans. Am. Geophys. Union, Vol. 39, No. 5, pp. 909-916, 1958.

De Vries, D.A., "The Theory of Heat and Moisture Transfer in Porous Media Revisited," Int. J. Heat Mass Transfer, Vol. 30, No. 7, pp. 1343-1350, 1987.

Eckert, E.R.G. and Faghri, M. "A General Analysis of Moisture Migration Caused by Temperature Differences in an Unsaturated Porous Medium", International Journal of Heat and Mass Transfer, Vol. 23, pp. 1613 - 1623, 1980.

Engelman M. S., Strang G. and Bathe K. J., 'the application of Quasi-Newton methods in Fluid Mechanics,' Int. J. Num. Meth. Eng., 17, 707 (1981).

Dennis J. and More J., 'Quasi-Newton method, motivation and theory,' SIAM Rev., 19, 46 (1965).

FIDAP - General Introduction Manual, Fluid Dynamics International Inc., Illinois; Revision 3.0, Jan., 1986.

Fitts, D.D., Non-Equilibrium Thermodynamics, McGraw-Hill, New York, 1962.

Fortes, M. and Okos, M.R., "A Non-Equilibrium Thermodynamics Approach to Transport Phenomena in Capillary Porous Media," Proceeding of the First

International Symposium on Drying, McGill University, Montreal, pp. 100-1009, 1978.

Fortes, M. and Okos, M.R., "Heat and Mass Transfer in Hygroscopic Capillary Extruded Products," Paper presented at the 71 st Annual Meeting of the A.I.Ch.E., meeting, Miami Beach, Florida, 1978.

Fortes, M. and Okos, M.R., "Drying Theories: Their Bases and Limitations as Applied to Food and Grains," in Advances in Drying, Vol. 1, Edited by Mujumdar, A.S., Hemisphere Publishing Co., N.Y., 1980.

Fullford, G.D., "A Survey of Recent Soviet Research on the Drying of Solids," Can. J. Chem. Eng., Vol. 47, pp. 378-391, 1969.

Groot, S.R. de, Thermodynamics of Irreversible Processes, 2d. Ed., Wiley, New York, 1951.

Groot, S.R. de, "On the Thermodynamics of Irreversible Heat and Mass Transfer", Int. J. Heat Mass Transfer, Vol. 4, pp. 63-70, 1961.

Groot, S.R. de and Mazur, P., Non-Equilibrium Thermodynamics, North Holland, Amsterdam, 1962.

Gupta, J.P. and S.W. Churchill "Moisture Transfer in Porous Medium Under a Temperature Gradient" Conservation in Heating, Cooling and Ventilating Buildings, Vol. 1, Hemisphere Publishing Corp., 1978.

Gurr, C.G, Marshall T.J. and Hutton J.T., "Movement of Water in Soil due to a Temperature Gradient," Soil Sci., Vol. 74, pp. 335-345, 1952.

Hall, C., "Water Movement in Porous Building Materials - I. Unsaturated Flow Theory and Its Applications," Building and Environment, Vol. 12, pp. 117-125, 1977.

Hall C., "Water Movement in Porous Building Materials - IV. The Initial Surface Absorption and the Sorptivity," Building and Environmental, Vol. 16, pp. 201-207, 1981.

Hall, C., Hoff, W.D. and Nixon, M.R., "Water Movement in Porous Building Materials - VI. Evaporation and Drying in Brick and Block Materials," Building and Environment, Vol. 19, No. 1, pp. 13-20, 1984.

Hall, C. and Kalimeris A.N., "Water Movement in Porous Building Materials - V. Absorption and Shedding of rain by Building Surfaces", Building and Environment, Vol. 17, No. 4, 1982.

Harmathy, T.Z., "Moisture Sorption of Building Materials," Technical Paper No. 242 of Division of Building Research, National Research Council of Canada, Ottawa, (NRC 9492), March 1967.

Harmathy, T.Z., "Simultaneous Moisture and Heat Transfer in Porous Systems with Particular Reference to Drying," Ind. Chem. Fundam., Vol. 8, No. 1, pp. 92-103, 1969.

Harmathy, T.Z., "Moisture and Heat Transport with Particular Reference to Concrete," Research Paper No. 494, DBR/NRCC., (NRCC 12143), Oct. 1971.

Henry, P.S.H., "Diffusion in Absorbing Media," Proc. R. Soc., Vol. 171A, pp. 215-241, London, 1939.

Hougen, O.A., et al., "Limitations of Diffusion Equations in Drying," Trans. AIChE, Vol. 36., No. 2, pp. 183-206, 1940.

Huang, C.L.D., "Multi-Phase Moisture Transfer in Porous Media Subjected to Temperature Gradient," Int. J. Heat and Mass Transfer, Vol. 22, pp. 1295-1307, 1979.

Kerestecioglu, A., Fairey, P. and Chandra, S., "algorithms to Predict Detailed Moisture Effects in Buildings," Proceedings, Thermal Performance of The Exterior Envelopes of Buildings III, ASHRAE/DOE/BTECC Conference, Clearwater Beach, FL, December 1985.

Kerestecioglu, A., The Detailed Mathematical Prediction of Simultaneous Heat and Mass Transfer in Cavities, Ph.D. Dissertation, Florida Institute of Technology, Melbourne, FL, June 1986.

Kielsgaard, H.K., "Sorption Isotherms - A Catalogue and A Data Base," Paper Presented at Symposium on Mechanisms and Measurement of Water Vapor Transmission Through Materials and Systems, Bal Harbour, Florida, Dec. 10 1987.

Kohonen, R., "Transient Analysis of the Thermal and Moisture Physical Behaviour of Building Constructions.. Building and Environment, Vol. 19, No. 1, pp. 1-11, 1984.

Kohonen, R., "A Method to Analyze the Transient Hygrothermal Behaviour of Building Materials and Components". Technical Research Center of Finland, Publications 21, Oct. 1984.

Krischer, O., "Die Wissenschaftlichen Grundlagen der Teocknungstechnik," Kap. IX, Springer, Berlin, 1963.

Kusuda, T., "Indoor Humidity Calculations," ASHRAE Transactions, Vol. 89, Part 2, 1983.

Kusuda, T. and Miki, M., "Measurement of Moisture Content for Building Interior Surfaces," in Moisture and Humidity, Measurement and Control in Science and Industry, Proceedings of the 1985 International Symposium on Moisture and Humidity, Washington, D.C., pp. 297-311, 1985.

Kusuda, T., "Measurement of Moisture Control for Building Interior Surfaces," Moisture and Humidity 1985, Proceedings for the 1985 International Symposium on Moisture and Humidity, Washington, D.C., April 15-18, 1985.

Kuzmak, J.M and Sereda, P.J., "The Mechanism by which Water Moves through a Porous Material Subjected to a Temperature Gradient: I. Introduction of a Vapor Gap into a Saturated System," Soil Sci., Vol. 84, pp. 291-299, 1957.

Kuzmak, J.M and Sereda, P.J., "The Mechanism by which Water Moves through a Porous Material Subjected to a Temperature Gradient: II. Salt Tracer and Streaming Potential to Detect Flow in the liquid Phase," Soil Sci., Vol. 84, pp. 419-422, 1957.

Labuza, T.P., "Sorption Phenomena in Foods," Food Technol., Vol. 22, pp. 15-25, 1968.

Labuza, T.P., "Interpretation of Sorption Data in Relation to the State of Constituent Water," in Duckworth R.B. (ed.), Water Relations of Foods, Academic Press, London, 1975.

Langlais, C. and Klansfeld, S., "Heat and Mass Transfer in Fibrous Insulations," Journal of Thermal Insulation, Vol. 8, July 1984.

Lewis, R.W, Morgan, K., and Thomas, H.R, "The Nonlinear Modeling of Drying Induced Stresses in Porous Materials," in Advances in Drying'80 Vol. 1 pp. 233-268, Edited by Mujumdar, A.S., Hemisphere Publishing Co., New York, 1980.

Lewis, W.K., "The Rate of Drying of Solid Materials," J. ind. Eng. Chem., Vol. 13, pp. 427-432, 1921.

Luikov, A.V., "Heat and Mass Transfer in Capillary Porous Bodies," in T.F. Irvine et al. (Eds.), Advances in Heat Transfer, Vol. 1, Academic Press, New York, 1964.

Luikov, A.V., Heat and Mass Transfer in Capillary-Porous Bodies, Pergamon Press, 1966.

Luikov, A.V., Analytical Heat Diffusion Theory, Academic Press, 1968.

Luikov, A.V., "Systems of Differential Equations of Heat and Mass Transfer in Capillary-Porous Bodies (review)," Int. J. Heat Mass Transfer, Vol. 18., pp 1-14, 1975.

Matthies H. and Strang G., 'The solution of non-linear finite element equations,' Int. J. Num. Meth. Eng., 11, 1155 (1977).

Meixner, J., Ann. Phys., Vol. 39, p. 333, 1941.

Meixner, J., Ann. Phys., Vol. 41, p. 409, 1942.

Meixner, J., Ann. Phys., Vol. 42, p. 244, 1943.

Morgan, K., Lewis, R.W, and Thomas, H.R, "Numerical Modeling of Drying Induced Stresses in Porous Materials," in Drying'80 Vol. 1 pp. 451-460, Proceedings of the 2nd International Symposium, Edited by Mujumdar, A.S., Hemisphere Publishing Co., New York, 1980.

Mikhailov, M.D., "General Solutions of the Diffusion Equations Coupled at Boundary Conditions," Int. J. Heat Mass Transfer, Vol. 16, pp. 2155-2164, 1973.

Miller E.E. and Miller R.D., "Theory of Capillary Flow: I. Practical Implications," Proc. Soil Sci. Soc. Am., Vol. 19, pp. 267-271, 1955.

Miller E.E. and Miller R.D., "Theory of Capillary Flow: II. Experimental Information," Proc. Soil Sci. Soc. Am., Vol. 19, pp. 272-275, 1955.

- Miller, J.D., "Development of Validation of a Moisture Mass Balance Model for Predicting Residential Cooling Energy Consumption," ASHRAE Transactions 90, pt. 2, pp. 275-293, 1984.
- Newmann, A.B., "Diffusion and Surface Emission Equations," Trans. AIChE, Vol. 27, pp. 203-220, 1931.
- Onsager, L., Phys. Rev., Vol. 37, p. 405, 1931.
- Onsager, L., Phys. Rev., Vol. 38, p. 2265, 1931.
- Philip, J.R. and De Vries, D.R., "Moisture Movement in Porous Media Under Temperature Gradients," Trans. Am. Geophysical Union, Vol. 38, pp. 222-232, 1957.
- Prigogine, I., Introduction to Thermodynamics of Irreversible Processes, Interscience Pub., Wiley, New York, 1961.
- Roques, M.A. and Cornish, A.R.H., "Phenomenological Coefficients for Heat and Mass Transfer Equations in Wet Porous Media," in Drying'80, Vol. 2, Edited by Mujumdar, A.S., Hemisphere Publishing Co., New York, 1980.
- Sherwood, T.K., "The Drying of Solids Part I," Ind. Eng. Chem., Vol.21, pp. 12-16, 1929.
- Sherwood, T.K., "The Drying of Solids Part II," Ind. Eng. Chem., Vol.21, pp. 976-980, 1929.
- Sherwood, T.K., "The Drying of Solids Part III Mechanism of the Drying of Pulp and Paper," Ind. Eng. Chem., Vol.22, pp. 132-136, 1930.
- Sherwood, T.K., "Application of the Theoretical Diffusion Equations to the Drying of Solids," Trans. AIChE, Vol. 27, pp. 190-202, 1931.
- Taylor, S.A. and Cary, J.W., "Linear Equations for the Simultaneous Flow Matter and Energy in Continuous Soil System," Soil Sci., Soc. Am. Proc., Vol. 28, pp. 167-172, 1964.
- Taylor, S.A., "The Influence of Steady Temperature Gradients upon Water Transport in Soil Materials," in Humidity and Moisture, Vol. 3, Reinhold, New York, 1965.
- Valchar, J., Papper E3, Proc. of the Int. Symp. on Heat and Mass Transfer Probl. in Food Eng., Wageningn, Netherlands, 1972.
- Valchar, J., "Heat and Moisture Transfer in Capillary Porous Materials from the Point of View of the Thermodynamics of Irreversible Processes," Third Int., Heat Transfer Conference, Chicago, Vol. 1, pp. 409-418, 1966.
- Valcharova, J., and Valchar, J., "The Thermokinetics of the Moisture Transport in Solids During Drying," in Drying'80 Vol. 2 pp. 53-60, Proceedings of the 2nd International Symposium, Edited by Mujumdar, A.S., Hemisphere Publishing Co., New York, 1980.
- Withaker, S., "Heat and Mass Transfer in Granular Porous Media," in Advances in Drying, Vol. 1, Hemisphere, Washington, 1980.

Young, J.H. and Nelson, G.L., "Research of Hysteresis between Sorption and Desorption Isotherms of Wheat," Trans. ASAE, Vol. 10, pp. 756-761, 1967.

APPENDIX A

DIFFERENT THEORIES ON COMBINED HEAT AND MASS TRANSFER

A.1 LIQUID DIFFUSION THEORY

The movement of moisture by liquid diffusion as the principal flow mechanism in a drying solid has been proposed by Lewis 1921, Newman 1931, Sherwood 1929a, 1929b, 1930 and 1931, and many other researchers. Fick's equation,

$$\frac{\partial U}{\partial \tau} = \nabla \cdot (D_L \nabla U) \quad (\text{A-1.1})$$

has been used since then with various assumptions, such as constant diffusion coefficients, isotropy, or first-kind (Dirichlet) boundary conditions. Solutions for several cases can be found in the literature.

However, liquid diffusion as the only mechanism for moisture movement has been subjected to severe criticism. Hougen et al. 1940 stated that the criterium for a model's validity is its ability to predict the correct moisture gradient in the solid during drying. Nevertheless, Hougen et al. 1940 pointed out that the model will give better results if variable diffusion coefficients are used.

Even when one accepts the fact that diffusion equations can fit experimental values for some solids, there remains the question of their physical validity. The liquid diffusion theory has been called misleading, since it has furnished wrong predictions and misinterpretations of the experimental results. The probable reason for its acceptance is the logarithmic behavior of the solution of the diffusion equations, resembling experimental drying curves.

Babit 1950 states that the driving force in diffusion through solids is not concentration but pressure. The relationship between pressure and concentration is seldom linear, owing to the complexities of adsorption and desorption. Equations phares in terms of concentration should be avoided, since they fail to distinguish diffusion from other flow mechanisms that may occur simultaneously.

Moisture movement through liquid diffusion cannot be denied. More sophisticated theories take Fick's law as representative of liquid and vapor movement. The criticism then lies in assuming liquid movement to be the only mechanism for moisture transfer in all stages of mass transfer. To apply the liquid diffusion equations as in Equation (A-1.1) is the same as assuming isothermal diffusion and thus, neglecting temperature gradients inside the medium.

As is true of most recent theories, the diffusion theory does not take into account shrinkage, case hardening, or sorption isotherms. The physical meaning of the diffusion coefficient is either lost or interpreted as a lumping of all simultaneous effects, besides being dependent on concentration and temperature.

A.2 CAPILLARY THEORY

The term capillary here refers to the flow of a liquid through the interstices and over the surface of a solid due to molecular attraction between the liquid and the solid. This phenomenon was first analyzed by Buckingham 1907, who introduced the concept of "capillary potential" as the driving force for unsaturated capillary flow.

The capillary potential or suction Ψ is the pressure difference between the water and the air at the curved air-water interface present in a capillary. The interface curvature is produced by the surface tension of the water. The equation for capillary-liquid flow is given as follows:

$$J_L = -D_H \rho_L \nabla \Psi \quad (\text{A-2.1})$$

In Equation (A-2.1) D_H denotes the hydraulic conductivity, and Ψ is the capillary potential. For isothermal conditions, the capillary potential is usually assumed to be proportional to the moisture content, and therefore Equation (A-2.1) becomes:

$$J_L = -D_H \rho_S \nabla U \quad (\text{A-2.2})$$

where

$$D_H = \frac{\sigma \cos \theta}{4\mu r^2 f(r)} \int_{r_0}^{r_1} r^2 f(r) dr \quad (\text{A-2.3})$$

Ceaglske and Hougen 1937 found that in the drying of granular solids, the water flow is determined entirely by capillary forces and hence is independent of water concentration. They showed, through an experiment, that moisture flow may be in the direction of increasing concentration. Miller and Miller 1955a and 1955b explain this by stating that the driving force is a tension gradient. Their argument is that both surface tension and viscous flow laws are based on pressure. Only for homogeneous media and negligible body forces tension is proportional to moisture content, and Equation (A-2.2) holds.

Water held in the interstices of solids, as liquid covering the surface and as free water in cell cavities, is subject to movement by gravity and capillarity, provided there are passageways for continuity of flow. Hougen et al. 1940 concluded that, in drying, the capillary-liquid flow equation applies to:

1. Water not held in solution and all water above saturation point, as in textiles, paper and leather;
2. All water above the equilibrium moisture content at atmospheric saturation, as in fine powders and granular solids, such as paint pigments, minerals, clays, soil and sand.

In the area of food research, capillary flow has been accepted as one of the fundamental drying mechanisms, mainly during the high-moisture stage. Equations (A-2.1) and (A-2.2), in principle, could give some support to the researchers who employ the diffusion equation. In this case, the equations for liquid diffusion and capillary flow are assumed to be lumped into just one equation, and this would improve the level of their assumption. However, an assumption of constant diffusion coefficient seems inappropriate.

A.3 EVAPORATION-CONDENSATION THEORY

Henry 1939 studied the diffusion of one substance through another in the pores of a solid body that may absorb (or desorb) and immobilize some of the diffusing substance. Even though his theory was not limited to vapor as an exclusive diffusing substance, in his work and in all modified models based on it, moisture was assumed to migrate entirely in the vapor phase. Henry's theory took into account the simultaneous diffusion of heat and mass, and assumed the pores to be a continuous network of spaces included in the solid. The derivation of the evaporation-condensation theory is as follows:

For a differential element having a unit-cross sectional area and a thickness of dx , the mass balance equation can be written as:

$$\epsilon \frac{\partial \rho_V}{\partial \tau} + (1-\epsilon) \rho_S \frac{\partial U}{\partial \tau} = \nabla \cdot (\epsilon \tau_0 D_A \nabla \rho_V) \quad (\text{A-3.1})$$

Equation (A-3.1) states that the net amount of vapor entering the differential element by diffusion equals the increase in moisture in the pores plus the increase in moisture in the solid.

For the same differential element, the energy balance equation can be written as follows:

$$\epsilon \rho_S C_S \frac{\partial T}{\partial \tau} = \nabla \cdot (k_T \nabla T) + \lambda \rho_S \frac{\partial U}{\partial \tau} \quad (\text{A-3.2})$$

According to Equation (A-3.2) the increase in the energy of the solid skeleton equals the amount of heat entering by conduction plus the heat evolved as the material absorbs or desorbs moisture.

The Neumann-type boundary conditions for Equation (A-3.1) and (A-3.2) can be formed as follows:

$$-\epsilon \tau_0 D_A \nabla \rho_V = h_{M,\rho} (\rho_V - \rho_{V,\alpha}) - q_M \quad (\text{A-3.3})$$

and

$$-k_T \nabla T = h_T (T - T_\alpha) - q_T \quad (\text{A-3.4})$$

The closure to the equations described in this section comes with the sorption isotherm data. The sorption isotherms can be represented with the following functional equation:

$$\rho_V = \rho_V(U, T) \quad (A-3.5)$$

Moisture movement in the vapor phase was substantiated by Gurr et al. 1952 and Kuzmak and Sereda 1957a, 1957b. They experimentally found that, in an unsaturated porous material such as soil, there is no flow in the liquid phase when moisture moves owing to a temperature gradient. The flow therefore occurs in the vapor phase. However, when there is pressure gradient, moisture flow occurs entirely in the liquid phase.

A further refinement of Henry's model was made by Harmathy 1969, who developed a theory for simultaneous mass and heat transfer during pendular state of a porous system. He based his model on the assumptions of the evaporation-condensation theory and on the assumption that the phases of a porous system are so finely distributed that from a macroscopic stand point, the system is a quasi-one-phase system. A system of equations was obtained that yielded the complete moisture content, temperature, and pressure history of the system. Harmathy concluded that the capillary flow mechanism is not the only one present at the beginning of the falling rate period, but that vapor transfer by diffusion also occurs.

Hougen et al. 1940 stated that moisture may move by vapor diffusion through a solid, provided that a temperature gradient is established, thus creating a vapor-pressure gradient toward the drying surface. Vaporization and vapor diffusion may be applied to any solid where heating is taking place on one surface and drying on the other, and when water is isolated between solid granules.

Another important point to be emphasized is that the product of tortuosity of the diffusion path and diffusion coefficient of moisture in air is equal to the vapor diffusivity; mathematically the following can be written:

$$D_V = \tau_0 D_A \quad (A-3.6)$$

A.4 LUIKOV'S THEORY

Luikov is credited by Russian researchers with discovering the phenomenon of moisture thermal diffusion and with establishing the fact that temperature gradient is also a factor causing moisture migration in materials. In the development of Luikov's theory, the principle of irreversible thermodynamics is used. The basic equation of the thermodynamics of irreversible processes

$$\frac{d_i S}{d\tau} = \sum_i J_i X_i > 0 \quad (A-4.1)$$

relates the rate of entropy production to the fluxes and thermodynamic forces. Equation (A-4.1) can be derived from the Gibbs equation:

$$T dS = dU + P dV - \sum_i \mu_i dn_i \quad (A-4.2)$$

Equations (A-4.1) and (A-4.2) assume that the entropy of the system, that is not in the equilibrium state, is determined by the same independent variables as in the equilibrium state. The following equation shows the linear relationships

between the driving forces and fluxes:

$$J_i = \sum_k L_{ik} X_k \quad \text{with } k=1,2,\dots,n \quad (\text{A-4.3})$$

where L_{ik} s' are the phenomenological coefficients. Equation (A-4.1) is restricted to the domain of validity of the linear equation (A-4.3), where the L_{ik} s' are assumed to be constant. However, in actuality, the phenomenological coefficients are functions of the thermodynamic forces. In high-rate transient processes, the conditions for linearity cannot be satisfied. For small deviations from the equilibrium state, the linear laws may be expressed as:

$$J_i = L_i^n J_i + \sum_k (L_{ik} X_k + L_{ik} X'_k) \quad (\text{A-4.4})$$

In the case of small perturbations of the thermodynamic forces, Equation (A-4.4) can be written as:

$$J_i = L_i^n J_i + \sum_k L_{ik} X_k \quad (\text{A-4.5})$$

where L_{in} may be called a relaxation coefficient. In the case of internal heat and mass transfer in capillary-porous bodies, Luikov assumed that the fluxes due to vapor diffusion and liquid diffusion are made up of two parts: one due to the total concentration gradient, and another due to temperature gradient.

$$J_L = -D_L \rho_S \nabla U - D_{LT} \rho_S \nabla T \quad (\text{A-4.6})$$

$$J_V = -D_V \rho_S \nabla U - D_{VT} \rho_S \nabla T \quad (\text{A-4.7})$$

Luikov's equations are then derived with the following assumptions:

1. Molecular and molar transport of vapor, air and water proceed simultaneously. The transfer of vapor and air takes place by diffusion, effusion and filtration, when under pressure gradients. The transport of liquid is assumed to occur by diffusion, capillary absorption, and filtration. All these types of transfer are called diffusion, and expressions similar to Fick's law are used, Equations (A-4.6) and (A-4.7).
2. Shrinkage and deformation are neglected.
3. Direct linkage between the governing equations and the sorption isotherms is not taken into account.
4. Isotropy is assumed and the relaxation term [Equation (A-4.5)] is ignored.

A mass balance over a differential element yields:

$$\rho_S \frac{\partial U_V}{\partial t} = -\nabla \cdot J_V + m_{ev} \quad (\text{A-4.8})$$

and

$$\rho_S \frac{\partial U_L}{\partial \tau} = -\nabla \cdot J_L - m_{ev} \quad (\text{A-4.9})$$

where in Equations (A-4.8) and (A-4.9) m_{ev} , denotes the rate of evaporation. Adding Equations (A-4.8) and (A-4.9)

$$\rho_S \frac{\partial (U_L + U_V)}{\partial \tau} = -\nabla \cdot (J_L + J_V) \quad (\text{A-4.10})$$

since $U_L \gg U_V$

$$U = U_L + U_V \approx U_L \quad (\text{A-4.11})$$

the energy balance leads to

$$C_S \rho_S \frac{\partial T}{\partial \tau} = -\nabla \cdot J_T + (h_V - h_L) m_{ev} - (C_L J_L + C_V J_V) \cdot \nabla T \quad (\text{A-4.12})$$

however

$$\nabla \cdot J_T \gg (C_L J_L + C_V J_V) \quad (\text{A-4.13})$$

The evaporation rate m_{ev} is also defined as follows:

$$m_{ev} = \gamma \rho_S \frac{\partial U}{\partial \tau} \quad (\text{A-4.14})$$

where γ is a dimensionless factor that characterizes the resistance to vapor diffusion. Consequently, from Equations (A-4.8) through (A-4.14), Luikov's equations can be obtained.

$$\frac{\partial U}{\partial \tau} = \nabla \cdot [D_W (\nabla U + \delta \nabla T)] \quad (\text{A-4.15})$$

and

$$C_S \rho_S \frac{\partial T}{\partial \tau} = \nabla \cdot (k_T \nabla T) + \lambda \gamma \rho_S \frac{\partial U}{\partial \tau} \quad (\text{A-4.16})$$

where

$$D_W = D_L + D_V \quad (\text{A-4.17})$$

$$\delta = \frac{D_{LT} + D_{VT}}{D_L + D_V} \quad (\text{A-4.18})$$

and

$$\lambda = h_V - h_L \quad (\text{A-4.19})$$

After some simple manipulations, Equations (A-4.15) and (A-4.16) can be rearranged to give the following elliptic equations:

$$\frac{\partial T}{\partial \tau} = \nabla \cdot (K_{11} \nabla T) + \nabla \cdot (K_{12} \nabla U) \quad (\text{A-4.20})$$

$$\frac{\partial U}{\partial \tau} = \nabla \cdot (K_{21} \nabla T) + \nabla \cdot (K_{22} \nabla U) \quad (\text{A-4.21})$$

with

$$K_{11} = \alpha + \frac{\lambda \gamma}{C_S} D_W \delta \quad (\text{A-4.22})$$

$$K_{12} = \frac{\lambda \delta}{C_S} D_W \quad (\text{A-4.23})$$

$$K_{21} = D_W \delta \quad (\text{A-4.24})$$

$$K_{22} = D_W \quad (\text{A-4.25})$$

When two different moist materials are in contact, there may be mass transfer from the body with lesser liquid concentration to the one of higher liquid concentration. To explain this fact, Luikov in 1964 and 1975 introduced the concept of mass transfer potential, in analogy with heat content (enthalpy) in the theory of heat transfer. The moisture transfer potential M is defined as a function of the moisture content and the temperature of the body.

$$M = M(U, T) \quad (\text{A-4.26})$$

Hence, differentiating Equation (A-4.26) the following equation can be obtained:

$$dM = \frac{\partial M}{\partial U} dU + \frac{\partial M}{\partial T} dT \quad (\text{A-4.27})$$

where

$$C_M = \frac{\partial U}{\partial M} \quad (\text{A-4.28})$$

and

$$M_T = \frac{\partial M}{\partial T} \quad (\text{A-4.29})$$

For references on general application of Luikov's theory, see Fullford 1969 and Luikov 1975. General analytical solutions of Equations (A-4.20) and (A-4.21) under a variety of boundary conditions are given by Mikhailov 1973. Similar approaches to heat and mass transfer in porous media, based on the principles of irreversible thermodynamics are given by Cary and Taylor 1962, Taylor and Cary 1964 and Taylor 1965.

Comini and Lewis 1975, and Comini and Giudice 1978 investigated heat and mass transfer in buildings by using the Luikov's equations. In their study they solved the governing equations with two-dimensional finite element model for linear properties. Morgan et al. 1980 and Lewis et al. 1980 used the same governing equations in order to study drying-induced stresses. The governing equations are solved with the two-dimensional finite element model and in these studies non linear and linear material properties are used. Valcharova and Valchar 1980 used the same governing equations to study the thermokinetics of the moisture transport in solids during drying. In this study once again the governing equations are solved by a two-dimensional finite element model and the material properties are assumed to be constant. In later research by Kohonen 1984, similar governing equations are used to analyze the transient hygrothermal behavior of building materials and components in two-dimensional space. Kohonen solved the system of equations by the finite difference method.

A.5 PHILIP AND DE VRIES' THEORY

Independent of Luikov's work, Philip and De Vries derived a set of equations describing the combined heat and mass transfer under temperature and moisture gradients. This approach is a mechanistic one that basically assumes that water moves by both vapor diffusion and capillarity. A brief description of their theory is given below:

The commonly used expression for the vapor flux is given by the following equation:

$$J_V = -\epsilon \tau_0 D_A \frac{P}{P - P_V} \nabla \rho_V \quad (A-5.1)$$

Philip and De Vries extended Equation (A-5.1) to show separately the effects of isothermal and thermal components of vapor transfer. This can be accomplished by writing the expression for the chemical potential of water under a meniscus, in a capillary tube:

$$\Delta\mu = \Psi g \quad (A-5.2)$$

In Equation (A-5.2), Ψ denotes the water pressure in thermodynamic equilibrium with the water in the medium, with atmospheric pressure as datum; consequently Ψ is negative in unsaturated media. It should be noted that Ψ is a function of moisture content and temperature, hence

$$\Psi = \Psi(U, T)$$

Equation (A-5.2) can be written in a slightly modified form to give

$$\Delta\mu = R_V T \ln \frac{\rho_V}{\rho_{V,sat}} \quad (A-5.3)$$

From Equations (A-5.2) and (A-5.3), the density of the water vapor can be defined as:

$$\rho_V = \rho_{V,sat} \Phi = \rho_{V,sat} \exp\left(\frac{\Psi g}{R_V T}\right) \quad (A-5.4)$$

Since

$$\rho_{V,sat} = \rho_{V,sat}(T)$$

and assuming that

$$\Phi = \Phi(U)$$

Equation (A-5.4) can be written as:

$$\nabla \rho_V = \Phi \frac{d\rho_{V,sat}}{dT} \nabla T + \frac{g \rho_V}{R_V T} \frac{\partial \Psi}{\partial U} \nabla U \quad (A-5.5)$$

Substitution of Equation (A-5.5) into Equation (A-5.1) gives the expression for the vapor flux in terms of concentration and temperature gradients:

$$J_V = -D_V \nabla U - D_{VT} \nabla T \quad (A-5.6)$$

with

$$D_V = \epsilon \tau_0 D_A \frac{P}{P - P_V} \frac{g \rho_V}{R_V T} \frac{\partial \Psi}{\partial U} \quad (A-5.7)$$

and

$$D_{VT} = \epsilon \tau_0 D_A \frac{P}{P - P_V} \Phi \frac{d\rho_{V,sat}}{dT} \quad (A-5.8)$$

In the above equations, D_V and D_{VT} denote the isothermal liquid diffusivity and thermal vapor diffusivity, respectively. The expression for the nonisothermal liquid flux can be obtained from Darcy's law for unsaturated porous media:

$$J_L = -D_H \rho_L \nabla \Psi \quad (A-5.9)$$

where in Equation (A-5.9) Ψ represents the total potential. In the range of capillary condensation, it is assumed that Ψ is proportional to the surface tension σ , so that

$$\frac{\partial \Psi}{\partial T} - \frac{\Psi}{\sigma} \frac{d\sigma}{dT} = \gamma \Psi \quad (\text{A-5.10})$$

Substituting Equation (A-5.10) into Equation (A-5.9), an expression for the liquid flux can be obtained.

$$J_L = - D_L \nabla U - D_{LT} \nabla T \quad (\text{A-5.11})$$

with

$$D_L = D_H \rho_L \frac{\partial \Psi}{\partial U} \quad (\text{A-5.12})$$

and

$$D_{LT} = D_H \rho_L \gamma \Psi \quad (\text{A-5.13})$$

By combining Equations (A-5.6) and (A-5.11), the total flux of water J_W is obtained as:

$$J_W = - D_W \nabla U - D_{WT} \nabla T \quad (\text{A-5.14})$$

where

$$D_{WT} = D_{LT} + D_{VT} \quad (\text{A-5.15})$$

$$D_W = D_L + D_V \quad (\text{A-5.16})$$

From Equation (A-5.14), by applying the continuity requirement, the general governing equations can be obtained:

$$\frac{\partial U}{\partial \tau} = \nabla \cdot (D_{WT} \nabla T) + \nabla \cdot (D_W \nabla U) \quad (\text{A-5.17})$$

$$\rho_S C_S \frac{\partial T}{\partial \tau} = \nabla \cdot (k_T \nabla T) + \lambda \nabla \cdot (D_V \nabla U) \quad (\text{A-5.18})$$

The major limitation of Philip and De Vries' theory lies in the use of Equations (A-5.4) and (A-5.10), which hold only for the capillary region of the isotherms, since only then is there liquid continuity in the pores and capillaries. A further refinement on this theory was made by De Vries 1958, to incorporate heat of wetting and transfer of sensible heat and to differentiate between changes in moisture content in the liquid and vapor phases.

A.6 KRISCHER'S AND BERGER AND PEI'S THEORIES

In an extensive treatise, Krischer 1963 analyzed heat and mass transfer in a variety of porous media. His work has served as a basis for much of the development of drying theories. Krischer assumes that moisture can migrate in the liquid state by capillarity, and in the vapor state by vapor concentration

gradients. In slightly modified form, the equations for the mass fluxes are:

$$J_L = -D_L \rho_L \nabla \theta \quad (\text{A-6.1})$$

$$J_V = -D_V \nabla P_V \quad (\text{A-6.2})$$

where D_L and D_V are the liquid and vapor diffusivities, respectively. Berger and Pei 1973 point out that the main difficulties encountered in Krischer's model are the application of the sorptional isotherm for the whole range of moisture content and the use of surface boundary conditions of the first kind. The Berger-Pei model employs the following basic assumptions:

1. The total internal mass transfer can be divided into two parts, the capillary flow of liquid due to gradient of liquid content, and the diffusion of vapor through the pores due to a gradient of partial vapor pressure. The internal heat transfer is governed by heat conduction through the solid skeleton and the latent heat-of-phase changes.
2. Inside the material, the rate-of-phase change is much faster than either of the rate of heat or mass transfer. Consequently, liquid content, partial vapor pressure, and temperature are in equilibrium at any location within the material.
3. For liquid contents larger than the maximum sorptional moisture contents, the partial vapor pressure is equal to its saturation value. For the sorptional region of liquid content, the partial vapor pressure is controlled by the sorptional isotherm.

Based on the supposition that for small temperature changes the partial vapor pressure gradient is proportional to the vapor density gradient, the following equation can be written:

$$\frac{1}{R_V T} \nabla P_V = \nabla \left(\frac{P_V}{R_V T} \right) = \nabla \rho_V \quad (\text{A-6.3})$$

thus, the vapor flux can be expressed as:

$$J_V = -D_V (\epsilon - \theta) \nabla \rho_V \quad (\text{A-6.4})$$

and the liquid flux can be expressed as:

$$J_L = -D_L \rho_L \nabla \theta \quad (\text{A-6.5})$$

In Equations (A-6.4) and (A-6.5), it is assumed that Fick's law is applicable to both mass transfer mechanisms. A mass balance over a differential element of unit cross sectional area and thickness, dx , leads to the differential equations for the liquid and vapor transfer.

$$D_L \rho_L \nabla^2 \theta - m_{ev} = \rho_L \frac{\partial \theta}{\partial t} \quad (\text{A-6.6})$$

and

$$D_V \nabla \cdot [(\epsilon - \theta) \nabla \rho_V] + m_{ev} = \frac{\partial}{\partial \tau} [(\epsilon - \theta) \rho_V] \quad (A-6.7)$$

In Equations (A-6.6) and (A-6.7), m_{ev} denotes the rate of evaporation within the material. If Equation (A-6.7) is differentiated by parts and m_{ev} is eliminated between Equations (A-6.6) and (A-6.7), the differential equation representing the total mass transfer can be obtained.

$$(\rho_L - \rho_V) \frac{\partial \theta}{\partial \tau} + (\epsilon - \theta) \frac{\partial \rho_V}{\partial \tau} = D_L \rho_L \nabla^2 \theta + D_V [(\epsilon - \theta) \nabla^2 \rho_V - \nabla \theta \nabla \rho_V]$$

If the heat flux is expressed by the Fourier law of conduction,

$$J_T = -k_T \nabla T \quad (A-6.9)$$

and realizing that the rate of latent heat required for or liberated by phase change is:

$$q_{ev} = m_{ev} \lambda \quad (A-6.10)$$

the energy balance for a differential element would be:

$$\frac{\partial T}{\partial \tau} = \alpha \nabla^2 T + \frac{\lambda}{\rho_S C_S} \{ D_V [(\epsilon - \theta) \nabla^2 \rho_V - \nabla \theta \nabla \rho_V] - (\epsilon - \theta) \frac{\partial \rho_V}{\partial \tau} + \rho_V \frac{\partial \theta}{\partial \tau} \} \quad (A-6.11)$$

Newmann-type boundary conditions for Equations (A-6.8) and (A-6.11) would be:

$$-D_L \rho_L \nabla \theta - D_V (\epsilon - \theta) \nabla \rho_V = h_M (\rho_V - \rho_{V,\alpha}) \quad (A-6.12)$$

and

$$-k_T \nabla T = \lambda D_L \rho_L \nabla \theta + h_T (T - T_\alpha) \quad (A-6.13)$$

Equation (A-6.12) states that the sum of liquid vapor flux to the surface must be equal to the vapor flux away from the surface into the media. In case of impermeable and adiabatic surface, Equations (A-6.12) and (A-6.13) would be:

$$D_L \rho_L \nabla \theta - D_V (\epsilon - \theta) \nabla \rho_V = 0 \quad (A-6.14)$$

and

$$k_T \nabla T = 0 \quad (A-6.15)$$

For the sorptional region of liquid content, the sorptional isotherm is used to obtain a closure. The sorption isotherm in general, can be represented by

$$\rho_V = \rho_V(\theta, T) \quad (A-6.16)$$

For liquid contents larger than the maximum sorptional content, the vapor pressure is equal to the saturation value. Thus, the Clausius-Clapeyron equation may be written as:

$$\rho_{V, \text{sat}} = \frac{1}{R_V T} \exp\left(58.7395 - \frac{6847.36}{T} - 5.62 \ln(T)\right) \quad (\text{A-6.17})$$

and the maximum sorptional liquid content Φ_M will be a function of temperature only.

$$\theta_M = \theta_M(T) \quad (\text{A-6.18})$$

Equations (A-6.16) and (A-6.18) can be obtained from experiments.

A.7 LOW-INTENSITY HEAT AND MOISTURE TRANSFER IN MOIST SOILS

In this section, macroscopic conservation equations for moist materials are presented in terms of the fluxes of vapor, air, and liquid. The equations to be developed are based upon the following assumptions:

1. The liquid water density is assumed to be constant; specific heats of material, water, vapor and air are allowed to vary with temperature; and the vapor and air in the pores are assumed to obey ideal gas law.
2. The material is isotropic, and the structure remains fixed.
3. The mass of water vapor present in the pores is negligible compared to the mass of liquid.
4. Flow of fluid due to gravity is neglected.

CONSERVATION EQUATIONS

According to Philip and De Vries 1957, Luikov 1966, Huang 1979 and Whitaker 1980, the governing conservation equations for mass and energy are written as:

$$\rho_L \frac{\partial \theta}{\partial \tau} = -\nabla \cdot (J_L + J_V) \quad (\text{A-7.1})$$

and

$$C^* \frac{\partial T}{\partial \tau} = -\nabla \cdot (-k_T \nabla T + h_L J_L + h_V J_V + h_A J_A) \quad (\text{A-7.2})$$

In Equation (A-7.2) C^* denotes the volumetric heat capacity and is defined as follows:

$$C^* = (\epsilon - \theta) (\rho_V C_V + \rho_A C_A) + \rho_L C_L + (1 - \epsilon) \rho_S C_S \quad (\text{A-7.3})$$

Denoting the sum of liquid and vapor fluxes as:

$$J_W = J_L + J_V$$

Equation (A-7.2) can be written as follows:

$$C^* \frac{\partial T}{\partial \tau} = -\nabla \cdot (-k_T \nabla T + h_L J_W + h_{LV} J_V + h_A J_A) \quad (\text{A-7.4})$$

The air density, ρ_A , can be written in terms of the density and the partial pressure of the air as:

$$\rho_A = \frac{P - P_V}{R_A T} \quad (\text{A-7.5})$$

The vapor density and pressure can be expressed using the relative humidity of the vapor.

$$\rho_V = \Phi \rho_{V,sat} \quad \text{and} \quad P_V = \Phi P_{V,sat} \quad (\text{A-7.6})$$

where the relative humidity can be obtained from a relation derived by Edlefsen and Andersen 1943.

$$\Phi = \exp\left(\frac{\Psi_M}{R_V T}\right) \quad (\text{A-7.7})$$

The matric potential, Ψ_M , is the negative of the suction and is a function of temperature and volumetric moisture content, therefore,

$$\Psi_M = \Psi_M(\theta, T) \quad (\text{A-7.8})$$

MASS FLUXES

The expressions for the liquid and vapor fluxes can be written as follows:

$$J_L = -D_L \rho_L \nabla \theta - D_{LT} \rho_L \nabla T \quad (\text{A-7.9})$$

and

$$J_V = -D_V \rho_L \nabla \theta - D_{VT} \rho_L \nabla T \quad (\text{A-7.10})$$

The total moisture flux

$$J_W = -D_W \rho_L \nabla \theta - D_{WT} \rho_L \nabla T \quad (\text{A-7.11})$$

where

$$D_W = D_V + D_L \quad \text{and} \quad D_{WT} = D_{VT} + D_{LT}$$

LIQUID FLUX

The flow of liquid in an unsaturated medium is described by a modified form of Darcy's law,

$$J_L = \frac{-\rho_L^2}{\mu_L} K_{sat} k_{rel} \nabla \Psi_M \quad (\text{A-7.12})$$

Substituting Equation (A-7.8) into Equation (A-7.12), the following expression for the liquid flux can be obtained:

$$J_L = \frac{-\rho_L^2}{\mu_L} K_{sat} k_{rel} \left(\frac{\partial \Psi_M}{\partial \theta} \nabla \theta + \frac{\partial \Psi_M}{\partial T} \nabla T \right) \quad (A-7.13)$$

Comparing Equation (A-7.13) with Equation (A-7.9), the following diffusivities can be obtained:

$$D_L = \frac{\rho_L K_{sat} k_{rel}}{\mu_L} \frac{\partial \Psi_M}{\partial \theta} \quad (A-7.14)$$

and

$$D_{LT} = \frac{\rho_L K_{sat} k_{rel}}{\mu_L} \frac{\partial \Psi_M}{\partial T} \quad (A-7.15)$$

VAPOR FLUX

The flow of water vapor can occur in bulk due to a pressure gradient or by diffusion due to temperature or moisture content gradients. In low intensity applications, no significant pressure gradients develop, and bulk flow is neglected, leaving out only flow by diffusion. Fick's law is generally used to describe the flow of air and water vapor by diffusion. The most frequently used form is:

$$J_V = -D_{VA} \rho_G \nabla \left(\frac{\rho_V}{\rho_G} \right) \quad (A-7.16)$$

and

$$J_A = -J_V \quad (A-7.17)$$

In Equation (A-7.16) D_{VA} is the molecular diffusivity of water vapor in air modified to account for the tortuosity and reduction in the flow area, and the density of the air vapor mixture in the pores is given by:

$$\rho_G = \rho_A + \rho_V \quad \text{or} \quad \rho_G = \rho_A + \Phi \rho_{V,sat}$$

since

$$\frac{\rho_V}{\rho_G} = \frac{\rho_V}{\rho_G}(T, \theta) \quad (A-7.18)$$

Substituting Equation (A-7.18) into Equation (A-7.16) and performing the differentiation, an expression for the vapor flux can be obtained.

$$J_V = -D_{VA} \rho_G \left[\frac{\partial(\rho_V/\rho_G)}{\partial\theta} \nabla\theta + \frac{\partial(\rho_V/\rho_G)}{\partial T} \nabla T \right] \quad (\text{A-7.19})$$

Comparing Equation (A-7.19) with Equation (A-7.10), the following diffusivities can be written:

$$D_V = D_{VA} \frac{\rho_G}{\rho_L} \frac{\partial(\rho_V/\rho_G)}{\partial\theta} \quad (\text{A-7.20})$$

$$D_{VT} = D_{VA} \frac{\rho_G}{\rho_L} \frac{\partial(\rho_V/\rho_G)}{\partial T} \quad (\text{A-7.21})$$

$$D_A = -D_V \quad (\text{A-7.22})$$

$$D_{AT} = -D_{VT} \quad (\text{A-7.23})$$

Using Equations (A-7.6) and (A-7.7), Equations (A-7.20) and (A-7.21) can be written as follows:

$$D_V = \frac{\nu \rho_{V,\text{sat}} D_{VA}}{\rho_L} \frac{\partial\Phi}{\partial\theta} = \frac{\nu \rho_{V,\text{sat}} D_{VA}}{\rho_L R_V T} \frac{\partial\Psi_M}{\partial\theta} \quad (\text{A-7.24})$$

and

$$D_{VT} = \frac{\nu \rho_{V,\text{sat}} D_{VA}}{\rho_L} \left(\frac{\Phi h_{LV}}{R_V T^2} + \frac{\partial\Phi}{\partial T} \right) \quad (\text{A-7.25.a})$$

or

$$D_{VT} = \frac{\nu \Phi \rho_{V,\text{sat}} D_{VA}}{\rho_L R_V T^2} \left(h_{LV} - \Psi_M + T \frac{\partial\Psi_M}{\partial T} \right) \quad (\text{A-7.25.b})$$

where

$$\nu = 1 - \frac{\Phi \rho_{V,\text{sat}}}{\rho_G} \left(1 - \frac{R_V}{R_A} \right) \quad (\text{A-7.26})$$

FINAL FORM OF GOVERNING EQUATIONS

Inserting the expressions for flux [Equations (A-7.9) through (A-7.11)] into the governing equations [Equations (A-7.1) and (A-7.2)] yields the final governing equations:

$$\frac{\partial\theta}{\partial\tau} = \nabla \cdot (D_W \nabla\theta + D_{WT} \nabla T) \quad (\text{A-7.27})$$

And for the conservation of energy

$$C^* \frac{\partial T}{\partial \tau} = \nabla \cdot ([k_T + \rho_L h_L D_{WT} + \rho_L (h_{LV} - h_A) D_{VT}] \nabla T + [\rho_L h_L D_W + \rho_L (h_{LV} - h_A) D_V] \nabla \theta) \quad (A-7.28)$$

The boundary conditions for Equations (A-7.27) and (A-7.28) would be:

$$-(D_W \nabla \theta + D_{TW} \nabla T) \cdot n = h_{M,\rho} (\rho_V - \rho_{V,\alpha}) - q_M \cdot n \quad (A-7.29)$$

and

$$-([k_T + \rho_L h_L D_{WT} + \rho_L (h_{LV} - h_A) D_{VT}] \nabla T + [\rho_L h_L D_W + \rho_L (h_{LV} - h_A) D_V] \nabla \theta) \cdot n = h_T (T - T_\alpha) - q_T \cdot n \quad (A-7)$$

A.8 HEAT AND MASS TRANSFER EQUATIONS AND IRREVERSABLE THERMODYNAMICS

A capillary porous medium that contains a certain amount of moisture can be subject to a set of gradients that will cause heat and/or mass to be transferred. These gradients may be

1. Water vapor partial pressure
2. Local humidity ratio
3. Temperature
4. Total pressure
5. Gravity.

If the total pressure is assumed to be constant and the effect of gravity is neglected, then the governing equations for heat and mass transfer can be derived. Additionally, reasonable values of the coefficients can be found either from the structural properties of the medium or from the experiments.

Linear thermodynamics of irreversible processes has been applied to the combined heat and mass transfer problem by several researchers. Luikov 1964, Cary and Taylor 1962, Valchar 1966 are some of the early researchers. Fortes and Okos 1978a, and 1978b have proposed a drying theory based on non-equilibrium thermodynamics; this theory was later shown to apply to food drying.

The procedure which leads to the constitutive equations by means of linear thermodynamics of irreversible processes is adapted from Prigogine 1961. It is important to realize that there are some limitations of the use of thermodynamics of irreversible processes.

In the derivation of the governing equations, the following assumptions are made:

1. The total pressure within the medium is constant.

2. The influence of gravity is negligible.
3. The inert gas velocity is negligible.
4. There is local equilibrium among liquid and vapor phases of water.

Consequently, under the above assumptions, the fluxes for pure heat, liquid water and water vapor can be written as follows:

$$J_i = \sum L_{ij} X_j \quad (\text{A-8.1})$$

$$J_T = L_{TT} X_T + L_{TL} X_L + L_{TV} X_V$$

$$J_L = L_{LT} X_T + L_{LL} X_L + L_{LV} X_V \quad (\text{A-8.2})$$

$$J_V = L_{VT} X_T + L_{VL} X_L + L_{VV} X_V$$

Equation (A-8.2) contains nine symmetrical phenomenological coefficients that fall into four categories:

1. Three direct coefficients L_{TT} , L_{LL} and L_{VV} .
2. Two typical cross coefficients L_{LV} and L_{VL} which represents the interaction among liquid and vapor phases.
3. Two Dufour-like coefficients L_{TL} and L_{TV} that characterize the flow of heat induced by vapor and liquid potential gradients.
4. Two Soret-like coefficients L_{LT} and L_{VT} that characterize the flow of matter induced by temperature gradient.

The driving forces may be written as:

$$X_T = - \frac{1}{T^2} \nabla T \quad (\text{A-8.3})$$

$$X_L = - \frac{1}{T} (\nabla \mu_L)_T \quad (\text{A-8.4})$$

$$X_V = - \frac{1}{T} (\nabla \mu_V)_T \quad (\text{A-8.5})$$

Since the vapor and liquid phases are in local equilibrium with each other, the chemical potential of the liquid and vapor phases are equal. Consequently, the driving forces for vapor and liquid transfer are equal.

$$X_L = X_V \quad (\text{A-8.6})$$

The chemical potential can be defined as:

$$\mu_V = \mu_L \approx \mu_L + R_V T \ln \frac{P_V}{P_{V,sat}} \quad (\text{A-8.7})$$

or using the definition of relative humidity (also called liquid activity)

$$\Phi = \frac{P_V}{P_{V,sat}} \quad (\text{A-8.8})$$

The chemical potential, Equation (A-8.6) can be rewritten as:

$$\mu_V = \mu_L \approx \mu_L^* + R_V T \ln(\Phi) \quad (\text{A-8.9})$$

Consequently, the driving forces for liquid and vapor transfer can be written as:

$$X_L = X_V = - \frac{1}{T} [\nabla(RT \ln \Phi)]_T = - \frac{R}{\Phi} (\nabla \Phi)_T \quad (\text{A-8.10})$$

Inserting Equation (A-8.10) into Equations (A-8.2)

$$J_T = - \frac{L_{TT}}{T^2} \nabla T - (L_{TL} + L_{TV}) \frac{R}{\Phi} (\nabla \Phi)_T \quad (\text{A-8.11})$$

$$J_L = - \frac{L_{LT}}{T^2} \nabla T - (L_{LL} + L_{LV}) \frac{R}{\Phi} (\nabla \Phi)_T \quad (\text{A-8.12})$$

$$J_V = - \frac{L_{VT}}{T^2} \nabla T - (L_{VL} + L_{VV}) \frac{R}{\Phi} (\nabla \Phi)_T \quad (\text{A-8.13})$$

For the mechanistic approach, the vapor flux, J_V , is assumed to be occurring by diffusion caused by a vapor concentration gradient and is given by:

$$J_V = -D_V \nabla \rho_V \quad (\text{A-8.14})$$

where the vapor diffusivity, D_V , is defined by

$$D_V = -\epsilon r_0 D_A \frac{P}{P - P_V} \quad (\text{A-8.15})$$

since

$$\Phi = \frac{\rho_V}{\rho_{V,sat}} \quad (\text{A-8.16})$$

Using Equation (A-8.16) in Equation (A-8.14) and differentiating, an expression for the vapor flux can be obtained.

$$J_V = -D_V (\rho_{V,sat} \frac{\partial \Phi}{\partial T} + \Phi \frac{d\rho_{V,sat}}{dT}) \nabla T - D_V \rho_{V,sat} (\nabla \Phi)_T \quad (A-8.17)$$

Similarly the liquid flux, J_L , can be defined by a modified form of Darcy's law

$$J_L = -k_L \rho_L \nabla \Psi_M \quad (A-8.18)$$

In Equation (A-8.18), Ψ_M denotes the water potential. The water potential is a combination of the gravimetric water potential, the osmotic water potential and the matric water potential.

$$\Psi_M = R_V T \ln \frac{P}{P_{V,sat}} = R_V T \ln \Phi \quad (A-8.19)$$

Hence, inserting Equation (A-8.19) into Equation (A-8.18) and carrying out the differentiation, the liquid flux equation can be obtained.

$$J_L = -k_L \rho_L R_V (\ln \Phi \nabla T + \frac{T}{\Phi} \nabla \Phi) \quad (A-8.20)$$

The phenomenological coefficients can be obtained by comparing Equation (A-8.17) to Equation (A-8.12) and Equation (A-8.20) to Equation (A-8.13). This can be accomplished by Onsager's reciprocal relations. The phenomenological coefficient of direct thermal effect can be obtained from Fourier's law as:

$$J_T = -k_T \nabla T \quad (A-8.21)$$

hence

$$L_{TT} = k_T T^2 \quad (A-8.22)$$

From Equation (A-8.12) and (A-8.20)

$$L_{LT} = k_L \rho_L R_V T^2 \ln \Phi \quad (A-8.23)$$

and

$$L_{LL} + L_{LV} = k_L \rho_L T \quad (A-8.24)$$

By comparing Equation (A-8.10) with Equation (A-8.17)

$$L_{VT} = D_V T^2 (\rho_{V,sat} \frac{\partial \Phi}{\partial T} + \Phi \frac{d\rho_{V,sat}}{dT}) \quad (A-8.25)$$

and

$$L_{VL} + L_{VV} = D_V \rho_{V,sat} \frac{\Phi}{R_V} \quad (A-8.26)$$

The final form of the heat flux can now be written using the Onsager relationship

$$J_T = -k_T \nabla T - [k_L \rho_L R_V \ln \Phi + D_V (\rho_{V, \text{sat}} \frac{\partial \Phi}{\partial T} + \Phi \frac{d\rho_{V, \text{sat}}}{dT})] \frac{RT^2}{\Phi} (\nabla \Phi)_T$$

and

$$\rho_{V, \text{sat}} = \frac{2.54 \times 10^8}{T} \exp\left(-\frac{5200}{T}\right) \quad (\text{A-8.28})$$

The final mass and energy conservation equation can be written as:

$$\rho_S \frac{\partial U}{\partial \tau} = -\nabla \cdot (J_L + J_V) \quad (\text{A-8.29})$$

and

$$\rho_S C_S \frac{\partial T}{\partial \tau} - \rho_S \Delta h_W \frac{\partial U}{\partial \tau} = -\nabla \cdot J_T - \Delta h_V \nabla J_V - (J_L C_L + J_V C_V)$$

The heat of vaporization and adsorption (wetting) of water in the material are given by the following equations:

$$\Delta h_V = \Delta h_o + \Delta h_W \quad (\text{A-8.31})$$

and

$$\Delta h_W = \frac{R_V T^2}{\Phi} \frac{\partial \Phi}{\partial T} \quad (\text{A-8.32})$$

where according to Brooker 1967 the latent heat of pure water vaporization is given by the following relation:

$$\Delta h_o = 3.11 \times 10^6 - 2.11 \times 10^3 T \quad (\text{A-8.33})$$

BOUNDARY CONDITIONS

$$J_L = J_V = 0$$

$$J_T = 0$$

$$J_L + J_V = h_{M,P} (P_V - P_{V,\alpha})$$

$$J_T + \Delta h_V J_L = h_T (T - T_\alpha)$$

NOMENCLATURE

C^*	Volumetric specific heat [W.h/m ³ .K]
C	Specific heat [W.h/kg.K]
C_A	Specific heat of dry air [W.h/kg.K]
C_L	Specific heat of liquid water [W.h/kg.K]
C_S	Specific heat of solid skeleton [W.h/kg.K]
C_V	Specific heat of water vapor [W.h/kg.K]
C_M	Specific isothermal moisture capacity [kg/kg.°M]
D_A	Molecular diffusivity of water vapor in air [m ² /h]
D_H	Unsaturated hydraulic conductivity [m/h]
D_L	Isothermal liquid water diffusivity [m ² /h]
D_{LT}	Thermal liquid water diffusivity [m ² /h.K]
D_V	Isothermal water vapor diffusivity [m ² /h]
D_{VT}	Thermal water vapor diffusivity [m ² /h.K]
D_W	Isothermal moisture (liquid+vapor) diffusivity [m ² /h]
D_{WT}	Thermal moisture (liquid+vapor) diffusivity [m ² /h.K]
$f(r)$	Differential curve for distribution of pore size by radius r
g	Acceleration due to gravity [m/h ²]
h_A	Enthalpy of dry air [W.h/kg]
h_L	Enthalpy of liquid water [W.h/kg]
$h_{M,p}$	Convective mass transfer coefficient based on pressure [kg/m ² .h.Pa]
$h_{M,\rho}$	Convective mass transfer coefficient based on concentration [m/h]
h_T	Convective heat transfer coefficient [W/m ² .K]
h_V	Enthalpy of water vapor [W.h/kg]
J_i	Flux
J_L	Liquid water flux [kg/m ² .h]
J_T	Thermal heat flux [W/m ²]

J_V	Water vapor flux [$\text{kg}/\text{m}^2 \cdot \text{h}$]
J_W	Moisture (liquid+vapor) flux [$\text{kg}/\text{m}^2 \cdot \text{h}$]
k_L	Liquid conductivity [h]
k_T	Effective (overall) thermal conductivity [$\text{W}/\text{m} \cdot \text{K}$]
k_{rel}	Liquid relative permeability [dimensionless]
K_{sat}	Saturated permeability [m^2]
K_{11}	Kinetic coefficient [m^2/h]
K_{12}	Kinetic coefficient [$\text{m}^2/\text{h} \cdot \text{K}$]
K_{21}	Kinetic coefficient [$\text{m}^2/\text{h} \cdot \text{K}$]
K_{22}	Kinetic coefficient [m^2/h]
L_{ij}	Phenomenological coefficients
M	Mass transfer potential [$^\circ\text{M}$]
M_T	temperature coefficient of mass transfer potential [$^\circ\text{M}/\text{K}$]
m_{ev}	Rate of internal evaporation [$\text{kg}/\text{m}^3 \cdot \text{h}$]
n	Unit outward normal vector [dimensionless]
U	Moisture (liquid+vapor) content dry basis [kg/kg]
U_L	Liquid content dry basis [kg/kg]
U_V	Vapor content dry basis [kg/kg]
P	Total pressure [$\text{kg}/\text{m} \cdot \text{h}^2$]
P_A	Dry air pressure [$\text{kg}/\text{m} \cdot \text{h}^2$]
P_V	Partial water vapor pressure [$\text{kg}/\text{m} \cdot \text{h}^2$]
q_M	Imposed moisture flux [$\text{kg}/\text{m}^2 \cdot \text{h}$]
q_T	Imposed heat flux [W/m^2]
R_A	Gas constant for dry air [$\text{W} \cdot \text{h}/\text{kg} \cdot \text{K}$]
R_V	Gas constant for water vapor [$\text{W} \cdot \text{h}/\text{kg} \cdot \text{K}$]
r	Radius [m]
r_o	Minimum radius [m]
r_l	Maximum radius [m]

S	Entropy [W.h/kg.K]
T	Temperature [K]
T_{α}	Ambient or medium temperature [K]
X_i	Thermodynamical force for substance i
X_L	Thermodynamical force for liquid water [W.h/kg.m.K]
X_T	Thermodynamical force energy equation [1/m.K]
X_V	Thermodynamical force water vapor [W.h/kg.m.K]

GREEK LETTERS

α	Thermal diffusivity [m^2/h]
γ	Resistance of vapor diffusion [dimensionless]
Δh_o	Specific latent heat of pure water vaporization [W.h/kg]
Δh_V	Specific latent heat of vaporization [W.h/kg]
Δh_W	Specific differential heat of wetting [W.h/kg]
δ	Thermogradient coefficient [1/K]
ϵ	Porosity or void fraction [m^3/m^3]
θ	Volumetric moisture content [m^3/m^3]
θ	Wetting angle in capillaries [radians]
λ	Latent heat of vaporization [W.h/kg]
μ	Dynamic viscosity [kg/m.h]
μ_i	Chemical potential of substance i
μ_L	Dynamic viscosity of liquid water [kg/m.h]
μ_L	Chemical potential of liquid water [W.h/kg]
μ_L^*	Chemical potential of pure water vapor [W.h/kg]
μ_V	Chemical potential of water vapor [W.h/kg]
ν	Kinematic viscosity [m^2/h]
ρ_A	Density of dry air [kg/m^3]
ρ_G	Density of air+vapor mixture [kg/m^3]

ρ_L	Density of liquid water, liquid water concentration [kg/m ³]
ρ_S	Density of solid skeleton [kg/m ³]
ρ_V	Density of water vapor, vapor concentration [kg/m ³]
$\rho_{V,a}$	Ambient or medium water vapor density or vapor concentration [kg/m ³]
σ	Surface tension [kg/h ²]
r	Time [s]
r_0	Factor taking into account the tortuosity of the diffusion path [dimensionless]
ϕ	Relative humidity [dimensionless]
ψ	Capillary potential, water pressure in thermodynamic equilibrium with the water [m]
ψ_M	Material moisture potential [W.h/kg]

SUBSCRIPTS

A	Air
G	Air-vapor mixture
L	Liquid
V	Vapor
W	Water (liquid+vapor)
S	Solid material
sat	Saturation
α	Ambient or medium

REFERENCES

- Babbit, J.D., "On the Differential Equations of Diffusion," Can. J. Res. A, Vol. 18, pp. 419-474, 1950.
- Berger, D. and Pei, D.C.T., "Drying of Hygroscopic Capillary Porous Solids-A Theoretical Approach," Int. J. Heat Mass Transfer, Vol. 16, pp. 293-302, 1973.
- Brooker, D.B., "Mathematical Model of the Psychrometric Chart," Trans. ASAE, Vol. 10, p. 558, 1967.
- Buckingham, E.A., "Studies on the Movement of Soil Moisture," U.S. Dept. Agr. Bull. 38, 1907.
- Cary, J.W. and Taylor, S.A., "The Interaction of Simultaneous Diffusion of Heat and Water Vapor," Soil Sci., Am. Proc., Vol. 28, pp. 167-172, 1962
- Ceaglske, N.H. and Hougen, O.A., "The Drying of Granular Solids," Trans. AIChE, Vol. 33, No. 3, pp. 283-312, 1937.
- Comini, G., and Giudice, S.D., "Finite Element Analysis of Heat and Mass Transfer in Buildings," in Energy Conservation in Heating, Cooling, and Ventilating Buildings, Edited by Hoogendoorn C.J., and Afgan N.H., Vol. 1 pp. 26-36, Hemisphere Publishing Co., New York, 1978.
- Comini, G., and Lewis, R.W., "A Numerical Solution of Two-Dimensional Problems Involving Heat and Mass Transfer," Int. J. Heat Mass Transfer, Vol. 19, pp. 1387-1392, 1975.
- De Vries, D.A., "Simultaneous Transfer of Heat and Moisture in Porous Media," Trans. Am. Geophys. Union, Vol. 39, No. 5, pp. 909-916, 1958.
- Fortes, M. and Okos, M.R., "A Non-equilibrium Thermodynamics Approach to Transport Phenomena in Capillary Porous Media," Proceeding of the First International Symposium on Drying, McGill University, Montreal, pp. 100-1009, 1978.
- Fortes, M. and Okos, M.R., "Heat and Mass Transfer in Hygroscopic Capillary Extruded Products," Paper presented at the 71 st Annual Meeting of the A.I.Ch.E., meeting, Miami Beach, Florida, 1978.
- Fullford, G.D., "A Survey of Recent Soviet Research on the Drying of Solids," Can. J. Chem. Eng., Vol. 47, pp. 378-391, 1969.
- Gurr, C.G, Marshall T.J. and Hutton J.T., "Movement of Water in Soil due to a Temperature Gradient," Soil Sci., Vol. 74, pp. 335-345, 1952.
- Harmathy, T.Z., "Simultaneous Moisture and Heat Transfer in Porous Systems with Particular Reference to Drying," Ind. Chem. Fundam., Vol. 8, No. 1, pp. 92-103, 1969.
- Henry, P.S.H., "Diffusion in Absorbing Media," Proc. R. Soc., Vol. 171A, pp. 215-241, London, 1939.

Hougen, O.A., et al., "Limitations of Diffusion Equations in Drying," Trans. AIChE, Vol. 36., No. 2, pp. 183-206, 1940.

Kohonen, R., "A Method to Analyze the Transient Hygrothermal Behaviour of Building Materials and Components," Technical Research Center of Finland, Publications 21, 88 p. 1984.

Krischer, O., "Die Wissenschaftlichen Grundlagen der Trocknungstechnik," Kap. IX, Springer, Berlin, 1963.

Kuzmak, J.M and Sereda, P.J., "The Mechanism by which Water Moves through a Porous Material Subjected to a Temperature Gradient: I. Introduction of a Vapor Gap into a Saturated System," Soil Sci., Vol. 84, pp. 291-299, 1957.

Kuzmak, J.M and Sereda, P.J., "The Mechanism by which Water Moves through a Porous Material Subjected to a Temperature Gradient: II. Salt Tracer and Streaming Potential to Detect Flow in the liquid Phase," Soil Sci., Vol. 84; pp. 419-422, 1957.

Lewis, R.W, Morgan, K., and Thomas, H.R, "The Nonlinear Modeling of Drying Induced Stresses in Porous Materials," in Advances in Drying'80 Vol. 1 pp. 233-268, Edited by Mujumdar, A.S., Hemisphere Publishing Co., New York, 1980.

Lewis, W.K., "The Rate of Drying of Solid Materials," J. ind. Eng. Chem., Vol. 13, pp. 427-432, 1921.

Luikov, A.V., "Heat and Mass Transfer in Capillary Porous Bodies," in T.F. Irvine et al. (eds)., Advances in Heat Transfer, Vol. 1, Academic Press, New York, 1964.

Luikov, A.V., "Systems of Differential Equations of Heat and Mass Transfer in Capillary-Porous Bodies (review)," Int. J. Heat Mass Transfer, Vol. 18., pp 1-14, 1975.

Morgan, K., Lewis, R.W, and Thomas, H.R, "Numerical Modeling of Drying Induced Stresses in Porous Materials," in Drying'80 Vol. 1 pp. 451-460, Proceedings of the 2nd International Symposium, Edited by Mujumdar, A.S., Hemisphere Publishing Co., New York, 1980.

Mikhailov, M.D., "General Solutions of the Diffusion Equations Coupled at Boundary Conditions," Int. J. Heat Mass Transfer, Vol. 16, pp. 2155-2164, 1973.

Miller E.E. and Miller R.D., "Theory of Capillary Flow: I. Practical Implications," Proc. Soil Sci. Soc. Am., Vol. 19, pp. 267-271, 1955.

Miller E.E. and Miller R.D., "Theory of Capillary Flow: II. Experimental Information," Proc. Soil Sci. Soc. Am., Vol. 19, pp. 272-275, 1955.

Newmann, A.B., "Diffusion and Surface Emission Equations," Trans. AIChE, Vol. 27, pp. 203-220, 1931.

Philip, J.R. and deVries, D.R., "Moisture Movement in Porous Media Under Temperature Gradients," Trans. Am. Geophysical Union, Vol. 38, pp. 222-232, 1957.

- Prigogine, I., Introduction to Thermodynamics of Irreversible Processes, Interscience Pub., Wiley, New York, 1961.
- Sherwood, T.K., "The Drying of Solids Part I," Ind. Eng. Chem., Vol.21, pp. 12-16, 1929.
- Sherwood, T.K., "The Drying of Solids Part II," Ind. Eng. Chem., Vol.21, pp. 976-980, 1929.
- Sherwood, T.K., "The Drying of Solids Part III Mechanism of the Drying of Pulp and Paper," Ind. Eng. Chem., Vol.22, pp. 132-136, 1930.
- Sherwood, T.K., "Application of the Theoretical Diffusion Equations to the Drying of Solids," Trans. AIChE, Vol. 27, pp. 190-202, 1931.
- Taylor, S.A. and Cary, J.W., "Linear Equations for the Simultaneous Flow Matter and Energy in Continuous Soil System," Soil Sci., Soc. Am. Proc., Vol. 28, pp. 167-172, 1964.
- Taylor, S.A., "The Influence of Steady Temperature Gradients upon Water Transport in Soil Materials," in Humidity and Moisture, Vol. 3, Reinhold, New York, 1965.
- Valchar, J., "Heat and Moisture Transfer in Capillary Porous Materials from the Point of View of the Thermodynamics of Irreversible Processes," Third Int., Heat Transfer Conference, Chicago, Vol. 1, pp. 409-418, 1966.
- Valcharova, J., and Valchar, J., "The Thermokinetics of the Moisture Transport in Solids During Drying," in Drying'80 Vol. 2 pp. 53-60, Proceedings of the 2nd International Symposium, Edited by Mujumdar, A.S., Hemisphere Publishing Co., New York, 1980.
- Withaker, S., "Heat and Mass Transfer in Granular Porous Media," in Advances in Drying, Vol. 1, Hemisphere, Washington, 1980.

APPENDIX B

FINITE ELEMENT SOLUTIONS

The basic concept of the finite element method is not new. It has been used throughout centuries for evaluating certain quantities (particularly area and volume) by adding or counting well-defined geometric figures (elements). Today the finite element method, however, is used to find an approximate solution for a boundary- and initial-value problem by assuming that the domain is divided into well-defined subdomains (elements) and that the unknown function of the state variable is defined approximately within each element. With these individually defined functions matching each other at the element nodes or at certain points at the interfaces, the unknown function is approximated over the entire domain.

There are, of course, many other approximate methods for the solution of boundary-value problems, such as finite-difference methods, weighted-residual methods, Rayleigh-Ritz methods, Galerkin methods, and more. The primary difference between the finite element method and most other methods is that in the former the approximation is confined to relatively small subdomains. It is, in a way, the localized version of the Rayleigh-Ritz method. Instead of finding an admissible function satisfying the boundary conditions for the entire domain (which, particularly for irregular domains, is often difficult), in the finite element methods the admissible functions are defined over the element domains with simple geometry and no attention is paid to the complications at the boundaries. This is one of the reasons that the finite element method has gained superiority over other approximate methods.

Since the entire domain is divided into numerous elements and the function is approximated in terms of its values at certain points (nodes), it is inevitable that the evaluation of such a function will require solution of simultaneous equations. Because of this, the finite element methods were not widely used until the middle of this century, when the computer became a powerful computational tool.

The variational principle provides an alternative statement of the differential equations that lends itself to the finite element method. The finite element method can be applied either with a variational method, based on a variational principle, or with the Galerkin method, which is applicable to all problems. The variational method is always equivalent to a Galerkin method, although the reverse is not true. The variational formulation allows one to obtain a firmer grasp on the underlying concepts behind the finite element method. It is by no means absolutely essential to the application of the method to practical problems. All variational formulations have a corresponding differential

formulation, but, unfortunately, the converse is not true: some differential formulations have no classical variational principle. (See Zienkiewicz 1977 for a procedure that yields a nonclassical variational formulation to some of these problems.) This does not mean that the finite element method cannot be used in these cases, because we simply resort to the more powerful weighted residual approach.

In this study, the Galerkin finite element method is used. In this appendix, the details of the finite element formulations and procedures are given. With the information contained here, a person who is familiar with numerical analysis and computer programming, can solve the governing equations that are given in Appendix A.

In Section B.1, some basic theory on the finite element formulations is provided, and later in Section B.2, the final Galerkin transient finite element equations are given. In Sections B.2 through B.9, the stiffness matrices, capacitance matrices and force vectors used in each of the combined heat and mass transfer theories are provided. In Section B.10, the formulation of the element types used in the analysis are given, and in Section B.11 for the same elements the isoparametric formulations are detailed. The element formulations are followed by the theory of numerical integrations that is used in the analysis. In Section B.12, the details of assemblage, storage and matrix solutions are given. Finally, Section B.13 presents the theories of the overall solution methods used.

B.1 ON THE THEORY OF FINITE ELEMENT FORMULATIONS

The finite element method formulations follow these basic steps:

1. Subdivision or discretization of the region of interest into a suitable number of finite elements
2. The process of localization, which includes the determination of the element characteristics
3. Generation of the assemblage system equations including the assemblage stiffness matrix and force vector
4. Application of prescribed boundary conditions
5. Elimination of known and trivial solutions from the system of equations
6. Solution of the problem and related quantities dictated by the type of results desired.

Each step of the finite element formulation is explained in detail in the following sections.

B.1.1 SUBDIVISION AND DISCRETIZATION

The first step in any finite element formulation, discretization, entails

subdivision of the area of interest into a specified or required number of suitable elements. In most finite element formulations, the number of elements used must be optimized. That is, depending on the problem size, computer time, and convergence criteria, one has to vary the number of elements until a "healthy" compromise is achieved.

In this study, one-dimensional line elements, two-dimensional rectangular elements and three-dimensional brick elements are used. For convenience in formulations, the nodal coordinates and element characteristics are changed to local normalized coordinates instead of global. Details of the elements are given in Section B.10.

B.1.2 PROCESS OF LOCALIZATION

For a typical element e , each parameter function may be written in terms of the nodal values at each node as

$$T = \sum_{i=1}^{non} N_i a_i^e = (N_1, N_2, \dots, N_n) (a_1, a_2, \dots, a_n)^T \quad (B-1.1)$$

where N_1, N_2, \dots, N_n are prescribed functions of local coordinates and a_1, a_2, \dots, a_n are the values of the unknowns at the nodal points. The nodal functions N_1, N_2, \dots, N_n are referred to as shape functions and are chosen so as to yield the values of the unknowns when the respective nodal coordinates are substituted into Equation (B-1.1).

Clearly, to satisfy the above statement, the values of the shape functions or position functions for the node under investigation should be unity at that node. The other position or shape functions should be zero for this node. In other words, we must have

$$N_1(x_1, y_1, z_1) = 1; \quad N_1(x_2, y_2, z_2) = 0$$

For the elements that are supported, the shape functions in terms of local normalized coordinates are given in Section B.10.

B.1.3 METHOD OF FORMULATION

As indicated earlier, the weighted residual method is used in this formulation for its simplicity, ease of application and versatility. The general weighted residual method has its basis in approximating the solution desired with an approximate function. For instance, if the nodal temperatures (T) were the nodal unknowns, then,

$$T = T(x, y, z, a_1, a_2, \dots, a_n) = \sum_{i=1}^{non} a_i N_i(x, y, z) \quad (B-1.2)$$

which has unknowns a_1, a_2, \dots, a_n . The functions N_1, N_2, \dots, N_n are the shape functions defined in Section B.10. Substitution of this approximate unknown T into the governing equations will not exactly satisfy the equation. If the

residual error is denoted as $R(x, y, z, a_1, a_2, \dots, a_n)$, then the weighted residual method requires the following:

$$\int w_i(x, y, z) R(x, y, z, a_1, a_2, \dots, a_n) dx dy dz = 0 \text{ for } i=1 \text{ to } n \quad (\text{B-1.3})$$

where the functions $w_i(x, y, z)$ are the non arbitrary weighting functions. Four weighting functions may be used in the finite element formulations.

1. Point collocation
2. Subdomain collocation
3. Least squares, and
4. Galerkin.

The Galerkin weighting functions are always taken to be the shape functions themselves, or

$$w_i(x, y, z) = N_i(x, y, z) \quad (\text{B-1.4})$$

With the relation given by Equation (B-1.4), Equation (B-1.3) becomes

$$\int N_i(x, y, z) R(x, y, z, a_1, a_2, \dots, a_n) dx dy dz = 0 \text{ for } i=1 \text{ to } n \quad (\text{B-1.5})$$

with one trial function for each unknown parameter. Equation (B-1.5) yields non equations, when solved, resulting in the values of a_1, a_2, \dots, a_n .

The finite element characteristics are derived next, using the Galerkin weighted residual method. The two parameter functions to be determined are listed below:

1. Temperature, and
2. Concentration

In the governing equations, each of these parameter functions is represented by a suitable polynomial that leads to the use of shape functions. Writing these parameter functions in terms of shape functions and nodal values gives the following

$$T = N a_T \quad C = N a_C \quad (\text{B-1.6})$$

In Equation (B-1.6) for mass transfer the field variable is assumed to be concentration. However, for different theories the field variables are different. For instance, in liquid diffusion theory the field variable is the moisture content, whereas in Luikov's theory the field variable is the mass transfer potential. Hence, depending on the governing equation, different field variables must be used and Equation (B-1.6) must be modified.

B.1.4 GOVERNING TRANSIENT FINITE ELEMENT EQUATION

The general governing finite element equation for a transient problem can be written as follows (a modified version of the equation given by Stasa 1985 and

Zienkiewicz 1977):

$$\begin{aligned}
 (C + K \Theta \Delta\tau) a^{\tau+\Delta\tau} &= + [C - (1-\Theta) K \Delta\tau] a^{\tau} \\
 &+ [(1-\Theta) F_1^{\tau} + \Theta F_1^{\tau+\Delta\tau}] \Delta\tau \\
 &+ F_2
 \end{aligned}
 \tag{B-1.7}$$

In Equation (B-1.7) C and K denote the capacitance and stiffness matrices, respectively, and F1 and F2 are the force vectors. The matrices and vectors used in Equation (B-1.7) for different heat and mass transfer theories are given in the subsequent sections.

The parameter Θ used in Equation (B-1.7) depends on the type of integration scheme. The type of numerical solution corresponding to each value of Θ is given in Table B-1.

TABLE B-1
Numerical Time Integration Constants

Θ	Type of Solution
0	Forward-difference scheme (Euler method)
1/3	Galerkin scheme (based on the shape function at the beginning of the time step)
1/2	Central-difference scheme (Crank-Nicholson)
2/3	Galerkin scheme (based on the shape function at the end of the time step)
1	Backward-difference scheme

FORWARD DIFFERENCE SCHEME

If the numerical time integration constant, Θ , is set to zero, then Equation (B-1.7) is referred to as a two-point recurrence scheme because the right-hand side is completely known at time τ , including $\tau=0$ for which the initial conditions apply. Consequently, Equation (B-1.7) may be applied recursively to obtain the nodal unknowns for a subsequent time given the unknowns for the preceding time. The forward difference method is also known as Euler's method.

If the lumped form of the capacitance matrix is used, the assemblage capacitance matrix C is diagonal. In this case the solution for the j-th nodal unknown is given explicitly by dividing the j-th row on the right-hand side of Equation (B-1.7) by the j-th diagonal entry in the C matrix. Hence, the solution in this case is frequently referred to as an explicit solution. This is the principal advantage of the forward difference (or Euler's) method. Conversely, if the consistent capacitance matrix is used, an implicit solution for a_{i+1} is required because C is no longer diagonal. In this case, an active zone equation solver

algorithm is used to determine the nodal unknowns at time $\tau + \Delta\tau$.

Euler's method is also convenient from the stand point of nonlinear analysis. For example, if the physical properties are functions of the nodal unknowns or thermal radiation is modeled, then the problems become nonlinear. Since the terms in Equation (B-1.7) must be evaluated at time τ and since the nodal unknowns are always known at this time, it is not necessary to iterate to obtain the solution for time $\tau + \Delta\tau$ for such problems.

The principal disadvantage of the Euler method, however, is the requirement of relatively small time steps. In other words, if the time step exceeds a certain critical value for the mesh used, the solution becomes oscillatory and fails to converge as the time increases. Even though the time step may be below this critical value, the results may still be quite inaccurate (but stable). The accuracy of this method generally improves for successively smaller time steps. In fact, a somewhat practical way to assess the accuracy of the solution is to compare the results for two different time steps, e.g., $\Delta\tau$ and $2\Delta\tau$. If the results for the two different time steps are within some acceptable tolerance, a good approximation to the true solution has been obtained.

BACKWARD DIFFERENCE SCHEME

If the numerical time integration constant used in Equation (B-1.7) is set to 1, then a backward difference scheme is simulated. As in the case of the recurrence formula from the forward difference method, the right-hand side is completely known at time τ including F_{i+1} because the vector F represents the forcing function for the analysis. Therefore, Equation (B-1.7) may be applied recursively to obtain the nodal unknowns for a subsequent time given the nodal unknowns for the previous time.

Note that even if the capacitance matrix C is diagonal, an implicit solution for the nodal unknown vector must be obtained because the stiffness matrix K is never a diagonal matrix. The backward difference method is stable for all $\Delta\tau$, but the accuracy deteriorates as the time step is increased. Again the accuracy can be assessed by comparing the results for two different time steps.

CENTRAL DIFFERENCE SCHEME

If the numerical time integration constant used in Equation (B-1.7) is set to 0.5, then a central difference scheme is simulated. As in the backward difference scheme, the recursion formula given by Equation (B-1.7) requires an implicit solution for the nodal unknowns at time $\tau + \Delta\tau$ given those at time τ . This method results in an oscillatory solution if the critical time step for stability is exceeded. For time steps smaller than this critical value, the accuracy of the solution improves as the time step is decreased. Not surprisingly, the central difference method is more accurate than both the forward and backward difference schemes because central differencing favors neither the nodal unknowns at time τ nor those at time $\tau + \Delta\tau$. The central difference method is also referred to as the Crank-Nicolson method.

Several examples on this subject are provided in Chapter 4 of this report.

LUMPED VERSUS CONSISTENT CAPACITANCE MATRICES

In the solution of the nodal unknowns, the initial part of the solution may tend to oscillate about the true solution if consistent capacitance matrix is used. These oscillations generally do not occur if the so-called lumped capacitance matrix is used. This does not imply that the solution with the lumped matrix is the exact solution. Some researchers argue that the wiggles that arise when consistent matrix is used are a signal to the analyst that smaller time steps should be used in the vicinity of the wiggles. Although Gresho and Lee 1979 contend that the results from the lumped matrix are more accurate due to the absence of wiggles, these results are erroneously accepted as correct.

The lumped matrix is a diagonal matrix and can be obtained by scaling the diagonal entries in the consistent capacitance matrix such that the total capacitance is preserved. In general, any lumping that preserves the total capacitance will lead to convergence. The reader may recall that the finite difference method always yields the lumped matrices directly. One advantage of the lumped form of the capacitance matrix is that the solution for the nodal unknowns (i.e., the nodal temperatures and concentrations) may be obtained in a more straightforward manner as explained above (i.e., a so called explicit solution results). The reader may want to consult Zienkiewicz 1977 for more information on the subject of lumping.

B.2 LIQUID DIFFUSION THEORY

The governing mass transfer equation with the proper boundary condition for the liquid diffusion theory follows:

$$\frac{\partial U}{\partial \tau} = \nabla \cdot (D_L \nabla U) \quad (\text{B-2.1})$$

Exposed to the boundary condition:

$$- D_L \nabla U = h_{M,\rho} (\rho_V - \rho_{V,\alpha}) - q_M \quad (\text{B-2.2})$$

The stiffness matrices, capacitance matrix and the force vectors used in the finite element formulations are given as:

$$C = + \int_{\Omega} N^T N \, d\Omega \quad (\text{B-2.3})$$

$$K = + \int_{\Omega} \frac{\partial N^T}{\partial x_i} D_L \frac{\partial N}{\partial x_i} \, d\Omega \quad (\text{B-2.4})$$

$$F1 = + \int_{\Gamma} N^T q_M \, d\Gamma - \int_{\Gamma} N^T h_{M,\rho} N (\rho_V - \rho_{V,\alpha}) \, d\Gamma \quad (\text{B-2.5})$$

The governing heat transfer equation with the proper boundary condition for the liquid diffusion theory is given by the following equations:

$$\rho_S C_p \frac{\partial T}{\partial \tau} = \nabla \cdot (k_T \nabla T) \quad (\text{B-2.6})$$

Exposed to the boundary condition:

$$-k_T \nabla T = h_T (T - T_\alpha) - q_T + \lambda h_{M,\rho} (\rho_V - \rho_{V,\alpha}) \quad (B-2.7)$$

The stiffness matrices, capacitance matrix and the force vectors used in the finite element formulations are given as:

$$C = + \int_{\Omega} N^T \rho_S C_p N \, d\Omega \quad (B-2.8)$$

$$K = + \int_{\Omega} \frac{\partial N^T}{\partial X_i} k_T \frac{\partial N}{\partial X_i} \, d\Omega \\ + \int_{\Gamma} N^T h_T N \, d\Gamma \quad (B-2.9)$$

$$F1 = + \int_{\Gamma} N^T h_T T_\alpha \, d\Gamma \\ + \int_{\Gamma} N^T q_T \, d\Gamma \\ - \int_{\Gamma} N^T \lambda h_{M,\rho} N (a_{\rho_V - \rho_{V,\alpha}}) \, d\Gamma \quad (B-2.10)$$

B.3 CAPILLARY THEORY

The governing mass transfer equation with the proper boundary condition for the capillary theory is given by the following equation:

$$\frac{\partial U}{\partial \tau} = \nabla \cdot (D_H \nabla U) \quad (B-3.1)$$

Exposed to the boundary condition:

$$- D_H \nabla U = h_{M,\rho} (\rho_V - \rho_{V,\alpha}) - q_M \quad (B-3.2)$$

The stiffness matrices, capacitance matrices and the force vectors used in the finite element formulations are given as:

$$C = + \int_{\Omega} N^T N \, d\Omega \quad (B-3.3)$$

$$K = + \int_{\Omega} \frac{\partial N^T}{\partial X_i} D_H \frac{\partial N}{\partial X_i} \, d\Omega \quad (B-3.4)$$

$$F1 = + \int_{\Gamma} N^T q_M \, d\Gamma \\ - \int_{\Gamma} N^T h_{M,\rho} N (a_{\rho_V - \rho_{V,\alpha}}) \, d\Gamma \quad (B-3.5)$$

The governing heat transfer equation with the proper boundary condition for the capillary theory is given by the following equation:

$$\rho_S C_p \frac{\partial T}{\partial \tau} = \nabla \cdot (k_T \nabla T) \quad (B-3.6)$$

Exposed to the boundary condition:

$$-k_T \nabla T = h_T (T - T_\alpha) - q_T + \lambda h_{M,\rho} (\rho_V - \rho_{V,\alpha}) \quad (B-3.7)$$

The stiffness matrices, capacitance matrix and the force vectors used in the finite element formulations are given as:

$$C = + \int_{\Omega} N^T \rho_S C_p N \, d\Omega \quad (B-3.8)$$

$$K = + \int_{\Omega} \frac{\partial N^T}{\partial X_i} k_T \frac{\partial N}{\partial X_i} \, d\Omega \\ + \int_{\Gamma} N^T h_T N \, d\Gamma \quad (B-3.9)$$

$$F1 = + \int_{\Gamma} N^T h_T T_\alpha \, d\Gamma \\ + \int_{\Gamma} N^T q_T \, d\Gamma \\ - \int_{\Gamma} N^T \lambda h_{M,\rho} N (\rho_V - \rho_{V,\alpha}) \, d\Gamma \quad (B-3.10)$$

B.4 EVAPORATION CONDENSATION THEORY

The governing mass transfer equation with the proper boundary condition for the evaporation condensation theory is given by the following equation:

$$\epsilon \frac{\partial \rho_V}{\partial \tau} + (1-\epsilon) \rho_S \frac{\partial U}{\partial \tau} = \nabla \cdot (\epsilon \tau \rho D_A \nabla \rho_V) \quad (B-4.1)$$

Exposed to the boundary condition:

$$- \epsilon \tau \rho D_A \nabla \rho_V = h_{M,\rho} (\rho_V - \rho_{V,\alpha}) - q_M \quad (B-4.2)$$

The stiffness matrices, capacitance matrix and the force vectors used in the finite element formulations are given as:

$$C = + \int_{\Omega} N^T \epsilon N \, d\Omega \quad (B-4.3)$$

$$K = + \int_{\Omega} \frac{\partial N^T}{\partial X_i} \epsilon \tau \rho D_A \frac{\partial N}{\partial X_i} \, d\Omega \\ + \int_{\Gamma} N^T h_{M,\rho} N \, d\Gamma \quad (B-4.4)$$

$$F1 = + \int_{\Gamma} N^T h_{M,\rho} \rho_{V,\alpha} \, d\Gamma \\ + \int_{\Gamma} N^T q_M \, d\Gamma \quad (B-4.5)$$

$$F2 = - \int_{\Omega} N^T (1-\epsilon) \rho_S N (a_U^{\tau+\Delta\tau} - a_U^\tau) \, d\Omega \quad (B-4.6)$$

The governing heat transfer equation with the proper boundary condition for the evaporation condensation theory follows:

$$\epsilon \rho_S C_S \frac{\partial T}{\partial \tau} - \nabla \cdot (k_T \nabla T) + \lambda \rho_S \frac{\partial U}{\partial \tau} \quad (\text{B-4.7})$$

Exposed to the boundary condition:

$$-k_T \nabla T = h_T (T - T_\alpha) - q_T \quad (\text{B-4.8})$$

The stiffness matrices, capacitance matrix and the force vectors used in the finite element formulations are given as:

$$C = + \int_{\Omega} N^T \epsilon \rho_S C_S N \, d\Omega \quad (\text{B-4.9})$$

$$K = + \int_{\Omega} \frac{\partial N^T}{\partial X_i} k_T \frac{\partial N}{\partial X_i} \, d\Omega + \int_{\Gamma} N^T h_T N \, d\Gamma \quad (\text{B-4.10})$$

$$F1 = + \int_{\Gamma} N^T h_T T_\alpha \, d\Gamma + \int_{\Gamma} N^T q_T \, d\Gamma \quad (\text{B-4.11})$$

$$F2 = + \int_{\Omega} N^T \lambda \rho_S N (a_U^{r+\Delta\tau} - a_U^r) \, d\Omega \quad (\text{B-4.12})$$

B.5 LUIKOV'S THEORY

The governing mass transfer equation with the proper boundary condition for the Luikov's theory is given by the following equation:

$$\rho_S C_M \frac{\partial M}{\partial \tau} - \nabla \cdot (K_{21} \nabla T) + \nabla \cdot (K_{22} \nabla M) \quad (\text{B-5.1})$$

Exposed to the boundary condition:

$$-K_{22} \nabla M - K_{21} \nabla T = h_{M,M} (M - M_\alpha) - q_M \quad (\text{B-5.2})$$

The stiffness matrices, capacitance matrix and the force vectors used in the finite element formulations are given as:

$$C = + \int_{\Omega} N^T \rho_S C_M N \, d\Omega \quad (\text{B-5.3})$$

$$K = + \int_{\Omega} \frac{\partial N^T}{\partial X_i} K_{22} \frac{\partial N}{\partial X_i} \, d\Omega + \int_{\Gamma} N^T h_{M,M} N \, d\Gamma \quad (\text{B-5.4})$$

$$\begin{aligned}
F1 = & - \int_{\Omega} \frac{\partial N^T}{\partial X_i} K_{21} \frac{\partial N}{\partial X_i} a_T d\Omega \\
& + \int_{\Gamma} N^T h_{M,M} M_{\alpha} d\Gamma \\
& + \int_{\Gamma} N^T q_M d\Gamma
\end{aligned} \tag{B-5.5}$$

The governing heat transfer equation with the proper boundary condition for the Luikov's theory is given by the following equation:

$$\rho_S C_p \frac{\partial T}{\partial \tau} = \nabla \cdot (K_{11} \nabla T) + \nabla \cdot (K_{12} \nabla M) \tag{B-5.6}$$

Exposed to the boundary condition:

$$-k_T \nabla T = h_T (T - T_{\alpha}) - q_T + (1-\gamma) \lambda h_{M,M} (M - M_{\alpha}) \tag{B-5.7}$$

The stiffness matrices, capacitance matrix and the force vectors used in the finite element formulations are given as:

$$C = + \int_{\Omega} N^T \rho_S C_p N d\Omega \tag{B-5.8}$$

$$\begin{aligned}
K = & + \int_{\Omega} \frac{\partial N^T}{\partial X_i} K_{11} \frac{\partial N}{\partial X_i} d\Omega \\
& + \int_{\Gamma} N^T h_T N d\Gamma
\end{aligned} \tag{B-5.9}$$

$$\begin{aligned}
F1 = & - \int_{\Omega} \frac{\partial N^T}{\partial X_i} K_{12} \frac{\partial N}{\partial X_i} a_M d\Omega \\
& + \int_{\Gamma} N^T \frac{K_{11}}{k_T} h_T T_{\alpha} d\Gamma \\
& + \int_{\Gamma} N^T \frac{K_{11}}{k_T} q_T d\Gamma \\
& - \int_{\Gamma} N^T \frac{K_{11}}{k_T} (1-\gamma) \lambda h_{M,M} N (a_M - M_{\alpha}) d\Gamma
\end{aligned} \tag{B-5.10}$$

B.6 PHILIP AND DE VRIES THEORY

The governing mass transfer equation with the proper boundary condition for the Philip and De Vries theory is given by the following equation:

$$\frac{\partial U}{\partial \tau} = \nabla \cdot (D_{WT} \nabla T) + \nabla \cdot (D_W \nabla U) \quad (B-6.1)$$

Exposed to the boundary condition of

$$- D_W \nabla U = h_{M,\rho} (\rho_V - \rho_{V,\alpha}) - q_M \quad (B-6.2)$$

The stiffness matrices, capacitance matrix and the force vectors used in the finite element formulations are also given as:

$$C = + \int_{\Omega} N^T N \, d\Omega \quad (B-6.3)$$

$$K = + \int_{\Omega} \frac{\partial N^T}{\partial X_i} D_W \frac{\partial N}{\partial X_i} \, d\Omega \quad (B-6.4)$$

$$\begin{aligned} F1 = & - \int_{\Omega} \frac{\partial N^T}{\partial X_i} D_{WT} \frac{\partial N}{\partial X_i} a_T \, d\Omega \\ & + \int_{\Gamma} N^T q_M \, d\Gamma \\ & - \int_{\Gamma} N^T h_{M,\rho} N (\rho_V - \rho_{V,\alpha}) \, d\Gamma \end{aligned} \quad (B-6.5)$$

The governing heat transfer equation with the proper boundary condition for the Philip and De Vries theory is given by the following equation:

$$\rho_S C_S \frac{\partial T}{\partial \tau} = \nabla \cdot (k_T \nabla T) + \lambda \nabla \cdot (D_V \nabla U) \quad (B-6.6)$$

Exposed to the boundary condition:

$$- k_T \nabla T = h_T (T - T_\alpha) - q_T \quad (B-6.7)$$

The stiffness matrices, capacitance matrix and the force vectors used in the finite element formulations are given as:

$$C = + \int_{\Omega} N^T \rho_S C_S N \, d\Omega \quad (B-6.8)$$

$$\begin{aligned} K = & + \int_{\Omega} \frac{\partial N^T}{\partial X_i} k_T \frac{\partial N}{\partial X_i} \, d\Omega \\ & + \int_{\Gamma} N^T h_T N \, d\Gamma \end{aligned} \quad (B-6.9)$$

$$\begin{aligned} F1 = & - \int_{\Omega} \frac{\partial N^T}{\partial X_i} \lambda D_V \frac{\partial N}{\partial X_i} a_U \, d\Omega \\ & + \int_{\Gamma} N^T q_T \, d\Gamma \\ & + \int_{\Gamma} N^T h_T T_\alpha \, d\Gamma \end{aligned} \quad (B-6.10)$$

B.7 KRISCHER AND BERGER-PEI'S THEORY

The governing mass transfer equation with the proper boundary condition for the Krischer and Berger-Pei's theory is given by the following equation:

$$\begin{aligned}
 (\rho_L - \rho_V) \frac{\partial \theta}{\partial \tau} + (\epsilon - \theta) \frac{\partial \rho_V}{\partial \tau} - \nabla \cdot (D_L \rho_L \nabla \theta) \\
 + D_V [(\epsilon - \theta) \nabla^2 \rho_V - \nabla \theta \nabla \rho_V]
 \end{aligned} \quad (B-7.1)$$

Exposed to the boundary condition of

$$-D_L \rho_L \nabla \theta - D_V (\epsilon - \theta) \nabla \rho_V = h_{M,\rho} (\rho_V - \rho_{V,a}) - q_M \quad (B-7.2)$$

The stiffness matrices, capacitance matrix and the force vectors used in the finite element formulations are given as:

$$C = + \int_{\Omega} N^T N (\epsilon - a_{\theta}) N \, d\Omega \quad (B-7.3)$$

$$\begin{aligned}
 K = + \int_{\Omega} \frac{\partial N^T}{\partial X_i} D_V N (\epsilon - a_{\theta}) \frac{\partial N}{\partial X_i} \, d\Omega \\
 + \int_{\Omega} N^T \frac{\partial N}{\partial X_i} D_V a_{\theta} \frac{\partial N}{\partial X_i} \, d\Omega \\
 + \int_{\Gamma} N^T h_{M,\rho} N \, d\Gamma
 \end{aligned} \quad (B-7.4)$$

$$\begin{aligned}
 F1 = - \int_{\Omega} \frac{\partial N^T}{\partial X_i} D_L \rho_L \frac{\partial N}{\partial X_i} a_{\theta} \, d\Omega \\
 + \int_{\Gamma} N^T h_{M,\rho} \rho_{V,\alpha} \, d\Gamma \\
 + \int_{\Gamma} N^T q_M \, d\Gamma
 \end{aligned} \quad (B-7.5)$$

$$F2 = - \int_{\Omega} N^T N (\rho_L - a_{\rho_V}) N (a_{\theta}^{\tau+\Delta\tau} - a_{\theta}^{\tau}) \, d\Omega \quad (B-7.6)$$

The governing heat transfer equation with the proper boundary condition for the Krischer and Berger-Pei's theory is given by the following equation:

$$\begin{aligned}
 \rho_S C_S \frac{\partial T}{\partial \tau} = + k_T \nabla^2 T + \lambda (D_V [(\epsilon - \theta) \nabla^2 \rho_V - \nabla \theta \nabla \rho_V] \\
 - (\epsilon - \theta) \frac{\partial \rho_V}{\partial \tau} + \rho_V \frac{\partial \theta}{\partial \tau})
 \end{aligned} \quad (B-7.7)$$

Exposed to the boundary condition:

$$-k_T \nabla T = h_T (T - T_\alpha) - q_T \quad (B-7.8)$$

The stiffness matrices, capacitance matrix and the force vectors used in the finite element formulations are given as:

$$C = + \int_{\Omega} N^T \rho_S C_S N \, d\Omega \quad (B-7.9)$$

$$K = + \int_{\Omega} \frac{\partial N^T}{\partial X_i} k_T \frac{\partial N}{\partial X_i} \, d\Omega \\ + \int_{\Gamma} N^T h_T N \, d\Gamma \quad (B-7.10)$$

$$F1 = - \int_{\Omega} N^T \lambda D_V N (\epsilon - a_\theta) \frac{\partial N}{\partial X_i} \frac{\partial N}{\partial X_i} a_{\rho V} \, d\Omega \\ - \int_{\Omega} N^T \frac{\partial N}{\partial X_i} \lambda D_V a_\theta \frac{\partial N}{\partial X_i} a_{\rho V} \, d\Omega \\ + \int_{\Gamma} N^T h_T T_\alpha \, d\Gamma \\ + \int_{\Gamma} N^T q_M \, d\Gamma \quad (B-7.11)$$

$$F2 = - \int_{\Omega} N^T N (\epsilon - a_\theta) \lambda N (a_{\rho V}^{\tau+\Delta\tau} - a_{\rho V}^\tau) \, d\Omega \\ + \int_{\Omega} N^T N a_{\rho V} \lambda N (a_\theta^{\tau+\Delta\tau} - a_\theta^\tau) \, d\Omega \quad (B-7.12)$$

B.8 MOIST SOILS MODELS

The governing mass transfer equation with the proper boundary condition for the moist soils theory is given by the following equation:

$$\frac{\partial \theta}{\partial \tau} = \nabla \cdot (D_W \nabla \theta) + \nabla \cdot (D_{WT} \nabla T) \quad (B-8.1)$$

Exposed to the boundary condition:

$$- D_W \nabla \theta - D_{WT} \nabla T = h_{M,\rho} (\rho_V - \rho_{V,\alpha}) - q_M \quad (B-8.2)$$

The stiffness matrices, capacitance matrix and the force vectors used in the finite element formulations are given as:

$$C = + \int_{\Omega} N^T N \, d\Omega \quad (B-8.3)$$

$$K = + \int_{\Omega} \frac{\partial N^T}{\partial X_i} D_W \frac{\partial N}{\partial X_i} d\Omega \quad (B-8.4)$$

$$\begin{aligned} Fl = & - \int_{\Omega} \frac{\partial N^T}{\partial X_i} D_{WT} \frac{\partial N}{\partial X_i} a_T d\Omega \\ & + \int_{\Gamma} N^T q_M d\Gamma \\ & - \int_{\Gamma} N^T h_{M,\rho} N (a_{\rho V} - \rho_{V,\alpha}) d\Gamma \end{aligned} \quad (B-8.5)$$

The governing heat transfer equation with the proper boundary condition for the moist soils theory is given by the following equation:

$$\begin{aligned} C^* \frac{\partial T}{\partial \tau} = & + \nabla [k_T + \rho_L h_L D_{WT} + \rho_L (h_{LV} - h_A) D_{VT}] \nabla T \\ & + \nabla [\rho_L h_L D_W + D_V \rho_L (h_{LV} - h_A)] \nabla \theta \end{aligned} \quad (B-8.6)$$

Exposed to the boundary condition:

$$- k_T \nabla T - D_M \nabla \theta = h_T (T - T_\alpha) - q_T \quad (B-8.7)$$

The stiffness matrices, capacitance matrix and the force vectors used in the finite element formulations are also given as:

$$C = + \int_{\Omega} N^T C^* N d\Omega \quad (B-8.8)$$

$$\begin{aligned} K = & + \int_{\Omega} \frac{\partial N^T}{\partial X_i} [k_T + \rho_L h_L D_{WT} + \rho_L (h_{LV} - h_A) D_{VT}] \frac{\partial N}{\partial X_i} d\Omega \\ & + \int_{\Gamma} N^T h_T N d\Gamma \end{aligned} \quad (B-8.9)$$

$$\begin{aligned} Fl = & - \int_{\Omega} \frac{\partial N^T}{\partial X_i} [\rho_L h_L D_W + D_V \rho_L (h_{LV} - h_A)] \frac{\partial N}{\partial X_i} a_\theta d\Omega \\ & + \int_{\Gamma} N^T h_T T_\alpha d\Gamma \\ & + \int_{\Gamma} N^T q_T d\Gamma \end{aligned} \quad (B-8.10)$$

B.9 IRREVERSIBLE THERMODYNAMICS

The governing mass transfer equation with the proper boundary conditions for Irreversible Thermodynamics is given by the following equation:

$$\rho_S \frac{\partial U}{\partial \tau} = \nabla \cdot (K_{11} \nabla T) + \nabla \cdot (K_{12} \nabla \Phi) \quad (B-9.1)$$

Exposed to the boundary condition:

$$-K_{11} \nabla T - K_{12} \nabla \Phi = h_{M,p} (P_V - P_{V,\alpha}) - q_M \quad (B-9.2)$$

where

$$K_{11} = K_L \rho_L R_V \ln \Phi + D_V \Phi \frac{d\rho_{V,sat}}{dT} + D_V \rho_{V,sat} \frac{\partial \Phi}{\partial T} \quad (B-9.3)$$

$$K_{12} = K_L \rho_L R_V \frac{T}{\Phi} + D_V \rho_{V,sat} \quad (B-9.4)$$

The stiffness matrices, capacitance matrix and the force vectors used in the finite element formulations are given below:

$$K = + \int_{\Omega} \frac{\partial N^T}{\partial X_i} K_{12} \frac{\partial N}{\partial X_i} d\Omega \quad (B-9.5)$$

$$F1 = - \int_{\Omega} \frac{\partial N^T}{\partial X_i} K_{11} \frac{\partial N}{\partial X_i} a_T d\Omega \\ + \int_{\Gamma} N^T q_M d\Gamma \\ - \int_{\Gamma} N^T h_{M,p} N (a_{pV} - \rho_{V,\alpha}) d\Gamma \quad (B-9.6)$$

$$F2 = - \int_{\Omega} N^T \rho_S N (a_{U, r+\Delta r} - a_{U, r}) d\Omega \quad (B-9.7)$$

The governing heat transfer equation with the proper boundary conditions for Irreversible thermodynamics is given by the following equation:

$$\rho_S C_S \frac{\partial T}{\partial \tau} - \rho_S \Delta h_W \frac{\partial U}{\partial \tau} = + \nabla (k_T \nabla T) + \nabla (K_{21} \nabla \Phi) \\ + \Delta h_V \nabla (K_{22} \nabla T) + \Delta h_V \nabla (D_V \rho_{V,sat} \nabla \Phi) \\ + K_{23} (\nabla T)^2 + K_{24} \nabla \Phi \nabla T \quad (B-9.8)$$

Exposed to the boundary condition:

$$-(k_T + \Delta h_V K_{22}) \nabla T - (K_{21} + \Delta h_V D_V \rho_{V,sat}) \nabla \Phi = h_T (T - T_{\alpha}) - q_T$$

where

$$K_{22} = D_V (\rho_{V,sat} \frac{\partial \Phi}{\partial T} + \Phi \frac{d\rho_{V,sat}}{dT}) \quad (B-9.10)$$

$$K_{21} = K_{11} \frac{R_V T^2}{\Phi} \quad (B-9.11)$$

$$K_{23} = C_L K_L \rho_L R_V \ln \Phi + C_V K_{22} \quad (\text{B-9.12})$$

$$K_{24} = C_L K_L \rho_L R_V \frac{T}{\Phi} + C_V D_V \rho_{V, \text{sat}} \quad (\text{B-9.13})$$

The stiffness matrices, capacitance matrix and the force vectors used in the finite element formulations are given below:

$$C = + \int_{\Omega} N^T \rho_S C_S N \, d\Omega \quad (\text{B-9.14})$$

$$\begin{aligned} K = & + \int_{\Omega} \frac{\partial N^T}{\partial X_i} (k_T + \Delta h_V K_{22}) \frac{\partial N}{\partial X_i} \, d\Omega \\ & - \int_{\Omega} N^T K_{21} \frac{\partial N}{\partial X_i} a_T \frac{\partial N}{\partial X_i} \, d\Omega \\ & - \int_{\Omega} N^T K_{24} \frac{\partial N}{\partial X_i} a_{\Phi} \frac{\partial N}{\partial X_i} \, d\Omega \\ & + \int_{\Gamma} N^T h_T N \, d\Gamma \end{aligned} \quad (\text{B-9.15})$$

$$\begin{aligned} F1 = & - \int_{\Omega} \frac{\partial N^T}{\partial X_i} (K_{11} + \Delta h_V D_V \rho_{V, \text{sat}}) \frac{\partial N}{\partial X_i} a_{\Phi} \, d\Omega \\ & + \int_{\Gamma} N^T (h_T T_{\alpha} + q_T) \, d\Gamma \end{aligned} \quad (\text{B-9.16})$$

$$F2 = + \int_{\Omega} N^T \rho_S \Delta h_W N (a_U^{\tau+\Delta\tau} - a_U^{\tau}) \, d\Omega \quad (\text{B-9.17})$$

B.10 SHAPE FUNCTIONS

Presently, only three different element types are supported. The element types are:

1. One-dimensional linear line element
2. Two-dimensional linear rectangular element
3. Three-dimensional linear brick element.

The shape functions associated with each type of element are given below:

One-dimensional linear line element:

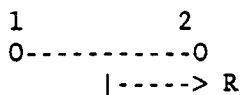


Figure B-1. One-dimensional linear line element and local normalized coordinates.

$$N = 1/2 \begin{vmatrix} (1+R) \\ (1-R) \end{vmatrix} \quad (B-10.1)$$

Two-dimensional linear rectangular element:

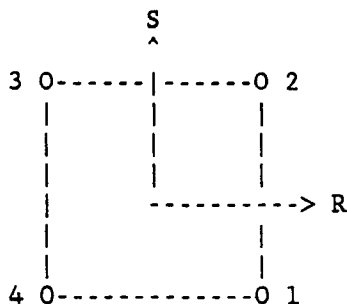


Figure B-2. Two-dimensional linear rectangular element and local normalized coordinates.

$$N = 1/4 \begin{vmatrix} (1+R) & (1-S) \\ (1+R) & (1+S) \\ (1-R) & (1+S) \\ (1-R) & (1-S) \end{vmatrix} \quad (B-10.2)$$

Three-dimensional linear brick element:

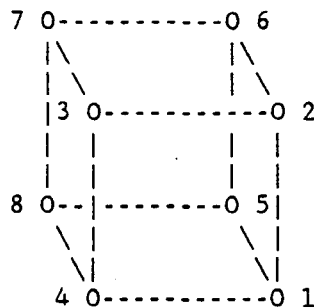


Figure B-3. Three-dimensional linear brick element and local normalized coordinates.

$$N = 1/8 \begin{vmatrix} (1+R) & (1-S) & (1+T) \\ (1+R) & (1+S) & (1+T) \\ (1-R) & (1+S) & (1+T) \\ (1-R) & (1-S) & (1+T) \\ (1+R) & (1-S) & (1-T) \\ (1+R) & (1+S) & (1-T) \\ (1-R) & (1+S) & (1-T) \\ (1-R) & (1-S) & (1-T) \end{vmatrix} \quad (B-10.3)$$

B.11 ISOPARAMETRIC FORMULATIONS

Let us first note that we have the shape functions in terms of the serendipity coordinates R, S and T for the parent elements as given in Section B.10. The serendipity coordinates are also functions of the global x, y and z coordinates, hence:

$$\begin{aligned} R &= R(x,y,z) \\ S &= S(x,y,z) \\ T &= T(x,y,z) \end{aligned} \quad (\text{B-11.1})$$

Additionally, the shape functions defined in Section B.10 are functions of the serendipity coordinates, and in general may be written as

$$N = N(R,S,T) \quad (\text{B-11.2})$$

Therefore, the total derivative of the shape function with respect to each serendipity coordinates would be

$$\begin{aligned} \frac{\partial N}{\partial R} &= \frac{\partial N}{\partial x} \frac{\partial x}{\partial R} + \frac{\partial N}{\partial y} \frac{\partial y}{\partial R} + \frac{\partial N}{\partial z} \frac{\partial z}{\partial R} \\ \frac{\partial N}{\partial S} &= \frac{\partial N}{\partial x} \frac{\partial x}{\partial S} + \frac{\partial N}{\partial y} \frac{\partial y}{\partial S} + \frac{\partial N}{\partial z} \frac{\partial z}{\partial S} \end{aligned} \quad (\text{B-11.3})$$

and

$$\frac{\partial N}{\partial T} = \frac{\partial N}{\partial x} \frac{\partial x}{\partial T} + \frac{\partial N}{\partial y} \frac{\partial y}{\partial T} + \frac{\partial N}{\partial z} \frac{\partial z}{\partial T}$$

Equation (B-11.3) can also be written in the following matrix form:

$$\begin{bmatrix} \frac{\partial N}{\partial R} \\ \frac{\partial N}{\partial S} \\ \frac{\partial N}{\partial T} \end{bmatrix} = \begin{bmatrix} \frac{\partial x}{\partial R} & \frac{\partial y}{\partial R} & \frac{\partial z}{\partial R} \\ \frac{\partial x}{\partial S} & \frac{\partial y}{\partial S} & \frac{\partial z}{\partial S} \\ \frac{\partial x}{\partial T} & \frac{\partial y}{\partial T} & \frac{\partial z}{\partial T} \end{bmatrix} \begin{bmatrix} \frac{\partial N}{\partial x} \\ \frac{\partial N}{\partial y} \\ \frac{\partial N}{\partial z} \end{bmatrix} \quad (\text{B-11.4})$$

The 3x3 matrix on the right-hand side is known as the Jacobian matrix and is denoted by J, or

$$J = \begin{bmatrix} \frac{\partial x}{\partial R} & \frac{\partial y}{\partial R} & \frac{\partial z}{\partial R} \\ \frac{\partial x}{\partial S} & \frac{\partial y}{\partial S} & \frac{\partial z}{\partial S} \\ \frac{\partial x}{\partial T} & \frac{\partial y}{\partial T} & \frac{\partial z}{\partial T} \end{bmatrix} \quad (\text{B-11.5})$$

The volume of an element can be calculated with the following equation:

$$d\Omega = dx dy dz = |\det J| dR dS dT \quad (\text{B-11.6})$$

In Equation (B-11.6), the determinant of the Jacobian matrix is indicated. This determinant is referred to simply as the Jacobian. From Equation (B-11.5) the desired derivatives of the shape functions can be obtained. The global coordinates used in Equation (B-11.5) can also be modified as follows:

$$\begin{aligned} x &= \sum N_i x_i \\ y &= \sum N_i y_i \\ z &= \sum N_i z_i \end{aligned} \quad (\text{B-11.7})$$

Consequently, from Equations (B-11.5) and (B-11.7) the desired expression for the Jacobian matrix can be obtained.

$$J = \begin{bmatrix} \sum \frac{\partial N_i}{\partial R} x_i & \sum \frac{\partial N_i}{\partial R} y_i & \sum \frac{\partial N_i}{\partial R} z_i \\ \sum \frac{\partial N_i}{\partial S} x_i & \sum \frac{\partial N_i}{\partial S} y_i & \sum \frac{\partial N_i}{\partial S} z_i \\ \sum \frac{\partial N_i}{\partial T} x_i & \sum \frac{\partial N_i}{\partial T} y_i & \sum \frac{\partial N_i}{\partial T} z_i \end{bmatrix} \quad (\text{B-11.8})$$

With the help of Equations (B-11.6) and (B-11.8) all the integrals given in Sections B.2 through B.9 can be transformed into a form that can be evaluated numerically. The equations that are given above are for three-dimensional formulations. However, equations that are given in Sections B.2 through B.9 are general and they are applicable for one-, two- and three-dimensional calculations. Depending on the dimensionality of the problem, the equations given in Sections B.2 through B.9 must be modified. The necessary modifications for one-, two- and three dimensional problems are given in Table B-2.

TABLE B-2
Integrands for Different Dimensions

Dimension	$d\Omega$	$d\Gamma$
One	A dR	1
Two	t dR dS	t dR
Three	dR dS dT	dR dS

In addition to the above modification, the equations given in Section B.11 must be modified for one- and two-dimensional problems. This modification can be easily performed by eliminating the y and z coordinate dependencies for one-dimensional problems and eliminating the z coordinate dependency for two-dimensional problems. It must also be emphasized that for three-dimensional problems the boundary integral term reduces to a volume integral term performed for two-dimensional elements with the thickness set to 1. Similarly, for two-dimensional problems the boundary integral term reduces to a volume integral term performed for one-dimensional elements with the area set to the thickness of the element.

B.12 NUMERICAL INTEGRATION

Integrals that arise in the finite element method have integrands that are explicit functions of the coordinates. If the global coordinates are changed to serendipity coordinates the following types of numerical integrations will be required:

$$I = \int_{-1}^{+1} f(R) dR \quad (B-12.1)$$

$$I = \int_{-1}^{+1} \int_{-1}^{+1} f(R,S) dR dS \quad (B-12.2)$$

$$I = \int_{-1}^{+1} \int_{-1}^{+1} \int_{-1}^{+1} f(R,S,T) dR dS dT \quad (B-12.3)$$

Equations (B-12.1), (B-12.2) and (B-12.3) denote the type of numerical integrations that need to be performed for one-, two- and three-dimensional elements, respectively. The numerical integrations can be performed by Gauss-Legendre quadrature and Equations (B-12.1), (B-12.2) and (B-12.3) can be transformed into the following equations:

$$I \approx \sum_{i=1}^n W_i f(R_i) \quad (B-12.4)$$

$$I \approx \sum_{i=1}^n \sum_{j=1}^m W_i W_j f(R_i, S_j) \quad (B-12.5)$$

$$I = \sum_{i=1}^n \sum_{j=1}^m \sum_{k=1}^p W_i W_j W_k f(R_i, S_j, T_j) \quad (\text{B-12.6})$$

The weights and the associated sampling points to be used in Equations (B-12.4) through (B-12.6) are given in Table B-3.

TABLE B-3
Sampling Point Values and Weights for Gauss-Legendre Quadrature

Order	R	W
1	0.000 000 000 000 000	2.000 000 000 000 000
2	-0.577 350 269 189 626	1.000 000 000 000 000
	+0.577 350 269 189 626	1.000 000 000 000 000
3	-0.774 596 669 241 483	0.555 555 555 555 556
	0.000 000 000 000 000	0.888 888 888 888 889
	+0.774 596 669 241 483	0.555 555 555 555 556
4	-0.861 136 311 594 053	0.347 854 845 137 454
	-0.339 981 043 584 856	0.652 145 154 862 546
	+0.339 981 043 584 856	0.652 145 154 862 546
	+0.861 136 311 594 053	0.347 854 845 137 454
5	-0.906 179 845 938 664	0.236 926 885 056 189
	-0.538 469 310 105 683	0.478 628 670 499 366
	0.000 000 000 000 000	0.568 888 888 888 889
	+0.538 469 310 105 683	0.478 628 670 499 366
	+0.906 179 845 938 664	0.236 926 885 056 189
6	-0.932 469 514 203 152	0.171 324 492 379 170
	-0.661 209 386 466 265	0.360 761 573 048 139
	-0.238 619 186 083 197	0.467 913 934 572 691
	+0.238 619 186 083 197	0.467 913 934 572 691
	+0.661 209 386 466 265	0.360 761 573 048 139
	+0.932 469 514 203 152	0.171 324 492 379 170

The derivation of the weights and sampling points is beyond the scope of this report; however, interested readers may wish to consult Carnahan et al. 1969. Before finalizing the numerical integration section one more point must be clarified. The number of sampling points (n, m and p) used in Equations (B-12.4) through (B-12.6) is function of the order of the function that needs to be integrated. The following equations can be used to find the number of sampling points to be used in each local normalized coordinate direction:

$$2n - 1 = \text{highest order of } R \quad (\text{B-12.7})$$

$$2m - 1 = \text{highest order of } S \quad (\text{B-12.8})$$

$$2p - 1 = \text{highest order of } T \quad (\text{B-12.9})$$

B.13 ACTIVE ZONE EQUATION SOLVER

The matrix inversion method to solve the system of algebraic equations implied in $Ka=f$ is not very practical in large finite element models because of computation of inverse of a large matrix can result in excessive computer time. A much more efficient solution method is discussed in this section. The basic idea is to decompose the matrix K into lower and upper triangular matrices L and U such that $K = LU$. It is shown below how this results in a straightforward solution for the unknown vector a , once this triangular decomposition (or LU decomposition) has been performed.

B.13.1 TRIANGULAR DECOMPOSITION

The triangular decomposition of K into L and U such that $K = LU$ is summarized below in the form of a short algorithm. Let us first illustrate the basis for the algorithm by working on a 3×3 matrix K . It follows from $K = LU$ that

$$\begin{bmatrix} K_{11} & K_{12} & K_{13} \\ K_{21} & K_{22} & K_{23} \\ K_{31} & K_{32} & K_{33} \end{bmatrix} = \begin{bmatrix} L_{11} & 0 & 0 \\ L_{21} & L_{22} & 0 \\ L_{31} & L_{32} & L_{33} \end{bmatrix} \begin{bmatrix} U_{11} & U_{12} & U_{13} \\ 0 & U_{22} & U_{23} \\ 0 & 0 & U_{33} \end{bmatrix} \quad (\text{B-13.1})$$

The number of unknowns on the right-hand side of Equation (B-13.1) is seen to be greater than the number of implied equations, that is twelve unknowns and nine equations. The number of unknowns may always be reduced to the number of implied equations by reducing each diagonal entry in L to be unity; or $L_{ii}=1$. Therefore, Equation (B-13.1) becomes

$$\begin{array}{c} \text{I} \quad | \quad \text{II} \quad | \quad \text{III} \\ \hline \begin{bmatrix} K_{11} & K_{12} & K_{13} \\ K_{21} & K_{22} & K_{23} \\ K_{31} & K_{32} & K_{33} \end{bmatrix} = \begin{bmatrix} 1 & 0 & 0 \\ L_{21} & 1 & 0 \\ L_{31} & L_{32} & 1 \end{bmatrix} \begin{bmatrix} U_{11} & U_{12} & U_{13} \\ 0 & U_{22} & U_{23} \\ 0 & 0 & U_{33} \end{bmatrix} \end{array} \quad (\text{B-13.2})$$

Note that the K matrix has been divided into three zones. In general, an $n \times n$ matrix K would be divided into n such zones. If the matrices on the right-hand side are multiplied and equated with the left-hand side, entry by entry, the following nine equations in nine unknowns (L_{21} , L_{31} , L_{32} , U_{11} , U_{12} , etc.) are obtained:

Zone I: $K_{11} = U_{11}$

Zone II: $K_{12} = U_{12}$

$K_{21} = L_{21} U_{11}$

$$K_{22} = L_{21} U_{12} + U_{22}$$

$$\text{Zone III: } K_{13} = U_{13}$$

$$K_{31} = L_{31} U_{11}$$

$$K_{32} = L_{31} U_{12} + L_{32} U_{22}$$

$$K_{23} = L_{21} U_{13} + U_{23}$$

$$K_{33} = L_{31} U_{13} + L_{32} U_{23} + U_{33}$$

These equations may in turn be solved for the nine unknowns to give the following

$$\text{Zone I: } U_{11} = K_{11}$$

$$\text{Zone II: } U_{12} = K_{12}$$

$$L_{21} = K_{21}/U_{11}$$

$$U_{22} = K_{22} - L_{21}/U_{12}$$

$$\text{Zone III: } U_{13} = K_{13}$$

$$L_{31} = K_{31}/U_{11}$$

$$L_{32} = (K_{32} - L_{31} U_{12})/U_{22}$$

$$U_{23} = K_{23} - L_{21} U_{13}$$

$$U_{33} = K_{33} - L_{31} U_{13} - L_{32} U_{23}$$

A few subtle points should be made here. Note how the calculations in each zone use only the entries in the K matrix that are in that zone and only those entries from the L and U matrices from previous and present zones. The present zone here is more commonly referred to as the active zone, hence the name active zone equation solver.

The above equations may be generalized for an nxn matrix K as follows. For the first active zone, we have

$$U_{11} = K_{11} \quad (\text{B-13.3})$$

$$L_{11} = 1 \quad (\text{B-13.4})$$

and for each subsequent active zone j from 2 to n, we have

$$L_{j1} = K_{j1}/U_{11} \quad (\text{B-13.5})$$

$$U_{1j} = K_{1j} \quad (\text{B-13.6})$$

and

$$L_{ji} = (K_{ji} - \sum_{m=1}^{i-1} L_{jm} U_{mi}) / U_{ii} \quad \text{for } i = 2, 3, \dots, j-1 \quad (\text{B-13.7})$$

$$U_{ij} = K_{ij} - \sum_{m=1}^{i-1} L_{im} U_{mj} \quad \text{for } i = 2, 3, \dots, j-1 \quad (\text{B-13.8})$$

and finally

$$L_{jj} = 1 \quad (\text{B-13.9})$$

$$U_{jj} = K_{jj} - \sum_{m=1}^{j-1} L_{jm} U_{mj} \quad (\text{B-13.10})$$

For a symmetric matrix, the entries in the lower triangular matrix L can be obtained directly from the upper triangular matrix U from

$$L_{ji} = U_{ij}/U_{ii} \quad \text{for } j \rightarrow i \quad (\text{B-13.11})$$

B.13.2 FORWARD ELIMINATION AND BACKWARD SUBSTITUTION

Let us now reconsider the system of algebraic equations $Ka = f$ and try to obtain the solution for the vector "a" by taking advantage of the material in the previous section. Beginning with $Ka = f$ and using $K = LU$, we may write

$$L U a = f \quad (\text{B-13.12})$$

Denoting Ua as the vector Z , we have, in effect, two systems of equations:

$$L Z = f \quad (\text{B-13.13})$$

$$U a = Z \quad (\text{B-13.14})$$

Let us write explicitly for the case of a 3x3 K matrix in order to gain some insight into the general algorithm to be presented. Equation (B-13.13) implies

$$\begin{aligned} Z_1 &= f_1 \\ L_{21} Z_1 + Z_2 &= f_2 \\ L_{31} Z_1 + L_{32} Z_2 + Z_3 &= f_3 \end{aligned} \quad (\text{B-13.15})$$

and Equation (B-13.14) implies

$$\begin{aligned} U_{11} a_1 + U_{12} a_2 + U_{13} a_3 &= Z_1 \\ U_{22} a_2 + U_{23} a_3 &= Z_2 \end{aligned} \quad (\text{B-13.16})$$

$$U_{33} a_3 = Z_3$$

From Equation (B-13.15) it follows that the Z_i 's may be obtained by a forward sweep as follows:

$$\begin{aligned} Z_1 &= f_1 \\ Z_2 &= f_2 - L_{21} Z_1 \\ Z_3 &= f_3 - L_{31} Z_1 - L_{32} Z_2 \end{aligned} \quad (\text{B-13.17})$$

From these and Equation (B-13.16), it follows that

$$\begin{aligned} a_3 &= Z_3/U_{33} \\ a_2 &= (Z_2 - U_{23} a_3)/U_{22} \\ a_1 &= (Z_1 - U_{13} a_3 - U_{12} a_2)/U_{11} \end{aligned} \quad (\text{B-13.18})$$

These steps may be generalized to the case of an $n \times n$ K matrix in the following manner:

$$Z_1 = f_1 \quad (\text{B-13.19})$$

$$Z_i = f_i - \sum_{j=1}^{i-1} L_{ij} Z_j \quad \text{for } j = 2, 3, \dots, n \quad (\text{B-13.20})$$

and

$$a_n = Z_n/U_{nn} \quad (\text{B-13.21})$$

$$a_i = (Z_i - \sum_{j=i+1}^n U_{ij} a_j) / U_{ii} \quad \text{for } i = n-1, n-2, \dots, 1 \quad (\text{B-13.22})$$

For obvious reasons, the steps in Equations (B-13.19) through (B-13.22) are referred to as the forward elimination and backward substitution steps.

B.13.3 STORAGE CONSIDERATIONS

It should be recalled that the assemblage stiffness matrix K is generally banded and for our case is symmetric. This is quite significant because it becomes possible to reduce significantly the storage requirements of such a matrix. Since the matrix is symmetric, the entries below the main diagonal need not be stored. This alone reduces the storage requirement by a factor of nearly one-half. If the matrix is banded or there are many leading zeros in the upper triangular portion of the matrix, then the storage requirements are reduced further.

Consider, for example, the 7×7 matrix K that is given below:

$$K = \begin{bmatrix} K_{11} & K_{12} & K_{13} & 0 & 0 & 0 & 0 \\ & K_{22} & K_{23} & 0 & 0 & K_{26} & 0 \\ & & K_{33} & K_{34} & 0 & K_{36} & 0 \\ & & & K_{44} & K_{45} & 0 & 0 \\ & & & & K_{55} & K_{56} & K_{57} \\ & & & & & K_{66} & K_{67} \\ & & & & & & K_{77} \end{bmatrix}$$

The half-bandwidth in this case is readily seen to be five, as dictated by the second row. It is far more efficient to store the K matrix in a column vector form as illustrated below. The method is most easily understood by way of an example. Reconsider the 7x7 matrix given above. Let us store the nonzero coefficients (and imbedded zeros in the column) in a column vector A(i) as shown in Figure B-4. Note how each column in the K matrix is stacked in A(i). Note further that leading zeros in the column need not be stored. Zeros that are imbedded in a column, however, must be stored.

i	A(i)
1	K11
2	K12
3	K22
4	K13
5	K23
6	K33
7	K34
8	K44
9	K45
10	K55
11	K26
12	K36
13	0
14	K56
15	K66
16	K57
17	K67
18	K77

Figure B-4. Skyline storage method for K matrix.

If two or more governing equations are simultaneously solved, then there are two different methods of assembling the stiffness matrix and force vector. These two methods can simply be described as follows:

1. Assemble all the governing equations to the same matrix and solve them simultaneously.
2. Assemble and solve one equation at a time.

In the first method the degree of freedom associated with each node will be equal to the number of governing equations; however, in the second method it will be equal to one. The effect of each method on the stability, convergence and storage requirement of the problem is rather drastic. It is our opinion that the second method allows more variations, and in the iteration scheme it has a corrective nature. This will be more obvious when the solution procedures (Section B.14) are discussed. In multi-equation solutions, the rate of convergence associated with each equation is different. Hence, with the second method the equation with the lower convergence rate may be solved a few more times than the others. For instance, in coupled heat and mass transfer solutions the energy equation's convergence rate is slower than the mass transfer's. Hence, the heat transfer equation is solved few times and then the mass transfer equation is solved, and the procedure is repeated till a healthy convergence is achieved. Whereas with the first method there will be some redundant solutions.

The storage requirements for each method are given by the following equations:

$$\text{SIZE} = \text{NOFBAN} * (1 + 2 * \text{NOFNOD} - \text{NOFBAN}) / 2 \quad (\text{B-13.23})$$

$$\text{Method 1} \text{ ---> } \text{STORAGE} = \text{NOE}^2 * \text{SIZE} - \text{NOE} * (\text{NOE} - 1) / 2 * \text{NOFNOD} \quad (\text{B-13.24})$$

$$\text{Method 2} \text{ ---> } \text{STORAGE} = \text{SIZE} \quad (\text{B-13.25})$$

Where

NOE Number of governing equations
 NOFBAN Half band width
 NOFNOD Number of nodes

For a one-dimensional problem with 500 nodal points, the required storage size for the second method will be only 999 (for most building simulations the half band width is equal to 2). In this study the second method is preferred for obvious reasons.

B.14 SOLUTION PROCEDURES

The choice of an iterative solution method for a general purpose code is governed by several considerations. First, the chosen algorithm should be convergent for a wide range of problems with minimal sensitivity to variations in initial conditions, flow conditions and parameters, and geometry. The rate of convergence should also be reasonably high for economy. Since none of the iterative procedure satisfies all these conditions, a number of different solution procedures are provided.

B.14.1 FIXED-POINT ITERATION

A particularly simple scheme is a fixed-point iteration procedure known as successive substitution (Picard iteration, functional iteration, successive approximation). The governing equation(s) which is under consideration is given by Equation (B-1.7). If the problem requires the simultaneous solution of two field variables, such as temperature and moisture concentration, then two equations in the form of Equation (B-1.7) must be solved simultaneously.

Although the convergence rate of this scheme can be slow (its convergence rate is asymptotically linear), the method converges for most of the problems. This, together with its simplicity of implementation and relative insensitivity to the initial conditions, accounts for its popularity and is recommended for the solution of a wide variety of problems.

The rate of convergence of the basic iteration procedure can be improved by the use of a relaxation procedure as shown below.

$$\begin{aligned} (C_{TT}^{r+\Delta\tau} + K_{TT}^{r+\Delta\tau} \theta \Delta\tau) a_T^{r+\Delta\tau} &= +[C_{TT}^r - (1-\theta) K_{TT}^r \Delta\tau] a_T^r \\ &\quad - [(1-\theta) K_{TM}^r a_M^r + \theta K_{TM}^{r+\Delta\tau} a_M^{r+\Delta\tau}] \Delta\tau \\ &\quad - [(1-\theta) f_T^r + \theta f_T^{r+\Delta\tau}] \Delta\tau \end{aligned} \quad (B-14.1)$$

and

$$\begin{aligned} (C_{MM}^{r+\Delta\tau} + K_{MM}^{r+\Delta\tau} \theta \Delta\tau) a_M^{r+\Delta\tau} &= +[C_{MM}^r - (1-\theta) K_{MM}^r \Delta\tau] a_M^r \\ &\quad - [(1-\theta) K_{MT}^r a_T^r + \theta K_{MT}^{r+\Delta\tau} a_T^{r+\Delta\tau}] \Delta\tau \\ &\quad - [(1-\theta) f_M^r + \theta f_M^{r+\Delta\tau}] \Delta\tau \end{aligned} \quad (B-14.2)$$

Equations (B-14.1) and (B-14.2) are special cases of Equation (B-1.7). In this particular case the subscripts T and M denote the temperature and mass transfer potential, respectively. The results obtained at the end of each iteration are relaxed by the following equations.

$$a_T^{r+\Delta\tau} = \mathcal{R}_T a_T^{r+\Delta\tau} + (1-\mathcal{R}_T) a_T^r \quad (B-14.3)$$

$$a_M^{r+\Delta\tau} = \mathcal{R}_M a_M^{r+\Delta\tau} + (1-\mathcal{R}_M) a_M^r \quad (B-14.4)$$

The value of the relaxation parameter, \mathcal{R} , varies between 0 and 1.

$$0.0 < \mathcal{R} < 1.0 \quad (B-14.5)$$

Unfortunately, there are no general rules as to the choice of a suitable value for the relaxation parameter; a commonly used value is 0.5.

B.14.2 NEWTON-TYPE METHODS

Consider the problem of solving a system of n non-linear equations in n unknowns given by the following equation:

$$K(a) = 0 \quad (\text{B-14.6})$$

Let a^* be an approximation to the exact solution a of equation (B-14.6) such that:

$$a = a^* + \Delta a \quad (\text{B-14.7})$$

Then in the neighborhood of a , the Taylor series expansion of K may be written as:

$$K(a) = K(a^*) + \frac{\partial K}{\partial a} (a^*) \Delta a + O(\Delta a^2) \quad (\text{B-14.8})$$

Using Equations (B-14.6) through (B-14.8) and truncating the series results in:

$$K(a^*) = - \frac{\partial K}{\partial a} (a^*) \Delta a \quad (\text{B-14.9})$$

Based on Equation (B-14.9) the following iterative algorithm can be obtained:

$$K(a_i) = - \frac{\partial K}{\partial a} (a_i) (a_{i+1} - a_i) \quad (\text{B-14.10})$$

or rearranging Equation (B-14.10)

$$a_{i+1} = a_i - \frac{\partial K^{-1}}{\partial a} (a_i) K(a_i) = a_i - J^{-1}(a_i) K(a_i) \quad (\text{B-14.11})$$

Where $J(a)$ is the Jacobian matrix of the system of Equations (B-14.6) and the iterative scheme of Equation (B-14.11) is the well known Newton-Raphson procedure, generalized here to a system of equations.

NOMENCLATURE

A	Cross sectional area of an one-dimensional element [m^2]
a_T	Temperature nodal unknown vector [K]
a_U	Moisture content (dry basis) nodal unknown vector [kg/kg]
a_θ	Moisture activity (relative humidity) nodal unknown vector [dimensionless]
$a_{\rho V}$	Water vapor concentration nodal unknown vector [kg/m^3]
C	Capacitance matrix
C	Specific heat [W.h/kg.K]
C^*	Volumetric specific heat [W.h/ m^3 .K]
C_A	Specific heat of dry air [W.h/kg.K]
C_L	Specific heat of liquid water [W.h/kg.K]
C_S	Specific heat of solid skeleton [W.h/kg.K]
C_V	Specific heat of water vapor [W.h/kg.K]
C_M	Specific isothermal moisture capacity [kg/kg. $^{\circ}M$]
D_A	Molecular diffusivity of water vapor in air [m^2/h]
D_L	Isothermal liquid water diffusivity [m^2/h]
D_{LT}	Thermal liquid water diffusivity [$m^2/h.K$]
D_V	Isothermal water vapor diffusivity [m^2/h]
D_{VT}	Thermal water vapor diffusivity [$m^2/h.K$]
D_W	Isothermal moisture (liquid+vapor) diffusivity [m^2/h]
D_{WT}	Thermal moisture (liquid+vapor) diffusivity [$m^2/h.K$]
F1	Nodal force vector
F2	Nodal force vector due to other time derivative term
h_A	Enthalpy of dry air [W.h/kg]
h_L	Enthalpy of liquid water [W.h/kg]
$h_{M,P}$	Convective mass transfer coefficient based on pressure [$kg/m^2.h.Pa$]
$h_{M,\rho}$	Convective mass transfer coefficient based on concentration [m/h]

h_T	Convective heat transfer coefficient [$W/m^2.K$]
h_V	Enthalpy of water vapor [$W.h/kg$]
J	Jacobian matrix
J_i	Flux
J_L	Liquid water flux [$kg/m^2.h$]
J_T	Thermal heat flux [W/m^2]
J_V	Water vapor flux [$kg/m^2.h$]
J_W	Moisture (liquid+vapor) flux [$kg/m^2.h$]
K	Stiffness matrix
k_L	Liquid conductivity [h]
k_T	Effective (overall) thermal conductivity [$W/m.K$]
k_{rel}	Liquid relative permeability [dimensionless]
K_{sat}	Saturated permeability [m^2]
K_{11}	Kinetic coefficient [m^2/h]
K_{12}	Kinetic coefficient [$m^2/h.K$]
K_{21}	Kinetic coefficient [$m^2/h.K$]
K_{22}	Kinetic coefficient [m^2/h]
M	Mass transfer potential [$^{\circ}M$]
N	Shape function vector [dimensionless]
non	Number of nodes per element [dimensionless]
U	Moisture (liquid+vapor) content dry basis. [kg/kg]
P	Total pressure [$kg/m.h^2$]
P_A	Dry air pressure [$kg/m.h^2$]
P_V	Partial water vapor pressure [$kg/m.h^2$]
q_M	Imposed moisture flux [$kg/m^2.h$]
q_T	Imposed heat flux [W/m^2]
R	Serendipity (local normalized) coordinate
R_V	Gas constant for water vapor [$W.h/kg.K$]

r	Radius [m]
r ₀	Minimum radius [m]
r ₁	Maximum radius [m]
S	Serendipity (local normalized) coordinate
S	Entropy [W.h/kg.K]
T	Serendipity (local normalized) coordinate
T	Temperature [K]
t	Thickness of a two-dimensional element [m]
T _α	Ambient or medium temperature [K]
W	Weights for Gauss-Legendre quadrature [dimensionless]

GREEK LETTERS

α	Thermal diffusivity [m ² /h]
γ	Resistance of vapor diffusion [dimensionless]
Δh ₀	Specific latent heat of pure water vaporization [W.h/kg]
Δh _v	Specific latent heat of vaporization [W.h/kg]
Δh _w	Specific differential heat of wetting [W.h/kg]
δ	Thermogradient coefficient [1/K]
ε	Porosity or void fraction [m ³ /m ³]
θ	Volumetric moisture content [m ³ /m ³]
θ	Wetting angle in capillaries [radians]
λ	Latent heat of vaporization [W.h/kg]
μ	Dynamic viscosity [kg/m.h]
μ _i	Chemical potential of substance i
μ _L	Dynamic viscosity of liquid water [kg/m.h]
μ _L	Chemical potential of liquid water [W.h/kg]
μ _L [*]	Chemical potential of pure water vapor [W.h/kg]
μ _v	Chemical potential of water vapor [W.h/kg]

ν	Kinematic viscosity [m^2/h]
ρ_A	Density of dry air [kg/m^3]
ρ_G	Density of air+vapor mixture [kg/m^3]
ρ_L	Density of liquid water, liquid water concentration [kg/m^3]
ρ_S	Density of solid skeleton [kg/m^3]
ρ_V	Density of water vapor, vapor concentration [kg/m^3]
$\rho_{V,a}$	Ambient or medium water vapor density or vapor concentration [kg/m^3]
τ	Time [h]
τ_0	Factor taking into account the tortuosity of the diffusion path [dimensionless]
Φ	Relative humidity [dimensionless]
Ψ	Capillary potential, water pressure in thermodynamic equilibrium with the water [m]
Ψ_M	Material moisture potential [W.h/kg]
\mathcal{R}	Relaxation parameter

SUBSCRIPTS

A	Air
G	Air-vapor mixture
L	Liquid
V	Vapor
W	Water (liquid+vapor)
S	Solid material
sat	Saturation
α	Ambient or medium

REFERENCES

Carnahan, B., Luther, H.A. and Wilkes, J.O., Applied Numerical Methods, Wiley, New York, pp. 100-116, 1969.

Gresho, P. and Lee, R.L., "Don't Suppress the Wiggles - They're Telling You Something," Finite Element Methods for Convection Dominated Flows, ADM-Vol. 34, pp. 37-61, Winter Annual Meeting of ASME, New York, Dec. 2-7, 1979.

Kardestuncer, H., Finite Element Handbook, McGraw-Hill, New York, 1987.

Stasa, F.L., Applied Finite Element Analysis for Engineers, Holt, Rinehart and Winston, New York, 1985.

Zienkiewicz, O.C., The Finite Element Method, McGraw-Hill (UK), London, 1977.

APPENDIX C

MATERIAL PROPERTIES NEEDED FOR VARIOUS THEORIES

TABLE C-1
Thermophysical Properties Required for Various
Heat and Mass Transfer Theories

THEORY	MATERIAL PROPERTIES
Liquid Diffusion	Isothermal Liquid Water diffusivity (D_L); Equilibrium relation (A-3.5)
Capillary	D_L (A-2.3); Heat of Phase Change (λ) Equilibrium relation (A-3.5)
Evaporation- condensation	Tortuosity ($\tau_0 = 1/\mu$), μ is obtained from Table (D-2); Molecular Diffusivity of Water Vapor in Air (D_A) is obtained from Section (D.2); Equilibrium relation (A-3.5); λ ; Porosity (ϵ).
Luikov's	Mass Transfer Potential relation (A-4.26); λ (A-4.19); Thermo-gradient Coefficient (δ) is obtained from (A-4.18); Isothermal moisture Diffusivity (D_W) is obtained from (A-4.17); Resistance of Vapor Diffusion (γ) and Specific Isothermal Moisture Capacity (C_M) is obtained from (A-4.28).
Phillip and De Vries	D_W is obtained from (A-5.16, A-5.12, A-5.7); Thermal Moisture Diffusivity (D_{WT}) is obtained from (A-5.15, A-5.8, A-5.13); λ .
Kricher, Berger and Pei's	Saturation Water Vapor Density ($\rho_{V, sat}$) is obtained from (A-6.17); Equilibrium relation (A-6.16); λ ; ϵ ; Density of Liquid Water (ρ_L); D_L ; Isothermal Water Vapor Diffusivity (D_V).
Moist Soils Model	D_W is obtained from (A-7.11, A-7.14, A-7.24); D_{WT} is obtained from (A-7.11, A-7.15, A-7.25); Volumetric Heat Capacity (C^*) is obtained from (A-7.3); ϵ ; ρ_L .
Irreversible Thermodynamics	$\rho_{V, sat}$ is obtained from (A-8.28); Specific Differential Heat of Wetting (Δh_W) and Specific Latent Heat of Vaporization (Δh_V) are obtained from (A-8.31 through A-8.33); Equilibrium relation; Liquid Conductivity (k_L); D_V ; Specific Heat of Water Vapor (C_V).

Note:

1. Thermal Conductivity (k_T), Specific Heat (C_S) and Density (ρ_S) are common to all theories.
2. Properties for which no reference is given are obtained experimentally.

APPENDIX D

LITERATURE COMPILED MATERIAL PROPERTIES

In this appendix the literature-compiled material properties are given. These material properties were either in tabular or graphical format. The data which were in graphical format were first digitized then curve fitted. In this appendix the following data are available:

1. Table D-1 equilibrium isotherm data. The content of Table D-1 can be explained as follows:
 - Column 1 : Classification of the material for easy reference.
 - Column 2 : Material name or description of the material.
 - Column 3 : Temperature or temperature range for the equilibrium data [$^{\circ}\text{C}$].
 - Column 4 : Dry-body density of the material [kg/m^3].
 - Column 5 : Experiment type,
 - A -- adsorption
 - D -- desorption
 - M -- mean.
 - Column 6 : Regression constant, a.
 - Column 7 : Regression constant, b.
 - Column 8 : Regression constant, c.
 - Column 9 : Regression constant, d.

The regression equation for the equilibrium equation is given as:

$$U = a \phi^b + c \phi^d$$

Where

U -- Moisture content in dry basis [kg/kg].
 ϕ -- Relative humidity [0 to 1].

2. Tables D-2 and D-3 water vapor diffusivity data. The content of Tables D-2 and D-3 can be explained as follows:
 - Column 1 : Classification of the material for easy reference.
 - Column 2 : Material name or description of the material.
 - Column 3 : Thickness of the specimen used in the experiments [mm].
 - Column 4 : Dry-body density of the material [kg/m^3].
 - Column 5 : Vapor diffusion resistance factor [dimensionless].

For a given vapor diffusion resistance factor, the water vapor diffusivity can be calculated from the following equations:

$$D_V = \frac{D_A}{\mu}$$

and

$$D_A = 0.083 \frac{10000}{P_b} \left(\frac{T}{273.0} \right)^{1.81}$$

Where

- D_A -- Molecular diffusion of water vapor in air [m^2/h].
 D_V -- Water vapor diffusivity [m^2/h].
 P_b -- Barometric pressure [kg/m^2].
 T -- Temperature [K].
 μ -- Vapor diffusion resistance factor [dimensionless].

3. Table D-4 moisture property data used in Luikov's theory. The content of Table D-4 can be explained as follows:
 Column 1 : Material name or description of the material.
 Column 2 : Dry-body density of the material [kg/m^3].
 Column 3 : Moisture content or moisture content range where the data are applicable [kg/kg].
 Column 4 : Temperature or temperature range for the equilibrium data [$^{\circ}C$].
 Column 5 : Moisture (liquid+vapor) diffusivity [m^2/h].
 Column 6 : Thermo-gradient coefficient [$1/^{\circ}C$].
 Column 7 : Moisture conductivity [$kg/m.h.^{\circ}M$].
 Column 8 : Specific isothermal moisture capacity [$kg/kg.^{\circ}M$].
4. Table D-5 liquid water diffusivity data. The content of Table D-5 can be explained as follows:
 Column 1 : Material name or description of the material.
 Column 2 : Moisture content or moisture content range where the data are applicable [kg/kg].
 Column 3 : Liquid water diffusivity [m^2/h].
5. Table D-6 moisture permeability data. The content of Table D-6 can be explained as follows:
 Column 1 : Classification of the material for easy reference.
 Column 2 : Material name or description of the material.
 Column 3 : Temperature or temperature range for the equilibrium data [$^{\circ}C$].
 Column 4 : Dry-body density of the material [kg/m^3].
 Column 5 : Regression constant.
 Column 6 : Regression constant.
 Column 7 : Regression constant.
 Column 8 : Regression constant.

The regression equation for the moisture permeability equation is given as:

$$\xi = a \phi^b + c \phi^d$$

Where

- ξ -- Moisture permeability [$g/m.h.mmHg$].
 ϕ -- Relative humidity [0 to 1].

TABLE D-1
Equilibrium Isotherms for Various Building Materials

Class	Material Name	T °C	ρ_3 kg/m ³	Exp	a	b	c	d
BRICK	Brick [2]	5-45	1720	A	0.003744	22.184770	0.002230	0.255390
		5-45	1840	A	0.002792	0.171445	0.010522	40.664750
	Brick [20]	20	1680	A				
		20	1860	A				
		20	1890	A				
		20	2030	A				
	Parnell Brick [1]	5	N/A	A	0.021053	1.017150	0.022365	11.285520
				D	0.016666	8.512250	0.025856	0.440512
				M	0.022418	0.590942	0.019302	9.321480
		15	N/A	A	0.012472	10.991360	0.024344	0.827079
				D	0.028790	0.372192	0.011002	8.601620
				M	0.012414	9.319372	0.025729	0.514964
		25	N/A	A	0.033034	0.980717	0.026450	12.295280
				D	0.034723	0.641719	0.026817	10.622700
				M	0.026433	10.174530	0.032570	0.712929
	Brick (The home steader) [1]	5	N/A	A	0.000269	0.684165	0.000855	10.904030
				D	0.000310	0.413623	0.000749	8.873786
				M	0.000800	11.783720	0.000342	0.718970
		15	N/A	A	0.001006	0.806932	0.000800	10.127700
				D	0.000616	6.337353	0.001350	0.202186
				M	0.001079	0.317415	0.000765	6.757072
		25	N/A	A	0.000715	11.021930	0.000696	1.041286
				D	0.000758	8.224447	0.000540	0.412256
M				0.000763	8.851550	0.000579	0.609507	
Red brick [3]	0-35	1700	A	0.000467	0.316240	0.004855	3.902922	
Tripoli brick [3]	0-35	480	A	0.041267	8.227257	0.029995	1.294379	
Veneer brick [1]	5	N/A	A	0.031400	1.003493	0.056273	11.495130	
			D	0.062256	9.819442	0.044448	0.588723	
			M	0.061170	10.098900	0.036060	0.680330	
	15	N/A	A	0.040598	0.994565	0.064208	11.514430	
			D	0.073844	10.107640	0.048598	0.631752	
			M	0.072232	11.108120	0.045329	0.783495	
	25	N/A	A	0.031499	0.898868	0.026590	10.757700	
			D	0.027000	9.634520	0.033587	0.589986	
			M	0.032150	0.694092	0.026485	9.797520	
CONCRETE AND CEMENT	Asbestos/cellulose cement (Hardiflex I) [1]	5	N/A	A	0.096110	11.147460	0.073510	1.006053
				D	0.094228	0.646410	0.073170	9.301769
				A	0.081657	0.753725	0.085280	9.674972
		15	N/A	A	0.086370	10.748620	0.085423	0.941907
				D	0.111499	0.640592	0.066360	9.385046
				M	0.077212	9.790125	0.097020	0.741827

	25	N/A	A	0.066134	0.989070	0.047285	11.114200
			D	0.023396	13.198100	0.089116	0.926835
			M	0.033888	11.750560	0.077990	0.955790
Asbestos/cellulose cement [20]	20	1510	A				
Asbestos cement [20]	20	1880	A				
	20	2030	A				
Cellular concrete [2]	5-45	460	A	0.061126	11.952830	0.009406	0.182729
	5-45	510	A	0.015204	0.330670	0.040595	8.402223
Cellular concrete [20]	20	475	A				
	20	500	A				
	20	500	A				
	20	510	A				
Cement mortar [20]	20	N/A	A				
	20	N/A	A				
Cement paste [9]	N/A	N/A	A	0.192503	0.264830	0.235570	20.765400
Cement paste [9]	N/A	N/A	A	0.236150	0.262687	0.176748	7.364265
Cement paste [9]	N/A	N/A	A	0.148857	0.162580	0.253757	1.169430
Cement sand mortar [3]	20	N/A	A	0.009190	0.620995	0.007892	3.478130
Concrete [20]	20	220	A				
	20	237	A				
	20	284	A				
	20	306	A				
	20	320	A				
	20	334	A				
	20	400	A				
	20	502	A				
Concrete block [1]	5	N/A	A	0.025650	1.056735	0.032420	11.775380
			D	0.031797	0.420070	0.027364	8.172718
			M	0.027557	0.606754	0.030777	9.586886
	15	N/A	A	0.023947	10.498800	0.037525	0.849945
			D	0.046040	0.380106	0.022665	7.882967
			M	0.024304	8.670148	0.040249	0.520760
	25	N/A	A	0.016777	10.437430	0.022899	0.859457
			D	0.010940	9.342740	0.026754	0.565665
			M	0.013850	9.638199	0.024615	0.676309
Cinders [3]	0	N/A	A	0.025789	0.705600	0.008239	5.823924
	35	N/A	A	0.010195	4.838340	0.019320	0.764573
Earthenware blocks [3]	N/A	N/A	A	0.009420	5.393850	0.003607	0.205223
Foam concrete [3]	0-35	345	A	0.043947	4.376072	0.039083	0.456663

	Gypsum slag concrete [3]	20	N/A	A	0.109930	0.756610	0.000000	0.000000
	Light-weight concrete [20]	20	270	A				
	Light-weight concrete [20]	20	640	A				
	Light-weight concrete [20]	20	715	A				
	Light-weight concrete [20]	20	1200	A				
	Lime cement mortar [20]	20	N/A	A				
	Lime sand stone [20]	20	1700	A				
		20	1800	A				
		20	1830	A				
	Slag concrete [3]	0	920	A	0.015743	6.435342	0.020692	0.455288
		35	920	A	0.011303	9.171323	0.023003	0.878349
CORK	Cork [2]	5-45	155	A	0.008486	0.368864	0.023822	5.623263
	Cork [3]	0	200	A	0.092466	0.861790	0.048627	5.870627
		35	200	A	0.059228	5.219846	0.068700	0.809798
	Cork [20]	20	N/A	A				
	Board pressed of garn. cork [2]	5-45	430	A	0.044540	9.070470	0.006964	0.585883
EARTH AND GROUND	Artic tuff [3]	0-35	960	A	0.001969	0.974140	0.003440	7.984554
	Activated charcoal (Steam activated charcoal) [8]	N/A	N/A	A	0.185427	0.501386	0.180112	0.503679
	Domestic coke [8]	N/A	N/A	A	0.010542	0.919939	0.010558	1.166619
	Expanded clay [20]	20	910	A				
	Kieselguhr [3]	24	N/A	A	0.020698	0.730957	0.020590	4.338963
FELT	Rag felt [3]	N/A	N/A	A	0.073129	1.067240	0.072437	1.071148
	Rag building felt [2]	5-45	500	A	0.155030	8.918695	0.051232	0.671865
	Rag building felt asphalt impr. [2]	5-45	920	A	0.038228	0.604026	0.101920	8.058596
	Wood felt [3]	0	120	A	0.135708	0.464387	0.230660	7.933550
		17	120	A	0.199204	10.059620	0.135044	0.891830
INSULATION	Asbestos fibre [3]	24	N/A	A	0.005413	2.687346	0.004667	0.488258
	Asbestos fiber (finely divided) [8]	N/A	N/A	A	0.007816	1.782664	0.002036	0.115087
	Carbamide foam [2]	5-45	14.3	A	0.002397	0.465397	0.000916	4.939812
	Expanded polystyrene [2]	5-45	17.2	A	0.000380	9.493858	0.000109	0.088410

	Expended polystyrene [20]	20	31	A				
	Fiberglass (Batts) [1]	5	N/A	A	0.047027	10.685760	0.021958	0.833640
				D	0.022563	0.524178	0.048903	10.066120
				M	0.020520	0.599597	0.051869	10.714840
		15	N/A	A	0.037590	0.787187	0.024539	9.990723
				D	0.027127	9.186606	0.047953	0.631495
				M	0.042620	0.683890	0.026438	9.300019
		25	N/A	A	0.015703	12.318370	0.058579	0.835330
				D	0.024384	7.171313	0.047110	0.363655
				M	0.050734	0.540385	0.022064	8.744134
	Glass fibres [4]	20	N/A	A	0.011744	0.667338	0.036274	13.324700
	Glass fibres [4]							
	d = 6 μm ; τ = 5.7%	50	20	A	0.009220	5.995554	0.002562	1.259258
	d = 5 μm ; τ = 9.7%	50	70	A	0.005782	2.037040	0.003840	11.324680
	d = 6 μm ; τ = 0.0%	50	100	A	0.064990	26.158060	0.002017	2.207223
	d = 6 μm ; τ = 12.8%	50	100	A	0.005940	0.832067	0.007492	7.734360
	d = 12 μm ; τ = 11.0%	50	121	A	0.001610	7.092125	0.007607	1.701209
	Glass wool [3]	N/A	N/A	A	0.004496	1.494255	0.000000	0.000000
	Mineral wool [20]	20	18	A				
	Mineral wool board [2]	5-45	175	A	0.007836	0.459843	0.012023	11.362020
	Mineral wool board [2]	5-45	400	A	0.013022	14.113446	0.005810	0.490509
	Polyester foam [2]	5-45	55.2	A	0.000400	11.598490	0.002020	1.054990
	Polyether foam [2]	5-45	26.6	A	0.000230	1.080185	0.000235	1.606183
	Polyester bonded fibreglass [2]	5-45	165	A	0.001573	0.442072	0.020743	7.829979
	Rockwool [20]	20	42	A				
	Rockwool bat [2]	5-45	100	A	0.002713	6.401205	0.001300	0.183926
	Urea Formaldehyde [1]	15	N/A	A	0.168378	10.906000	0.257984	0.930105
				D	0.124615	10.318120	0.329326	0.685490
				M	0.286406	0.760630	0.155748	10.033632
	Urethane foam [20]	20	25	A				
	Wool felt [2]	5-45	200	A	0.021749	0.751252	0.038275	5.774993
	Wool felt [2]	5-45	300	A	0.037812	0.621772	0.052028	7.767620
LEATHER	Leather [2]	5	940	A	0.214082	0.354347	0.268030	6.811124
		25	940	A	0.203852	0.408090	0.197957	6.898870
		45	940	A	0.122817	4.128172	0.172875	0.350514

	Leather (Sole oak - tanned) [8]	N/A	N/A	A	0.259628	0.702416	0.133610	9.140092
	Linoleum [2]	5	2.1	A	0.047436	0.351589	0.065578	4.771276
		25	2.1	A	0.052246	0.546057	0.074477	7.927515
		45	2.1	A	0.045499	0.654287	0.055819	6.076293
	Linoleum carpet [20]	20	N/A	A				
	Nylon [6]	N/A	N/A	A	0.038705	5.814072	0.062470	0.768932
	Plastic carpet [20]	20	N/A	A				
	Rubber (Solid tires) [8]	N/A	N/A	A	0.005515	0.932733	0.005514	1.112846
PAPER	Cellulose building paper [2]	5	600	A	0.174677	5.504476	0.069182	0.461679
		25	600	A	0.115488	5.794530	0.074729	0.655132
		45	600	A	0.064367	0.695687	0.091640	4.865170
	Cellulose building paper [2]	5	860	A	0.106438	0.549470	0.266137	7.505054
		25	860	A	0.150156	7.887783	0.119315	0.807976
		45	860	A	0.072930	0.475658	0.111200	3.585629
	Comm. ledger (75% Rag - 1% ash) [8]	N/A	N/A	A	0.124083	6.394190	0.079116	0.390250
	Kraft wrapping (Coniferous) [8]	N/A	N/A	A	0.083519	3.613129	0.097226	0.474043
	Macerated paper [4]	20	N/A	A	0.416794	15.767940	0.137870	0.988136
	Macerated paper Ammonium sulphate treated [1]	15	N/A	A	1.724364	16.231570	0.330080	1.548526
				D	1.647258	14.051750	0.349080	1.066276
				M	1.691997	14.858580	0.319954	1.198910
	Macerated paper Borax or Boric treated [1]	15	N/A	A	0.610468	11.060000	0.295197	0.925237
				D	0.265016	0.629843	0.708032	10.971130
				M	0.687082	10.770600	0.258300	0.691559
	M.F. news-print (Wood pulp - 24% ash) [8]	N/A	N/A	A	0.062463	4.516385	0.070962	0.488255
	H.M.F. writing (Wood pulp - 3% ash) [8]	N/A	N/A	A	0.091019	0.481886	0.081807	3.626582
	Building paper standad type [1]	15	N/A	A	0.140307	10.931450	0.137895	1.021389
				D	0.108820	0.440682	0.156286	8.040502
				M	0.124098	0.724080	0.152976	10.160480
	White bond (Rag - 1% ash) [8]	N/A	N/A	A	0.075346	4.802483	0.092310	0.575048
PARTICLE AND FIBERBORDS	Board [20]	20	300	A				
	Board semihard [20]	20	780	A				

Board oil-hardened [20]	20	1050	A				
Hard board [20]	20	1000	A				
Hardboard standard [1]	15	N/A	A	0.054039	11.113080	0.124834	0.864770
			D	0.040177	11.140190	0.151654	0.686398
			M	0.055558	10.277230	0.133820	0.737376
Hardboard oil tempered [1]	15	N/A	A	0.067900	10.547640	0.120777	0.863664
			D	0.153203	0.678870	0.055980	10.139990
			M	0.138046	0.756342	0.058972	10.350840
Hardboard (Weatherside) [1]	15	N/A	A	0.118229	0.861080	0.035555	12.091490
			D	0.034932	10.728560	0.125596	0.657796
			M	0.037749	10.984600	0.119742	0.736977
Particleborad (Sabreline) [1]	15	N/A	A	0.089663	10.909360	0.175190	0.897544
			D	0.190304	0.619994	0.089580	9.213884
			M	0.099064	9.613488	0.177513	0.714165
Particleborad (Bison Borad) [1]	15	N/A	A	0.170490	0.865268	0.077646	10.944230
			D	0.084378	8.984095	0.182846	0.585475
			M	0.090577	9.456628	0.171635	0.679634
Particleborad medium density [1]	15	N/A	A	0.172828	0.871116	0.106296	10.465220
			D	0.111049	8.704210	0.184115	0.589516
			M	0.113700	9.466062	0.174736	0.696784
Particleborad flooring grade [1]	15	N/A	A	0.061760	11.416090	0.168788	0.853995
			D	0.184835	0.612104	0.061449	9.845212
			M	0.067277	10.121770	0.173160	0.694885
Softborad (Pinex) [1]	15	N/A	A	0.114228	10.575250	0.178640	0.898697
			D	0.107275	8.960898	0.202278	0.607968
			M	0.187197	0.716922	0.113644	9.641624
Fibreborad (Customwood) [1]	15	N/A	A	0.074068	10.711130	0.140360	0.845134
			D	0.064680	9.303152	0.167399	0.570157
			M	0.071690	9.803980	0.151995	0.667882
Fibreborad flooring grade [1]	15	N/A	A	0.039886	12.824160	0.173809	0.818840
			D	0.038640	10.917420	0.181065	0.578242
			M	0.037148	11.942170	0.177280	0.676163
Wood particle board [2]	5	560	A	0.195618	9.349666	0.071074	0.479738
	25	560	A	0.064765	0.516527	0.118435	8.472525
	45	560	A	0.097213	8.386842	0.059689	0.552162
Wood partiel board [20]	20	610	A				
Wood fibre board [2]	5	215	A	0.063235	8.896166	0.031560	0.437160
	25	215	A	0.042429	7.153105	0.027772	0.462162
	45	215	A	0.024302	0.457866	0.036924	7.118702

	Wood fibre board [2]	5	610	A	0.077594	0.515816	0.130736	9.915459
		25	610	A	0.076060	9.480125	0.072070	0.577840
		45	610	A	0.091168	10.538700	0.065759	0.636717
	Wood fibre board [2]	5	870	A	0.341020	15.426120	0.120110	0.484537
		25	870	A	0.109178	7.646888	0.102728	0.464374
		45	870	A	0.058039	4.792619	0.089273	0.493884
	Wood fibre board [2]	5	960	A	0.222922	8.532650	0.114930	0.407768
		25	960	A	0.105460	0.456258	0.120703	7.037468
		45	960	A	0.050020	3.664755	0.093789	0.459456
	Wood fibre board with 6% asphalt impr. [2]	5-45	280	A	0.045129	6.820820	0.030594	0.370256
	Wood fibre board with 6% asphalt impr. [2]	5	860	A	0.171722	7.877448	0.109843	0.529206
		25	860	A	0.109566	0.633299	0.112747	8.717624
		45	860	A	0.074648	6.204236	0.097166	0.676350
	Wood fibre board with 6% asphalt impr. [2]	5	960	A	0.334598	14.894890	0.119088	0.482093
		25	960	A	0.106248	0.477882	0.113566	11.542490
		45	690	A	0.065300	9.246260	0.098119	0.511593
	Wood fibre board oil impr. [2]	5	1040	A	0.122333	0.480190	0.223703	12.711260
		25	1040	A	0.106470	8.282250	0.101024	0.394569
		45	1040	A	0.093349	0.436143	0.067794	6.437566
PLASTER-BOARD	Cement asbestos board [2]	5-45	775	A	0.068560	10.145370	0.006334	0.203290
	Fibrous [1]	5	N/A	A	0.012815	1.099860	0.165694	0.001642
				D	0.014144	8.186860	0.007130	0.353847
				M	0.010276	0.596172	0.001674	12.255020
		15	N/A	A	0.071556	0.789930	0.070008	1.082794
				D	0.032028	5.042665	0.075389	0.088672
				M	0.046154	0.338432	0.046148	0.331410
		25	N/A	A	0.052222	1.133502	0.079102	0.800598
				D	0.027129	4.951737	0.068760	0.075860
				M	0.043254	0.344539	0.043256	0.341127
	Gypsum plaster with paper [1]	5	N/A	A	0.027987	1.147282	0.085804	0.006580
				D	0.023536	7.570097	0.023213	0.346970
				M	0.005647	10.365420	0.024960	0.543676
	15	N/A	A	0.048344	1.147645	0.049887	0.809267	
			D	0.037363	5.560157	0.055749	0.125103	
			M	0.008485	11.214390	0.070094	0.404147	
	25	N/A	A	0.052940	1.131866	0.054927	0.801622	
			D	0.030856	5.307925	0.055687	0.104699	
			M	0.072549	0.397173	0.007774	11.705680	
Gypsum without paper [1]	5	N/A	A	0.051696	0.078536	0.051687	0.066278	
			D	0.010779	6.413036	0.018440	0.270059	
			M					
	15	N/A	A	0.089808	0.910320	0.005713	24.171370	
			D	0.029796	0.172585	0.029790	0.131583	
			M	0.010646	8.801787	0.061520	0.331076	

		25	N/A	A	0.005670	24.378500	0.090078	0.913910	
				D	0.026176	4.987109	0.063273	0.079312	
				M	0.006012	11.265230	0.059635	0.352047	
	Plaster [20]	20	1240	A					
	Plaster board [2]	5-45	730	A	0.009620	0.202660	0.196697	11.476600	
STONE	Limestone [1]	5	N/A	A	0.009372	11.788290	0.003314	0.942267	
				D	0.009873	10.228250	0.003133	0.544549	
				M	0.010327	11.456260	0.003045	0.684999	
		15	N/A	A	0.003238	0.283524	0.005247	7.438119	
	D			0.004944	8.172178	0.003342	0.458594		
	M			0.004310	0.833883	0.004147	9.951977		
		25	N/A	A	0.003534	0.358796	0.004430	7.400820	
	D								
	M								
		Limestone [3]	0-35	1300	A	0.001990	5.917070	0.001715	1.772220
		Limestone [20]	20	2700	A				
		Peat slab [3]	0	225	A	0.083830	7.730830	0.200263	0.882798
	35		225	A	0.175677	0.952510	0.090495	6.772648	
		Sphagnumpeat [3]	0-35	280	A	0.212620	0.717180	0.089590	4.761913
	Stone [20]	20	2700	A					
	Volcanic Rock [1]	5	N/A	A	0.002703	0.918435	0.003946	10.665450	
D				0.003053	0.504350	0.004050	8.284812		
M				0.002863	0.661100	0.004100	9.457277		
	15	N/A	A	0.003138	9.612249	0.003663	0.770217		
D			0.003893	6.877840	0.002958	0.239516			
M			0.003124	0.433870	0.003620	7.746225			
	25	N/A	A	0.002894	9.951792	0.004274	0.803289		
D			0.003254	6.887292	0.003495	0.317414			
M			0.003730	0.498354	0.003178	7.984943			
TEXTILE AND FIBRES	Acetate [12]	N/A	N/A	A					
	Cotton [6]	20	N/A	A	0.121512	5.142645	0.075312	0.378559	
	Cotton [11]	N/A	N/A	A					
	Cotton (Sea Island-roving) [8]	N/A	N/A	A	0.089756	3.535650	0.083564	0.519728	
	Cotton (American-cloth) [8]	N/A	N/A	A	0.137990	7.383585	0.083772	0.516120	
	Cotton (Absorbent) [8]	N/A	N/A	A	0.143152	0.690200	0.143768	0.690754	
	Cuprammonium cellulose acetate (Average skein) [8]	N/A	N/A	A	0.045740	2.083984	0.016330	0.339372	

	Fibrolite [3]	0-35	325	A	0.123734	0.551746	0.224515	4.713773
	Hemp (Manila and sisal-rope) [8]	N/A	N/A	A	0.056642	3.945043	0.128730	0.651700
	Jute (Average of several grades) [8]	N/A	N/A	A	0.086366	3.672244	0.154375	0.687455
	Jute web [20]	20	N/A	A				
	Linen (Table cloth) [8]	N/A	N/A	A	0.070042	0.556879	0.054413	3.978427
	Linen (Dry spun-yarn) [8]	N/A	N/A	A	0.082490	9.446458	0.113094	0.475750
	Orlon acrylic fibre [15]	N/A	N/A	A				
	Silk [13]	N/A	N/A	A				
	Silk (Raw cheveness-skein) [8]	N/A	N/A	A	0.134600	0.581210	0.120534	7.179449
	Terylene polyester fibre [15]	N/A	N/A	A				
	Wool [14]	N/A	N/A	A				
	Wool (Australian Merino-skein) [8]	N/A	N/A	A	0.178457	0.583749	0.095156	3.517180
	Viscose nitro cellulose (Average skein) [8]	N/A	N/A	A	0.082018	2.281830	0.100294	0.393952
	Viscose rayon [12]	N/A	N/A	A				
WOOD	Abachi [2]	5	370	A	0.075048	4.242048	0.051257	0.476255
		25	370	A	0.050703	0.584309	0.059790	4.702588
		45	370	A	0.047384	0.652608	0.054343	4.835848
	Balsa [2]	5	125	A	0.016722	0.489309	0.030714	5.690960
		25	125	A	0.014022	0.503004	0.027242	5.852653
		45	125	A	0.013965	0.655414	0.033013	8.259300
	Beech [20]	20	750	A				
	Birch [20]	20	600	A				
	Doussie [2]	5	660	A	0.072679	0.281146	0.070776	2.664116
		25	660	A	0.067990	3.441290	0.072336	0.370192
		45	660	A	0.057296	2.957994	0.064834	0.371123
	Oak [5]	N/A	N/A	A	0.150628	6.666482	0.126180	0.493184
	Oak [20]	20	780	A				
	Oregon pine [20]	20	560	A				

Pine [2]	5	530	A	0.072922	0.362360	0.087706	3.419070
	25	530	A	0.075279	0.473989	0.088280	5.094006
	45	530	A	0.075908	3.832880	0.061398	0.407650

Pine [20]	20	510	A				
Pinus radiata untreated [1]	15	N/A	A	0.087617	11.071180	0.191523	0.885963
			D	0.209907	0.734253	0.087260	10.255360
			M	0.089290	10.527170	0.200517	0.783496

Pinus radiata boric treated [1]	15	N/A	A	0.105062	10.755220	0.198055	0.882426
			D	0.107040	9.772727	0.210712	0.718040
			M	0.110492	10.066070	0.201280	0.780925

Pinus radiata CCA treated [1]	15	N/A	A	0.207683	0.873598	0.090423	11.097300
			D	0.096120	9.748652	0.213335	0.685539
			M	0.210205	0.765789	0.091048	10.380780

Pinus radiata AAC treated [1]	15	N/A	A	0.105740	11.023500	0.200094	0.915958
			D	0.080398	10.866700	0.237134	0.739543
			M	0.093998	10.444470	0.212513	0.780120

Plywood [20]	20	600	A				

Spruce [20]	20	750	A				

Spruce with vertical fibers [2]	5	410	A	0.064266	0.476742	0.078134	5.556426
	25	410	A	0.065073	6.581450	0.060809	0.540779
	45	410	A	0.044383	0.461255	0.047097	3.410469

Spruce with horizontal fibers [2]	5	450	A	0.075874	3.948554	0.069492	0.465295
	25	450	A	0.066900	0.550567	0.062213	4.273869
	45	450	A	0.058135	3.465735	0.053732	0.528938

Teak [2]	5	600	A	0.067164	2.418370	0.056589	0.333554
	25	600	A	0.073147	4.013810	0.058984	0.414012
	45	600	A	0.064765	2.772287	0.043498	0.357033

Wood [3]	-20	N/A	A	0.151922	5.410355	0.151338	0.490738
	0	N/A	A	0.138353	6.958823	0.161059	0.660522
	20	N/A	A	0.151862	0.727746	0.131848	6.866099
	40	N/A	A	0.132223	0.737857	0.133018	6.029177
	60	N/A	A	0.132110	5.746005	0.114583	0.741467
	80	N/A	A	0.113188	0.855983	0.136485	8.177380
	100	N/A	A	0.165785	11.277070	0.102156	0.843419

Wood [7]	4	N/A	A	0.163695	0.792386	0.122324	6.696172
	10	N/A	A	0.122777	6.940739	0.164183	0.799178
	16	N/A	A	0.163615	0.807227	0.122644	7.162130
	21	N/A	A	0.123445	7.233199	0.161089	0.801567
	27	N/A	A	0.122884	7.282050	0.155867	0.805194
	32	N/A	A	0.123107	7.470260	0.155920	0.811302
	38	N/A	A	0.122436	7.432344	0.152346	0.813004
	43	N/A	A	0.149406	0.824012	0.121288	7.603406
	49	N/A	A	0.119918	7.627708	0.145756	0.831902

		54	N/A	A	0.141228	0.835565	0.119210	7.606832
		60	N/A	A	0.117247	7.871782	0.138524	0.853137
		66	N/A	A	0.134609	0.862292	0.114624	7.906389
		71	N/A	A	0.132120	0.893380	0.111353	8.099529
		77	N/A	A	0.127498	0.904243	0.109180	8.017570
		82	N/A	A	0.123663	0.927978	0.107203	8.219320
		88	N/A	A	0.103828	8.427196	0.120752	0.968760
		93	N/A	A	0.115797	0.995339	0.101236	8.300570
		99	N/A	A	0.098084	8.411994	0.111883	1.038776
	Wood (Timber average) [8]	N/A	N/A	A	0.151457	3.711355	0.125610	0.639215
	Wood pulp (Pine) [3]	N/A	N/A	A	0.125643	0.626416	0.000000	0.000000
	Wood slab [3]	N/A	N/A	A	0.156522	0.944302	0.000000	0.000000

Note: The data adapted from reference [2] are in terms of volumetric moisture content not in terms of dry basis.

TABLE D-2
Water Vapor Diffusivity Values of Various Building Materials

Class	Material Name	t mm	ρ kg/m ³	μ
BUILDING MATERIAL	Asbestos cement sheeting [16]	6.50	1850.0	64.0
	Broken clinker [16]	15.00	N/A	62.5
	Cement rendering 1:1 [16]	21.60	N/A	32.0
	Cement rendering 1:3 [16]	21.80	N/A	21.0
	Cement rendering 1:4 [16]	21.50	N/A	14.0
	Epoxide-resin board, reinforced with fibreglass [16]	3.00	N/A	198000.0
	Gas concrete [16]	50.30 48.60	671.0 782.0	5.1 5.4
	Glazed tiles with 3.6% jointing	15.00	N/A	117.5
	4.6% jointing [16]	15.00	N/A	145.0
	Flintkote floor finish A [16]	15.30	N/A	143.0
	Flintkote floor finish B [16]	14.10	N/A	166.0
	Lean cement rendering 1:6 [16]	22.30	N/A	14.5
	Lime mortat rendering 1:3 [16]	14.30	N/A	9.1
	Marinite board (asbestos based)	12.40	N/A	14.1
	Plaster board [16]	10.00	N/A	13.5
	Sandstone [16]	43.50	2250.0	22.5
	COMPOSITE BOARDS	Cork board+bituminous undercoat (1 part bitumen+6 parts water) [16]	32.00	250.0
Cork board+bituminous undercoat (1 part bitumen+3 parts water) [16]		33.50	250.0	21.3
Cork board+bituminous undercoat (2 parts bitumen+1 part water) [16]		34.52	250.0	42.4
Cork board coated with filler & Flintkote primer U [16]		15.30	N/A	15.0
Cork board with protective coating : 1 part cement ,3 parts sand & 1 part Flintkote III (by				

volume) [16]	25.00	N/A	18.0
Cork board with 4 coats of Diofan [16]	16.00	N/A	28.0
Cork board with bitumen Wadimex A [16]	17.0	N/A	65.0
Cork board with protective coating : 0.5 part ground slate, 0.5 part cement , 3 parts Flintkote III (by volume) & hard-wearing finish of Hebolit [16]	25.00	N/A	67.0
	25.00	N/A	84.0
Cork board with protective coating : 4 coats of Diofan and 2 layers of tape [16]	16.70	N/A	141.0
Cork board with protective coating : 3 coats of glazing lacquer, 2 layers of tape and 2 coats of asphalt lacquer [16]	16.50	N/A	306.0
Cork board with protective coating : 3 coats of glazing lacquer, 2 layers of tape and 2 coats of insulating lacquer [16]	16.50	N/A	345.0
Cork board with protective coating : 3 parts of Flintkote III, 0.5 part ground slate and 0.5 part cement (by volume) with tape worked in [16]	16.50	N/A	345.0
Cork board with protective coating : 3 parts of Flintkote III, part ground slate and part cement (by volume) with tape worked in [16]	18.00	N/A	536.0

Felt with two coats of epoxide resin [16]	1.15	N/A	12360.0
Felt with three coats of epoxide resin [16]	1.20	N/A	15920.0

Fibreboard coated with melamine resin (Reniplast) [16]	3.50	N/A	1305.0
Fibreboard coated with melamine resin (Noratex) [16]	3.20	N/A	1330.0
Fibreboard coated with melamine resin (Thermopal) [16]	3.00	N/A	2790.0

Foamed plastic board + two coats (Seraltox + Duratox) [16]	10.35	N/A	102.0
Foamed plastic board + two coats (Acronal + Super-Imonite) [16]	10.20	N/A	440.0
Foamed plastic board + two coats (Bitumen + Acronal 14D) [16]	7.50	N/A	616.0
Foamed plastic board+three coats (Acronal + LWK + Duratox) [16]	10.65	N/A	390.0
Foamed plastic board+three coats (Seraltox + Duratox) [16]	10.60	N/A	420.0

Foamed plastic board coated with filler, followed by 2 coats of Diofan and 1 coat of Duratox mildew-resistant) [16]	11.00	N/A	174.0
Foamed plastic board + 2 coats Diofan + 1 coat Duratox [16]	10.50	N/A	183.0
Foamed plastic board with sprayed cocooning on fibreglass matting [16]	20.00	N/A	195.0
Foamed plastic board with PVC foil fixed with adhesive [16]	19.00	N/A	219.0
Foamed plastic board coated with filler +2 coats of Diofan [16]	10.80	N/A	560.0
Foamed plastic board coated with filler +2 coats of Diofan after 10 cycles of temperature from 22 to -20 °C [16]	10.80	N/A	450.0
Foamed plastic board coated with filler +3 coats of Diofan [16]	10.50	N/A	1070.0
Foamed plastic board coated with filler +3 coats of Diofan after 10 cycles of temperature from 22 to -20 °C [16]	10.50	N/A	1170.0

Hornitex moulded wood-fibreboard + synthetic plastic coating	3.00	N/A	1390.0

Marinite board coated with plastic + Rulon filler [16]	12.60	N/A	526.0
	12.10	N/A	537.0

Mineral wool board + single coat of Mowilith [16]	22.85	N/A	8.4
Mineral wool board + two coats of Herbopan [16]	20.12	N/A	10.0
Mineral wool board + three coats of Herbopan [16]	20.21	N/A	22.0
Mineral wool board + three coats of Special Protegol [16]	22.40	N/A	50.0
Mineral wool board + three coats of Procolor [16]	22.50	N/A	158.0
Mineral wool board with one layer of sprayed cocooning [16]	17.50	N/A	4.4
Mineral wool board, coated with Acronal 14d, blue + fibreglass matting [16]	21.00	N/A	8.8
Mineral wool board, coated with Acronal 14d, grey + fibreglass matting [16]	21.00	N/A	10.9
Mineral wool board, coated with Acronal 14d, blue, without fibreglass matting [16]	21.00	N/A	13.9
Mineral wool board treated with primer (of Mowilith and additives) followed by 3 coats of sprayed			

	cocooning [16]	40.00	N/A	62.0
	Mineral wool board with a coating of Diofan [16]	40.00	N/A	64.0
INSULATING MATERIALS	Baked cork brick [16]	38.00	121.0	20.0
		37.00	160.0	15.0
	Compostite board of expanded cork and foamed polystyrene; boards bonded with bitumen [16]	27.50	N/A	45.0
	Foamed polystyrene, impregnated to be flame-resistant [16]	48.00	13.5	25.0
	Foamed polystyrene [16]	31.00	37.0	76.0
	Foamed polystyrene [16]	10.00	12.0	35.0
		10.00	12.2	42.0
		10.00	13.0	46.0
		10.00	14.0	44.0
		10.00	15.0	48.0
		10.00	18.0	36.0
		10.00	19.0	57.0
		10.00	20.0	41.0
		10.00	21.0	40.0
		10.00	22.0	47.0
		10.00	23.0	42.0
		10.00	24.0	48.0
		10.00	25.0	51.0
		10.00	26.0	59.0
		10.00	28.0	58.0
		10.00	29.0	40.0
		10.00	31.0	48.0
		10.00	38.0	68.0
		10.00	48.0	59.0
	Foamed polystyrene [16]	20.00	15.0	21.0
	Foamed polystyrene [16]	30.00	30.0	74.0
	Foamed polyurethane [16]	19.80	23.0	32.0
		20.80	40.0	37.0
		20.40	146.0	99.0
		20.60	34.3	111.0
		19.90	33.0	115.0
		21.00	254.0	279.0
	Foamed PVC [16]	58.00	26.0	413.0
		29.00	35.0	206.0
	Mineral wool board [16]	18.30	347.0	5.1
	Mineral wool board with paint	16.80	390.0	6.7
	Monoblock (mineral wool board) [16]	16.00	220.0	2.7

	Styrofoam [16]	20.00	15.0	51.0
		31.00	26.0	92.0
PAINTS AND COATINGS	Acronal D14 [16]	0.15	N/A	1390.0
	Acronal D14 and Dyckerhoffweiss [16]	0.10	N/A	1800.0
	Acronal D14 and Lithopone [16]	0.09	N/A	1400.0
	Acronal 14D, blue, with interlay of fiberglass matting [16]	0.60	N/A	264.0
	Acronal 14D, grey, with interlay of fiberglass matting [16]	0.60	N/A	341.0
	Acronal 14D, without fiberglass interlay [16]	0.40	N/A	667.0
	Albertlac number 1 [16]	0.15	N/A	115000.0
	Albertlac number 2 [16]	0.15	N/A	105000.0
	Albertlac number 3 [16]	0.15	N/A	74000.0
	Bitumen coating, Wadimex A	2.00	N/A	500.0
	Bitumen first coat [16]	1.00	N/A	740.0
		1.50	N/A	890.0
	Cocooning, sprayed [16]	0.60	N/A	5250.0
		0.70	N/A	8730.0
	Cocooning, sprayed(3-coat) [16]	0.55	N/A	14520.0
	Cocooning, sprayed(4-coat) [16]	0.84	N/A	9310.0
	Cocooning over absorbent material(mineral wool board)[16]	0.70	N/A	74.0
	Diofan single coat [16]	0.04	N/A	12000.0
	Diofan two-coat [16]	0.08	N/A	113000.0
	Diofon 2 coats + 1 coat Duratox (mildew-resistant) [16]	0.28	N/A	6050.0
	Diofon 2 coats + 1 coat Duratox (upon a smooth base) [16]	0.14	N/A	134800.0
	Diofon 2 coats upon smooth base [16]	0.24	N/A	24400.0
	Diofon 2 coats upon smooth base after 10 cycles of temperature from 22 to -20 °C [16]	0.24	N/A	19000.0
	Diofan three-coat [16]	0.10	N/A	199000.0
	Diofon 3 coats upon smooth base [16]	0.25	N/A	37000.0
	Diofon 3 coats upon smooth base after 10 cycles of temperature from 22 to -20 °C [16]	0.24	N/A	49000.0
	Diofon [16]	0.06	N/A	41400.0
Epoxide resin, 2-coat [16]	0.23	N/A	61800.0	
Epoxide resin, 3-coat [16]	0.28	N/A	67900.0	
Flintkote I (bituminous mixture) [16]	4.60	N/A	760.0	
Flintkote III (bituminous mixt.)				

[16]	5.50	N/A	350.0
Flintkote V (bituminous mixture)			
[16]	4.50	N/A	760.0
Flintkote VII (bituminous mixt.)			
[16]	4.10	N/A	765.0
Flintkote primer U [16]	0.30	N/A	7600.0
Flintkote with hard surface film of:1 part Flintkote V + 1 part sand (by volume) [16]	7.00	N/A	470.0
Flintkote with hard surface film of:1 part Flintkote V + 1.5 part sand (by volume) [16]	6.50	N/A	337.0
Flintkote with hard surface film of:1 part Flintkote VII + 2 part sand (by volume) [16]	5.50	N/A	33.0
Flintkote with hard surface film of:1 part Flintkote I + 1 part cement + 2 parts cork powder [16]	6.50	N/A	100.0
Flintkote protective coating comprising 3 parts by volume Flintkote III, 0.5 part ground slate & 0.5 part cement (top- -cap--Hebolit) [16]	9.00	N/A	177.0
	9.00	N/A	224.0
Flintkote-Monoform, 2.2 kg/m ² [16]	2.00	N/A	3220.0
Flintkote protective coating comprising 3 parts by volume Flintkote III, 0.5 part ground slate & 0.5 part cement with tape worked in [16]	2.00	N/A	3585.0
	2.00	N/A	4800.0

Foster-Mastic 625, 2.88 kg/m ² . [16]	3.50	N/A	22920.0

Hard-wearing coating comprising of:1 part Flintkote I + 1 part cement + 2 parts cork powder (by volume) [16]	7.40	N/A	31.0

Hasol coating T60/55 [16]	0.12	N/A	5340.0
	0.12	N/A	10550.0

Herbopan, two coats [16]	0.60	N/A	280.0
Herbopan, three coats [16]	0.70	N/A	600.0

Layer of bitumen + Acronal [16]	1.00	N/A	4500.0

Melamine resin [16]	0.15	N/A	21060.0
	0.20	N/A	41000.0
	0.20	N/A	19750.0

Mowilith [16]	0.45	N/A	380.0

	Plastic coating with Rulon filler [16]	0.40	N/A	16140.0
		0.40	N/A	154250.0
	Polyster, reinforced with fibre-glass [16]	1.30	N/A	52235.0
	Procolor 'EP' undercoat and finishing coat [16]	1.50	N/A	2360.0
	Prodoral chlorinated rubber lacquer [16]	0.15	N/A	71000.0
	Prodoral with two coats of paint DP30 [16]	4.00	N/A	2500.0
	Prodoral treated five times with Protegol M [16]	4.00	N/A	3770.0
	Protective coating comprising 1:3 cement/sand mixture with 1 part by volume Flintkote III [16]	9.00	N/A	42.0
	Protective coating : 4 coats Diofan & 2 layer of tape [16]	1.00	N/A	3100.0
	Protective coating : 3 coats glazing lacquer, 2 layers of tape & 2 coats asphalt lacquer [16]	1.00	N/A	4970.0
	Protective coating : 3 coats glazing lacquer, 2 layers of tape & 2 coats insulating lacquer [16]	1.00	N/A	4970.0
	Protegol, special three-coat application [16]	1.50	N/A	730.0
	Super-Imonite (once) [16]	0.11	N/A	10200.0
	Super-Imonite (twice) [16]	0.20	N/A	20800.0
	Synthetic plastic coating [16]	0.18	N/A	23000.0
	Two-coat combination system [16]	0.35	N/A	10100.0
		0.25	N/A	2800.0
	Three-coat combination system [16]	0.40	N/A	9800.0
	Four-coat combination system [16]	0.25	N/A	37000.0
BUILDING PAPERS AND FELTS AND FOILS	Asphalt paper ,140 g/m ² [16]	0.20	N/A	2580.0
	Bitumen paper, one-sided [16]	0.15	N/A	580.0
	Bitumen paper [16]	0.30	N/A	3000.0
	Bituminous felt, 725 g/m ² [16]	0.70	N/A	1510.0
	Bituminous felt, 723 g/m ² [16]	0.70	N/A	1630.0
	Coroplast ,black and self-adhesive, 200 g/m ² [16]	0.15	N/A	28030.0

Corothene ,black and self- adhesive, 220 g/m ² [16]	0.25	N/A	132100.0
	0.20	N/A	181700.0
Felt [16]	0.92	N/A	108.0
Felt,620 kg/m ² [16]	0.70	N/A	110.0
Samcolastic felt,unimpregnated [16]	1.50	N/A	70.0
Samcolastic felt,impregnated with 52% acetone [16]	1.20	N/A	179.0
Fibreglass matting (for roofs) GB5,3000 g/m ² [16]	2.00	N/A	21880.0
Fibreglass matting roof sheeting and ultraplast,No. 5,2550 g/m ² [16]	2.00	N/A	23430.0
Filter paper with coating of Hasol [16]	0.30	N/A	2220.0
Filter paper X with coating of Hasol [16]	0.30	N/A	4300.0
Glass wool felt,talcumed,2805 g/m ² . [16]	2.50	N/A	7100.0
Hostophan foil, 45 g/m ² [16]	0.04	N/A	140000.0
Jute fabric waterproof sheeting (AIB),with jute fabric interlay (H305),2910 g/m ² [16]	3.00	N/A	17660.0
Luvitherm foil [16]	0.03	N/A	139000.0
Percalor Standard,green/gray, 338 g/m ² [16]	0.70	N/A	122.0
Percalor-Diplex,reinforced with glass-fibre,330 g/m ² [16]	0.70	N/A	82.0
Perforated Paratect skin [16]	4.00	N/A	31.0
Non-perforated Paratect skin [16]	2.50	N/A	100000.0
Polyethylene foil [16]	0.10	N/A	65000.0
PVC foil [16]	0.40	N/A	8560.0
Roofing felt [16]	1.20	N/A	1300.0
Roofing felt,sanded and stewn with chippings,2800 g/m ² [16]	2.60	N/A	19500.0
Roofing felt,T80-300,with chipp- -ings,3850 g/m ² [16]	1.90	N/A	5600.0
Vaporex [16]	0.80	N/A	3700.0
Vaporex, bituminized [16]	0.80	N/A	6400.0
Vaporex, bituminized 863g/m ²			

	[16]	0.90	N/A	8560.0
	Vaporex, heavily bituminized and sanded [16]	2.00	N/A	15200.0
	Ultraplast insulating foil (PVC-based) [16]	0.50	N/A	16700.0
METALS	Aluminium sheeting with holes			
	28 holes/m ² [16]	1.50	N/A	6195.0
	56 holes/m ²	1.50	N/A	1345.0
	112 holes/m ²	1.50	N/A	610.0
	224 holes/m ²	1.50	N/A	343.0
	448 holes/m ²	1.50	N/A	164.0
	Aluminium sheeting with joints formed in grooves in aluminium rail. Joints sealed once. (Gregson system) [16]	1.50	N/A	61800.0
	Ditto with joints sealed twice (Gregson system) [16]	1.50	N/A	147600.0
	Bituminous felt with 0.03 mm thick interlay of aluminium foil [16]	1.60	N/A	134300.0
	Bituminous felt with 0.05 mm thick interlay of aluminium foil [16]	1.60	N/A	268600.0
	Aluminium foil, coated on one side with plastic [16]	0.06	N/A	1700000.0
	Aluminium foil, coated on one side with plastic (Metalon, an epoxy adhesive) [16]	0.06	N/A	1700000.0
	Aluminium foil with high pressure polyethylene glued to sodium paper, 152g/m ² [16]	0.15	N/A	2084000.0
	Laminated aluminum foil [16]	0.03	N/A	733000.0
	Percalor foil [16]	0.50	N/A	
	Sand paper, double pitched, with aluminum foil interlay [16]	0.25	N/A	520000.0

TABLE D-3
Water Vapor Diffusivity Value Ranges for Various Building Materials

Material Name	Diffusion Resistance Factor μ		
	Low	Medium	High
BUILDING MATERIALS			
Brickwork 1600 to 1800 kg/m ³ [16]	8	9	10
Roofing tiles 1600 kg/m ³ [16]	36	40	44
Clinker or broken clinker walling [16] 2000 kg/m ³	60	120	180
Tiled Finish [16]	150	300	N/A
Concrete 2300 kg/m ³ [16]	28	34	40
Sandstone 2250 kg/m ³ [16]	N/A	22	N/A
Calcareous sandstone 1900 kg/m ³ [16]	N/A	16	N/A
Lime mortar rendering/plaster [16]	9	10	11
Lean cement mortar rendering [16]	10	12	14
Cement mortar rendering [16]	15	20	25
Flintkote mortar rendering [16]	30	65	100
Flintkote floor finish [16]	N/A	150	N/A
Luberfix adhesive mortar [16]	N/A	55	N/A
Gypsum plaster finish [16]	5	6	7
Pumice concrete 780 kg/m ³ [16]	N/A	3	N/A
Porous concrete, gas concrete [16]	5	6	7
Pumice slabs 900 kg/m ³ [16]	N/A	5	N/A
Plasterboard, Marinite boarding [16]	N/A	13	N/A
Broken brick concrete [16]	N/A	5	N/A
Asbestos cement sheeting 1800 to 1850 kg/m ³ [16]	60	65	70
Fibre board [16]	N/A	62	N/A
Lightweight wood-wool boarding [16]	4	6	8

Pine timber [16]	110	170	230
Beech wood [16]	2	36	70
Epoxide-resin boarding, reinforced with fibre glass [16]	N/A	200,000	N/A
INSULATING MATERIALS			
Baked cork brick 100 to 150 kg/m ³ [16]	5	15	30
Expanded cork brick, with pitch binding agent 150 to 230 kg/m ³ [16]	3	5	14
Foamed polystyrene 15 to 50 kg/m ³ [16]	25	40	60
Foamed polyurethane 40 to 150 kg/m ³ [16]	30	40	100
Foamed PVC 25 to 35 kg/m ³ [16]	N/A	200	400
Foamed urea formaldehyde 12 kg/m ³ [16]	N/A	2	N/A
Peat insulation board 220 kg/m ³ [16]	N/A	3	N/A
Soft wood-fibre boarding [16]	N/A	4	N/A
Mineral wool felts and boards 30 to 100 kg/m ³ [16]	1	1	1
Heavy mineral wool boards 300 kg/m ³ [16]	5	6	7
Monoblock 220 kg/m ³ [16]	N/A	3	N/A
Foamed glass layers [16]	5,000	70,000	∞
BARRIER LAYERS (FELTS AND FOILS)			
Roofing felt, laid in bitumen [16]	3,000	10,000	20,000
Vaporex, standard [16]	N/A	3,500	N/A
Vaporex, bituminized [16]	N/A	6,000	N/A
Vaporex, strong, bituminized and sanded [16]	N/A	15,000	N/A
Vaporex, super [16]	N/A	56,000	N/A
Bituminous felt and aluminium foil interlay, 0.03 mm [16]	N/A	135,000	N/A
Bituminous felt and aluminium foil interlay, 0.05 mm [16]	N/A	270,000	N/A
Bituminous felt and aluminium foil interlay,	N/A	700,000	N/A

0.1 mm [16]			
Aluminium foil, laminated on one side (with plastic) 0.025 mm [16]	N/A	700,000	N/A
Aluminium foil, laminated on one side (with plastic) 0.06 mm [16]	N/A	1,700,000	N/A
Aluminium foil, laminated on one side (with plastic) 0.08 mm [16]	N/A	2,000,000	N/A
Luvitherm foil (PVC) 0.03 mm [16]	N/A	140,000	N/A
Polyethylene foil, 0.10 mm [16]	N/A	65,000	N/A
Polyethylene foil, 0.30 mm [16]	N/A	34,000	N/A
PVC foil, 0.40 mm [16]	N/A	8,500	N/A
Ursuplast foil (PVC), 0.50 mm [16]	N/A	17,000	N/A
Igelit foil (PVC) 0.27 mm [16]	N/A	14,000	N/A
PAINTS AND COATINGS			
Diofan, single coat (0.04 mm) [16]	12,000	16,000	20,000
Diofan, two coats (0.08 mm) [16]	N/A	113,000	N/A
Diofan, three coats (0.1 mm) [16]	N/A	200,000	N/A
Acronal D14 [16]	1,400	1,600	1,800
Chlorinated rubber lacquer, cyclo-rubber lacquer, Albertlack [16]	70,000	90,000	110,000
Sprayed cocooning [16]	5,000	9,000	14,000
Melamine resin [16]	20,000	30,000	40,000
Epoxide resin [16]	60,000	64,000	68,000

TABLE D-4
Coefficients of Moisture Transfer

Material Name	$\rho \times 10^3$ kg/m ³	U%	T °C	$a_M \times 10^5$ m ² /h	$\delta \times 10^2$ 1/°C	$k_M \times 10^4$ kg/m.h.°M	$C_M \times 10^4$ kg/kg. M
Asbestos cement slabs [3]	390.0	10.0	20.0	1.40	0.540	N/A	N/A
	390.0	20.0	20.0	3.20	1.140	N/A	N/A
	390.0	10.0	20.0	6.20	0.880	N/A	N/A
	390.0	20.0	20.0	7.90	0.420	N/A	N/A
	390.0	10.0	20.0	8.30	0.210	N/A	N/A
	390.0	20.0	20.0	8.30	0.140	N/A	N/A
Autoclaved concrete [3]	400.0	10.0	20.0	1.90	0.400	N/A	N/A
	400.0	20.0	20.0	2.00	0.800	N/A	N/A
	400.0	30.0	20.0	2.50	0.920	N/A	N/A
	400.0	40.0	20.0	4.00	0.960	N/A	N/A
Brick [17]	1200.0	N/A	N/A	10.00	? ???	2.160	18.00
Ceramic [18]	2000.0	N/A	N/A	24.00	? ???	8.640	18.00
Concrete [18]	N/A	N/A	N/A	19.20	? ???	0.504	N/A
	N/A	N/A	N/A	111.00	? ???	2.880	N/A
Mineral wool [3]	200.0	20.0	20.0	0.90	0.920	N/A	N/A
	to	100.0	20.0	3.90	0.920	N/A	N/A
	800.0	140.0	20.0	4.80	N/A	N/A	N/A
		180.0	20.0	5.60	N/A	N/A	N/A
Diatomite slabs [3]	500.0	10.0	20.0	1.00	0.500	N/A	N/A
	500.0	20.0	20.0	3.50	0.520	N/A	N/A
	500.0	30.0	20.0	7.00	0.350	N/A	N/A
	500.0	40.0	20.0	9.10	0.250	N/A	N/A
	500.0	50.0	20.0	9.10	0.170	N/A	N/A
Expanded polystyrene [19]	N/A	N/A	N/A	140.00	N/A	N/A	N/A
Kaolin [3]	N/A	5.0	25.0	8.00	0.150	N/A	N/A
	N/A	10.0	25.0	9.00	0.230	N/A	N/A
	N/A	20.0	25.0	25.00	0.270	N/A	N/A
	N/A	40.0	25.0	46.00	0.250	N/A	N/A
	N/A	50.0	25.0	47.00	0.190	N/A	N/A
Quartz sand [3]	N/A	5.0	45.0	70.00	0.120	N/A	N/A
	N/A	10.0	45.0	120.00	0.190	N/A	N/A
	N/A	15.0	45.0	208.00	0.180	N/A	N/A
	N/A	20.0	45.0	N/A	0.080	N/A	N/A
Kuchino clay [3]	N/A	12.0	20.0	4.00	N/A	N/A	N/A
	N/A	12.0	30.0	7.50	N/A	N/A	N/A
	N/A	12.0	40.0	12.50	N/A	N/A	N/A
	N/A	10.0	50.0	18.00	N/A	N/A	N/A
	N/A	10.0	25.0	7.50	N/A	N/A	N/A

	N/A	5.0	25.0	N/A	0.060	N/A	N/A
	N/A	10.0	25.0	N/A	0.125	N/A	N/A
	N/A	20.0	25.0	N/A	0.076	N/A	N/A
Moscow brown coal [3]	N/A	21.0	45.0	N/A	0.300	N/A	N/A
	N/A	25.0	45.0	N/A	0.750	N/A	N/A
	N/A	28.0	45.0	N/A	2.800	N/A	N/A
Loess-like loam [3]	N/A	5.0	40.0	N/A	0.200	N/A	N/A
	N/A	10.8	40.0	N/A	0.270	N/A	N/A
	N/A	19.0	40.0	N/A	0.625	N/A	N/A
	N/A	27.9	40.0	N/A	0.870	N/A	N/A
Peat, lowland (40% rotted) [3]	N/A	25.0	30.0	N/A	0.210	N/A	N/A
	N/A	43.0	30.0	N/A	0.320	N/A	N/A
	N/A	66.0	30.0	N/A	0.400	N/A	N/A
	N/A	100.0	30.0	N/A	0.230	N/A	N/A
	N/A	150.0	30.0	N/A	0.250	N/A	N/A
Peat, lowland [3]	N/A	50.0	45.0	23.00	0.800	N/A	N/A
	N/A	100.0	45.0	31.00	1.800	N/A	N/A
	N/A	150.0	45.0	40.00	2.400	N/A	N/A
	N/A	200.0	45.0	49.00	2.700	N/A	N/A
	N/A	300.0	45.0	59.00	2.300	N/A	N/A
	N/A	400.0	45.0	59.00	1.200	N/A	N/A
Polystyrene [17]	N/A	N/A	N/A	N/A	N/A	3.78×10^{-2}	N/A
Soil, clay [17]	N/A	N/A	N/A	14.70	N/A	3.960	N/A
Vapor barrier [17]	N/A	N/A	N/A	N/A	N/A	1.01×10^{-4}	N/A
Wood, pine [3]	N/A	10.0	40.0	0.18	1.000	N/A	N/A
	N/A	25.0	40.0	0.46	2.000	N/A	N/A
	N/A	50.0	40.0	0.62	2.000	N/A	N/A
	N/A	75.0	40.0	0.62	0.600	N/A	N/A
Tuzlovo mud [3]	N/A	4.3	22.0	N/A	0.144	N/A	N/A
	N/A	8.3	22.0	N/A	0.252	N/A	N/A
	N/A	12.5	22.0	N/A	0.224	N/A	N/A
	N/A	18.3	22.0	N/A	0.196	N/A	N/A
	N/A	55.0	22.0	N/A	0.022	N/A	N/A
	N/A	122.2	22.0	N/A	0.011	N/A	N/A

TABLE D-5
Coefficients of Water Diffusion at 20°C

Material Name	U%	$a_M \times 10^5$ m ² /h
Gypsum [3]	0.0	0.110
	3.0	0.140
	6.0	0.170
	8.0	0.200
	10.0	0.230
	12.0	0.270
	15.0	0.330
	20.0	0.500
Gas concrete [3]	0.0	0.170
	5.0	0.175
	10.0	0.180
	15.0	0.190
	20.0	0.195
	25.0	0.200
	30.0	0.205
Foam concrete [3]	0.0	0.113
	5.0	0.450
	10.0	0.620
	15.0	0.680
	20.0	0.700
	25.0	0.650

TABLE D-6
Moisture Permeability for Various Building Materials

Class	Material Name	T °C	ρ kg/m ³	a	b	c	d
BRICK	Brick [2]	5-45	1720	0.000530	0.094560	0.000532	0.115540
	Brick [2]	5-45	1840	0.000296	0.050838	0.000296	0.056512
CONCRETE AND CEMENT	Cellular concrete [2]	5-45	460	0.001428	0.049739	0.000869	1.962446
	Cellular concrete [2]	5-45	510	0.000334	2.599087	0.000690	0.093965
CORK	Cork [2]	5-45	155				
	Board pressed of garn. cork [2]	5-45	430	0.000149	0.006497	0.000068	6.854995
FELT	Rag building felt [2]	5-45	500	0.000403	0.102459	0.000990	6.084116
	Rag building felt asphalt impr. [2]	5-45	920	0.000019	3.867242	0.000084	8.190987
INSULATION	Carbamide foam [2]	5-45	14.3	0.001823	0.235040	0.001823	0.234460
	Expended polystyrene [2]	5	17.2	0.000064	-0.174930	0.000248	0.374799
		25	17.2	0.000128	0.093110	0.000128	0.093407
		45	17.2	0.000086	2.653169	0.000287	0.218575
	Mineral wool board [2]	5-45	175	0.000820	0.061994	0.000820	0.062920
	Mineral wool board [2]	5-45	400	0.001788	0.116999	0.001788	0.117080
	Polyester foam [2]	5-45	55.2	0.000590	0.232459	0.000589	0.130896
	Polyether foam [2]	5	26.6	0.001458	0.422289	0.001458	0.184669
		25	26.6	0.001820	0.014349	0.001752	0.983617
		45	26.6	0.001767	0.134282	0.001768	0.308476
	Polyester bonded fibreglass [2]	5-45	165				
	Rockwool bat [2]	5-45	100				
	Wool felt [2]	5-45	200	0.002290	0.271862	0.002290	0.271835
Wool felt [2]	5-45	300	0.002192	0.368360	0.002190	0.367746	
LEATHER	Leather [2]	5-45	940	0.000374	0.101853	0.000299	6.330303
	Linoleum [2]	5-45	2.1	0.000003	0.182210	0.000005	4.320802
PAPER	Cellulose building paper [2]	5-45	600	0.000663	0.148310	0.001085	7.036223

PARTICLE AND FIBERBORDS	Cellulose building paper [2]	5	860	0.001510	9.896840	0.000470	0.216342
		25	860	0.001078	9.773487	0.000398	0.205018
		45	860	0.000190	0.459998	0.000200	0.459770
	Wood particle board [2]	5-45	560	0,000245	3.632870	0.000158	0.268519
	Wood fibre board [2]	5	215	0.001208	0.115087	0.001208	0.115135
		25	215	0.001407	0.055493	0.001250	1.473120
		45	215	0.001207	0.233305	0.001207	0.233850
	Wood fibre board [2]	5-45	610	0.003980	3.317516	0.004303	0.019256
	Wood fibre board [2]	5-45	870	0.000117	0.076865	0.000438	8.931798
Wood fibre board [2]	5-45	960	0.000080	0.093082	0.000127	3.384946	
Wood fibre board with 6% asphalt impr. [2]	5	280	0.000553	0.029458	0.000554	0.029952	
	25	280	0.000630	0.215820	0.000630	0.005886	
	45	280	0.000778	0.165686	0.000778	0.170907	
Wood fibre board with 6% asphalt impr. [2]	5-45	860	0.000120	3.907568	0.000068	0.096816	
Wood fibre board with 6% asphalt impr. [2]	5-45	960	0.000173	8.863690	0.000033	0.095604	
Wood fibre board oil impr. [2]	5-45	1040	0.000022	0.859364	0.000068	5.705475	
PLASTER- BOARD	Cement asbestos board [2]	5-45	775	0.000497	0.307816	0.000645	2.748160
	Plaster board [2]	5-45	730	0.003133	10.562230	0.000308	0.198397
WOOD	Abachi [2]	5	370	0.000993	1.200579	0.000403	6.689495
		25	370	0.001050	1.593129	0.000293	11.512570
		45	370	0.000690	1.725895	0.000338	1.787027
	Balsa [2]	5-45	125	0.001223	3.325168	0.000104	0.326892
	Doussie [2]	5-45	660	0.000310	6.511740	0.000132	1.163469
	Pine [2]	5-45	530	0.001174	13.406200	0.000122	2.336779
	Spruce with vertical fibers [2]	5	410	0.000246	1.555783	0.002818	11.768300
		25	410	0.002847	15.829630	0.000367	2.816836
		45	410	0.002392	83.752850	0.000345	3.325343
	Spruce with horizontal fibers [2]	5	450	0.002607	0.403743	0.002505	0.998833
		25	450	0.001836	0.390450	0.001836	0.392037
		45	450	0.001840	0.393095	0.001840	0.394776
	Teak [2]	5-45	600				

NOMENCLATURE

- a Regression coefficient [dimensionless]
- a_M Moisture (liquid+vapor) diffusivity [m^2/h]
- a_W Liquid water diffusivity [m^2/h]
- b Regression coefficient [dimensionless]
- c Regression coefficient [dimensionless]
- C_M Specific isothermal moisture capacity [$kg/kg \cdot ^\circ M$]
- d Average diameter [μm]
- d Regression coefficient [dimensionless]
- k_M Moisture (liquid+vapor) conductivity [$kg/m \cdot h \cdot ^\circ M$]
- T Temperature [$^\circ C$]
- t Thickness [mm]
- U Moisture (liquid-vapor) content on dry basis [kg/kg]

GREEK LETTERS

- δ Thermo-gradient coefficient [$1/^\circ C$]
- μ Vapor diffusion resistance factor [dimensionless]
- ρ Density [kg/m^3]
- τ Binder content

REFERENCES

1. Cunningham, M.J. and Sprott, T.J., "Sorpton Properties of New Zealand Building Materials," Building Research Association of New Zealand Research Report, No. R43, 1984.
2. Tviet, A., "Measurement of Moisture Sorpton and Permeability of Porous Materials," Norwegian Building Research Institute Report No. 45, Oslo, 1966.
3. Luikov A.V., Heat and Mass Transfer in Capillary-Porous Bodies, Pergamon Press, Oxford, 1966.
4. Langlais, C., Hyrien, M. and Klarsfled, S. "Moisture Migration In Fibrous Insulating Materials Under the Influence of a Thermal Gradient and its Effect on Thermal Resistance,"
5. Morton, W.E. and Hearle, H.W.S., "Physical Properties of Textile Fibres," The Textile Institute, Butterworths, Manchester and London, pp. 23-244, 1962.
6. Ahlgren, L., "Moisture Fixation in porous Building Materials," Report 36, Division of Building Technology, Lund Institute of Technology, Lund, Sweden, 1972.
7. Wood handbook, Forest Products Laboratory, Forest Service, U.S. Department of Agriculture, Agriculture Handbook No. 72, U.S. Government Printing Office, Washington, D.C., 1974.
8. ASHRAE Applications Handbook, Chapter 13, "Process and Product Air Conditioning," p. 13.5, 1974.
9. Huang, C.L.D., Siang, H.H. and Best, C.H., "Heat and Moisture Transfer in Concrete Slabs," Int. J. Heat and Mass Transfer, Vol. 22, pp. 257-266, 1979.
10. Pierce, D.A. and Benner, S.M., "Thermally Induced Hygroscopic Mass Transfer in a Fibrous Medium," Int. J. Heat Mass Transfer, Vol. 29, No. 11, pp. 1683-1694, 1986.
11. Urquhart, A.R. and Williams, A.M., J. Text. Inst. Vol. 15, T138, 1924.
12. Urquhart, A.R. and Eckersall, J. Text. Inst. Vol. 23, T163, 1932.
13. Hutton, E.A. and Gartside, J., J. Text. Inst. Vol. 40, T161, 1949.
14. Speakman, J.B., J. Soc. Chem. Industr., Vol. 49, 209T, 1930.
15. Hill, R., (Editor), "Fibres from Synthetic Polymers," Elsevier, Amsterdam, Netherlands, 1953.

16. Seiffert, K., Damp Diffusion and Buildings, Elsevier Publishing Company Limited, Barking, Essex, England, 1970.
17. Comini, G. and Del Giudice, S., " Finite Element Analysis of Heat and Mass Transfer in Buildings," Energy Conservation in Heating, Cooling and Ventilating Buildings, Vol. 1, Edited by Hoogen C.J. and Afgan N.H., Hemisphere Publishing Co., Washington, 1978.
18. Comini, G. and Lewis R.W., "A Numerical Solution of Two-Dimensional Problem Involving Heat and Mass Transfer," Int. J. Heat Mass Transfer, Vol. 19, pp. 1387-1392, 1976.
19. Glicksman, L.R. and Katsenelenbogen, S., "A Study of Water Vapor Transmission Through Insulation Under Steady-State and Transient Conditions," ASHRAE Transactions, No. 2792, pp. 483-499, 1983.
20. Ahlgren, L., "Moisture Fixation in Porous Building Materials," Division of Building Technology the Lund Institute of Technology, Report 36, Lund Sweden, (in Swedish), 1972.

APPENDIX E

ZONE ENERGY AND MASS BALANCE EQUATIONS

As explained in the earlier sections of this report, the building is divided into two separate domains, namely, air and solid domains. Mathematically, these two domains can be defined either by lumped or distributed equations. If the field variables (temperature and humidity ratio) are not functions of the spatial coordinates, lumped equations may be used. However, if the field variables are functions of the spatial coordinates, distributed equations must be used.

In Appendices A and J, details of the equations of combined heat and mass transfer were discussed for solid and air domains, respectively. In this appendix the equations for lumped heat and mass transfer equations are given. In the lumped analysis, the domain is represented by field variables that are functions of time only. In the following sections, the word "zone" is used to represent an air domain bounded by solid walls. The zone definition does not include the solid domains. However, the zone and the solid domains are coupled at their boundaries (surfaces) through convection.

In Sections E.1 and E.2, the zone energy and mass transfer balance equations are mathematically defined for a lumped model. In Section E.3, the analysis procedures used to define the internal mass and furniture in terms of lumped model are highlighted. In Section E.4, details of the "effective air mass multiplier" concept are given. Finally, in Section E.5 the overall solution strategies are explained.

In Sections E.1 and E.2, the quantity Q used in the zone energy and moisture balance equations denotes the heat (in kW) and moisture (in kg/h) flows, respectively. The three letters following the quantity Q is used to indicate the component, and the following letter "s" (sensible) or "l" (latent) are used to indicate the sensible (energy) and latent (moisture) contributions. For instance, Q_{inf-s} denotes the net heat flow due to infiltration, whereas Q_{inf-l} denotes the net moisture flow due to infiltration.

E.1 ZONE ENERGY BALANCE EQUATION

The governing energy balance equation in a given zone, i , may be written as follows:

$$\begin{aligned}
 (\rho VC_p)_i \frac{dTr_i}{dt} = & Q_{equ-s_i} + Q_{fur-s_i} + Q_{inf-s_i} + Q_{lig-s_i} + Q_{mix-s_i} + \\
 & Q_{peo-s_i} + Q_{sin-s_i} + Q_{sor-s_i} + Q_{sup-s_i} + Q_{ven-s_i} + \\
 & Q_{wal-s_i}
 \end{aligned} \quad (E-1.1)$$

Equation (E-1.1) describes the conservation of energy in a control volume (zone or room). The significance of each term appearing on the right-hand side of Equation (E-1.1) starting with the first term is explained below.

Q_{equ-s} represents the convective energy gains from equipment such as typewriters, computers, coffee pots, copy machines, dishwashers, cloth washers and dryers, refrigerators, etc. and is defined by the following equation.

$$Q_{equ-s_i} = Ue_i We-s_i (1-Re_i) \quad (E-1.2)$$

Q_{fur-s} represents the amount of energy that is stored or released by the furniture within the zone. Furniture can be simulated using one or a combination of the following methods:

1. "Effective air mass multiplier" analysis
2. Lumped ("effective penetration depth") analysis
3. Detailed (distributed) analysis.

In the "effective air mass multiplier" model, the amount of air in the zone is artificially increased through an artificial mass multiplier. The details of "effective air mass multiplier" concept are given in Section E.4 of this appendix. In lumped analysis, the furniture is represented by lumped nodal points. Each lump is represented by a single temperature that is a function of time only. The details of lumped analysis are given in Section E.3 of this appendix. In the detailed (distributed) analysis, the furniture is treated similar to walls, and the equations that are described in Appendix A are applied. In the lumped and detailed simulations, the heat of sorption is accounted for through the surface temperatures. In other words, if the furniture adsorbs moisture its surface temperature increases, and later the heat gets convected to the room air. For the lumped analysis see Equation (E-3.4), and for the detailed analysis see Equations (B-2.7), (B-3.7), etc.

Q_{inf-s} represents the energy gain or loss due to infiltration. If the infiltration and exfiltration rates are known, the magnitude of this term can be calculated using the following equation.

$$Q_{inf-s_i} = V_i (II_i \rho C_p Ta - EI_i \rho C_p Tr_i) \quad (E-1.3)$$

In Equation (E-1.3) II and EI denote the infiltration and exfiltration rates, respectively, for the zone. If only one zone is simulated and the zone is not pressurized, the infiltration and exfiltration rates will be the same. On the other hand, for multi zone simulations with internal air flow between zones, the infiltration and exfiltration rates for a particular zone may not be the same. Detailed knowledge of the internal air flow between zones would be required. It should be also noted that in Equation (E-1.3) the density and the specific heat of air must be evaluated at correct reference temperatures.

Qlig-s represents the convective energy gains from lights and may be defined with the following equation.

$$Q_{lig-s_i} = U_{l_i} W_{l_i} f_{c_i} \quad (E-1.4)$$

Qmix-s represents the amount of energy that is brought into or removed from a given zone by internal flows between connected zones. For instance, if the kitchen or bathrooms are separated from the living areas, the energy generated in these sections will be diffused and convected to the living areas. If the internal mass flow rates between the connected zones are known, the amount of energy that is brought into or removed from the zone can be calculated by the following equation.

$$Q_{mix-s_i} = V_i \left(\sum_{\substack{j=1 \\ j \neq i}}^{noz} I_{M_{i,j}} \rho C_p Tr_j - \sum_{\substack{j=1 \\ j \neq i}}^{noz} E_{M_{i,j}} \rho C_p Tr_i \right) \quad (E-1.5)$$

Qpeo-s represents the amount of energy that is added to the zone due to the presence of occupants and is given by the following equation.

$$Q_{peo-s_i} = N_{p_i} W_{p-s_i} (1 - R_{p_i}) \quad (E-1.6)$$

In Equation (E-1.6) Wp-s denotes the sensible heat gain from a person, and is a function of the occupant's metabolic rate and zone air temperature.

Qsin-s and Qsor-s represent the amount of energy that is removed or added by various sinks and sources, respectively. These terms can be defined by any functional relation or can be simulated in detail. Examples of energy sink and source term simulations are given in Chapter 3 of this report, and additional information can be found in Appendix J.

$$Q_{sin-s_i} = \text{Functional definition} \quad (E-1.7)$$

$$Q_{sor-s_i} = \text{Functional definition}$$

Qsup-s represents the amount of energy added to or removed from the zone by the supply air and is given by the following equation:

$$Q_{sup-s_i} = m_{s_i} C_p (T_{s_i} - T_{r_i}) \quad (E-1.8)$$

In Equation (E-1.8) ms and Ts denote the mass flow rate and temperature of the supply air, respectively. The magnitude of these variables can be calculated with additional algorithms, and may be functions of the mechanical unit and control strategies employed.

Qven-s represents the energy gain or loss due to ventilation. If the incoming and outgoing ventilation rates are known, the magnitude of this term can be calculated using the following equation:

$$Q_{ven-s_i} = \epsilon_v V_i (IV_i \rho C_p T_a - EV_i \rho C_p Tr_i) \quad (E-1.9)$$

In Equation (E-1.9) IV and EV denote the rates of air coming into and exiting the zone, respectively. In the case of multi-zone simulations with internal air flows, these rates may not be the same. In other words, the air coming into the

zone by ventilation may leave the zone by ventilation and internal air flow. If only one zone is simulated and the zone is not pressurized, then these rates will be equal. It should also be noted that in Equation (E-1.3) the density and the specific heat of air must be evaluated at correct reference temperatures.

In Equation (E-1.9) ϵ_v denotes the "ventilation air mixing efficiency factor" which is defined by the following equation:

$$\epsilon_v = \frac{IV_i \rho C_p T_a - EV_i \rho C_p T_{o_i}}{IV_i \rho C_p T_a - EV_i \rho C_p T_{r_i}} \quad (E-1.10)$$

The necessity of defining a "ventilation air mixing efficiency factor" comes from the fact that if the zone is not well mixed then the temperature of the outgoing ventilation air will not be equal to the temperature of the zone. The ventilation air mixing efficiency factor can be experimentally determined, and some examples on this subject are given in Chapter 3 of this report. In the case of perfect air mixing within the zone the value of ventilation air mixing efficiency factor is equal to 1.

Q_{wal-s} is the energy flow rate across the air film between the zone air and interior surface of the building shell and is given by the following equation.

$$Q_{wal-s_i} = \sum_{k=1}^{nos} h_{T_{i,k}} A_{s_{i,k}} (T_{w_{i,k}} - T_{r_i}) \quad (E-1.11)$$

Equation (E-1.11) is very important due to the fact that it couples the air domain to the solid domain. Further information on this subject is provided in Section E.5 of this appendix and also in Appendix F. In the wall simulations the heat of sorption is accounted for through the boundary conditions applied to the energy equation [see Equations (B-2.7), (B-3.7), etc.].

E.2 ZONE MASS BALANCE EQUATION

The governing moisture balance equation in a zone, i , may be written as follows:

$$(\rho V)_i \frac{dW_{r_i}}{dt} = Q_{con-l_i} + Q_{equ-l_i} + Q_{fur-l_i} + Q_{inf-l_i} + Q_{mix-l_i} + Q_{peo-l_i} + Q_{rev-l_i} + Q_{sin-l_i} + Q_{sor-l_i} + Q_{sup-l_i} + Q_{ven-l_i} + Q_{wal-l_i} \quad (E-2.1)$$

Equation (E-2.1) describes the conservation of moisture in a control volume. The significance of each term appearing on the right-hand side of Equation (E-2.1) starting with the first term is explained below.

Q_{con-l} represents the amount of moisture that can condense over cold surfaces in the zone and is described by the following equation:

$$Q_{con-l_i} = \sum_{k=1}^{nos} h_{c_{i,k}} A_{c_{i,k}} (W_{r_i} - W_{c_{i,k}}) \quad (E-2.2)$$

Q_{equ-1} represents the convective moisture gains from equipment and is defined by the following equation:

$$Q_{equ-1_i} = Ue_i W_{e-1_i} / \lambda \quad (E-2.3)$$

Q_{fur-1} represents the amount of moisture that is adsorbed or desorbed by the furniture within the zone. Furniture can be simulated using one or a combination of the following methods:

1. "Effective air mass multiplier" analysis
2. Lumped ("effective penetration depth") analysis
3. Detailed (distributed) analysis.

In the "effective air mass multiplier" model, the amount of air that is simulated is multiplied by an artificial mass multiplier. The details of "effective air mass multiplier" concept is given in Section E.4 of this appendix. In lumped analysis the furniture is represented by lumped nodal points. Each lump is represented by a single moisture content which is a function of time only. The details of lumped analysis are given in Section E.3 of this appendix. In the detailed (distributed) analysis the furniture is treated similar to walls, and the equations that are described in Appendix A are applied.

Q_{inf-1} represents the amount of moisture that is brought into or removed from the zone by infiltration. Considerations similar to those discussed for Q_{inf-s} are applicable in case of multi zone simulation with internal air flow. If the infiltration and exfiltration rates are known, the magnitude of this term can be calculated using the following equation:

$$Q_{inf-1_i} = V_i (II_i \rho W_a - EI_i \rho W_{r_i}) \quad (E-2.4)$$

Q_{mix-1} represents the amount of moisture that is brought into or removed from a given zone by internal flows between connected zones. For instance, if the kitchen or bathrooms are separated from the living areas, the moisture generated in these sections will be diffused and convected to the living areas. If the internal mass flow rates between the connected zones are known, the amount of moisture that is brought into or removed from the zone can be calculated by the following equation:

$$Q_{mix-1_i} = V_i \left(\sum_{\substack{j=1 \\ j \neq i}}^{noz} IM_{i,j} \rho W_{r_j} - \sum_{\substack{j=1 \\ j \neq i}}^{noz} EM_{i,j} \rho W_{r_i} \right) \quad (E-2.5)$$

Q_{peo-1} represents the amount of moisture that is generated by people and is given by the following equation:

$$Q_{peo-1_i} = Np_i W_{p-1_i} / \lambda \quad (E-2.6)$$

In Equation (E-2.6) $Wp-1$ denotes the latent heat gain from a person, and it is a function of the occupant's metabolic rate and zone air temperature.

$Qrev-1$ is the amount of moisture that is re-evaporated into the conditioned space from the mechanical cooling and/or dehumidification coil surfaces and their condensate collection pans. This term is dictated by the velocity field prevailing over the cooling coils and condensate pans and it can be significant, especially in the case of continuous fan operations. The amount of moisture that is added into the zone by re-evaporation can be estimated by the following equation:

$$Qrev-1_i = hr_i Ar_i (Wst_i - Ws_i) \quad (E-2.7)$$

$Qsin-1$ and $Qsor-1$ represent the amount of moisture that is removed or added by various sinks and sources, respectively. These terms can be defined by functional relations or can be simulated in detail. Examples of moisture sink and source term simulations are given in Chapter 3 of this report, and additional information can also be found in Appendix J.

$$Qsin-1_i = \text{Functional definition} \quad (E-2.8)$$

$$Qsor-1_i = \text{Functional definition}$$

$Qsup-1$ represents the amount of moisture that is removed by the supply air and is given by the following equation:

$$Qsup-1 = ms_i (Ws_i - Wr_i) \quad \text{or} \quad -f (Ta, Tr_i, Twe_i) \quad (E-2.9)$$

In Equation (E-2.9) ms and Ws denote the mass flow rate and humidity ratio of the supply air, respectively. The magnitude of these variables can be calculated with additional algorithms and may be functions of the mechanical unit and control strategies employed.

$Qven-1$ represents the amount of moisture that is brought into or removed from the zone by ventilation. If the incoming and outgoing ventilation rates are known, the magnitude of this term can be calculated using the following equation:

$$Qven-1_i = \epsilon_v V_i (IV_i \rho Wa - EV_i \rho Wr_i) \quad (E-2.10)$$

In Equation (E-2.10) ϵ_v denotes the "ventilation air mixing efficiency factor" which is defined by Equation (E-1.10).

$Qwal-1$ represents the amount of moisture that is adsorbed and/or desorbed by the envelope walls. As it will be shown later, this term couples the solid and air domains of the building. The amount of moisture that is adsorbed and/or desorbed by the envelope and internal mass is given by the following equation:

$$Qwal-1_i = \sum_{k=1}^{nos} h_{Mi,k} As_{i,k} (Ww_{i,k} - Wr_i) \quad (E-2.11)$$

Equation (E-2.11) is very important due to the fact that it couples the air domain to the solid domain. Further information on this subject is provided in Section E.5 of this appendix and also in Appendix F.

E.3 LUMPED ANALYSIS ("EFFECTIVE PENETRATION DEPTH" CONCEPT)

In many instances, defining the geometry in exact detail or obtaining all material properties required for a detailed analysis may be impossible. In such cases, it is prudent to simplify the problem to suit immediate needs without completely distorting the physics of the problem. Certain artificial coefficients that may be problem-specific or depend on the operating conditions may be required. If the geometrical configuration is changed or the operating characteristics are altered, then a new set of numbers or coefficients must be found. The coefficients may be determined either through experiments or through other rigorous models.

Such a model is introduced in this section. The primary assumption in this model is that only a small layer of the solid material is assumed to participate in the overall process. The name "effective penetration depth" model therefore applies. The following assumptions underline the lumped approach analysis:

1. The solid domain is represented by a single lumped temperature (T_s) and a single moisture content (U_s). In other words, both T_s and U_s are independent of the spatial coordinates and dependent only on time.
2. The heat and mass Biot numbers are less than or equal to 0.1, or

$$Bi_T = \frac{h_T L}{k_T} \leq 0.1 \quad (E-3.1)$$

$$Bi_M = \frac{h_M L}{k_M} \leq 0.1 \quad (E-3.2)$$

L is the characteristic length and it may be approximated by

$$L \approx \frac{V_S}{A_S} \quad (E-3.3)$$

If both the thermal and mass Biot numbers are less than 0.1, the temperature and the moisture content inside the solid are essentially uniform to within 5 percent. However, for larger Biot numbers, the results using this lumped approach may be erroneous and a detailed analysis is recommended. However, for most materials in a building environment, the Biot numbers are higher than 0.1.

3. Thermodynamic equilibrium exists at the boundary between the air and the solid domains. Figure E-1 illustrates the equilibrium at the solid and air interface.

$$(P_{sa}, T_{sa}, W_{sa}) < \text{-----}$$

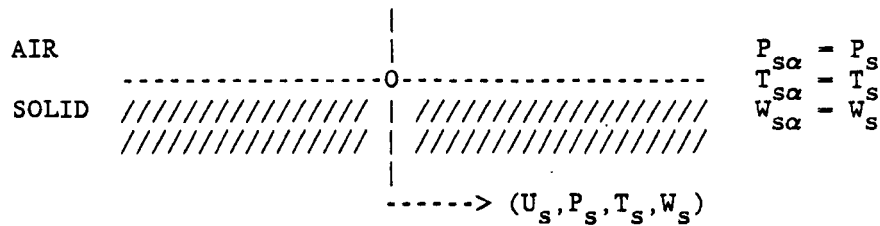


Figure E-1. Thermodynamic surface equilibrium.

Before proceeding with the mathematics of this concept, a few points must be clarified. The field variables for the solid domain are temperature and moisture content. The field variables for the air domain are temperature and humidity ratio. It should be realized that the field variable for the energy equation for both domains is the temperature, and is common (continuous) to both domains. However, for the mass equation the field variables are the moisture content and humidity ratio for the solid and air domains, respectively. Due to different field variables used in the mass balance equations, a relation must be used to relate these field variables. This relation is assumed to be governed by the equilibrium sorption isotherm of the material. Consequently, if the temperature and the moisture content are known, the surface humidity ratio can be calculated. This particular argument can be further clarified with the following example.

Assume that a small solid material is left within a large controlled chamber for a very long time. The chamber is kept at a constant temperature of 25 °C and at a humidity ratio of 0.0098 kg/kg (= 50% relative humidity). Further assume that the equilibrium moisture content of the material at 50% relative humidity and 25 °C is about 0.12 kg/kg. Now let us try to answer the following question. What will happen if the temperature of the solid is suddenly raised by 10 °C? First, since the control chamber is large, neither its temperature nor its humidity ratio will change. Second, since the initial moisture content of the material is 0.12 kg/kg, the initial relative humidity of the surface air will be 50%. Third, with increasing surface temperature the saturation humidity ratio of the surface air will increase. However since the relative humidity of the surface air is 50%, the humidity ratio of the surface air will increase ($RH = W/W_{sat}$). Fourth, due to this the solid material will lose moisture to the chamber air. The actual physics of the problem is more complicated; however, this simple example should clarify the concept. Note: Surface air indicates, air condition evaluated surface temperature and surface moisture content of the material, and its humidity ratio is calculated through the moisture isotherm relations.

If the temperature and the moisture content at the surface is known (for a lumped analysis both are uniform throughout the solid) the corresponding relative humidity can be obtained from Equation (G-22). This relative humidity can be employed to calculate the corresponding humidity ratio from Equation (G-10).

Substantial work in lumped analysis has been done by Cunningham 1983(a), 1983(b) and 1984. He developed a model of moisture concentration in a building cavity containing hygroscopic material which allowed for fluctuating external climatic conditions. The following assumptions were made in Cunningham's model:

1. The storage vapor pressure P_V or relative humidity is a linear function of the moisture content.

$$P_V = kU$$

where k is a function of temperature.

2. The water vapor obeys the ideal gas law.
3. A lumped value of the mass transfer coefficient is assumed.

Very similar models with identical assumptions were also used by Burch 1985, Cleary and Sherman 1985 for predicting the performance of attics. Kusuda 1983 and Kusuda and Miki 1985 again used a similar model for estimating the indoor humidity levels.

The lumped energy equation for the i -th solid domain is given by

$$(\rho A \delta_T C_p)_i \frac{dT_i}{dr} = h_{Ti} A_i (T_r - T_i) + \lambda h_{Mi} A_i (W_r - W_{si}) \quad (E-3.4)$$

The lumped moisture content equation for the i -th solid domain is given by

$$(\rho A \delta_M)_i \frac{dU_i}{dr} = h_{Mi} A_i (W_r - W_{si}) \quad (E-3.5)$$

The effective penetration depth concept and the lumped analysis can be further clarified by the aid of Figures E-2.

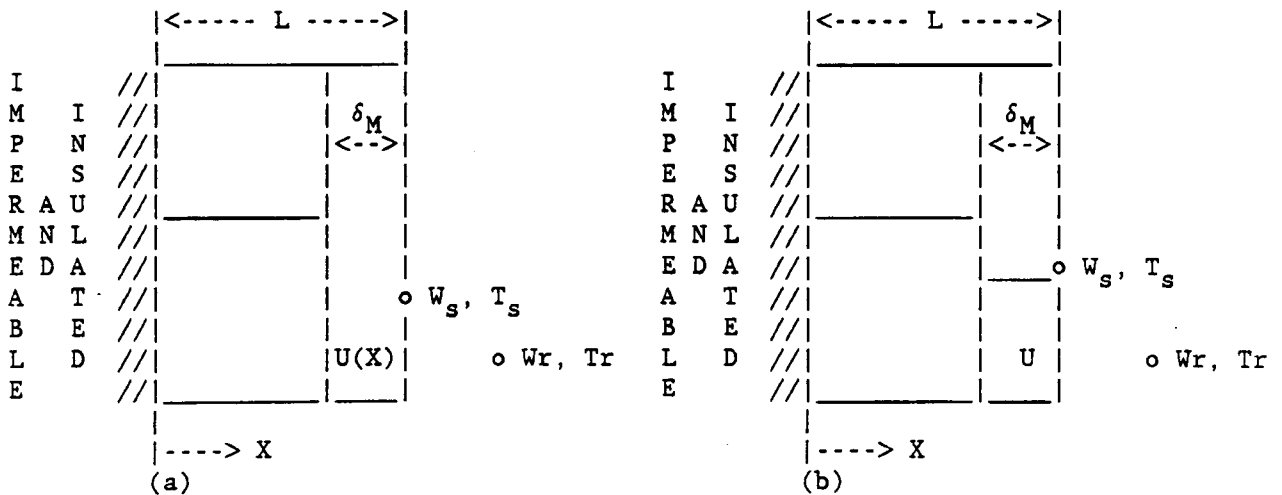


Figure E-2. Schematics of lumped analysis concept. (a) Real moisture content profile, (b) lumped moisture content profile note $U \neq U(x)$.

Figures E-2.(a) and E-2.(b) depict a hypothetical drying stage of a specimen placed in a dry environment. In the early stages of drying the moisture content of the inner regions of the specimen remains unaltered by the environment

conditions. However, a thin layer (δ_M) close to the surface behaves dynamically and loses moisture to the environment. The shape of the moisture content curve shown in Figure E-2.(a) is very close to the ones obtained with detailed simulations (see Chapter 3). If the specimen is left in the same environment for a long time, then the inner regions of the specimen will be affected, and at that point this approach will fail. However, for short time periods or where the cyclic integral of the total moisture adsorption and desorption is zero, this concept can be used. In other words, the following constraint must be met:

$$\int_0^{24} \frac{dU}{dr} dr = 0 \quad (E-3.6)$$

If the above conditions are satisfied, the lumped analysis can be used. In the lumped analysis no moisture content variation within this thin surface layer is assumed. As shown in Figure E-2.(b), the moisture content of this layer is constant and is discontinuous between the inner regions and this thin layer. However, the following condition is satisfied at each discrete time interval:

$$\int_{L-\delta_M}^L U(X) dX = U \delta_M \quad (E-3.7)$$

The thickness of the surface layer varies from one material to another, and in addition, it may vary from one operating condition to another. The thickness of this layer is named as the "effective penetration depth". Equations (E-3.4) and (E-3.5) define this concept. However, these equations alone cannot define the problem completely because the surface conditions are not defined. The surface conditions can be defined through the equilibrium relations. In other words, if the moisture content of the surface (same as the moisture content throughout the effective penetration layer) is known, then the surface relative humidity can be determined from Equation (G-22). If the surface temperature is known and the relative humidity is calculated, then the surface humidity ratio can be calculated [Equation (G-10)]. This surface humidity ratio and the humidity ratio of the environment drives the whole problem.

As mentioned above, the "effective penetration depth" is a function of the material and the operating conditions (boundary and initial conditions). Its value can be determined either through detailed simulations or experiments. Some examples using this approach are provided in Chapter 3 of this report.

The major limitations of this concept can be summarized as follows:

1. Long time performances (storage) cannot be determined.
2. A new set of "penetration depths" are required for different operating conditions.
3. The heat of sorption is assumed to be uniformly distributed throughout the lump, which may yield erroneous results.

Additional information on this subject is provided in Chapter 2.

For the legs 1-2 and 3'-4', the angles $\langle c_2-c_1-n_1 \rangle$ and $\langle c_1-c_2-n_2 \rangle$ are less than 90 degrees. Hence, they are facing each other.

For the legs 1-2 and 4'-1', the angle $\langle c_3-c_1-n_1 \rangle$ is less than 90 degrees but angle $\langle c_1-c_3-n_3 \rangle$ is greater than 90 degrees. Hence, they do not face each other and the view factor between them is set to zero.

For the legs 3'-4' and 4'-1', both angles $\langle c_2-c_3-n_3 \rangle$ and $\langle c_3-c_2-n_2 \rangle$ are greater than 90 degrees. Hence, they do not face each other and the view factor between them is set to zero.

H.4.1.2 DETAILED SHADOW CHECKING

In the detailed shadow checking, a check is carried out between a pair of radiating surfaces to see if a leg or face of another solid element is blocking the line of sight.

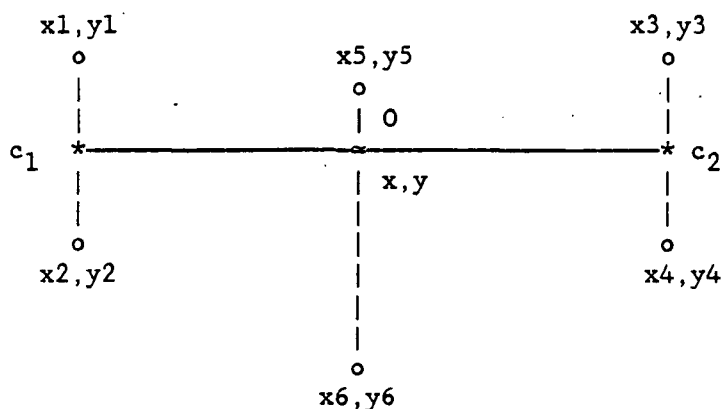


Figure H-5. Two-dimensional detailed shadow checking configuration.

Let 1-2 and 3-4 be two radiating legs and 5-6 be an arbitrary leg of a solid element. The task is to determine if the leg 5-6 is blocking the sight between legs 1-2 and 3-4. In, FEMALP 2.1, the line of sight is assumed to be between the centers of the radiating legs.

The condition for leg 5-6 to be an obstructing leg is that the point of intersection $O(x,y)$ of line passing through c_1-c_2 and the passing through point 5-6, must lie on both segments 5-6 and c_1-c_2 .

Line c_1-c_2 is given by the vector

$$[0.5(x_1+x_2)-0.5(x_3+x_4)] i + [0.5(y_1+y_2)-0.5(y_3+y_4)] j + 0 k \quad (\text{H-4.1})$$

Line 5-6 is given by the vector

$$(x_6-x_5) i + (y_6-y_5) j + 0 k \quad (\text{H-4.2})$$

The intersection point $O(x,y)$ of the two vectors is determined by solving the equations for the two vectors.

Line 5-6 is an obstruction if and only if both conditions below are met:

1. sum of distances c_1-O and $O-c_2$ equals distance c_1-c_2 and
2. sum of distances $5-O$ and $O-6$ equals distance $5-6$.

If the above conditions are met, the view factor is set to zero.

H.4.2 THREE-DIMENSIONAL SHADOW CHECKING

Before three-dimensional shadow checking is performed, a coordinate screening is applied in order to determine which elements are in the vicinity of the radiating elements. If the shading element is not in the vicinity of the radiating elements, then no further three-dimensional shadow checking is performed. The coordinate screening is performed as follows:

The zone equations for lumped analysis are similar to equations (E-1.1) and (E-2.1). Thus, if we have "nos" solid domains or storage media and one zone, the total number of equations to be solved simultaneously is $2*(nos+1)$. These equations can be solved using a forward finite-difference scheme. Details of the solution procedure are given in Section E.5.

E.4 "EFFECTIVE AIR MASS MULTIPLIER" CONCEPT

The "effective air mass multiplier" concept can be best explained with the following example. If there exist two identical insulated containers, one filled only with air, the other with air and concrete, and suddenly they are exposed to the same level of heat input, the temperature of the air in the container filled only with air will rise faster. This can be attributed to the thermal capacities. The container filled with air and concrete will have higher thermal capacitance than the other one; therefore its temperature will rise slowly. If one wants to simulate this phenomena, then one way would be to assign an effective thermal capacity to the container field with air and concrete. The same is true for a building, the furniture, appliances, clothing materials, etc., which have some thermal as well as mass capacitances. In the absence of these materials, the behavior of the building will be more dynamic; in other words, a less massive house will have larger temperature swings than the one with high mass.

From a simulation point of view, the physical properties of some building materials are not well defined. For instance, what would be the surface area, volume or the mass properties of the clothing materials? Even with answers to these questions, what would happen if one's current software did not support detailed simulations? With these problems in mind the following equations are said to represent the zone energy and mass balance.

$$\epsilon_T (\rho VC_p)_i \frac{dTr_i}{dr} = Q_{equ-s_i} + Q_{fur-s_i} + Q_{inf-s_i} + Q_{lig-s_i} + Q_{mix-s_i} + Q_{peo-s_i} + Q_{sin-s_i} + Q_{sor-s_i} + Q_{sup-s_i} + Q_{ven-s_i} + Q_{wal-s_i} \quad (E-4.1)$$

$$\epsilon_M (\rho V)_i \frac{dWr_i}{dr} = Q_{con-l_i} + Q_{equ-l_i} + Q_{fur-l_i} + Q_{inf-l_i} + Q_{mix-l_i} + Q_{peo-l_i} + Q_{rev-l_i} + Q_{sin-l_i} + Q_{sor-l_i} + Q_{sup-l_i} + Q_{ven-l_i} + Q_{wal-l_i} \quad (E-4.2)$$

In Equation (E-5.1) and (E-5.2) ϵ_T and ϵ_M represent the effective air mass multipliers for the energy and mass balance equations, respectively. These multipliers can be visualized as damping coefficients used to decrease the swings of the field variables. Their magnitudes can be determined from experiments; such experiments for a full-scale residential building are reported in Chapter 3.

This concept has some severe limitations, which are discussed in Chapter 2, but nevertheless, as shown in Chapter 3, it can be used to predict the internal humidity ratios with some degree of confidence. Furthermore, most of the existing building energy analysis programs can adapt this concept with minimum difficulty.

E.5 SOLUTION PROCEDURES

In this section the numerical solutions of the equations given in Sections E.1 and E.2 are provided. Furthermore, the exact solution of the combined equations given in Sections E.2 and E.3 for one lumped mass case are also provided.

E.5.1 LUMPED ZONE THERMAL AND MASS EQUATIONS

After substituting Equations (E-1.2) through (E-1.10) into Equation (E-1.1), Equations (E-2.2) through (E-2.11) into Equation (E-2.1), and collecting the common terms, the following two equations can be obtained:

$$\frac{dTr_i}{d\tau} + P1(\tau) Tr_i = Q1(\tau) \quad (E-5.1)$$

$$\frac{dWr_i}{d\tau} + P2(\tau) Wr_i = Q2(\tau) \quad (E-5.2)$$

Where

$P1(\tau)$ is the summation of all coefficients of terms containing the zone temperature.

$Q1(\tau)$ is the summation of all terms not containing the zone temperature.

$P2(\tau)$ is the summation of all coefficients of terms containing the zone humidity ratio.

$Q2(\tau)$ is the summation of all terms not containing the zone humidity ratio.

Equations (E-5.1) and (E-5.2) represent the zone energy and moisture balance equations, respectively. These equations are ordinary differential equations and in order for them to be considered complete, their initial conditions must be given. Therefore, the initial conditions for Equations (E-5.1) and (E-5.2) can be written as:

$$@ \tau = 0 \quad Tr_i = To_i \quad (E-5.3)$$

and

$$@ \tau = 0 \quad Wr_i = Wo_i \quad (E-5.4)$$

The analytical solutions to Equations (E-5.1) and (E-5.2) subject to initial conditions defined by Equations (E-5.3) and (E-5.4) are given as follows:

$$Tr_i(\tau) = \frac{Q1(\tau)}{P1(\tau)} + [To_i - \frac{Q1(\tau)}{P1(\tau)}] \exp[-P1(\tau) \tau] \quad (E-5.5)$$

and

$$Wr_i(\tau) = \frac{Q2(\tau)}{P2(\tau)} + [Wo_i - \frac{Q2(\tau)}{P2(\tau)}] \exp[-P2(\tau) \tau] \quad (E-5.6)$$

If Equations (E-5.5) and (E-5.6) are solved, then the zone temperature and the humidity ratio at the end of a time step can be calculated. However, under certain circumstances, an integrated average value may be desirable rather than the end value. For instance, if the hourly load due to infiltration is desired, then the load can be accurately estimated by the use of integrated average value. The integrated average temperature and humidity ratio from now on will be termed as "effective temperature" and "effective humidity ratio". The effective zone temperature and zone humidity ratio can be calculated through the following equations:

$$Te_i = \frac{\int_{\tau}^{\tau+\Delta\tau} Tr_i(\tau) d\tau}{\Delta\tau} \quad (E-5.7)$$

and

$$We_i = \frac{\int_{\tau}^{\tau+\Delta\tau} Wr_i(\tau) d\tau}{\Delta\tau} \quad (E-5.8)$$

Substituting Equations (E-5.5) and (E-5.6) into Equations (E-5.7) and (E-5.8) respectively and performing the integration results in the following expressions for the effective zone temperature and zone humidity ratio:

$$Te_i = \frac{\frac{Q1(\tau)}{P1(\tau)} \tau + [To_i - \frac{Q1(\tau)}{P1(\tau)}] \frac{1.0}{P1(\tau)} (1.0 - \exp[-P1(\tau) \tau])}{\Delta\tau} \quad (E-5.9)$$

and

$$We_i = \frac{\frac{Q2(\tau)}{P2(\tau)} \tau + [Wo_i - \frac{Q2(\tau)}{P2(\tau)}] \frac{1.0}{P2(\tau)} (1.0 - \exp[-P2(\tau) \tau])}{\Delta\tau} \quad (E-5.10)$$

E.5.2 LUMPED INTERNAL MASS EQUATIONS AND ZONE INTERACTIONS

For the sake of simplicity in representation, only the Q_{wal-s} and Q_{wal-l} terms along with Q_{sin-s} and Q_{sin-l} are considered in Equations (E-1.1) and (E-1.2), respectively. The sink and source terms for both the zone energy and mass equations are represented by $QT(\tau)$ and $QM(\tau)$. Taking these simplifications into consideration and using the definition of Q_{wal-s} [Equation (E-1.11)] and Q_{wal-l} [Equation (E-2.11)], the zone heat and mass transfer equations for a single zone can be written as follows:

$$\rho V C_p \frac{dTr}{d\tau} = QT(\tau) + \sum_{k=1}^{nos} h_{T_k} A_k (T_k - Tr) \quad (E-1.1.a)$$

$$\rho V \frac{dW_r}{dr} = QM(\tau) + \sum_{k=1}^{\text{nos}} h_{Mk} A_k (W_k - W_r) \quad (\text{E-2.1.a})$$

where subscript k is the k-th exposed lump and subscript r denotes the zone.

Equations (E-1.1.a) and (E-3.4) along with Equations (E-2.1.a) and (E-3.5), in that order, for "nos" surfaces exposed to a single zone, can be written in the finite difference form. The forward-finite difference for any property V is defined as

$$\frac{dV}{dr} = \frac{V(\tau+\Delta\tau) - V(\tau)}{\Delta\tau} \quad (\text{E-5.11})$$

Employing this definition in Equations (E-1.1.a), (E-3.4), (E-2.1.a) and (E-3.5), in that order, the finite-difference equations can be written in the following matrix form:

$$A X = b \quad (\text{E-5.12})$$

where

$$A = \begin{bmatrix} (1.0 + \sum_{i=1}^{\text{nos}} B_i) & -B_1 & \dots & -B_{\text{nos}} & 0 & 0 & \dots & 0 \\ -C_1 & (1.0 + C_1) & 0 & \dots & 0 & -D_1 & 0 & \dots & 0 \\ \cdot & 0 & \cdot \\ \cdot & \cdot \\ -C_{\text{nos}} & 0 & \dots & (1.0 + C_{\text{nos}}) & -D_{\text{nos}} & 0 & \dots & 0 \\ 0 & 0 & \cdot & \cdot & \cdot & 0 & \dots & 0 \\ \cdot & 0 & \cdot & \cdot & \cdot & 0 & \dots & 0 \\ \cdot & \cdot \\ 0 & 0 & \cdot & \cdot & \cdot & 0 & \dots & 1.0 \end{bmatrix} \quad (\text{E-5.13})$$

$$X = [T_r \ T_1 \ \dots \ T_{\text{nos}} \ W_r \ U_1 \ \dots \ U_{\text{nos}}]^T \quad (\text{E-5.14})$$

$$\begin{aligned}
 & \tau \\
 & T_r + A \\
 & \tau \\
 & T_1 - D_1 W_1 \\
 & \vdots \\
 & \tau \\
 & T_{\text{nos}} - D_{\text{nos}} W_{\text{nos}} \\
 & \tau \\
 & W_r + E + \sum_{i=1} F_i W_i \\
 & \vdots \\
 & \tau \\
 & U_1 - G_1 W_1 \\
 & \vdots \\
 & \tau \\
 & U_{\text{nos}} - G_{\text{nos}} W_{\text{nos}}
 \end{aligned}
 \tag{E-5.15}$$

The constants - A, B_i, C_i, D_i, E, F_i and G_i are defined below:

$$A = \frac{QT(\tau) \Delta\tau}{(\rho VC_p)_a} \tag{E-5.16}$$

$$B_i = \frac{h_{Ti} A_i \Delta\tau}{(\rho VC_p)_a} \tag{E-5.17}$$

$$C_i = \frac{h_{Ti} A_i \Delta\tau}{(\rho VC_p)_i} \tag{E-5.18}$$

$$D_i = \frac{\lambda h_{Mi} A_i \Delta\tau}{(\rho VC_p)_i} \tag{E-5.19}$$

$$E = \frac{QM(\tau) \Delta\tau}{(\rho V)_a} \tag{E-5.20}$$

$$F_i = \frac{h_{Mi} A_i \Delta\tau}{(\rho V)_a} \tag{E-5.21}$$

$$G_i = \frac{h_{Mi} A_i \Delta\tau}{(\rho V)_i} \tag{E-5.22}$$

for $i = 1, \dots, \text{nos}$

The X vector (E-5.14) contains the unknowns -- zone temperature, storage temperature, zone humidity ratio and storage moisture content at next time step $r+\Delta r$. The A matrix [Equation (E-5.13)] contains the coefficients of the unknowns defined by the vector X [Equation (E-5.14)]. The b vector contains all those terms in the finite-difference equations that do not contain the unknowns defined by vector X. Such terms include the heat generation (constant A), mass generation (constant E) and all other terms that contain the surface humidity ratio (W_k , $k=1, \dots, nos$). The surface humidity ratio is also an unknown but it is included in the b vector therefore making the solution procedure iterative. As mentioned later in the solution procedure, the surface humidity ratio is evaluated with the help of equilibrium and psychometric relations, for any given surface moisture content.

The constants (E-5.16)-(E-5.22) are all those terms in the finite difference equations which are either coefficients of the unknown variables (constants with subscript i- B, C, D, F and G) or constants by themselves like A and E. Constant A contains the heat generation term and the constant E contains the mass generation term, both of which could be functions of time.

The system of equations defined by Equation (E-5.12) can be solved by the following two methods:

1. MATRIX INVERSION ITERATION SCHEME

In the matrix inversion iteration scheme the following solution procedure is employed:

```

Input ----> for i=1, ..., nos
                Tr0, Ti0, Wr0, Ui0
[1] Define ----> for i=1, ..., nos
                Tr1 = Tr0
                Ti1 = Ti0
                Wr1 = Wr0
                Ui1 = Ui0
Store ----> for i=1, ..., nos
                X1 = [Tr1 Ti1 Wr1 Ui1]T
[2] Calculate ----> for i=1, ..., nos
                Φi from [Eq. (G-22)] using Ui1
                Wi from [Eq. (G-10)] using Φi, Ti1
Calculate ----> b [Eq. (E-5.15)] vector and A [Eq. (E-5.13)]
                matrix
Solve ----> for X in (E-5.12) by matrix inversion X = A-1 b
Convergence ----> |X - X1| < error tolerance

```

If converged,

Define ----> for i=1, ..., nos

$$\begin{aligned} Tr_0 &= Tr \\ Ti_0 &= Ti \\ Wr_0 &= Wr \\ Ui_0 &= Ui \end{aligned}$$

Tr, Ti, Wr and Ui are obtained from X for i=1, ..., nos.

Go to ----> [1] for next time

else,

Relax ----> for i=1, ..., nos

$$\begin{aligned} Tr_1 &= (1-R) Tr_1 + R Tr \\ Ti_1 &= (1-R) Ti_1 + R Ti \\ Wr_1 &= (1-R) Wr_1 + R Wr \\ Ui_1 &= (1-R) Ui_1 + R Ui \end{aligned}$$

Tr, Ti, Wr and Ui are obtained from X for i=1, ..., nos.

Go to ----> [2] for next iteration

2. NEWTON RAPHSON ITERATION SCHEME

The Newton Raphson iteration equation in matrix equation can be written as:

$$J \Delta X = b - A X_1 \quad (E-5.23)$$

where J is called the Jacobian matrix. The entries of the Jacobian matrix J_{ij} are given as:

$$J_{ij} = \left(\frac{\partial A_{ij} X_j}{\partial X_i} \right) X_k = \text{const}$$

$$\text{for } i, j, k = 1, \dots, \text{nos and } k \neq i \quad (E-5.24)$$

where A_{ij} are the entries of the matrix A. The vector DX is given as:

$$\Delta X = X - X_1 \quad (E-5.25)$$

The following solution procedure is employed:

Input ----> for i=1, ..., nos

$$Tr_0, Ti_0, Wr_0, Ui_0$$

[1] Define ----> for i=1, ..., nos

$$\begin{aligned} Tr_1 &= Tr_0 \\ Ti_1 &= Ti_0 \\ Wr_1 &= Wr_0 \end{aligned}$$

$$U_{i1} = U_{i0}$$

Store ----> for $i=1, \dots, \text{nos}$

$$X_1 = [\text{Tr}_1 \text{Ti}_1 \text{Wr}_1 U_{i1}]^T$$

[2] Calculate ----> for $i=1, \dots, \text{nos}$

Φ_i from [Eq. (G-22)] using U_{i1}
 W_i from [Eq. (G-10)] using Φ_i, Ti_1

Calculate ----> b [Eq. (E-5.15)] vector, A [Eq. (E-5.13)] and
 J [Eq. (E-5.24)] matrices

Solve ----> for ΔX in [Eq. (E-5.22)] by matrix inversion

$$\Delta X = J^{-1} (b - AX_1)$$

Convergence ----> $|\Delta X/X| < \text{error tolerance}$

If converged,

Solve ----> $X = X_1 + \Delta X$

Define ----> for $i=1, \dots, \text{nos}$

$$\begin{aligned} \text{Tr}_0 &= \text{Tr} \\ \text{Ti}_0 &= \text{Ti} \\ \text{Wr}_0 &= \text{Wr} \\ \text{Ui}_0 &= \text{Ui} \end{aligned}$$

$\text{Tr}, \text{Ti}, \text{Wr}$ and Ui are obtained from X for $i=1, \dots, \text{nos}$.

Go to ----> [1] for next time

else,

Relax ----> for $i=1, \dots, \text{nos}$

$$\begin{aligned} \text{Tr}_1 &= (1-R) \text{Tr}_1 + R \text{Tr} \\ \text{Ti}_1 &= (1-R) \text{Ti}_1 + R \text{Ti} \\ \text{Wr}_1 &= (1-R) \text{Wr}_1 + R \text{Wr} \\ \text{Ui}_1 &= (1-R) \text{Ui}_1 + R \text{Ui} \end{aligned}$$

$\text{Tr}, \text{Ti}, \text{Wr}$ and Ui are obtained from X for $i=1, \dots, \text{nos}$.

Go to ----> [2] for next iteration

E.5.3 EXACT SOLUTION FOR LUMPED MASS TRANSFER AND ZONE EQUATIONS

The governing moisture balance equation for one zone is given as follows (see also Section E.2 for detailed description):

$$d\text{Wr}$$

$$\begin{aligned}
 (\rho V) \frac{d}{dr} = & Q_{con-1} + Q_{equ-1} + Q_{fur-1} + Q_{inf-1} + Q_{mix-1} + \\
 & Q_{peo-1} + Q_{rev-1} + Q_{sin-1} + Q_{sor-1} + Q_{sup-1} + \\
 & Q_{ven-1} + Q_{wal-1}
 \end{aligned} \quad (E-5.26)$$

In Equation (E-5.26) Q_{wal-1} denotes the amount of moisture that is adsorbed or desorbed, and is given as follows:

$$Q_{wal-1} = h_M A (W_s - W_r) \quad (E-5.27)$$

The lumped moisture content equation was given by Equation (E-3.5) and for easy reference it is also repeated here for a single solid domain.

$$(\rho V \delta_M) \frac{dU}{dr} = h_M A (W_r - W_s) \quad (E-5.28)$$

The following moisture isotherm has been used in solving the above equations.

$$U = a + b\phi \quad (E-5.29)$$

where

$$\phi \approx \frac{W_s}{W_{sat}} \quad (E-5.30)$$

Making use of the Equations (E-5.26) through (E-5.30), the following governing differential equations can be obtained:

$$\frac{dW_r}{dr} + E_1 W_r + E_2 U = E_3 \quad (E-5.31)$$

$$\frac{dU}{dr} + E_4 U + E_5 W_r = E_6 \quad (E-5.32)$$

Where E_1 through E_6 represent the various constants resulting from the rearrangement of Equation (E-5.26) through (E-5.30). Equations (E-5.31) and (E-5.32) can now be written in the following form:

$$(D^2 + F_1 D + F_2) W_r = F_3 \quad (E-5.33)$$

$$(D^2 + F_1 D + F_2) U = F_4 \quad (E-5.34)$$

where

$$D = \frac{d}{dr} \quad \text{and}$$

$$F_1 = E_1 + E_4 \quad F_2 = E_1 E_4 - E_2 E_5 \quad F_3 = E_3 E_4 - E_2 E_6 \quad F_4 = E_1 E_6 - E_3 E_5 \quad (E-5.35)$$

Equations (E-5.33) and (E-5.34) will have the following roots:

$$m_1 = \frac{-F_1 + (F_1^2 - 4F_2)^{0.5}}{2} \quad \text{and} \quad m_2 = \frac{-F_1 - (F_1^2 - 4F_2)^{0.5}}{2} \quad (E-5.36)$$

2.0

2.0

Depending upon the nature of the roots, the exact solution for various cases is as follows:

Case i) If both roots are real and distinct:

$$W_r = C_1 e^{m_1 r} + C_2 e^{m_2 r} + \frac{F_3}{m_1 m_2}$$

$$U = -C_1 \frac{E_1 + m_1}{E_2} e^{m_1 r} - C_2 \frac{E_1 + m_2}{E_2} e^{m_2 r} + \frac{F_4}{m_1 m_2}$$

where

$$C_1 = W_{r0} - C_2 - \frac{F_3}{m_1 m_2}$$

$$C_2 = \left[W_{r0} + \frac{E_2}{E_1 + m_1} U_0 - \frac{1}{m_1 m_2} \left(F_3 + \frac{E_2 F_4}{E_1 + m_1} \right) \right] \frac{E_1 + m_1}{m_1 - m_2}$$

Case ii) If both roots are real and equal:

$$W_r = C_1 e^{m_1 r} + C_2 r e^{m_1 r} + \frac{F_3}{m_1 m_1}$$

$$U = -C_1 \left(\frac{E_1 + m_1}{E_2} \right) + \frac{F_4}{m_1 m_1} + C_2$$

where

$$C_1 = W_{r0} - \frac{F_3}{m_1 m_1}$$

$$C_2 = U_0 - \frac{F_4}{m_1 m_1} + \frac{1}{E_2} (E_1 + m_1) \left(W_{r0} - \frac{F_3}{m_1 m_1} \right)$$

Case iii) If roots are imaginary:

$$W_r = e^{-p r} [C_1 \cos(qr) + C_2 \sin(qr)] + \frac{F_3}{F_2}$$

$$U = e^{-p r} \cos(qr) \left[-\frac{C_2 q}{E_2} + (p - E_1) \frac{C_1}{E_2} \right] +$$

$$e^{-Pr} \sin(qr) \left[-\frac{C1q}{E2} + (p-E1) \frac{C2}{E2} \right] + \frac{F4}{F2}$$

where

$$q = (F2 - F1^2/4)^{0.5}$$

$$p = F1/2$$

$$C1 = Wro - \frac{F3}{F2}$$

$$C2 = -\frac{E2Uo}{q} + \frac{p-E1}{q} \left(Wro - \frac{F3}{F2} \right) + \frac{E2F4}{qF2}$$

NOMENCLATURE

A	Matrix defined by Equation (E-5.12) or surface area [m^2]
A_c	Condensation surface area [m^2]
A_r	Re-evaporation surface area [m^2]
A_s	Heat and moisture transfer surface area [m^2]
b	Vector defined by Equation (E-5.14)
Bi_M	Mass transfer Biot number [dimensionless]
Bi_T	Heat transfer Biot number [dimensionless]
C_p	Specific heat [W.h/kg.K]
C1	Integration constant [kg/kg]
C2	Integration constant [kg/kg]
EI	Rate of air leaving the zone by infiltration [1/h]
EM	Rate of air leaving the zone by internal air flows [1/h]
EV	Rate of air leaving the zone by ventilation [1/h]
E1	Constant used in Equation (E-5.31) [1/h]
E2	Constant used in Equation (E-5.31) [1/h]
E3	Constant used in Equation (E-5.31) [kg/kg.h]
E4	Constant used in Equation (E-5.32) [1/h]
E5	Constant used in Equation (E-5.32) [1/h]
E6	Constant used in Equation (E-5.32) [kg/kg.h]
fc	Ratio of convective heat to total sensible heat from lights [dimensionless]
F1	Constant defined by Equation (E-5.35) [1/h]
F2	Constant defined by Equation (E-5.35) [1/h]
F3	Constant defined by Equation (E-5.35) [1/h]
F4	Constant defined by Equation (E-5.35) [1/h]
hc	Convective mass transfer coefficient applied to the condensation surface [$kg/m^2.h$]

hr	Convective mass transfer coefficient applied to the re-evaporation surface [kg/m ² .h]
h _M	Convective moisture transfer coefficient [kg/m ² .h.°M]
h _T	Convective heat transfer coefficient [W/m ² .K]
II	Rate of air coming to the zone by infiltration [1/h]
IM	Rate of air coming to the zone by internal air flows [1/h]
IV	Rate of air coming to the zone by ventilation [1/h]
J	Jacobian matrix defined by Equation (E-5.23)
k _M	Moisture conductivity
k _T	Thermal conductivity [W/m.K]
ms	Mass flow rate of the supply air [kg/h]
m1	Root of a differential equation defined by Equation (E-5.36) [1/h]
m2	Root of a differential equation defined by Equation (E-5.36) [1/h]
nos	Number of heat and mass transfer surfaces in the zone [dimensionless]
noz	Number of zones to be simulated simultaneously [dimensionless]
Np	Number of people in the zone [dimensionless]
P	Variable part of the energy and moisture balance equations
P _s	Partial vapor pressure of the storage surface
Qcon-l	Moisture loss due to surface condensation [kg/h]
Qequ-l	Convective moisture gain from equipment [kg/h]
Qequ-s	Convective sensible heat gain from equipment [kW]
Qfur-l	Convective moisture gain from furniture [kg/h]
Qfur-s	Convective sensible heat gain from furniture [kW]
Qinf-l	Moisture gain or loss due to infiltration [kg/h]
Qinf-s	Sensible heat gain or loss due to infiltration [kW]
Qlig-s	Convective heat gain from lighting [kW]
Qmix-l	Moisture gain or loss due to intrazonal air flows [kg/h]
Qmix-s	Sensible heat gain or loss due to intrazonal air flows [kW]

Q _{peo-l}	Convective moisture gain gain from people [kg/h]
Q _{peo-s}	Convective sensible heat gain from people [kW]
Q _{rev-l}	Moisture gain due to re-evaporation [kg/h]
Q _{sin-l}	Moisture loss due to functionally defined sink term(s) [kg/h]
Q _{sin-s}	Sensible heat loss due to functionally defined sink term(s) [kW]
Q _{sor-l}	Moisture gain due to functionally defined source term(s) [kg/h]
Q _{sor-s}	Sensible heat gain due to functionally defined source term(s) [kW]
Q _{sup-l}	Moisture gain or loss by supply air [kg/h]
Q _{sup-s}	Sensible heat gain or loss by supply air [kW]
Q _{ven-l}	Moisture gain or loss due to ventilation [kg/h]
Q _{ven-s}	Sensible heat gain or loss due to ventilation [kW]
Q _{wal-l}	Convective moisture flow rate from building surface into the zone [kg/h]
Q _{wal-s}	Convective heat gain from building surface into the zone [kW]
Q	Constant part of the energy and moisture balance equations
Re	Ratio of radiative heat to total sensible heat from equipment [dimensionless]
R _p	Ratio of radiative heat to total sensible heat from people [dimensionless]
R	Relaxation parameter [dimensionless]
U _s	Moisture content of the storage media or surface moisture content [kg/kg]
T	Temperature [K]
T _a	Ambient temperature [K]
T _o	Initial zone air dry-bulb or ventilation air exit temperature [K]
T _r	Zone air dry-bulb temperature [K]
T _s	Supply air dry-bulb temperature [K]
T _w	Temperature of the heat transfer surface towards the zone side [K]
T _{w_e}	Zone air wet-bulb temperature [K]
U	Moisture content on Dry basis [kg/kg]
U _e	Equipment utilization coefficient [dimensionless]
U _l	Lighting utilization coefficient [dimensionless]

U _o	Initial moisture content [kg/kg]
V	Volume of the zone [m ³]
V _s	Volume of the storage material or internal mass [m ³]
W _a	Ambient air humidity ratio [kg/kg]
W _c	Humidity ratio of the air evaluated at condensation surface conditions [kg/kg]
W _{e-l}	Latent heat gain from equipment [kW]
W _{e-s}	Sensible heat gain from equipment [kW]
W _l	Sensible heat gain from light [kW]
W _o	Initial zone air or ventilation air exit humidity ratio [kg/kg]
W _{p-l}	Latent heat gain from people [kW]
W _{p-s}	Sensible heat gain from people [kW]
W _r	Humidity ratio of the zone air [kg/kg]
W _{ro}	Initial zone air humidity ratio [kg/kg]
W _s	Humidity ratio of the supply air [kg/kg]
W _s	Humidity ratio of the surface air [kg/kg]
W _{st}	Humidity ratio of air at saturation [kg/kg]
W _w	Humidity ratio of the surface air [kg/kg]
X	Vector defined by Equation (E-5.13)

GREEK LETTERS

ΔX	Matrix defined by Equation (E-5.24)
δ _M	"Effective penetration depth" for the energy equation [m]
δ _T	"Effective penetration depth" for the moisture equation [m]
ε _M	"Effective air mass multiplier" for the energy equation [dimensionless]
ε _T	"Effective air mass multiplier" for the moisture equation [dimensionless]
ε _V	Ventilation air mixing efficiency factor [dimensionless]
λ	Latent heat of vaporization [J/kg]

ρ Density [kg/m³]
 τ Time [h]
 ϕ Relative humidity [0 to 1]

SUBSCRIPTS

a Ambient air
i I-th storage lump
0, 1 Iteration indices
S Storage media
s Surface
sat Saturation
 α Fluid

REFERENCES

- Burch, D., "Experimental Validation of a Mathematical Model for Predicting Moisture in Attics," in Moisture and Humidity, Measurement and Control in Science and Industry, Proceedings of the 1985 International Symposium on Moisture and Humidity, Washington, D.C., pp. 287-296, 1985.
- Cleary, P. and Sherman, M., "Seasonal Storage of Moisture in Roof Sheathing," in Moisture and Humidity, Measurement and Control in Science and Industry, Proceedings of the 1985 International Symposium on Moisture and Humidity, Washington, D.C., pp. 313-323, 1985.
- Cunningham, M.J., "A New Analytical Approach to the Longterm Behavior of Moisture Concentrations in Building Cavities - I. Non-Condensing Cavity," Building and Environment, Vol. 18, No. 3, pp. 109-116, 1983.
- Cunningham, M.J., "A New Analytical Approach to the Longterm Behavior of Moisture Concentrations in Building Cavities - II. Condensing Cavity," Building and Environment, Vol. 18, No. 3, pp. 117-124, 1983.
- Cunningham, M.J., "Further Analytical Studies of Building Cavity Moisture Concentrations," Building and Environment, Vol. 19, No. 1, pp. 21-29, 1984.
- Kusuda, T., "Indoor Humidity Calculations," ASHRAE Transactions, Vol. 89, Part 2, 1983.
- Kusuda, T. and Miki, M., "Measurement of Moisture Content for Building Interior Surfaces," in Moisture and Humidity, Measurement and Control in Science and Industry, Proceedings of the 1985 International Symposium on Moisture and Humidity, Washington, D.C., pp. 297-311, 1985.

APPENDIX F

INTERFACE EQUATIONS AND HEAT AND MASS TRANSFER COEFFICIENTS

Various heat and mass transfer equations along with their boundary conditions for different heat and mass transfer theories were discussed in Appendix A. In case of a convective boundary, the heat and mass transfer coefficients are usually unknown but can be found through heat and mass transfer analogies mentioned in this appendix. An effective way of interfacing the zone heat and mass transfer equations with the storage media equations is also explained in this appendix.

F.1 HEAT AND MASS TRANSFER COEFFICIENT RELATIONS

All heat and mass transfer relations are derived from the various heat-mass transfer analogies developed. Most expressions for the convective mass transfer coefficient, h_M , are determined from expressions for the heat transfer coefficient, h_T . This is because a strong theoretically based analogy exists between heat and mass transfer. The analogy can be applied to both laminar and turbulent flows.

The following restrictions apply to the various heat-mass transfer analogies mentioned in this section:

1. The surface shapes should be similar in both cases.
2. The ratio of the velocity normal to the mass transfer surface and the ambient velocity should be less than 0.01.
3. All relations are valid for low mass transfer rates only. Relations for higher mass transfer rates are given by Bird et al 1960 and Chilton and Colburn 1934.

F.1.1 REYNOLDS ANALOGY

Reynolds analogy gives a plausible correlation between friction factors and heat-mass transfer coefficients for common gases (where $Pr=1$) with moderate temperature potential. This analogy can be expressed by the following equation

$$\frac{h_{M,\rho}}{u P_{am}} = \frac{h_T}{\rho C_p u} = \frac{f}{2} \quad (\text{F-1})$$

The term P_{am} in Equation (F-1) is approximately equal to unity for dilute mixtures, such as water vapor in air at near atmospheric conditions.

F.1.2 J-FACTOR ANALOGY

This analogy accounts for the effect of the Prandtl number which is neglected in Reynolds analogy. It was first suggested by Chilton and Colburn 1934 who showed that the correlation of heat-mass transfer data with friction data could be greatly improved by accounting for the Prandtl number. This analogy can be expressed by the following equations:

$$j_H = \left(\frac{h_T}{\rho C_p u} \right) \left(\frac{C_p \mu}{k} \right)^{2/3} = f/2 \quad (\text{F-2})$$

$$j_M = \left(\frac{h_{M,\rho} P_{am}}{u} \right) \left(\frac{\mu}{\rho D} \right)^{2/3} = f/2 \quad (\text{F-3})$$

where j_H and j_M are dimensionless numbers and are called the Colburn heat and mass transfer groups respectively. The expressions for j_H and j_M can be equated, and if the heat transfer coefficient is known then the mass transfer coefficient can be calculated.

The j-factor analogy is valid only for low mass-transfer rates and to some extent is dependent on the flow geometry.

F.1.3 GILLILAND'S ANALOGY

Gilliland (Eckert and Drake 1972) found that the exponent for $(\mu/\rho D)$ in Equation (F-3) for the j-factor analogy should be 0.56 instead of 2/3, to represent the effect of the Schmidt number. This is shown by the fact that Gilliland's equation may be written as:

$$j_M = 0.023 \text{Re}^{-0.17} \left(\frac{\mu}{\rho D} \right)^{0.11} \quad (\text{F-4})$$

F.1.4 LEWIS RELATION

Heat and mass transfer coefficients are related by equating the Chilton-Colburn j-factors. This leads to

$$\frac{h_T}{h_{M,\rho} \rho C_p} = P_{am} (\alpha/D) \quad (\text{F-5})$$

where α/D is called the Lewis number, Le .

For low diffusion rates, Equation (F-5) is further simplified to

$$\frac{h_T}{h_{M,\rho} \rho C_p} = 1 \quad (\text{F-6})$$

For a mass transfer coefficient with humidity ratio as the driving force; the Lewis relation becomes

$$\frac{h_T}{h_{M,W} \rho} = (1.0 + W) C_p \quad (\text{F-7})$$

In case the driving force for the mass-transfer coefficient is the water vapor density, the mass transfer coefficient $h_{M,\rho}$ can be expressed as:

$$h_{M,\rho} = \frac{h_T}{(\rho_a + \rho_v) C_p} \quad (\text{F-8})$$

The various mass transfer coefficients for different theories mentioned in Appendix A are tabulated below:

TABLE F-1
Mass Transfer Coefficient Conversions

Mass Transfer coefficient	Units	Formula
$h_{M,\rho}$	m/h	(F-8)
$h_{M,W}$	m/h	(F-7)
$h_{M,M}$	kg/m ² .h.M	$h_{M,\rho} \rho_a / M_a$
$h_{M,P}$	kg/m ² .h	$h_{M,\rho} \rho_a$
$h_{M,U}$	m/h	$h_{M,\rho}$

F.2 HEAT AND MASS INTERFACE EQUATIONS

For a mathematical modeling of the real life situation of a room, the room air is treated as a zone and the room walls are treated as a storage media. Whenever a storage block or media is linked to zone, an effective method of interfacing is necessary. Interfacing is necessary for two reasons, namely,

1. Moisture is in vapor phase in the zone, whereas it is in liquid phase inside the storage media. The change in phase occurs at the boundary wall when moisture from one domain enters the other domain. The change in phase is accompanied with a heat-of-phase change.
2. The zone heat and mass transfer equations [(E-5.1) and (E-5.2)], are in a lumped form, whereas the storage heat and mass transfer equations [(A-3.1) and (A-3.2)] are both space and time dependent. A link between the storage media and the zone has to be established since the temperature and moisture conditions at the wall interface effects the temperature and moisture conditions in the zone and vice-versa.

Temperature is the governing variable in the thermal equations for the zone (E-1.1) and the storage media (A-3.2). The governing variables for the moisture equation for the storage media are different for different heat and mass transfer models mentioned in Appendix A. These variables are tabulated below:

TABLE F-2
Mass Transfer Variables

Mass Transfer variable	Reference
ρ_V	(A-3.1)
U	(A-4.21) (A-5.18)
M	(A-4.21) (A-4.26)
θ	(A-6.8) (A-7.27)
Φ	(B-8.10)

As shown before, thermodynamic equilibrium is assumed to exist at the wall interface between the storage media and the zone. This is illustrated in Figure E-1 and explained briefly in the same appendix. Thus the zone moisture and storage media moisture variables are related through equilibrium and psychometric relations. The interface is carried out through what the authors call the Beta concept. This concept is explained in detail in the next section.

F.2.1 THE BETA CONCEPT

The various zone equations for different heat and mass transfer theories along with their Beta's are tabulated in Table F-3. As can be seen from Table F-3, the Beta concept serves two purposes, namely,

1. It is used to convert wall moisture conditions to zone moisture conditions as in Low Intensity and Irreversible thermodynamics models. For the Low Intensity model the Q_{w-1} term in the zone equation is stated in terms of the vapor density ρ_v . The wall vapor density $\rho_{v,w}$ is converted to U_w by using bq_v and the zone vapor density $\rho_{v,r}$ is related to the humidity ratio by the simple relation

$$\rho_{v,r} = \rho_{a,r} W \quad (F-2.1.1)$$

2. It is used to convert zone moisture conditions to wall moisture conditions as in Philip and De Vries and Luikov's models. For the Luikov's model the Q_{w-1} term in the zone equation is in terms of the Mass transfer potential. Since the storage equations in Luikov's model (A-4.21) are solved in terms of the mass transfer potential, no conversion is necessary for the M_w term in the zone equation. But the M_r term in the zone equation needs to be converted to a humidity ratio W , which is done through β_M (Table F-4).

TABLE F-3
Interface Equations

Mass Transfer theory	Reference	Zone equation	Beta reference
Evaporation Condensation	(A-3.1)	$\rho_a V \frac{dW}{dr} = \Sigma h_{\rho v} A (\rho_w - \rho_a W) + Q_M$	N/A
Low Intensity	(A-7.27)	$\rho_a V \frac{dW}{dr} = \Sigma h_{\rho v} A (\beta_{\rho v} U_w - \rho_a W) + Q_M$	Procedure I
Philip and DeVries	(A-5.18)	$\rho_a V \frac{dW}{dr} = \Sigma h_U A (U_w - \beta_U W) + Q_M$	Procedure II
Irreversible Thermodynamics	(B-9.1)	$\rho_a V \frac{dW}{dr} = \Sigma h_{\rho v} A (\beta_{\phi} U_w - \rho_a W) + Q_M$	Procedure III
Luikov	(A-4.21)	$\rho_a V \frac{dW}{dr} = \Sigma h_M A (M_w - \beta_M W) + Q_M$	Procedure IV

- Note : a) Only the mass generation term Q_m has been included in the zone equation for simplicity in representation.
 b) The various procedures to obtain Betas are tabulated in Table F-4.
 c) The summation Σ is carried over all surfaces exposed to the zone.

The Betas mentioned in Table F-3 can be obtained from the procedures tabulated in Table F-4. The different relations used in finding the Betas for the different heat and mass theories are the various equilibrium and psychrometric

relations outlined in Appendix G.

TABLE F-4
Betas for Different Models

Function	Procedure I	Procedure II	Procedure III	Procedure IV
Input	U_w, T_w	W_i, T_i	Φ_w, T_w	W_i, T_i
Calculate	Φ_w from(G-22) ρ_w from(G-15)	Φ_i from(G-20) U_i from(G-9)	ρ_w from(G-15)	Φ_i from(G-21) M_i from(G-4)
Calculate	$\beta_{\rho V} = \frac{\rho_w}{U_w}$	$\beta_U = \frac{U_i}{W_i}$	$\beta_{\Phi} = \frac{\rho_w}{\Phi_w}$	$\beta_M = \frac{M_i}{W_i}$

F.2.2 NUMERICAL SOLUTION

All the zone equations tabulated in Table F-3 can be expressed in the form of equation (E.5-2), the closed form solution for which is given by Equation (E.5-6). Consider for example the zone mass transfer equation for the Evaporation-Condensation theory (Table F-3). The terms $P2(\tau)$ and $Q2(\tau)$ in Equation (E-5.2) are defined as:

$$P2(\tau) = \frac{\sum h_{\rho V} A}{V} \quad (F-2.2.1)$$

$$Q2(\tau) = QM(\tau) + \frac{\sum h_{\rho V} A \rho_w}{\rho_a V} \quad (F-2.2.2)$$

Similarly if the zone energy equation is given by Equation (E-5.1.a) then the terms $P1(\tau)$ and $Q1(\tau)$ in equation (E-5.1) are defined as

$$P1(\tau) = \frac{\sum h_T A}{\rho V C_p} \quad (F-2.2.3)$$

$$Q1(\tau) = QT(\tau) + \frac{\sum h_T A T_w}{\rho V C_p} \quad (F-2.2.4)$$

Note: The summation Σ is carried over all surfaces exposed to the zone.

A direct iteration technique with successive relaxation is employed in solving the zone and storage equations simultaneously. A detailed algorithm employed for the Irreversible Thermodynamics model is described below. The algorithm is similar for other models.

- Notes: 1. 'i' represents the i-th zone number.
 2. 'k' represents the k-th exposed surface.
 3. 'i,k' represents the k-th surface exposed to the i-th zone.
 4. ' α,k ' represents the ambient condition for k-th exposed surface.

Input -----> $T_i^{\tau}, T_{wi,k}^{\tau}, W_i^{\tau}, \Phi_{wi,k}^{\tau}$

[1] Define -----> $T_i^{\tau} = T_i^{\tau}, W_i^{\tau} = W_i^{\tau}, T_{wi,k}^{\tau} = T_{wi,k}^{\tau}, \Phi_{wi,k}^{\tau} = \Phi_{wi,k}^{\tau}$

[2] Store -----> T_i in boundary location for $T_{\alpha,k}$

Calculate -----> $\beta_{\Phi_{i,k}}$ using procedure III (Table F-4)

Set -----> $\rho_{v,i} = \rho_a W_i$

Store -----> $\rho_{v,i}$ in boundary location for $\rho_{v,\alpha,k}$

Solve -----> Thermal FEM Equation (B-8.8) to obtain $T_{wi,k}^{\tau+\Delta\tau}$

Check -----> $|T_{wi,k}^{\tau+\Delta\tau} - T_{wi,k}^{\tau}| < \text{error tolerance}$

Relax -----> $T_{wi,k}^{\tau+\Delta\tau} = (1-R)T_{wi,k}^{\tau+\Delta\tau} + RT_{wi,k}^{\tau}$

Set -----> $T_{wi,k}^{\tau+\Delta\tau} = T_{wi,k}^{\tau+\Delta\tau}$

Calculate -----> $P1(s)$ and $Q1(s)$ in Equation (E-5.1)

Solve -----> zone energy balance Equation (E-5.1) to obtain $T_i^{\tau+\Delta\tau}$ from (E-5.5)

Check -----> $|T_i^{\tau+\Delta\tau} - T_i^{\tau}| < \text{error tolerance}$

Relax -----> $T_i^{\tau+\Delta\tau} = (1-R)T_i^{\tau+\Delta\tau} + RT_i^{\tau}$

Set -----> $T_i^{\tau+\Delta\tau} = T_i^{\tau+\Delta\tau}$

Solve -----> Mass FEM Equation (B-8.1) to obtain $\Phi_{wi,k}^{\tau+\Delta\tau}$

Check -----> $|\Phi_{wi,k}^{\tau+\Delta\tau} - \Phi_{wi,k}^{\tau}| < \text{tolerance}$

Relax -----> $\Phi_{wi,k}^{\tau+\Delta\tau} = (1-R)\int_{wi,k}^{\tau+\Delta\tau} + R\int_{wi,k}^{\tau}$

```

Set ----->  $\Phi_{wi,k}^{r+\Delta\tau} = \Phi_{wi,k}^{r+\Delta\tau}$ 
Calculate -----> P2(s) and Q2(s) in Equation (E-5.2)

Solve -----> zone mass balance Equation (E-5.2) to obtain  $W_i^{r+\Delta\tau}$  from (E-5.6)

Check ----->  $|W_i^{r+\Delta\tau} - W_i^r| < \text{tolerance}$ 

Relax ----->  $W_i^{r+\Delta\tau} = (1-R)W_i^r + RW_i^{r+\Delta\tau}$ 

Set ----->  $W_i^{r+\Delta\tau} = W_i^{r+\Delta\tau}$ 

Check -----> Overall Convergence

If true
Set ----->  $\tau = \tau + \Delta\tau$ 

Set ----->  $T_i^{\tau} = T_i^{\tau}$ 
            $W_i^{\tau} = W_i^{\tau}$ 
            $T_{wi,k}^{\tau} = T_{wi,k}^{\tau}$ 
            $\Phi_{wi,k}^{\tau} = \Phi_{wi,k}^{\tau}$ 

Goto -----> [1]

else

Goto -----> [2]

```

The relaxation parameter R ranges from 0 to 1 and has to be chosen by the user.

NOMENCLATURE

A	Surface area [m^2]
C_p	Specific heat at constant pressure [W.h/kg.k]
D	Air diffusivity [m^2/h]
f	Friction factor [dimensionless]
h_M	Mass transfer coefficient [m/h]
h_T	Heat transfer coefficient [$W/m^2.K$]
j_H	Colburn heat transfer number [dimensionless]
j_M	Colburn mass transfer number [dimensionless]
M	Mass transfer potential [M]
P	Total Pressure [$kg/m.s^2$]
P_{am}	Logarithmic mean density factor [kg/m^3]
T	Temperature [K]
u	Average free steam velocity [m/hr]
U	Moisture Content [kg/kg]
V	Volume [m^3]
W	Humidity Ratio [kg/kg]

GREEK LETTERS

ρ	Density [kg/m^3]
μ	Absolute viscosity [N.h/m]
Φ	Relative humidity [dimensionless]
Θ	Volumetric moisture content [m^3/m^3]
\Re	Relaxation parameter [dimensionless]
τ	Time [h]

SUBSCRIPTS

a Air
 α Ambient
w Wall
M Mass
i i-th zone
i,k i-th zone exposed to k-th storage surface
V Vapor

REFERENCES

ASHRAE 1981, Handbook of Fundamentals, Chapter 3, Atlanta: American Society of Heating, Refrigerating and Air-conditioning Engineers.

Bird, R.B., Stewart, W.E. and Lightfoot E.N., Transport Phenomena, Wiley, New York, 1960.

Chilton, T.H. and Colburn, A. P., "Mass Transfer (absorption) Coefficients - Prediction from Data on Heat Transfer and Fluid Friction," Industrial and Engineering Chemistry, p. 1183, 1934.

Eckert, E.R.G. and Drake, R.M., Analysis of heat and mass transfer, McGraw-Hill, New York, 1972.

APPENDIX G

PSYCHROMETRIC AND EQUILIBRIUM FUNCTIONS

In this appendix the psychrometric and moisture equilibrium functions used in the study are given.

$$1.0 \quad h = h(T, W)$$

$$h = [(T - 273.15) + (2007.96425 + 1.805 T) W]/3.6 \quad (G-1)$$

$$2.1 \quad \Delta h_W = \Delta h_W(T, \rho_V, \phi)$$

$$\Delta h_W = \frac{R_V T^2}{\phi} \frac{\partial \phi}{\partial T}(\rho_V, T) \quad (G-2)$$

$$2.2 \quad \Delta h_o = \Delta h_o(T)$$

$$\Delta h_o = 3.11 \times 10^6 - 2.11 \times 10^3 T \quad (G-3)$$

$$3.0 \quad M = M(\phi)$$

$$M = +0.357544 + 129.928 \phi - 443.087 \phi^2 + 942.941 \phi^3 - 648.953 \phi^4 \\ - 330.918 \phi^5 + 450.698 \phi^6 \quad (G-4)$$

$$4.1 \quad P_V = P_V(\phi, T)$$

$$P_V = \phi \exp\left(+23.7093 - \frac{4111.0}{T - 35.45}\right) \quad (G-5)$$

$$4.2 \quad P_{V,sat} = P_{V,sat}(T)$$

$$P_{V,sat} = \exp\left(+23.7093 - \frac{4111.0}{T - 35.45}\right) \quad (G-6)$$

$$5.0 \quad T_d = T_d(W, P_b)$$

$$P_V = \frac{P_b W}{0.62198 + W}$$

$$T_d = T_{sat}(P_V) \quad (G-7)$$

$$6.0 \quad T_w = T_w(T, W, P_b)$$

The wet bulb temperature can be obtained by iterative solution of the following equations.

$$W_{sat} = \frac{W (3149.7313 + 1.805 T - 4.18 T_{nw}) + (T - T_{nw})}{3151.3702 - 2.381 T_{nw}}$$

$$P_{V,sat} = \frac{W_{sat} P_b}{0.62198 + W_{sat}}$$

$$T_{n+1w} = 35.45 + \frac{4111.0}{23.7093 - \ln(P_{V,sat})} \quad (G-8)$$

$$7.0 \quad U = U(\phi)$$

$$U = a \phi^b + c \phi^d \quad (G-9)$$

The constants a, b, c and d can be obtained from Appendix D (Table D-1).

$$8.1 \quad W = W(T, P_b, \phi)$$

$$W = \frac{0.62198 \phi}{\exp(-23.7093 + \frac{4111.0}{T - 35.45}) P_b - \phi} \quad (G-10)$$

$$8.2 \quad W = (T_d, P_b)$$

$$P_{V,sat} = \exp(+23.7093 - \frac{4111.0}{T_d - 35.45})$$

$$W = 0.62198 \frac{P_{V,sat}}{P_b - P_{V,sat}} \quad (G-11)$$

$$8.3 \quad W = W(T, T_w, P_b)$$

$$P_{V,sat} = \exp(+23.7093 - \frac{4111.0}{T_w - 35.45})$$

$$W_{sat} = 0.62198 \frac{P_{V,sat}}{P_b - P_{V,sat}}$$

$$W = \frac{(3151.3702 - 2.381 T_w) W_{sat} - T + T_w}{3149.7313 + 1.805 T - 4.18 T_w} \quad (G-12)$$

$$8.4 \quad W = W(T, h)$$

$$W = \frac{3.6 h - T + 273.15}{2007.96425 + 1.805 T} \quad (G-13)$$

$$8.5 \quad W_{sat} = W_{sat}(P_b, P_{V,sat})$$

$$W_{sat} = 0.62198 \frac{P_{V,sat}}{P_b - P_{V,sat}} \quad (G-14)$$

$$9.1 \quad \rho_V = \rho_V(\phi, T)$$

$$\rho_V = \frac{\phi}{R_V T} \exp\left(+23.7093 - \frac{4111.0}{T - 35.45}\right) \quad (G-15)$$

$$9.2 \quad \rho_{V,sat} = \rho_{V,sat}(T)$$

$$\rho_{V,sat} = \frac{1}{R_V T} \exp\left(+23.7093 - \frac{4111.0}{T - 35.45}\right) \quad (G-16)$$

$$9.3 \quad \rho_V = \rho_V(T, W, P_b)$$

$$\rho_V = \frac{W P_b}{R_V T (W + 0.62198)} \quad (G-17)$$

$$10.1 \quad \phi = \phi(\rho_V, T)$$

$$\phi = \rho_V R_V T \exp\left(-23.7093 + \frac{4111.0}{T - 35.45}\right) \quad (G-18)$$

$$10.2 \quad \phi = \phi(T, T_d)$$

$$\phi = \exp\left[\frac{4111.0 (T_d - T)}{(T - 35.45) (T_d - 35.45)}\right] \quad (G-19)$$

$$10.3 \quad \phi = \phi(W, T, P_b)$$

$$\phi = \frac{W P_b \exp\left(-23.7093 + \frac{4111.0}{T - 35.45}\right)}{W + 0.62198} \quad (G-20)$$

$$10.4 \quad \phi = \phi(M)$$

$$\begin{aligned} \phi = & +4.66934 \times 10^{-3} + 2.33479 \times 10^{-5} M + 1.2899 \times 10^{-3} M^2 - 3.10179 \times 10^{-5} M^3 \\ & + 2.75323 \times 10^{-7} M^4 - 7.6617 \times 10^{-10} M^5 - 7.61305 \times 10^{-13} M^6 \end{aligned} \quad (G-21)$$

$$10.5 \quad \phi = \phi(U, T)$$

The relative humidity can be obtained by iterative solution of the following equation.

$$\phi_{n+1} = \phi_n - \frac{a \phi_n^b + c \phi_n^d - U}{a b \phi_n^{b-1} + c d \phi_n^{d-1}} \quad (G-22)$$

$$11.0 \quad \frac{\partial \phi}{\partial \rho_V} = \frac{\partial \phi}{\partial \rho_V}(T)$$

$$\frac{\partial \phi}{\partial \rho_V} = R_V T \exp(-23.7093 + \frac{4111.0}{T - 35.45}) \quad (G-23)$$

$$12.0 \quad \frac{\partial \phi}{\partial T} = \frac{\partial \phi}{\partial T}(\rho_V, T)$$

$$\frac{\partial \phi}{\partial T} = R_V \rho_V \exp(-23.7093 + \frac{4111.0}{T - 35.45}) [1.0 - \frac{4111.0 T}{(T - 35.45)^2}] \quad (G-24)$$

$$13.0 \quad \frac{d\rho_{V,sat}}{dT} = \frac{d\rho_{V,sat}}{dT}(T)$$

$$\frac{d\rho_{V,sat}}{dT} = \frac{\exp(+23.7093 - \frac{4111.0}{T - 35.45})}{R_V T} \left[\frac{4111.0}{(T - 35.45)^2} - \frac{1}{T} \right] \quad (G-25)$$

$$14.0 \quad \frac{\partial U}{\partial \phi} = \frac{\partial U}{\partial \phi}(\phi, T)$$

$$\frac{\partial U}{\partial \phi} = a b \phi^{b-1} + c d \phi^{d-1} \quad (G-26)$$

$$15.1 \quad \beta_M = \beta_M(W, T)$$

Get $\phi = \phi(W, T)$ from Equation (G-20)
Get $M = M(\phi)$ from Equation (G-4)

$$\beta_M = M/W \quad (G-27)$$

$$15.2 \quad \beta_U = \beta_U(U, T)$$

Get $\phi = \phi(U, T)$ from Equation (G-22)
Get $\rho_V = \rho_V(\phi, T)$ from Equation (G-15)

$$\beta_U = \rho_V/U \quad (G-28)$$

$$15.3 \quad \beta_{\rho_V} = \beta_{\rho_V}(\rho_V, T)$$

Get $\phi = \phi(\rho_V, T)$ from Equation (G-18)
Get $U = U(\phi, T)$ from Equation (G-9)

$$\beta_{\rho_V} = U/\rho_V \quad (G-29)$$

$$15.4 \quad \beta_\phi = \beta_\phi(\phi, T)$$

Get $P_V = P_V(\phi, T)$ from Equation (G-5)

$$\beta_\phi = P_V/\phi$$

(G-30)

NOMENCLATURE

- a Constant used to define the equilibrium relation [dimensionless]
- b Constant used to define the equilibrium relation [dimensionless]
- c Constant used to define the equilibrium relation [dimensionless]
- d Constant used to define the equilibrium relation [dimensionless]
- h Enthalpy of moist air [W.h/kg]
- h_o Specific latent heat of pure water vaporization [W.h/kg]
- h_w Specific differential heat of wetting [W.h/kg]
- M Mass transfer potential [$^{\circ}$ M]
- n Iteration index [dimensionless]
- P_V Partial water vapor pressure [$\text{kg/m}\cdot\text{s}^2$]
- P_b Barometric pressure [$101325.0 \text{ kg/m}\cdot\text{s}^2$]
- R_V Ideal gas constant for water vapor [461.52 J/kg.K]
- T Dry bulb temperature [K]
- T_d Dew point temperature [K]
- T_w Wet bulb temperature [K]
- U Moisture content on dry basis [kg/kg]
- W Humidity ratio [kg/kg]
- ρ_V Water vapor density [kg/m^3]
- ϕ Relative humidity [0 to 1]

SUPERSCRIPTS

sat Saturation

APPENDIX H

THERMAL RADIATION MODELING

In enclosures, thermal radiation may be a more significant portion of the total heat transfer than convection and conduction. The details of thermal radiation in enclosures and the parameters governing it are explained in this appendix. Here, only radiation from a solid surface to a receiver or to another solid surface is considered. Gas radiation is excluded.

An important factor in radiation heat transfer is the relative geometric orientation of the participating surfaces. One way to account for geometry is to introduce a quantity called the geometric configuration factor (view factor). The geometric configuration is defined as the fraction of radiant energy leaving a surface that arrives at the other surface it depends on the geometric orientations of the surfaces with respect to each other. Although the geometric dependency discussed here is for black surfaces, the results have wider generality as they can be applied for uniform diffuse radiation leaving any surface. More information on how to calculate the view factors for one-, two- and three-dimensional elements by using specific methods such as Hottel's crossed-string or integration methods, is provided in Section H.2. There is yet another concept used in the many simulations involving radiation called script-F factor. The script-F factor is directly related to the view factors and surface emissivities, and they can be determined using the definition of radiosity. Details on how to obtain the script-F factors are explained in Section H.3.

In modelling radiation exchange using view factors (or script-F factors), there are three basic assumptions. First, it is assumed that each surface is gray, which emits and reflects thermal radiation diffusely. Second, each surface is further assumed to be isothermal, a condition which may be easily met in practice by subdividing a non-isothermal surface into smaller isothermal elements. Finally, thermal radiation incident on a surface is assumed to be uniformly distributed on that surface.

If an opaque body is blocking the radiant exchange between two participating surfaces, as happens in many applications, it is necessary to modify the view factors (or script-F factors) to account for the shading effect. In Section H.4, details of some mathematical concepts that are used in shadow checking procedures for two- and three-dimensional elements are discussed.

H.1 RADIATIVE BOUNDARY CONDITIONS AND FINITE ELEMENT FORMULATIONS

Thermal radiation affects the governing equations through the boundary conditions applied to the domain of interest. If radiation is modelled, the terms contributing to radiant exchange will evolve at the boundaries when an energy balance is carried out. The energy balance requires that heat conducted to a solid boundary should be equal to the sum of total imposed, convective, and radiative heat fluxes, as shown in Figure H-1.

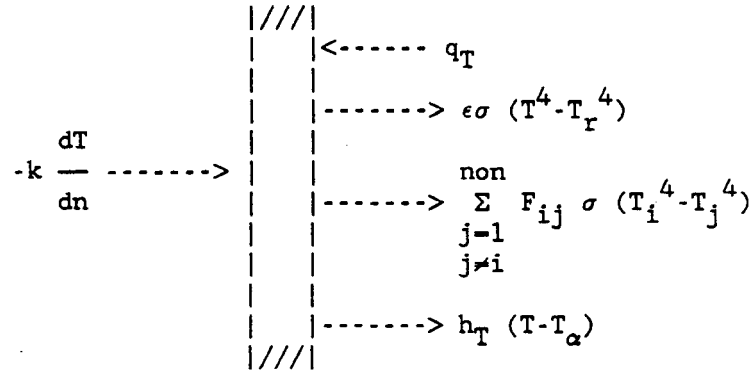


Figure H-1. Schematic of energy balance at a boundary.

The equation corresponding to Figure H-1 can be expressed as follow:

$$-k \frac{dT}{dn} = -q_T + h_T (T - T_\alpha) + \epsilon \sigma (T^4 - T_r^4) + \sum_{\substack{j=1 \\ j \neq i}}^{\text{non}} F_{ij} \sigma (T_i^4 - T_j^4) \quad (\text{H-1.1})$$

As shown in Equation (H-1.1), two radiation terms are involved. The first term accounts for the radiation exchange between a solid surface and some infinite receiver such as the night sky. The second term accounts for the radiation exchange among solid surfaces such as radiation exchange between two plates. Thermal radiation among two surfaces is calculated through the script-F concept and is explained in detail in Section H.3.

The stiffness matrix and the force vector used in the finite element formulation arising from Equation (H-1.1) are given below:

$$K = \int_{\Gamma} \epsilon \sigma N^T (N a_T)^3 N d\Gamma + \int_{\Gamma} \sigma \sum_{\substack{j=1 \\ j \neq i}}^{\text{non}} F_{ij} N^T (N a_T)^3 N d\Gamma \quad (\text{H-1.2})$$

$$F_1 = \int_{\Gamma} \epsilon \sigma N^T T_r^4 d\Gamma + \int_{\Gamma} \sigma \sum_{\substack{j=1 \\ j \neq i}}^{\text{non}} N^T F_{ij} T_j^4 d\Gamma \quad (\text{H-1.3})$$

Equations (H-1.2) and (H-1.3) will be the additional stiffness matrix and force vector that need to be added to the ones already defined in Appendix B. However, it must be noted that the stiffness matrix and force vector due to

convection and imposed heat fluxes are already given in Appendix B. Only the terms derived for radiation need to be added.

H.2 VIEW FACTOR CALCULATIONS

In FEMALP 2.1, two methods are used for view factor calculations depending on the type of surfaces involved. The first method is the Hottel's cross-string method and is discussed in Section H.2.1. If the surfaces are infinitely long then this method can be used. In the second method, the differential equation defining the view factors between arbitrarily oriented infinitesimal elemental areas are integrated numerically over the entire radiating surfaces to obtain the configuration factors. Section H.2.2 explains this method.

H.2.1 HOTTEL'S CROSSED-STRING METHOD

This is a convenient way of determining configuration factors in a two-dimensional geometry; it was first pointed out by Hottel. Typical configurations where the Hottel's crossed-string method can be applied are given in Figure H-2. In Figure H-2.(a) the surfaces are directly viewing each other; however in Figure H-2.(b) the surfaces are blocked by two other surfaces.

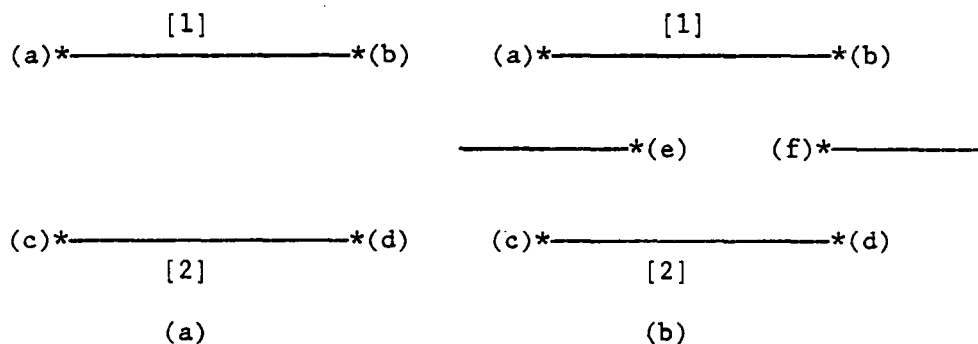


Figure H-2. Hottel's crossed-string method for view factor determination.

The equations used to determine the view factors for each of the above cases are given below:

$$F_{1-2} = \frac{ad+bc-ac-bd}{2 ab} \quad (\text{H-2.1})$$

$$F_{1-2} = \frac{ad+bc-aec-bfd}{2 ab} \quad (\text{H-2.2})$$

Additional information on Hottel's crossed-string method can be found in Siegel and Howel 1972.

H.2.2 INTEGRAL METHOD

Consider the configuration factor for radiation emitted from an isothermal surface A_1 shown in Figure H-3 and reaching A_2 . By definition, F_{1-2} is the fraction of the energy leaving A_1 that arrives at A_2 . Since A_1 is isothermal at T_1 , the total energy leaving the black surface A_1 is $\sigma T_1^4 A_1$. The radiation leaving an element dA_1 that reaches dA_2 is given as:

$$d^2Q_{d1-d2} = \sigma T_1^4 \frac{\cos\theta_1 \cos\theta_2}{\pi d^2} dA_1 dA_2 \quad (\text{H-2.3})$$

If Equation (H-2.3) is integrated over both A_1 and A_2 , the result will be the energy leaving A_1 that reaches A_2 . The configuration factor is then found as:

$$F_{1-2} A_1 = \int_{A_1} \int_{A_2} \frac{\cos\theta_1 \cos\theta_2}{\pi d^2} dA_1 dA_2 \quad (\text{H-2.4})$$

Equation (H-2.4) can also be written in terms of the configuration factors involving differential as:

$$F_{1-2} = \frac{1}{A_1} \int_{A_1} \int_{A_2} dF_{d1-d2} dA_1 = \frac{1}{A_1} \int_{A_1} F_{d1-2} dA_1 \quad (\text{H-2.5})$$

In a manner similar to the derivation of Equation (H-2.4), the configuration factor from A_2 to A_1 would be

$$F_{2-1} A_2 = \int_{A_1} \int_{A_2} \frac{\cos\theta_1 \cos\theta_2}{\pi d^2} dA_1 dA_2 \quad (\text{H-2.6})$$

The double integrals in Equations (H-2.4) and (H-2.6) are identical. Hence the following reciprocity relation will result.

$$A_1 F_{1-2} = A_2 F_{2-1} \quad (\text{H-2.7})$$

The equations given above are too complex for exact solution. However, if numerical integration is employed, then Equation (H-2.4) can be written as follows:

$$A_1 F_{1-2} = \sum_{i=1}^{no1} \sum_{j=1}^{no2} \left| \frac{\cos\theta_{i-j} \cos\theta_{j-i} A_i A_j}{\pi d_{i-j}^2} \right| \quad (\text{H-2.8})$$

Where

$$\cos\theta_{i-j} = \frac{n_1 \cdot d_{i-j}}{|n_1| |d_{i-j}|} \quad \text{and} \quad \cos\theta_{j-i} = \frac{n_2 \cdot d_{j-i}}{|n_2| |d_{j-i}|} \quad (\text{H-2.9})$$

$$A_i = A_1 / (no1) \quad \text{and} \quad A_j = A_2 / (no2) \quad (\text{H-2.10})$$

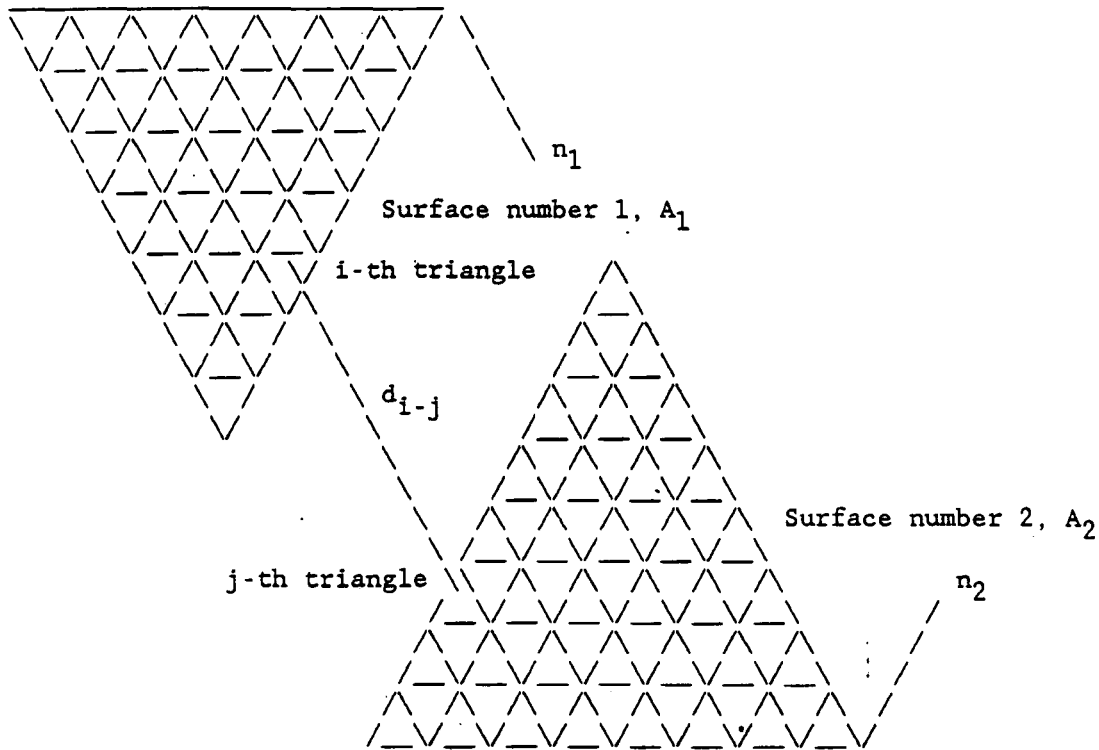


Figure H-3. Calculation of radiation view factors with integral method.

H.3 SCRIPT-F CALCULATIONS

The total radiosity of a surface i may be expressed mathematically as:

$$A_i R_i = \epsilon_i A_i \sigma T^4 + \rho_i \sum_{j=1}^{\text{non}} A_j F_{ji} R_j \quad (\text{H-3.1})$$

where F_{ji} is the well-known view factor from surface j to surface i . Since the surfaces are opaque and gray,

$$\rho_i = 1 - \epsilon_i \quad (\text{H-3.2})$$

and since the surfaces emit and reflect radiant energy diffusely,

$$A_i F_{ij} = A_j F_{ji} \quad (\text{H-3.3})$$

Equation (H-3.1) may be written, therefore, as

$$R_i = \epsilon_i \sigma T^4 + (1 - \epsilon_i) \sum_{j=1}^{\text{non}} F_{ij} R_j \quad (\text{H-3.4})$$

or in more convenient form as

$$\frac{1}{\epsilon_i} R_i - \frac{1 - \epsilon_i}{\epsilon_i} \sum_{j=1}^{\text{non}} F_{ij} R_j = \sigma T^4 \quad (\text{H-3.5})$$

Equation (H-3.5) represents a system of algebraic equations linear in radiosity. This system may be represented in matrix form as

$$P X = C \quad (\text{H-3.6})$$

where the ij -th entry of P (P_{ij}) is given by

$$P_{ij} = \frac{1}{\epsilon_i} \delta_{ij} - \left(\frac{1 - \epsilon_i}{\epsilon_i} \right) F_{ij} \quad (\text{H-3.7})$$

The i -th entries of X and C are given by

$$X_i = R_i \quad (\text{H-3.8})$$

and

$$C_i = \sigma T^4 \quad (\text{H-3.9})$$

Note that P is an $n \times n$ matrix, X is an $n \times 1$ matrix and C is the $n \times 1$ constant matrix. If the inverse of P exists, then the following can be written:

$$X = P^{-1} C \quad (\text{H-3.10})$$

But the net rate of heat loss Q_i from surface i is given by Sparrow 1978 as

$$Q_i = \frac{\epsilon_i A_i}{1 - \epsilon_i} (\sigma T^4 - R_i) \quad (\text{H-3.11})$$

or in matrix form

$$Q = G [C - X] \quad (\text{H-3.12})$$

where the ij -th entry of the matrix G is given by

$$G_{ij} = \frac{\epsilon_i A_i}{1 - \epsilon_i} \delta_{ij} \quad (\text{H-3.13})$$

Noting that G is a diagonal matrix and substituting X from Equation (H-3.10) into Equation (H-3.12) yields

$$Q = G [C - P^{-1} C] \quad (\text{H-3.14})$$

But the vector C may be factored from the right to give

$$Q = G [I - P^{-1}] C \quad (\text{H-3.15})$$

where I is an n x n identity matrix. An alternate expression for the vector Q may be written based on the definition of the F-factor, namely

$$Q_i = \sum_{\substack{j=1 \\ j \neq i}}^{\text{non}} A_i F_{ij} (\sigma T_i^4 - \sigma T_j^4) \quad (\text{H-3.16})$$

or in matrix notation

$$Q = B C \quad (\text{H-3.17})$$

where the ij-th entry of B is given by

$$B_{ij} = -A_i F_{ij} \quad \text{for } i \neq j \quad (\text{H-3.18})$$

and

$$B_{ij} = A_i \sum_{\substack{j=1 \\ j \neq i}}^{\text{non}} F_{ij} \quad \text{for } i=j \quad (\text{H-3.19})$$

Equating the right-hand side of Equation (H-3.15) to that of Equation (H-3.17) gives

$$B C = G [I - P^{-1}] C \quad (\text{H-3.20})$$

So that

$$R = G [I - P^{-1}] \quad (\text{H-3.21})$$

Equation (H-3.21) gives the formula for converting ϵ_i , A_i , and F_{ij} as embodied in G and P to the $A_i F_{ij}$ as embodied in B. The matrix B may be shown to be necessarily symmetrical, since $B_{ij} = -A_i F_{ij}$ and $B_{ji} = -A_j F_{ji}$ and $A_i F_{ij} = A_j F_{ji}$ for $i=j$. For completeness, another relation exists among the view factors, namely

$$\sum_{j=1}^{\text{non}} F_{ij} = 1 \quad (\text{H-3.22})$$

H.4 SHADOW CHECKING

FEMALP 2.1 performs two types of shadow checking for different element types. The first type of shadow checking is called two-dimensional shadow checking and is applicable for radiation between line segments (one-dimensional line elements and a leg of a two-dimensional triangular or rectangular element) where Hottel's crossed string method is applied for finding the radiation view factors. The second type of shadow checking is called three-dimensional shadow checking and is applicable for radiation between element faces and element legs.

H.4.1 TWO-DIMENSIONAL SHADOW CHECKING

FEMALP 2.1 performs two types of two-dimensional shadow checking, namely simple and detailed.

H.4.1.1 SIMPLE SHADOW CHECKING

A simple shadow checking between two radiating surfaces is a check to determine whether two surfaces are facing each other. The details of the shadow checking are given below:

Consider the two elements (1-2-3-4 and 1'-2'-3'-4') in which nodes 1, 2, 3' 4' and 1' are specified as radiating nodes. The task is to determine whether the radiating legs are facing each other.

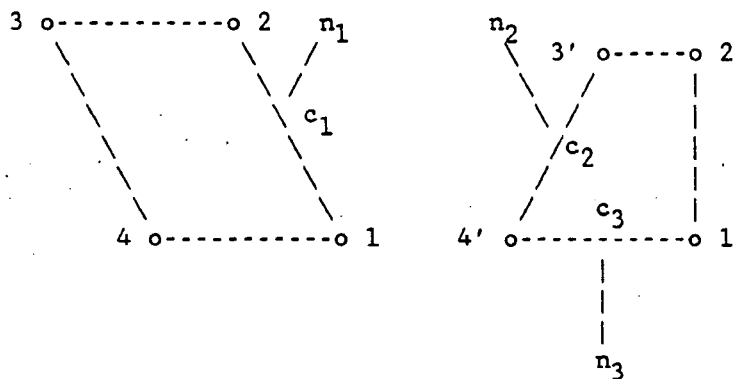


Figure H-4. Two-dimensional simple shadow checking configuration.

The normals to the radiating legs are

$$n_1 = v_{12} \times n_s$$

$$n_2 = v_{4'3'} \times n_s$$

$$n_3 = v_{1'4'} \times n_s$$

where

n_s denotes the normal to the plane of the element

v_s denotes the vectors of the lines containing the points

and

\times denotes cross product.

First, the normal vectors to each of the legs at their center are determined (n_1 , n_2 and n_3 at points c_1 , c_2 and c_3 respectively). Next, the angles between the normal and the line joining the two centers are determined for each pair of radiating legs. In order for the legs to be facing each other, both angles must be less than 90 degrees.

For the legs 1-2 and 3'-4', the angles $\langle c_2-c_1-n_1 \rangle$ and $\langle c_1-c_2-n_2 \rangle$ are less than 90 degrees. Hence, they are facing each other.

For the legs 1-2 and 4'-1', the angle $\langle c_3-c_1-n_1 \rangle$ is less than 90 degrees but angle $\langle c_1-c_3-n_3 \rangle$ is greater than 90 degrees. Hence, they do not face each other and the view factor between them is set to zero.

For the legs 3'-4' and 4'-1', both angles $\langle c_2-c_3-n_3 \rangle$ and $\langle c_3-c_2-n_2 \rangle$ are greater than 90 degrees. Hence, they do not face each other and the view factor between them is set to zero.

H.4.1.2 DETAILED SHADOW CHECKING

In the detailed shadow checking, a check is carried out between a pair of radiating surfaces to see if a leg or face of another solid element is blocking the line of sight.

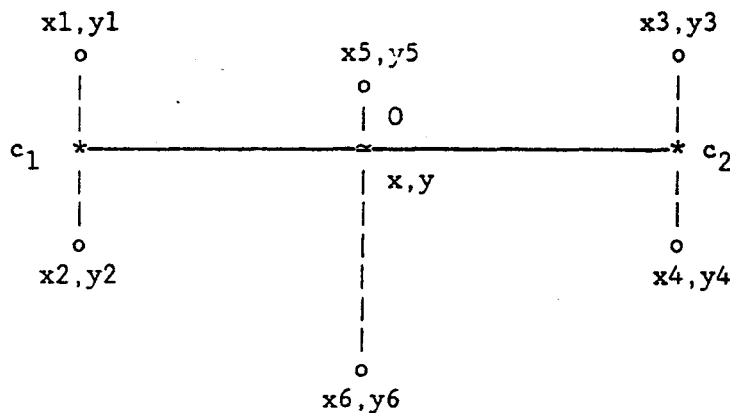


Figure H-5. Two-dimensional detailed shadow checking configuration.

Let 1-2 and 3-4 be two radiating legs and 5-6 be an arbitrary leg of a solid element. The task is to determine if the leg 5-6 is blocking the sight between legs 1-2 and 3-4. In, FEMALP 2.1, the line of sight is assumed to be between the centers of the radiating legs.

The condition for leg 5-6 to be an obstructing leg is that the point of intersection $O(x,y)$ of line passing through c_1-c_2 and the passing through point 5-6, must lie on both segments 5-6 and c_1-c_2 .

Line c_1-c_2 is given by the vector

$$[0.5(x_1+x_2)-0.5(x_3+x_4)] i + [0.5(y_1+y_2)-0.5(y_3+y_4)] j + 0 k \quad (\text{H-4.1})$$

Line 5-6 is given by the vector

$$(x_6-x_5) i + (y_6-y_5) j + 0 k \quad (\text{H-4.2})$$

The intersection point $O(x,y)$ of the two vectors is determined by solving the equations for the two vectors.

Line 5-6 is an obstruction if and only if both conditions below are met:

1. sum of distances c_1-O and $O-c_2$ equals distance c_1-c_2 and
2. sum of distances $5-O$ and $O-6$ equals distance $5-6$.

If the above conditions are met, the view factor is set to zero.

H.4.2 THREE-DIMENSIONAL SHADOW CHECKING

Before three-dimensional shadow checking is performed, a coordinate screening is applied in order to determine which elements are in the vicinity of the radiating elements. If the shading element is not in the vicinity of the radiating elements, then no further three-dimensional shadow checking is performed. The coordinate screening is performed as follows:

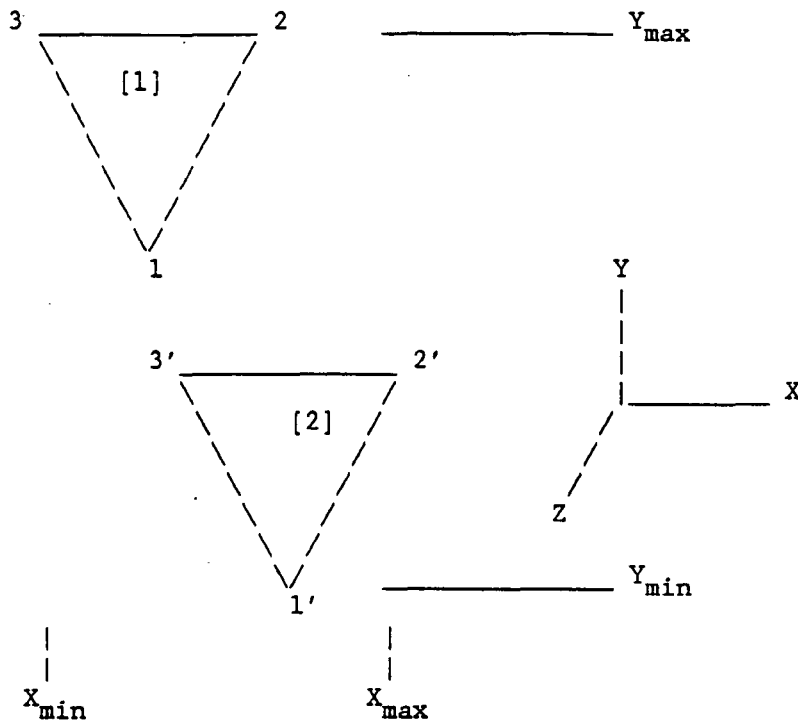


Figure H-6. Three-dimensional shadow checking layout.

Find X_{\max} , X_{\min} , Y_{\max} , Y_{\min} , Z_{\max} and Z_{\min} for surface [1] and [2]. Then check each nodal coordinate of the shading surface for following constraints.

$$X_{\max} \rightarrow X_1 \rightarrow X_{\min} \quad \text{or} \quad X_{\max} \rightarrow X_2 \rightarrow X_{\min} \quad \text{or} \quad X_{\max} \rightarrow X_3 \rightarrow X_{\min} \quad (\text{H-4.3})$$

$$Y_{\max} \rightarrow Y_1 \rightarrow Y_{\min} \quad \text{or} \quad Y_{\max} \rightarrow Y_2 \rightarrow Y_{\min} \quad \text{or} \quad Y_{\max} \rightarrow Y_3 \rightarrow Y_{\min} \quad (\text{H-4.4})$$

$$Z_{\max} \rightarrow Z_1 \rightarrow Z_{\min} \quad \text{or} \quad Z_{\max} \rightarrow Z_2 \rightarrow Z_{\min} \quad \text{or} \quad Z_{\max} \rightarrow Z_3 \rightarrow Z_{\min} \quad (\text{H-4.5})$$

If the above criteria is not satisfied for the three principal coordinate directions, then the shadow element is out of the radiation domain and no further checks are needed.

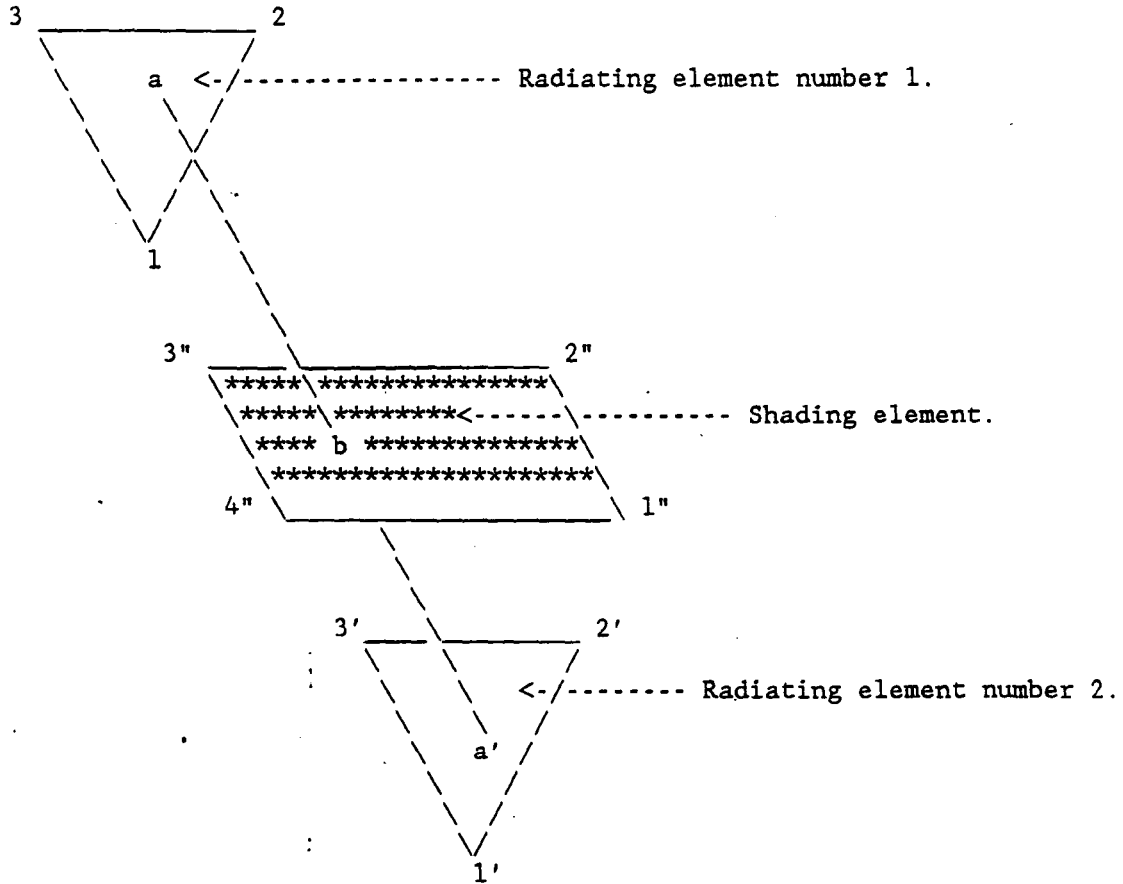


Figure H-7. Three-dimensional shadow checking layout.

Note that a and a' are the centroids of the radiating elements 1 and 2, and aa' is the line joining these two centroids. If line aa' intersects the shading element in its domain, then the shading element will cast a shadow over the radiating elements.

The equation of the plane passing from points 1234 is defined as follows:

$$a X + b Y + c Z + d = 0 \tag{H-4.6}$$

where

$$a = (y_2 - y_1)(z_3 - z_1) - (y_3 - y_1)(z_2 - z_1) \tag{H-4.7}$$

$$b = (z_2 - z_1)(x_3 - x_1) - (z_3 - z_1)(x_2 - x_1) \tag{H-4.8}$$

$$c = (x_2 - x_1)(y_3 - y_1) - (x_3 - x_1)(y_2 - y_1) \tag{H-4.9}$$

$$d = -(a \cdot x_1 + b \cdot y_1 + c \cdot z_1) \tag{H-4.10}$$

Equation of the line passing through points a (X_a, Y_a, Z_a) and a' (X_{a'}, Y_{a'}, Z_{a'}) is defined as:

$$\frac{X - X_a}{X_{a'} - X_a} = \frac{Y - Y_a}{Y_{a'} - Y_a} = \frac{Z - Z_a}{Z_{a'} - Z_a} \quad \text{or} \quad \frac{X - X_a}{s_1} = \frac{Y - Y_a}{s_2} = \frac{Z - Z_a}{s_3} \tag{H-4.11}$$

Equation (H-4.11) can be rewritten as follows:

Case i- $s_1 \neq 0$ then

$$Y - Y_a = s_2/s_1 (X - X_a); \quad Z - Z_a = s_3/s_1 (X - X_a) \quad (H-4.12)$$

and the intersection coordinates of line aa' with the shade plane are:

$$X_b = -(b*e+c*g+d)/(a*b*f+c*h); \quad Y_b = e + f*X_b; \quad Z_b = g + h*X_b \quad (H-4.13)$$

Case ii- $s_2 \neq 0$ then

$$X - X_a = s_1/s_2 (Y - Y_a); \quad Z - Z_a = s_3/s_2 (Y - Y_a) \quad (H-4.14)$$

and the intersection coordinates of line aa' with the shade plane are:

$$Y_b = -(a*e+c*g+d)/(a*f+b*c*h); \quad X_b = e + f*Y_b; \quad Z_b = g + h*Y_b \quad (H-4.15)$$

Case iii- $s_3 \neq 0$ then

$$X - X_a = s_1/s_3 (Z - Z_a); \quad Y - Y_a = s_2/s_3 (Z - Z_a) \quad (H-4.16)$$

and the intersection coordinates of line aa' with the shade plane are:

$$Z_b = -(a*e+b*g+d)/(a*f+b*h+c); \quad X_b = e + f*Z_b; \quad Y_b = g + h*Z_b \quad (H-4.17)$$

After the intersection coordinates (X_b, Y_b, Z_b) are calculated, the task is then to determine if the intersection is within the domain of the shading element. The criteria of finding whether intersection point b is within the shade domain is:

$$\text{Area } 1234 = \text{Area } 12b + \text{Area } 23b + \text{Area } 34b + \text{Area } 41b$$

If the shading element is a triangle, then points 3 and 4 are the same.

NOMENCLATURE

A_1	Area of the emitting triangle [m^2]
A_2	Area of the first receiving triangle [m^2]
A_i	Discretized area over surface number one [m^2]
A_j	Discretized area over surface number two [m^2]
B	Matrix defined by Equation (H-3.17)
C	Matrix defined by Equation (H-3.6)
d_{i-j}	Distance between the centroids of the discretized triangles [m]
F_1	Nodal force vector due to radiation
F_{1-2}	Radiation view factor [dimensionless]
F_{ij}	Script factor between surfaces [dimensionless]
G	Matrix defined by Equation (H-3.13)
h_T	Convective heat transfer coefficient [$W/m^2.K$]
i	Summation index over surface number one [dimensionless]
j	Summation index over surface number two [dimensionless]
K	Stiffness matrix due to radiation
k	Thermal conductivity [$W/m.K$]
n	Normal vector to the boundary
non	Number of radiation surfaces [dimensionless]
$no1$	Number of triangles on surface number one [dimensionless]
$no2$	Number of triangles on surface number two [dimensionless]
P	Matrix defined by Equation (H-3.6)
Q_i	Net radiation heat loss from surface i
q_T	Heat flux receiving at the surface [W/m^2]
R_i	Radiosity [dimensionless]
T	Temperature [K]
T_α	Ambient temperature for convection [K]

T_r Receiver temperature (infinite source) [K]
 T_j Temperature of the other surface [K]
 X Matrix defined by Equation (H-3.10)

GREEK LETTERS

ϵ Emissivity of boundary surfaces [dimensionless]
 θ Angle between the distance vector and surface normal [dimensionless]
 ρ Reflectivity [dimensionless]
 σ Stefan-Boltzmann constant [$W/m^2 \cdot K^4$]

REFERENCES

Siegel, R. and Howell, J.R., Thermal Radiation Heat Transfer, McGraw-Hill Book Company, New York, 1972.
Sparrow, E.M. and Cess, R.D., Radiation Heat Transfer, Augmented Edition, McGraw-Hill Book Company, New York, 1978.



APPENDIX I

VALIDATIONS

To validate a computer code is a very difficult and time-consuming task, and it must be performed with maximum care. The major difficulty encountered in the validation process is the lack of reliable and complete data to which the results of the code can be compared. It is to be stressed that the validation presented here is by no means complete or exhaustive. Rather, it utilizes comparisons of hypothetical test cases which equivalent computer codes would be expected to pass. It should be understood that detailed data from moisture transfer experiments is quite rare. Data from simultaneous heat and mass transfer experiments is even more difficult to obtain. In this study the data for comparison is obtained from the following sources:

1. Closed form solutions of simple problems
2. Known and accepted numerical solutions
3. Experimental laboratory data.

Each source has some advantages and some disadvantages, and one must be familiar with these. The closed form solutions are excellent validation sources and each code must pass them. However, they are limited to very simple problems and boundary conditions. Other computer programs and numerical solutions also provide reasonable studies for comparison. But one must understand the limitations and the numerical techniques used in these programs. Experimental data is the ultimate validation tool; however, it is very difficult to find, and even if it is found in most of the cases it is incomplete.

Test cases one through five are for homogenous solids having exact analytical solutions depending on the boundary conditions imposed. The exact solutions for these cases are available in Arpaci 1966. Three levels of mass levels were considered. Table I-1 gives the material properties used for each mass level as well as the test cases in which they were used.

TABLE I-1
Material Properties Used in Validation Test Cases I through V

Mass level	Material	k_T W/m.k	ρ kg/m ³	C_P W.h/kg.K	L m	Test case
Low-mass	Gypsum	0.4327	1249.0	0.3025	0.0127	II
Mid-mass	Concrete	0.9350	2307.0	0.1861	0.1016	I,II,III
High-mass	Concrete	0.9350	2307.0	0.1861	0.1778	all

I.1 TEST CASE NUMBER I

Test case one is a slab of thickness L at an initial temperature of T_i , (275 K) insulated at the left and suddenly exposed to an imposed temperature equal to T_α (350 K) at the right face. Assuming one-dimensional conduction in x , the temperature distribution at any x with time is sought. Figure I-1 describes the geometry and boundary conditions of the problem.

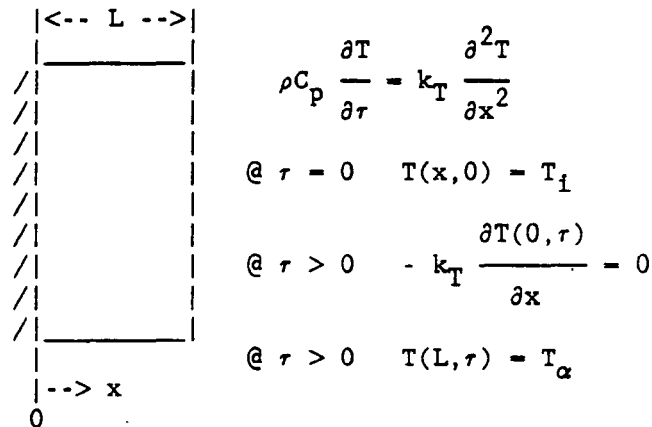


Figure I-1. A Slab suddenly exposed to a prescribed temperature on one side.

The exact solution to the problem (Arpaci 1966) is given by the following equation:

$$T(x, \tau) = T_\alpha + (T_i - T_\alpha) 2 \sum_{n=0}^{\infty} \frac{(-1)^n}{\lambda_n L} \exp(-\alpha \lambda_n^2 \tau) \cos(\lambda_n x) \quad (\text{I-1.1})$$

where

$$\lambda_n = \frac{(2n+1) \pi}{2L} \quad n = 0, 1, 2, \dots, \infty \quad (\text{I-1.2})$$

$$\alpha = \frac{k_T}{\rho C_p}$$

Figures I-2.(a) and (b) show, for medium and high mass respectively, the comparison of the exact solution with those obtained from FEMALP 2.1 at the mid-plane ($x=L/2$) of the solid. The agreement is very close in both cases at all times except near the start of simulation. The small disparities observed there are due to inherent startup problems associated with any numerical simulation. These may however be reduced by having smaller time steps at the initial startup period. Note also that the discrepancy near the initial time increases with higher mass levels.

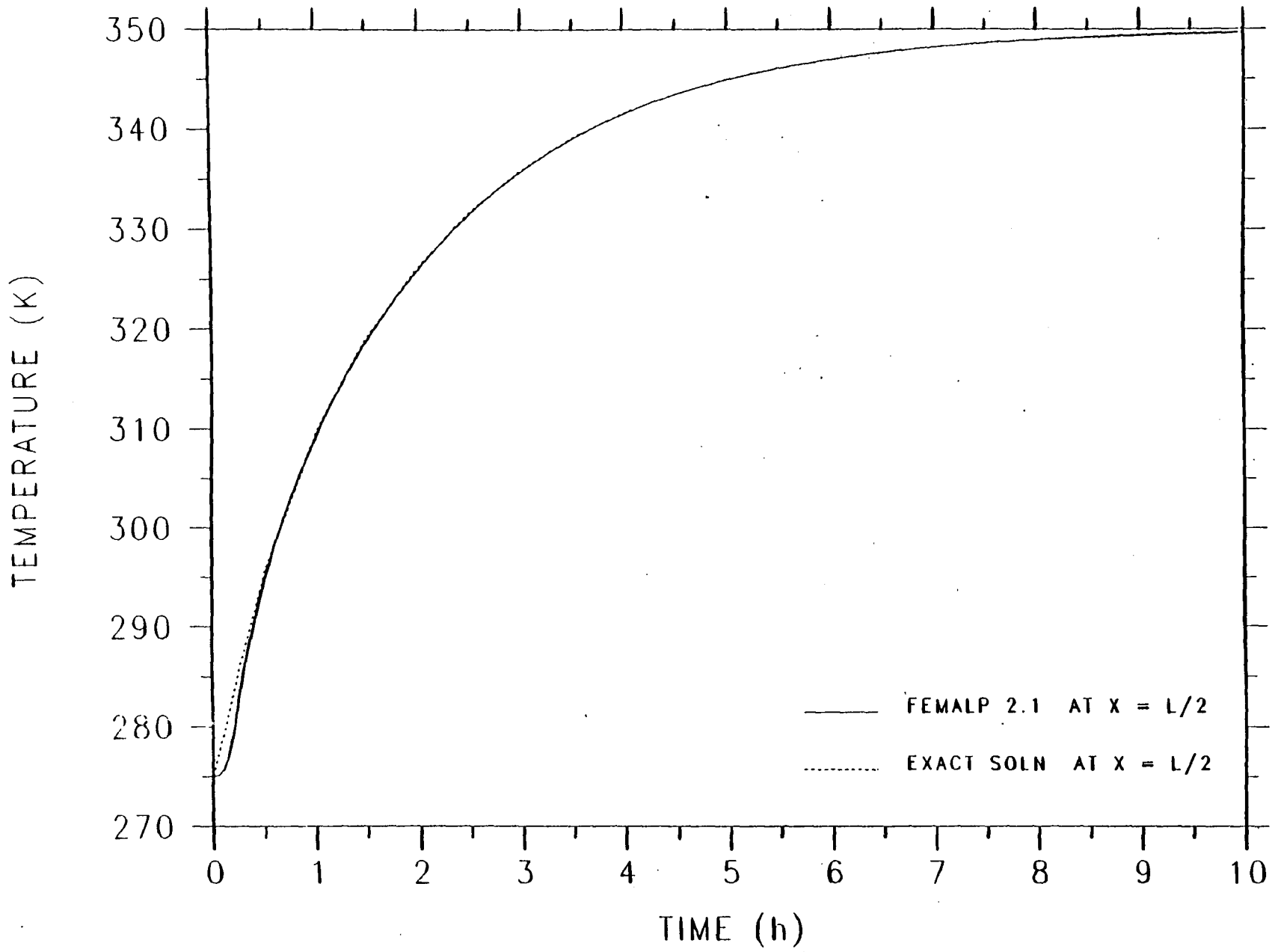


Figure I-2-(a).

FEMALP 2.1 VALIDATION CASE (I) FOR MID-MASS.

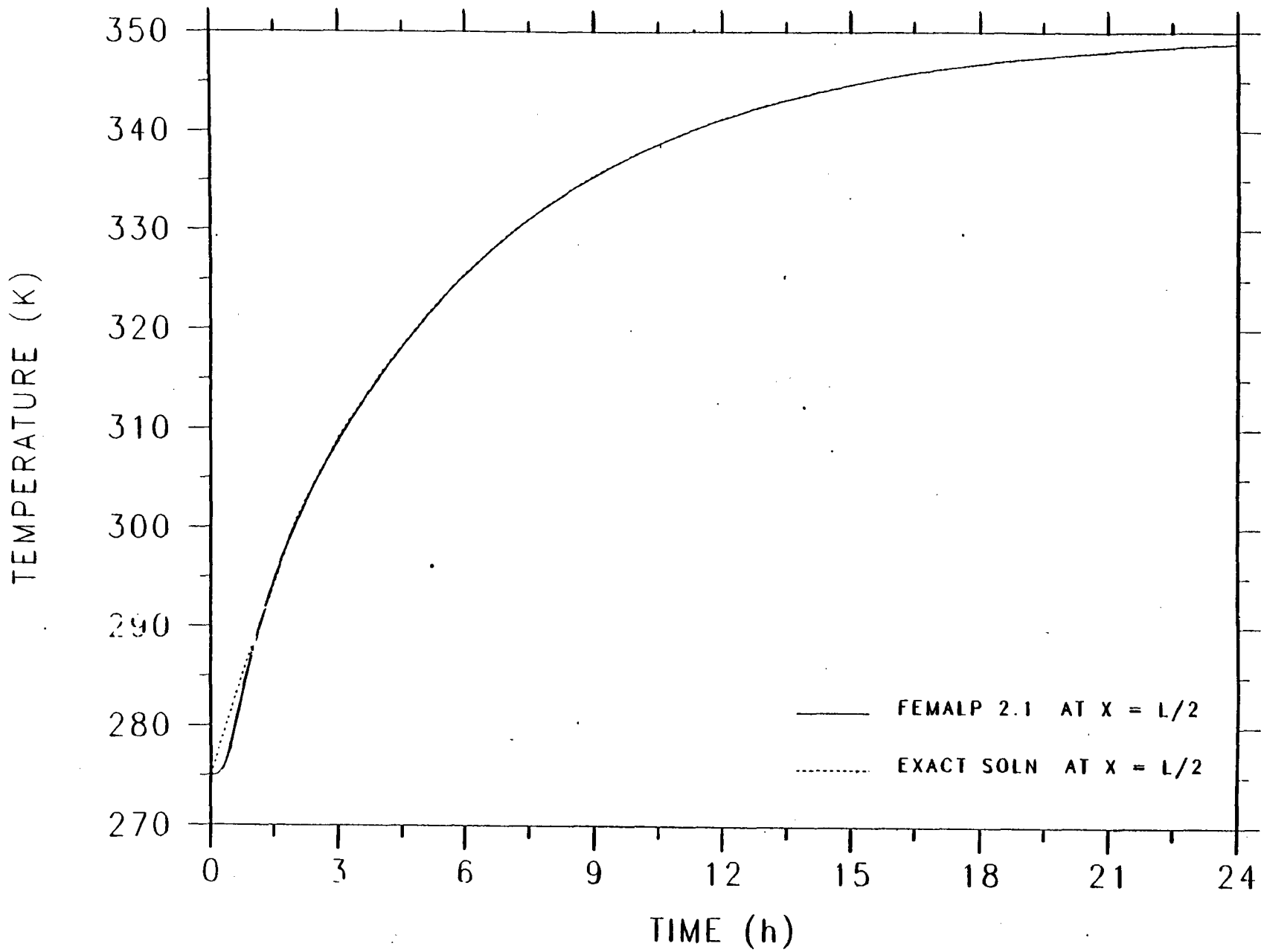
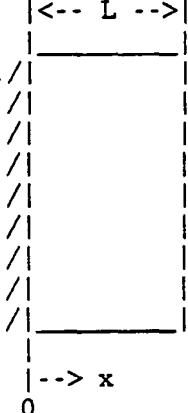


Figure I-2-(b). FEMALP 2.1 VALIDATION CASE (I) FOR HIGH-MASS.

I.2 TEST CASE NUMBER II

Test case two is a slab of thickness L at an initial temperature of T_i , (275 K) insulated at the left and suddenly exposed to a convective temperature equal to T_α (350 K) at the right face. Assuming one-dimensional conduction in x , the temperature distribution at any x with time is sought. Figure I-3 describes the geometry and boundary conditions of the problem.



$$\rho C_p \frac{\partial T}{\partial \tau} = k_T \frac{\partial^2 T}{\partial x^2}$$

$$@ \tau = 0 \quad T(x, 0) = T_i$$

$$@ \tau > 0 \quad -k_T \frac{\partial T(0, \tau)}{\partial x} = 0$$

$$@ \tau > 0 \quad -k_T \frac{\partial T(L, \tau)}{\partial x} = h_T (T - T_\alpha)$$

Figure I-3. A Slab suddenly exposed to convection on one side.

The exact solution to the problem (Arpaci 1966) is given by the following equation:

$$T(x, \tau) = T_\alpha + (T_i - T_\alpha) 2 \sum_{n=1}^{\infty} \exp(-\lambda_n^2 \alpha \tau) \frac{\sin(\lambda_n L) \cos(\lambda_n x)}{\lambda_n L + \sin(\lambda_n L) \cos(\lambda_n L)} \quad (\text{I-2.1})$$

where

$$(\lambda_n L) \tan(\lambda_n L) = \frac{h_T L}{k_T} \quad (\text{I-2.2})$$

$$\alpha = \frac{k_T}{\rho C_p}$$

Figures I-4.(a), (b) and (c) show, for low, medium, and high mass respectively, the comparison of the exact solution with those obtained from FEMALP 2.1 at the mid-plane ($x=L/2$) of the solid. The agreement of all three cases is excellent. The same validation case is also given by Judkoff et al. 1983 as a methodology for validating building energy analysis programs.

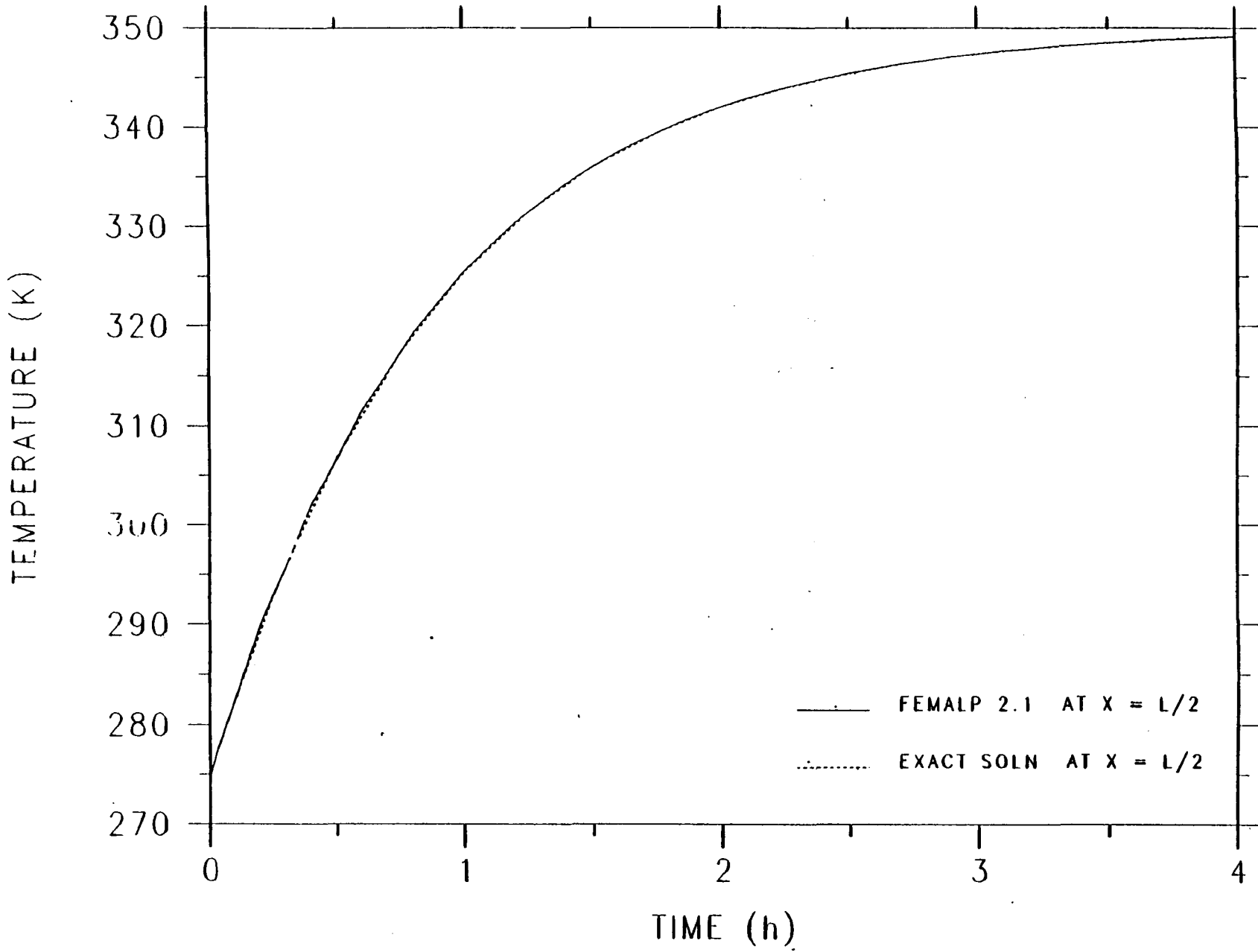


Figure I-4-(a).

FEMALP 2.1 VALIDATION CASE (II) FOR LOW-MASS

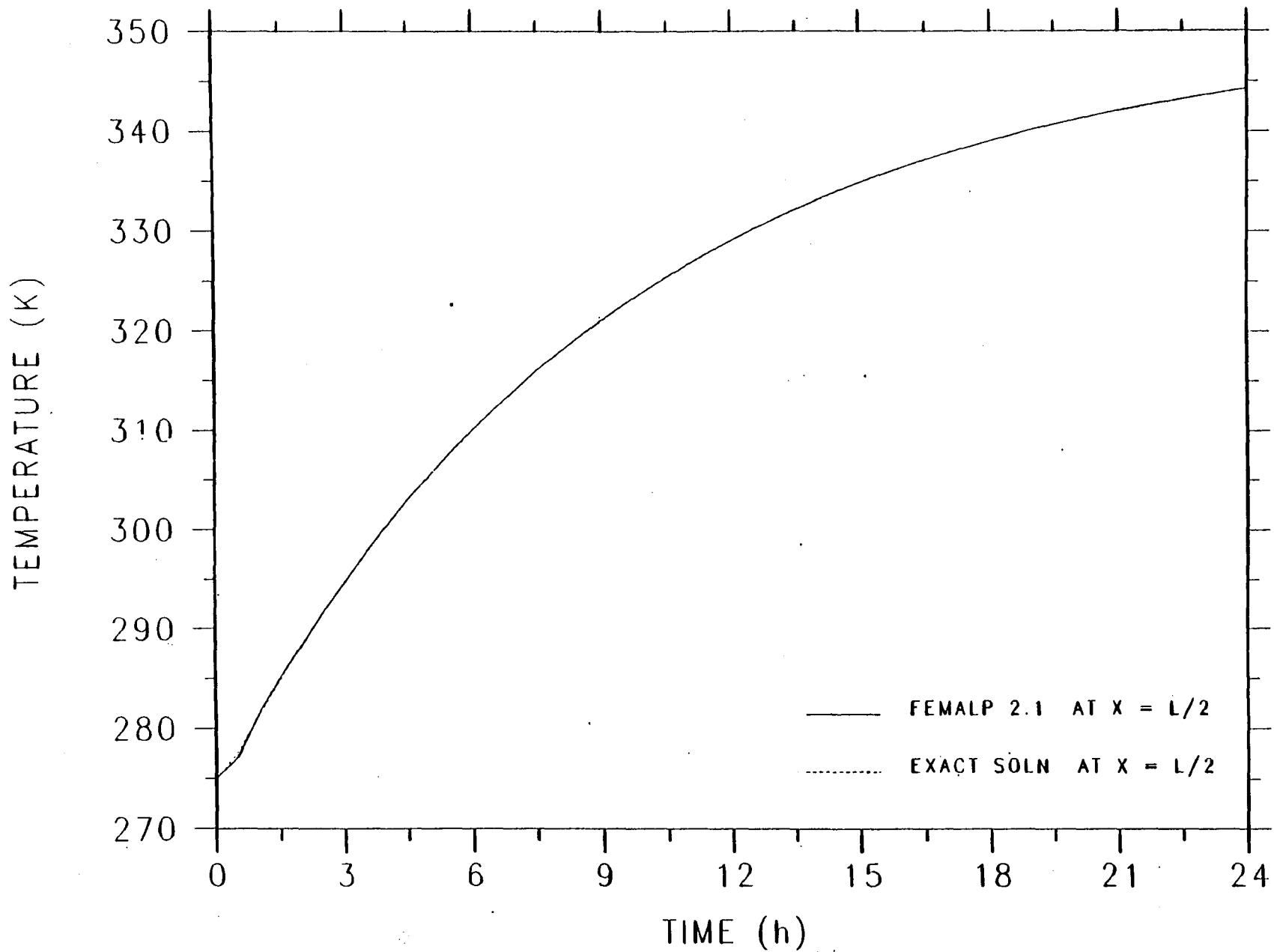


Figure I-4-(b).

FEMALP 2.1 VALIDATION CASE (II) FOR MID-MASS

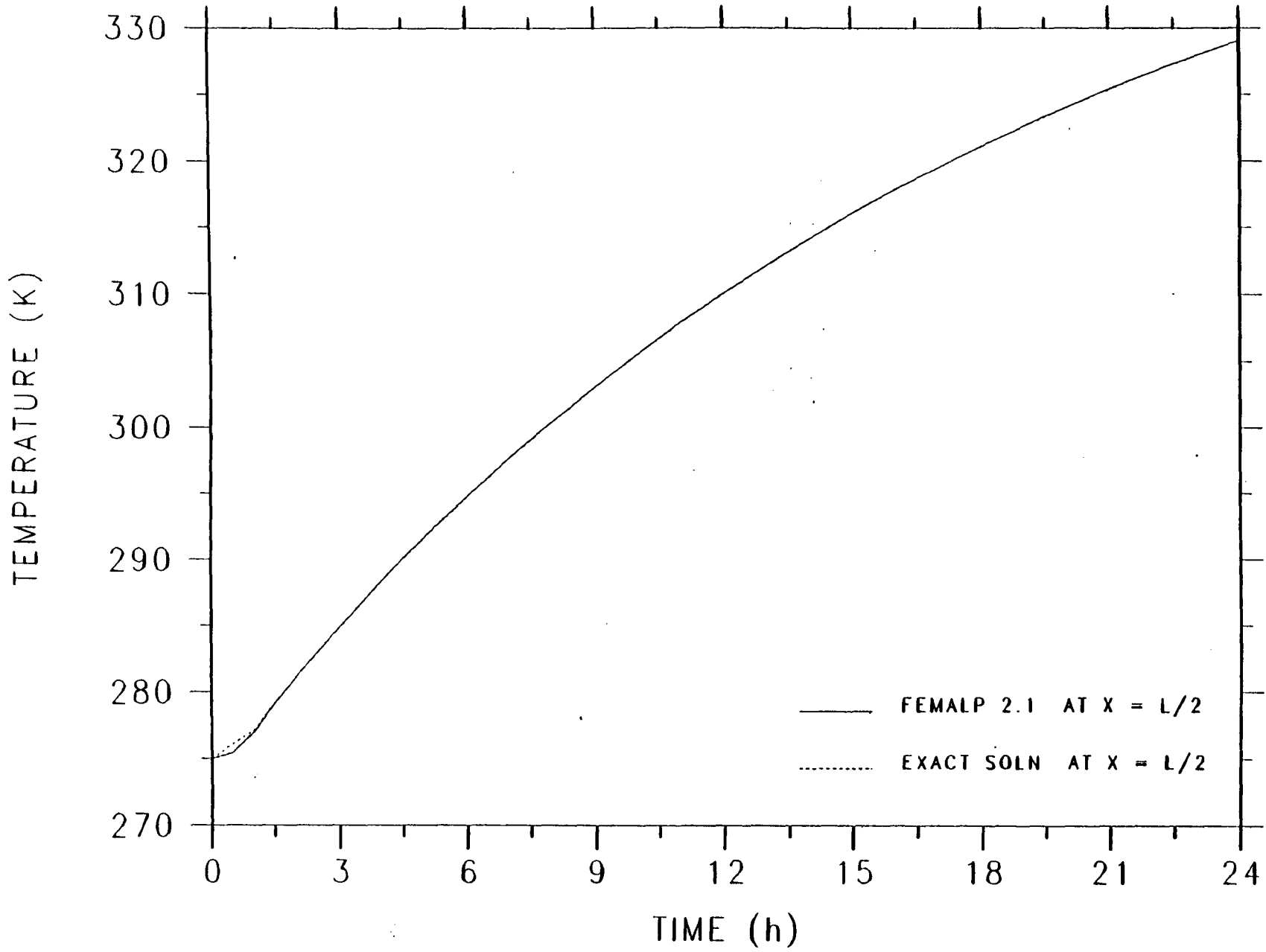


Figure I-4-(c).

FEMALP 2.1 VALIDATION CASE (II) FOR HIGH-MASS

I.3 TEST CASE NUMBER III

Test case three is a slab of thickness L at an initial temperature of T_i , (275 K) insulated at the left and suddenly exposed to an imposed heat flux equal to q_T at the right face. Assuming one-dimensional conduction in x , the temperature distribution at any x with time is sought. Figure I-5 describes the geometry and boundary conditions of the problem.

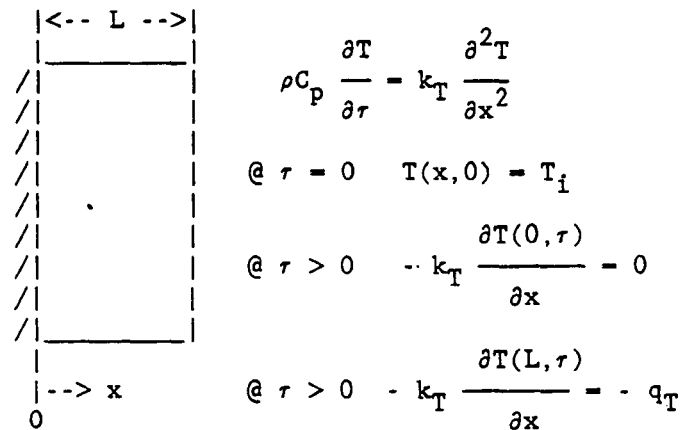


Figure I-5. A slab suddenly exposed to a constant heat flux on one side.

The exact solution to the problem (Arpaci 1966) is given by the following equation:

$$T(x, \tau) = T_i + \frac{q_T L}{k_T} \left(\frac{\alpha \tau}{L^2} + \frac{1}{2} \left(\frac{x}{L} \right)^2 - \frac{1}{6} \right) - 2 \sum_{n=1}^{\infty} \frac{(-1)^n}{(\lambda_n L)^2} \exp(-\lambda_n^2 \alpha \tau) \cos(\lambda_n x) \quad (\text{I-3.1})$$

where

$$\lambda_n = \frac{n \pi}{L} \quad n = 0, 1, 2, \dots, \infty \quad (\text{I-3.2})$$

$$\alpha = \frac{k_T}{\rho C_p}$$

Figures I-6.(a) and (b) show, for medium and high mass respectively, the comparison of the exact solution with those obtained from FEMALP 2.1 at the mid-plane of the solid. The agreement for the two cases is excellent. The same validation case is also given by Judkoff et al. 1983 as a methodology for validating building energy analysis programs.

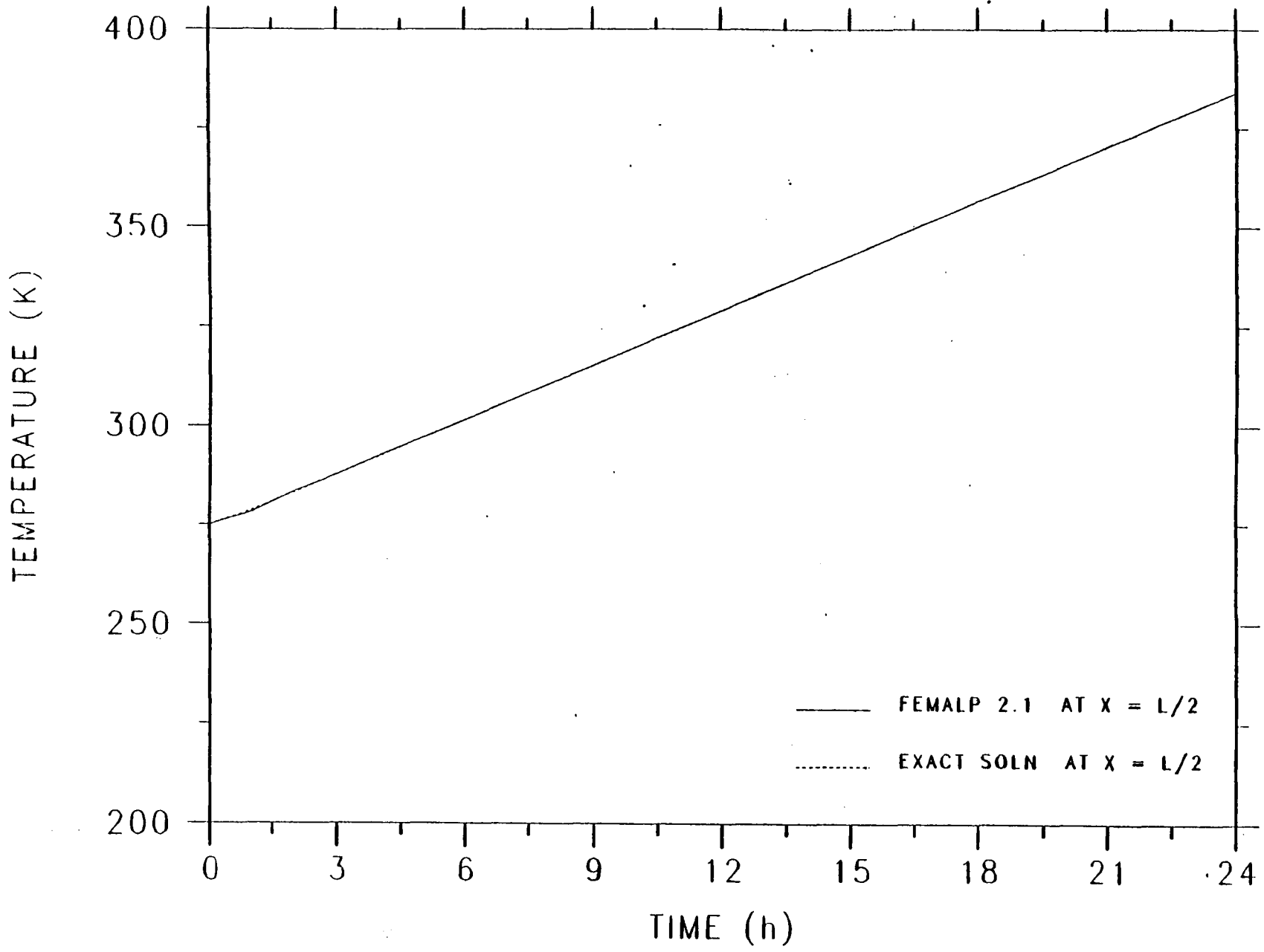


Figure I-6-(a).

FEMALP 2.1 VALIDATION CASE (III) FOR MID-MASS

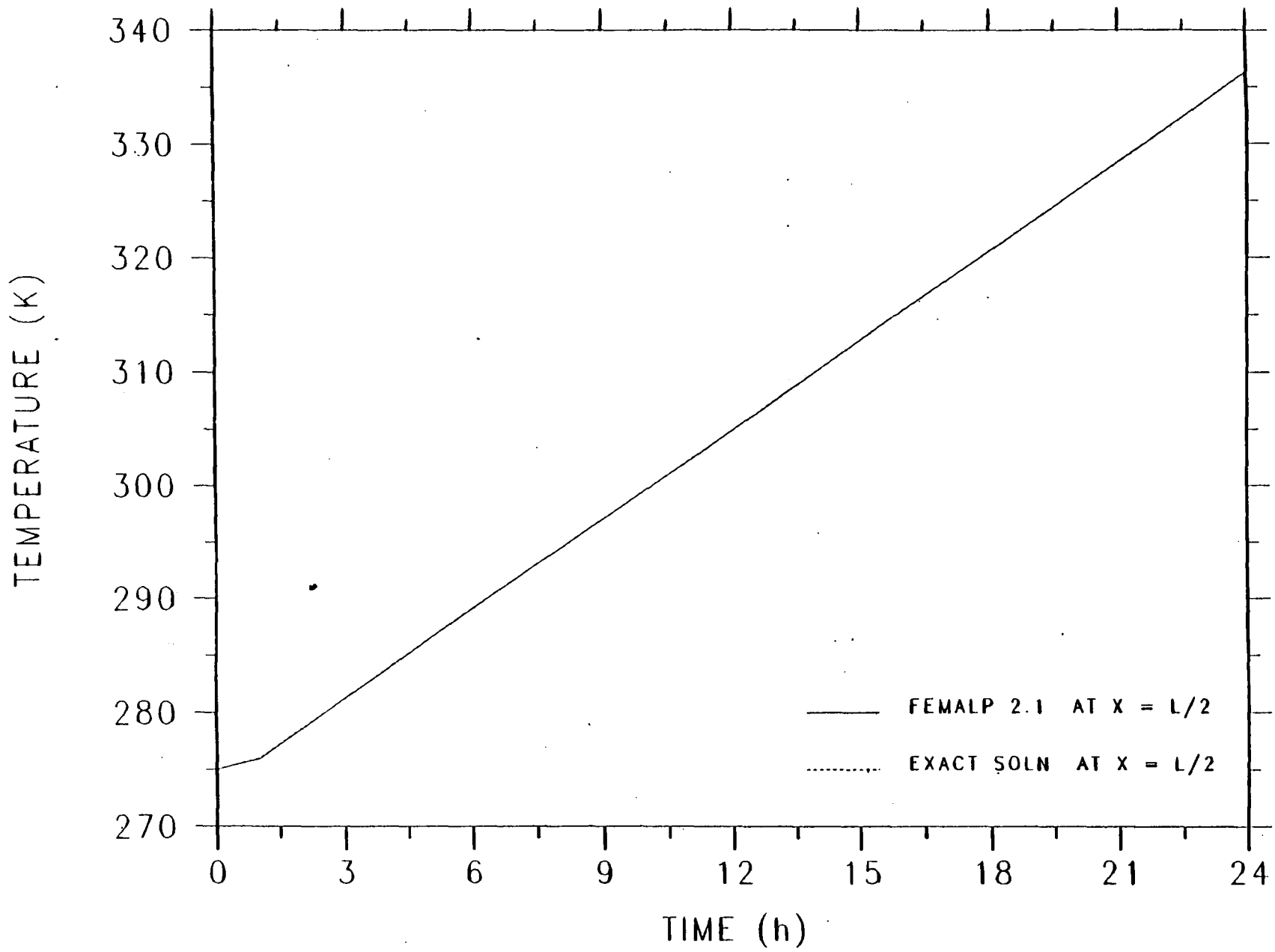


Figure I-6-(c).

FEMALP 2.1 VALIDATION CASE (III) FOR HIGH-MASS

I.4 TEST CASE NUMBER IV

Test case four is a semi-infinite solid at an initial temperature of T_i , (275 K) suddenly exposed to a prescribed temperature equal to T_α at the left face. Such a solid extends to infinity in all but one direction and is characterized by a single identifiable surface. If a sudden change of conditions is imposed on this surface, transient one-dimensional conduction will occur in the solid. The temperature distribution at any x with time is sought. Figure I-7 describes the geometry and boundary conditions of the problem.

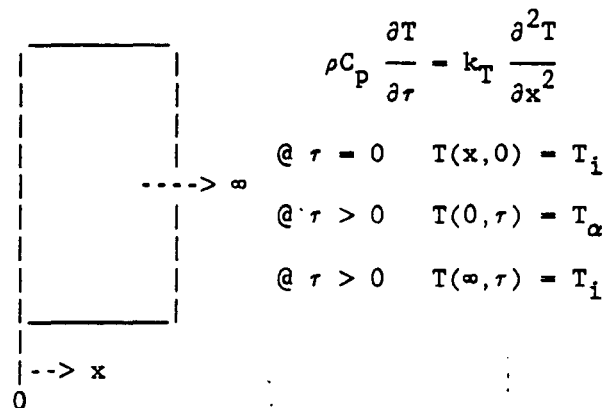


Figure I-7. A semi-infinite solid suddenly exposed to a prescribed temperature.

The exact solution to the problem (Arpaci 1983) is given by the following equation:

$$T(x, \tau) = T_\alpha + (T_i - T_\alpha) \operatorname{erf}\left[\frac{x}{(4\alpha\tau)^{0.5}}\right] \quad (\text{I-4.1})$$

where

$$\alpha = \frac{k_T}{\rho C_p}$$

The numerical simulation for this test case was done only for high-mass. Figure I-8 shows the comparison of the exact solution with those obtained from FEMALP 2.1 at $x=0.25$ m. The agreement is excellent.

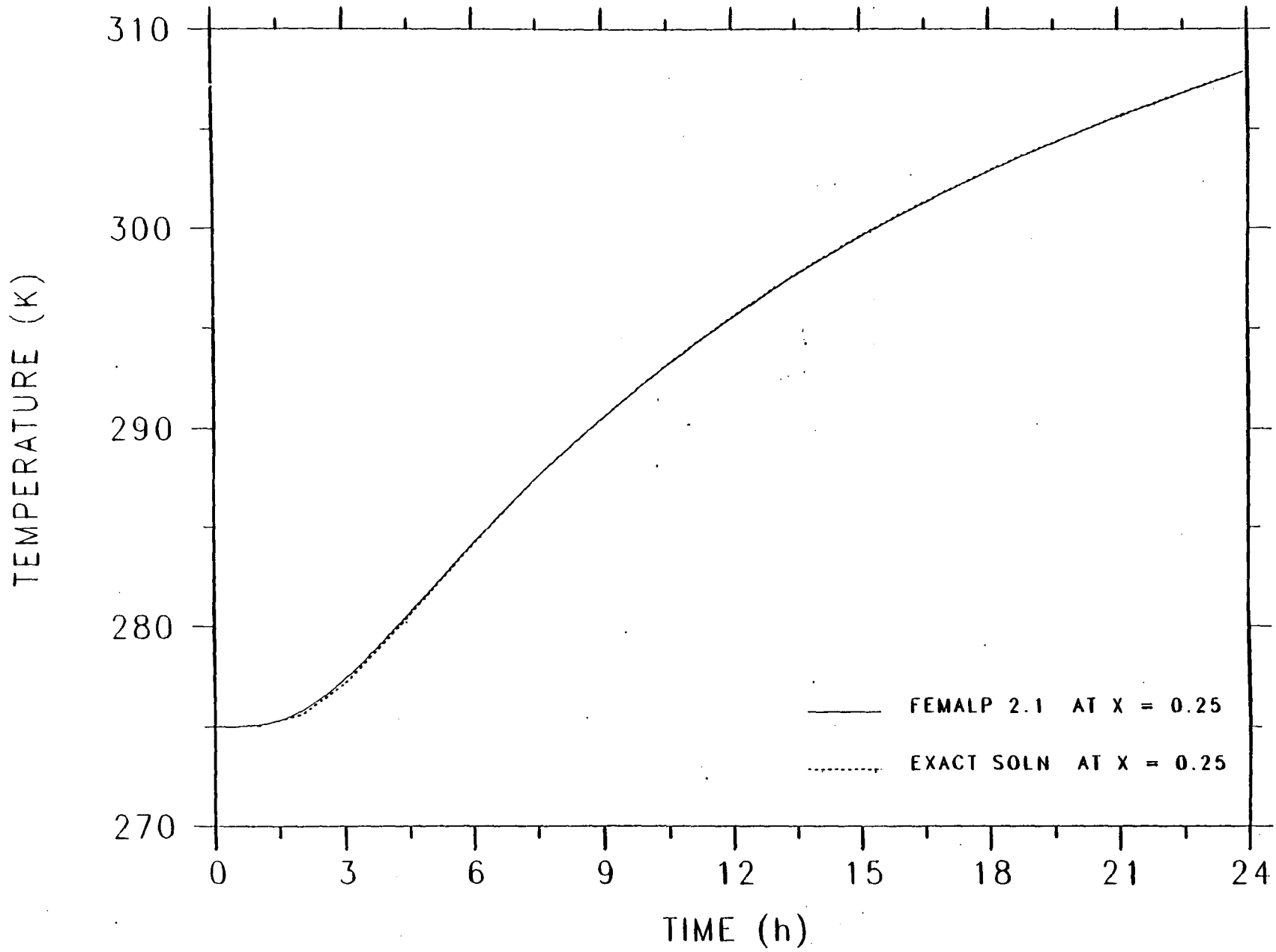


Figure I-8.

FEMALP 2.1 VALIDATION CASE (IV) FOR HIGH-MASS

I.5 TEST CASE NUMBER V

Test case five is a semi-infinite solid at an initial temperature of T_i , (275 K) suddenly exposed to a convective temperature equal to T_α at the left face. Such a solid extends to infinity in all but one direction and is characterized by a single identifiable surface. If a sudden change of conditions is imposed on this surface, transient one-dimensional conduction will occur in the solid. The temperature distribution at any x with time is sought. Figure I-9 describes the geometry and boundary conditions of the problem.

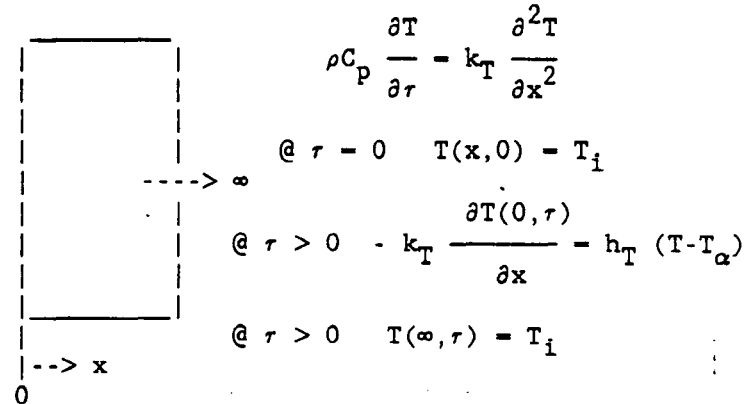


Figure I-9. A semi-infinite solid suddenly exposed a convection.

The exact solution to the problem (Arpaci 1983) is given by the following equation:

$$T(x, r) = T_i + (T_\alpha - T_i) \left(1 - \operatorname{erf}(\xi) - \exp\left(\frac{h_T x}{k_T} + \frac{h_T^2 \alpha r}{k_T^2}\right) \left[1 - \operatorname{erf}\left(\xi + \frac{h_T (\alpha r)^{0.5}}{k_T}\right) \right] \right) \quad (\text{I-5.1})$$

where

$$\xi = \frac{x}{(4\alpha r)^{0.5}} \quad (\text{I-5.2})$$

$$\alpha = \frac{k_T}{\rho C_p}$$

The numerical simulation for this test case was done only for high-mass. Figure I-10 shows the comparison of the exact solution with those obtained from FEMALP 2.1 at $x=0.25$ m. The agreement is excellent.

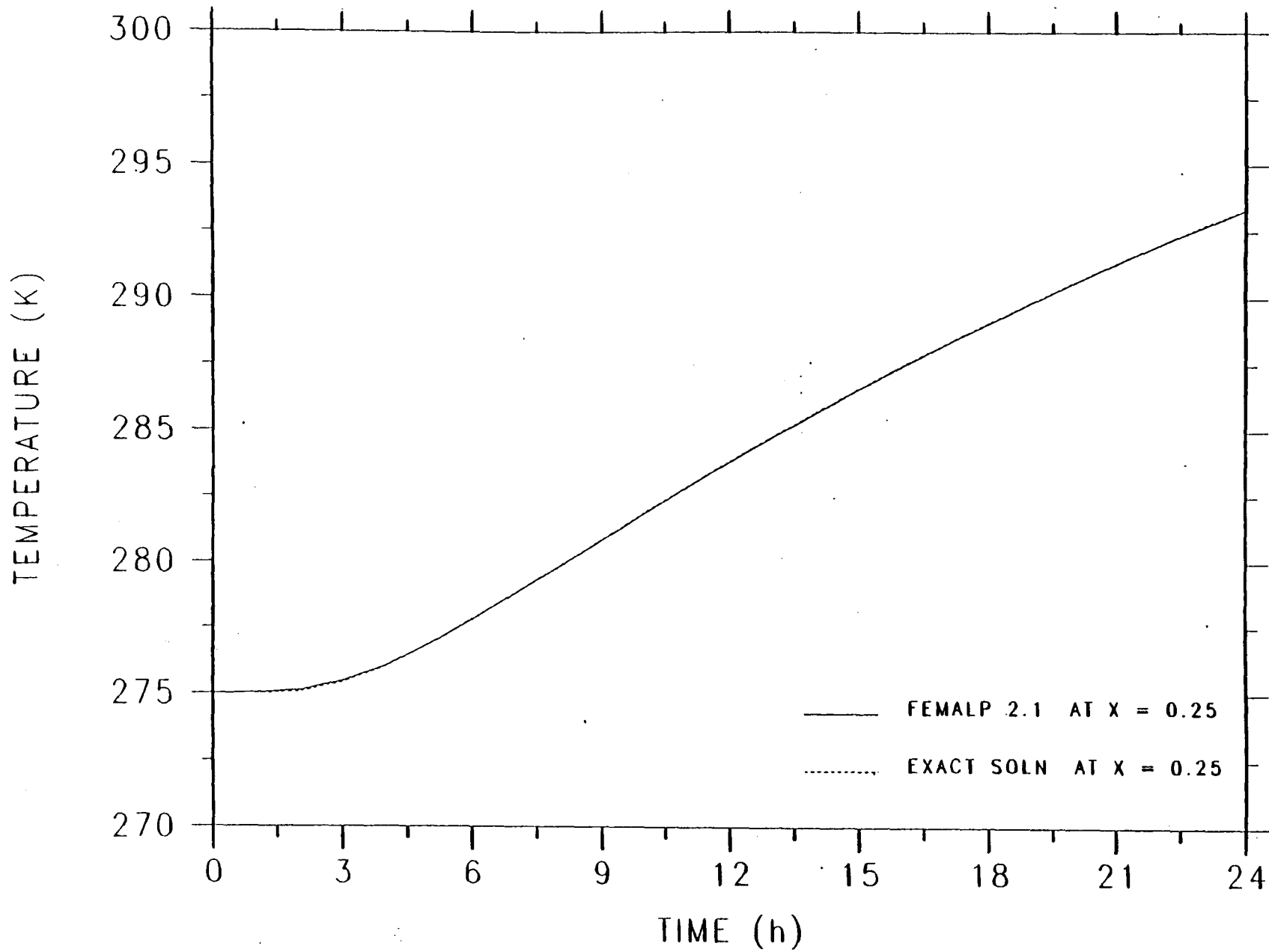


Figure I-10

FEMALP 2.1 VALIDATION CASE (V) FOR HIGH-MASS

I.6 TEST CASE NUMBER VI

While the previous test cases were for homogenous solids exposed to a myriad of boundary conditions, this test case is for composite solids. The analytical solution for the heat flux using conduction transfer functions, for such composite solids, are given in ASHRAE 1976. Four constructs, each having three layers, were chosen for the purposes of comparison. Table I-2 gives the general description of the constructs. A full description of the constructs, their material properties and the inside and outside film coefficients may be found in ASHRAE 1976.

TABLE I-2
Description of ASHRAE constructs used for comparison.

ASHRAE Construct	Description	Remarks
19	Wall with fibreglass insu. and stucco outside finish	low mass
32	Wall 4" concrete with 2" insulation on the outside	high mass
76	4" high weight concrete	high mass
79	4" face brick with 4" common brick	medium to high mass

The geometry of the problem is a composite plane wall at an initial temperature of T_i , exposed to a convective temperature, T_s , at the left face and another convective temperature, T_r , at the right face. The convective temperature on the left face is the sol-air temperature and is changing with time. The film coefficients coupling the faces to the convecting temperatures were taken from ASHRAE 1976. Figure I-11 describes the geometry and boundary conditions of the problem. The heat flux crossing the right face as a function of time is sought. One-dimensional conduction in x direction is assumed.

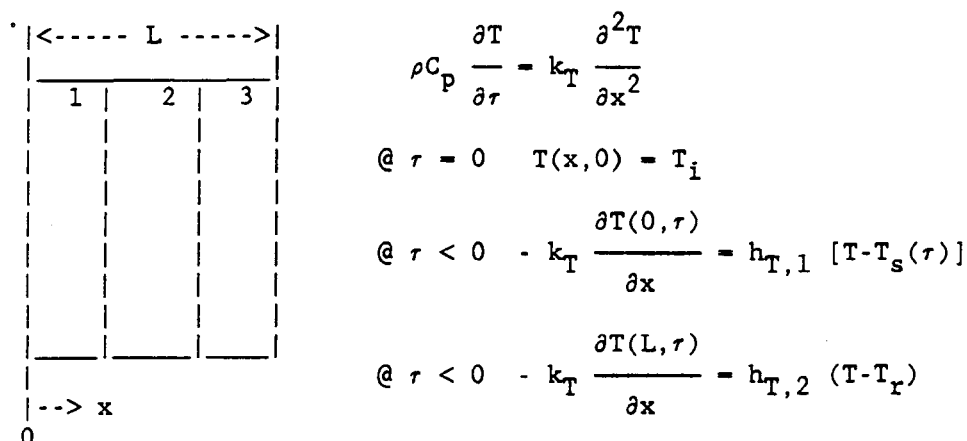


Figure I-11. A composite plane wall suddenly exposed to convection on both sides.

The solution to the problem (ASHRAE 1976) is given by the following equation:

$$Q_T = A \left[\sum_{n=0} b_n (T_{s, \tau - n\Delta\tau}) - \sum_{n=1} d_n \frac{Q_{T, \tau - n\Delta\tau}}{A} - T_r \sum_{n=0} c_n \right] \quad (I-6.1)$$

Figure I-12 shows the comparison of the analytical solution for the heat flux crossing the right face with those obtained from FEMALP 2.1. The agreement for all four constructs is excellent.

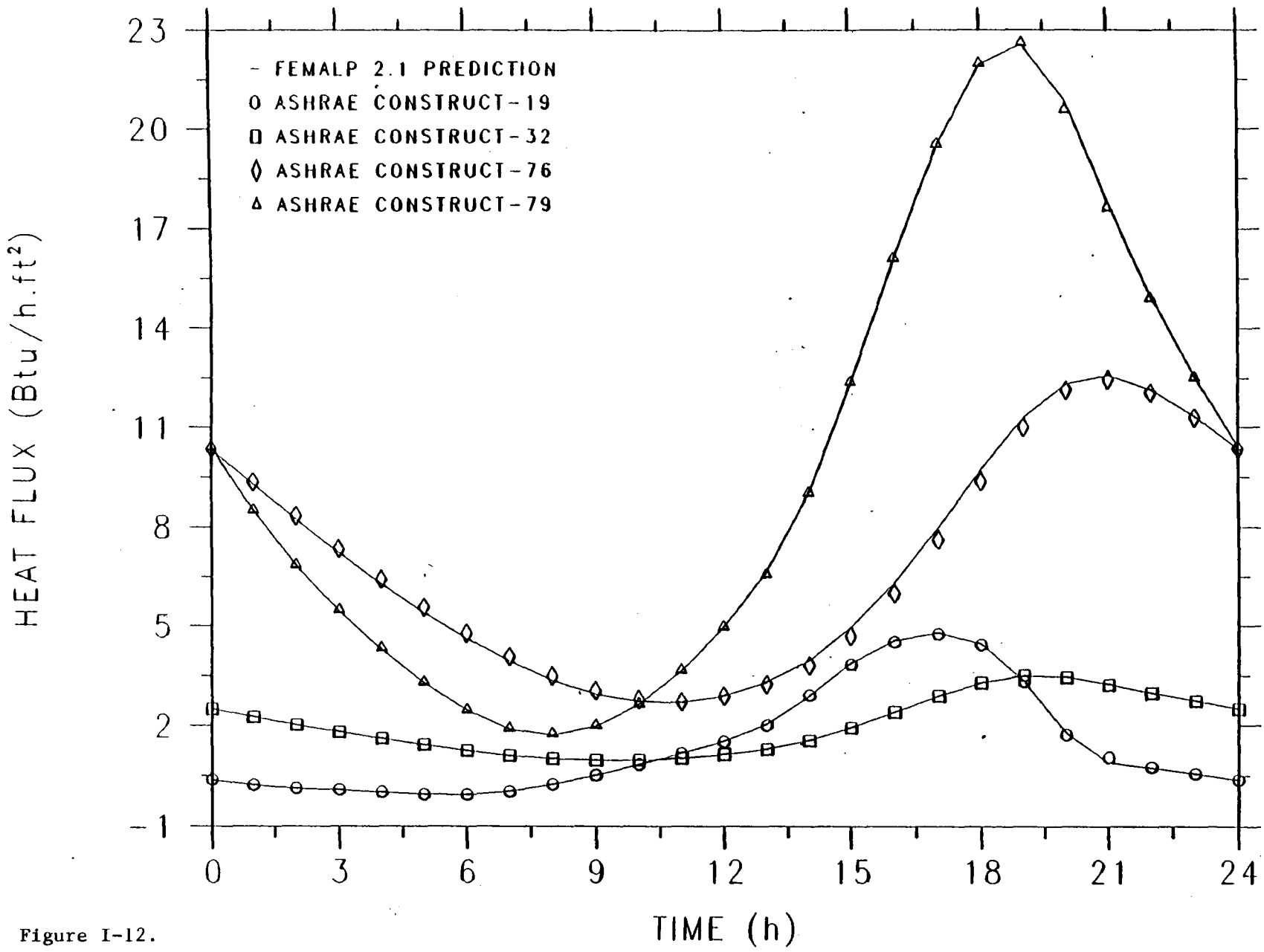


Figure I-12.

ASHRAE TRANSFER FUNCTION CALCULATIONS VERSUS FEMALP 2.1 PREDICTIONS

I.7 TEST CASE NUMBER VII

In the previous sections, FEMALP 2.1 was compared against the closed form solutions of various hypothetical test cases for only solid domains. The objective here is to validate the solution schemes used for the simultaneous room and wall energy balance. The results of TARP 1983 are used for comparison. It must be emphasized that identical assumptions were employed in TARP 1983 and FEMALP 2.1 for this study.

In all simulations, a 5.09 cm thick polystyrene wall exposed to a scheduled ambient profile is used. In the simulations the volume of the zone is set to 340 m^3 and the surface area of the walls set to 398 m^2 . The material properties and the ambient air temperatures used are given in Tables I-3 and I-4, respectively.

TABLE I-3
Material Properties Used in Test Case VII

k	ρ	C_p
W/m.K	kg/m ³	W.h/kg.K
0.043	91.20	0.2328

TABLE I-4
Scheduled Ambient Temperature Used in Test Case VII

Time	T	Time	T	Time	T	Time	T
h	K	h	K	h	K	h	K
01	297.59	02	297.59	03	297.04	04	296.48
05	296.48	06	297.04	07	298.71	08	300.37
09	302.59	10	304.82	11	307.04	11	309.26
13	316.48	14	322.59	15	327.04	16	328.15
17	325.93	18	318.71	19	303.71	20	302.59
21	301.48	22	300.37	23	299.26	24	298.15

Figures I-13 through I-15 show the internal wall surface and zone temperature comparisons for a variety of operating conditions that are defined in Table I-5. Very close agreement is observed in all the simulation runs.

TABLE I-5
Zone Operating Conditions Used in Test Case VII

Figure No	Zone Temperature	Internal Heat G.
I-13	24 hrs. 294.26 K	24 hrs. 0.0 W
I-14.(a)	24 hrs. floating	24 hrs. 0.0 W
I-14.(b)	24 hrs. floating	24 hrs. 1465.5 W
I-14.(c)	24 hrs. floating	5 hrs. 1465.5 W 12 hrs. 0.0 W 7 hrs. 1465.5 W
I-15.(a)	12 hrs. 299.81 K 6 hrs. floating 6 hrs. 299.81 K	24 hrs. 1465.5 W
I-15.(b)	15 hrs. 299.81 K 7 hrs. floating 2 hrs. 299.81 K	24 hrs. 1465.5 W

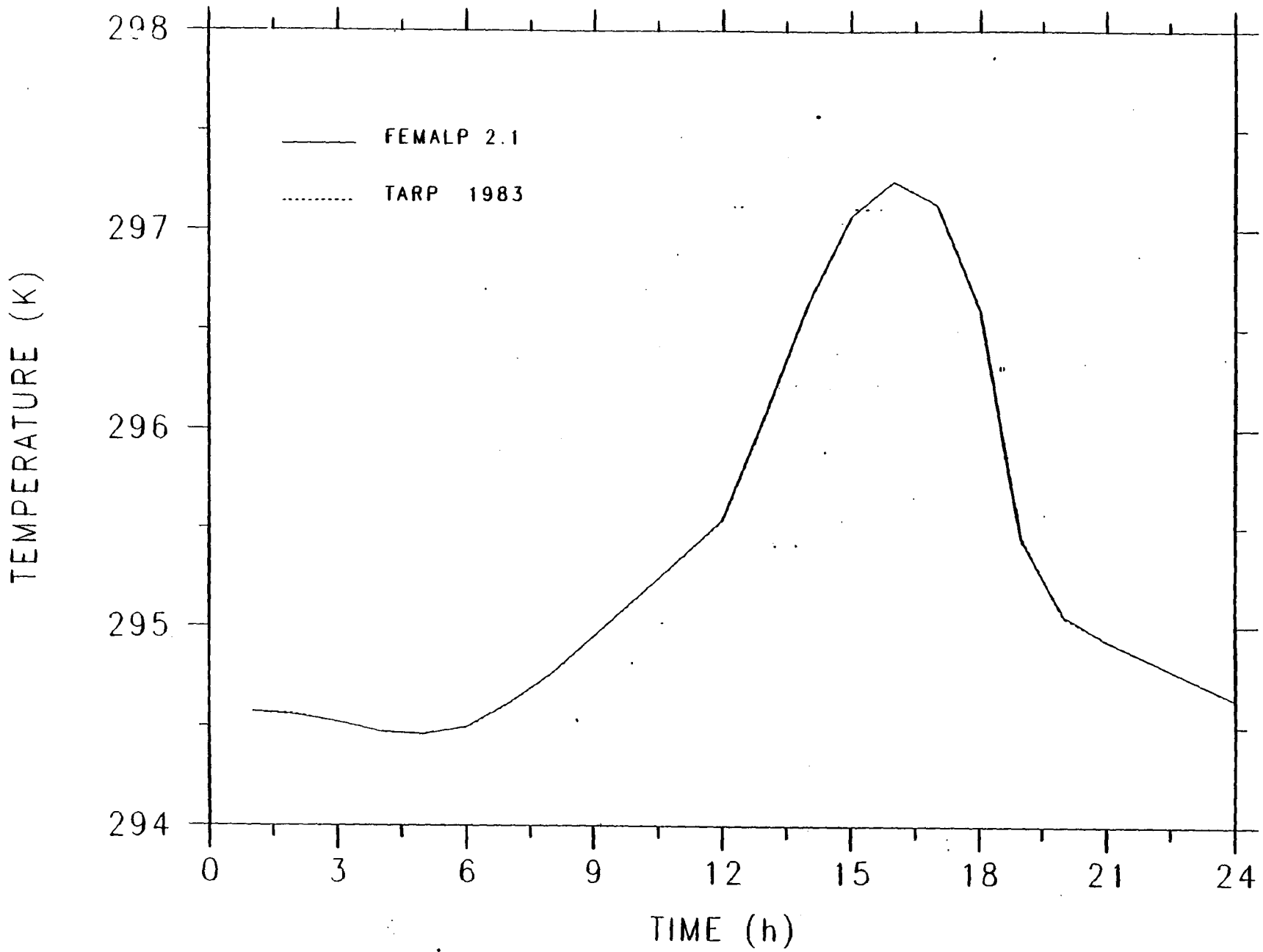


Figure I-13.

FEMALP 2.1 VALIDATION CASE (VII) FOR $T_r = 294.26$ K

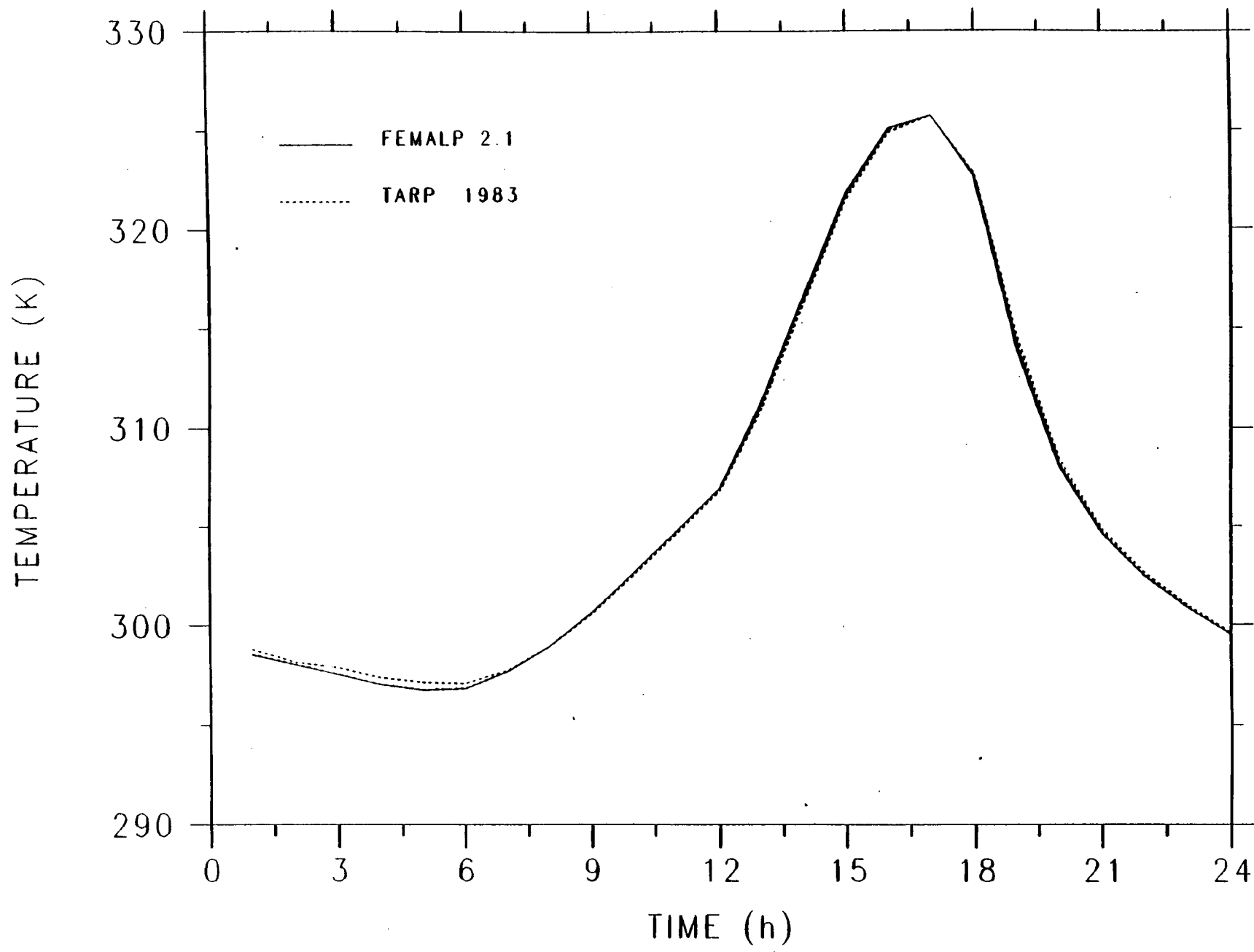


Figure I-14-(a).

FEMALP 2.1 VALIDATION CASE (VII) FOR $Q_r = 0$

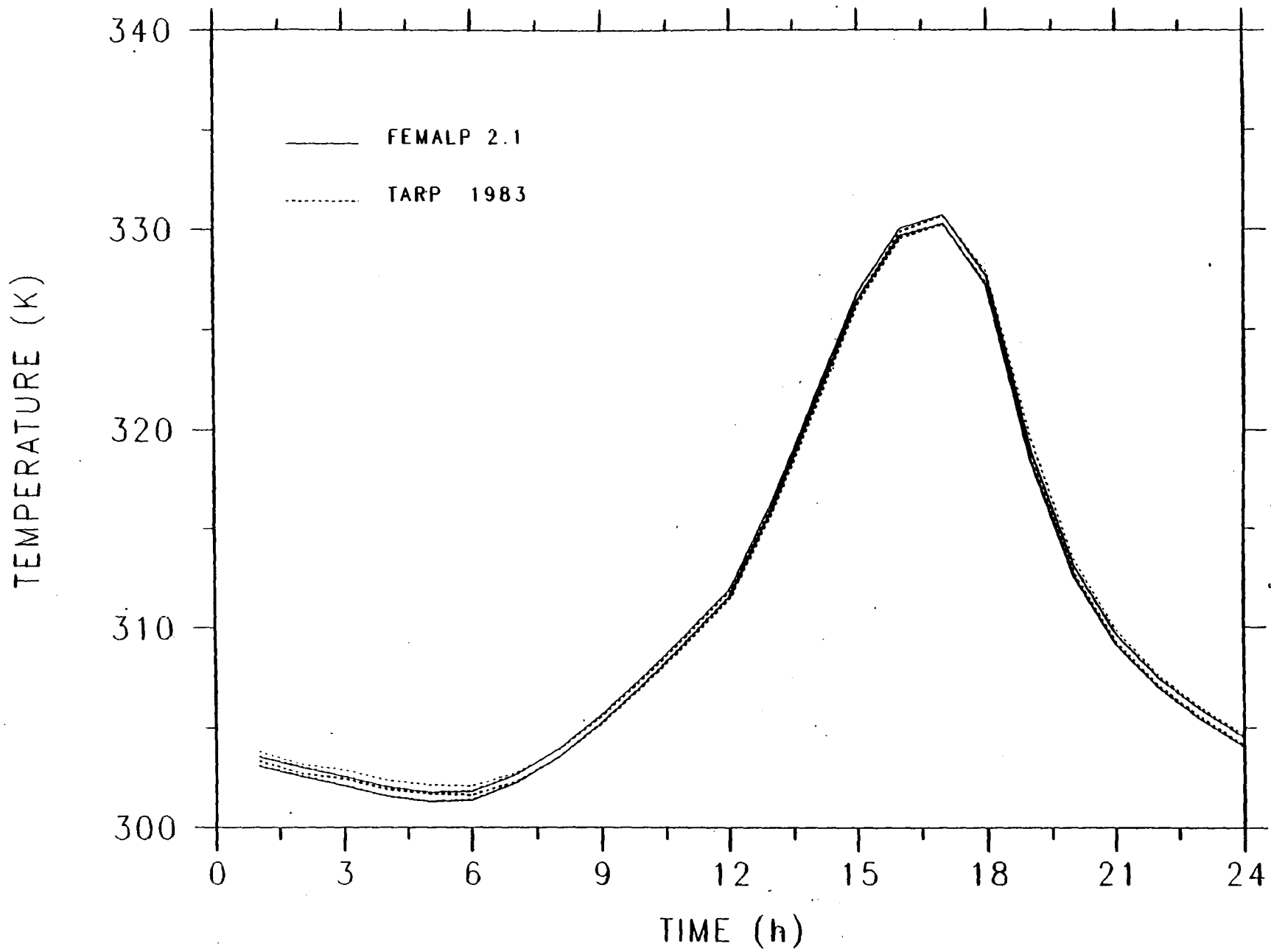


Figure I-14-(b). FEMALP 2.1 VALIDATION CASE (VII) FOR $Q_T = 1465.5 \text{ W}$

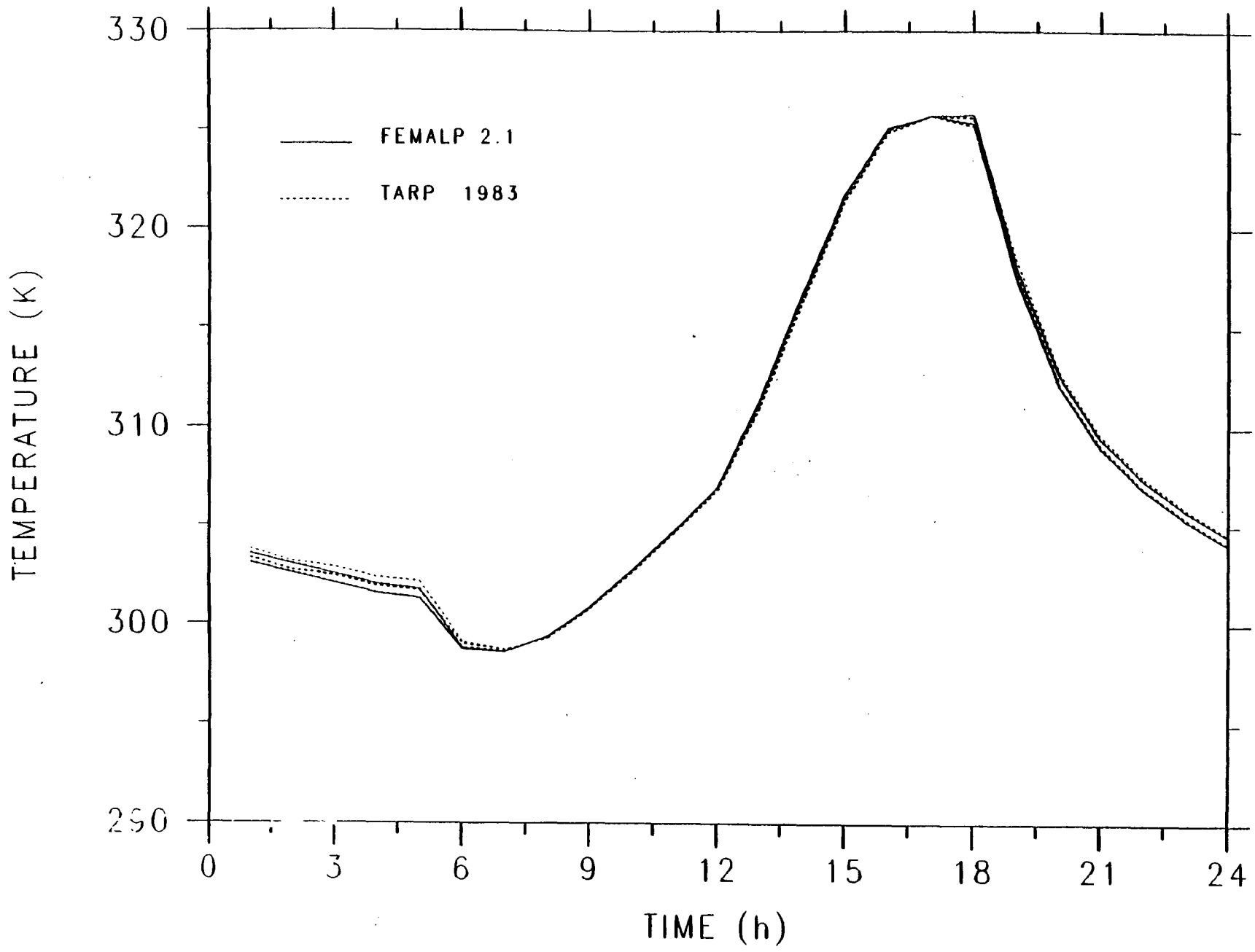


Figure I-14-(c). FEMALP 2.1 VALIDATION CASE (VII) FOR $Q_T = 1465.5$ W

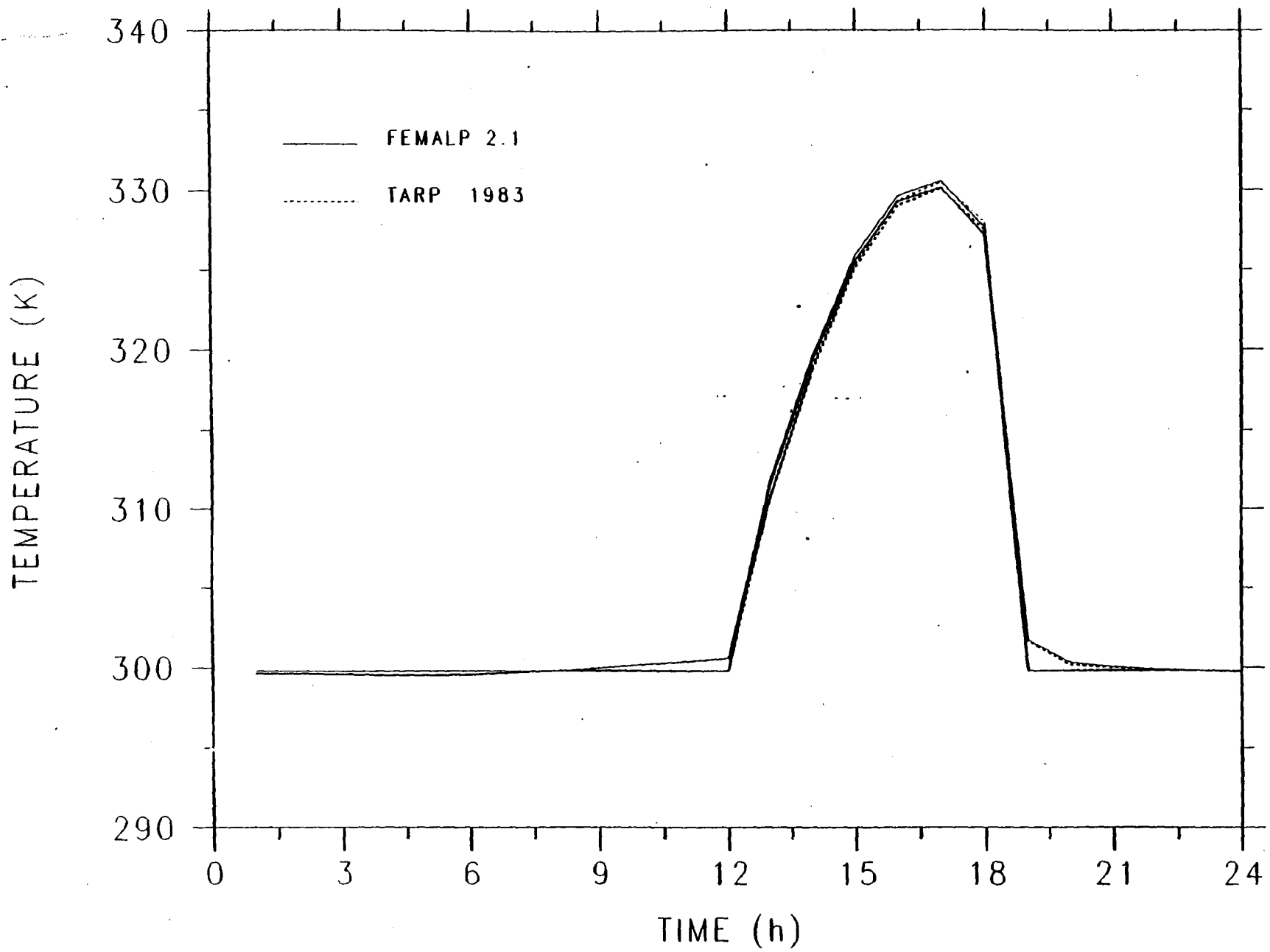


Figure I-15-(a). FEMALP 2.1 VALIDATION CASE (VII) FOR $Q_T = 1465.5$ W

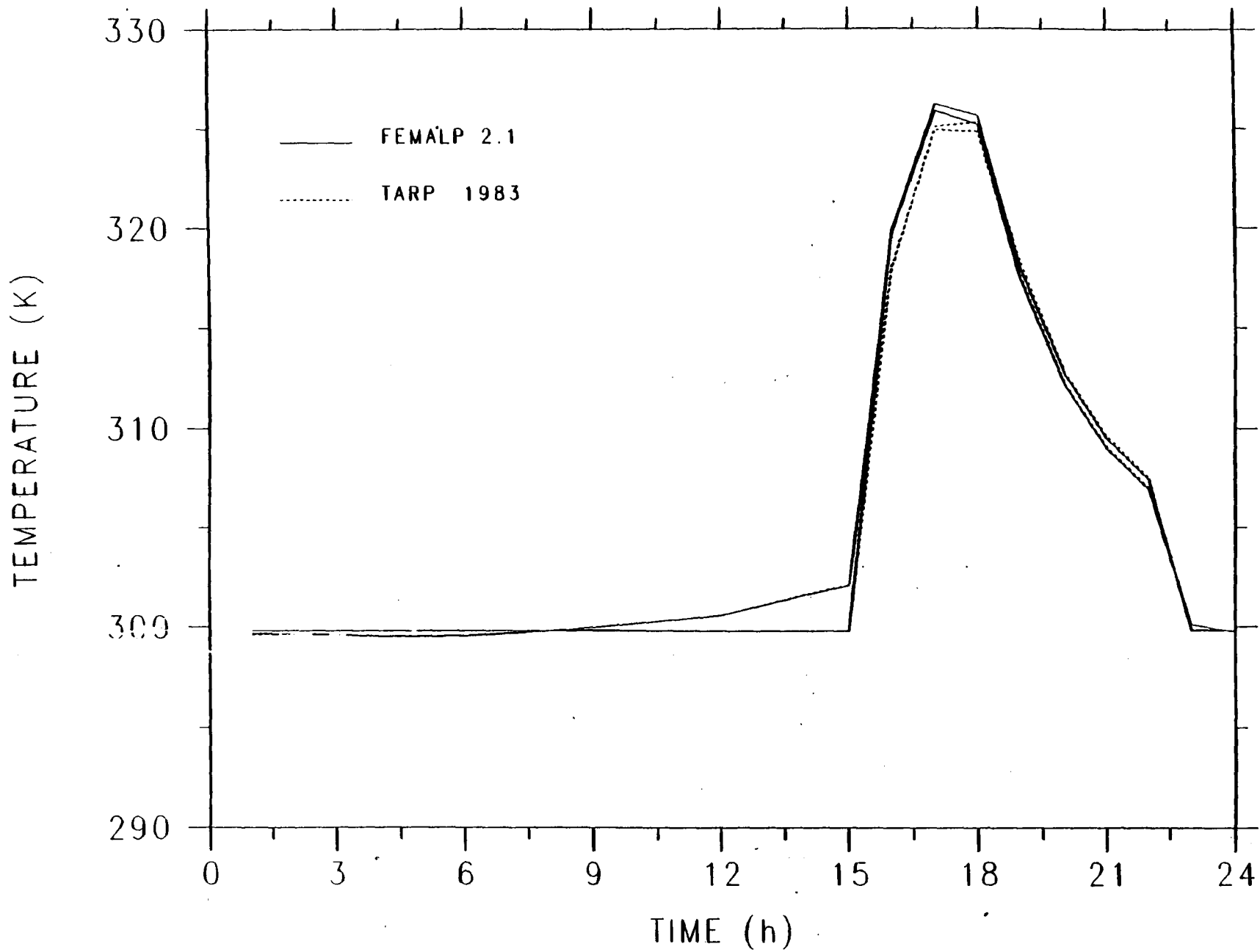


Figure I-15-(b). FEMALP 2.1 VALIDATION CASE (VII) FOR $Q_T = 1465.5$ W

I.8 TEST CASE NUMBER VIII

In this test case, the results from FEMALP 2.1 have been compared with experimental data from FSEC's PCL attics. Figure I-16 shows the layout of cell 2 of the PCL attic. For the purposes of simulation, the attic air space is divided into seven lumped zones with ventilation air entering into zone 1 at C'-I' and leaving the seventh zone at C-I. The seven zones are coupled by interzone air flow; that is, all air entering into a zone leaves to the next zone until it exits from zone seven. The dash lines in Figure I-16 show the zone partitions. The materials and boundary conditions used in this problem are given in Tables I-6 and I-7, respectively. A single-zone model would have required an additional parameter, namely, the "ventilation air mixing efficiency factor" for the attic. This parameter should either be assumed or determined from measurements. Appendix E discusses the use of this parameter. A multiple zone model, on the other hand, would allow for the temperature to vary from one zone to another although a single temperature would define the thermal state of a given zone. A seven-zone model was chosen because such was the kind of division used in the PCL instrumentation. Material properties for the attic components were taken from ASHRAE 1985.

Figure I-17.(a) shows the comparison of experimentally measured heat fluxes crossing the ceiling bottom with the results obtained from FEMALP 2.1. The agreement is good. Figure I-17.(b) shows a plot of deck bottom temperature prediction error and the measured moisture removal of the vent air plotted with respect to time. One can safely infer that much of the difference between the predicted and measured temperature is due to moisture effects which have not been modelled in this test case. Results from simulations including the effects of moisture are given in Chapter 3.

TABLE I-6
Material Description for Test Case VII

SURFACE	MATERIAL	COMMENT
A-A'-B'-B	SHINGLE	ROOF
B-B'-C'-C	PLYWOOD	ROOF
E-E'-F'-F	INSULATION	CEILING
F-F'-G'-G	GYPSUM	CEILING
I-D-G-H	POLYISO	WEST WALL
I'-D'-G'-H'	POLYISO	EAST WALL
E-D-D'-E'	ZONE AIR	

TABLE I-7
Boundary Condition Description for Test Case VII

BOUNDARY	PRES. TEMP	CONVECTION TO	INTERELEMENT RADIATION
B-B'	MEASURED INPUT		
C-J'		ZONE-7 AIR	YES
J'-K'		ZONE-6 AIR	YES
K'-L'		ZONE-5 AIR	YES
L'-M'		ZONE-4 AIR	YES
M'-N'		ZONE-3 AIR	YES
N'-O'		ZONE-2 AIR	YES
O'-C'		ZONE-1 AIR	YES
E-J		ZONE-7 AIR	YES
J-K		ZONE-6 AIR	YES
K-L		ZONE-5 AIR	YES
L-M		ZONE-4 AIR	YES
M-N		ZONE-3 AIR	YES
N-O		ZONE-2 AIR	YES
O-E'		ZONE-1 AIR	YES
G-G'	MEASURED INPUT		
D-E		ZONE-7 AIR	YES
D'-E'		ZONE-1 AIR	YES
I-H		AMBIENT	
I'-H'		AMBIENT	

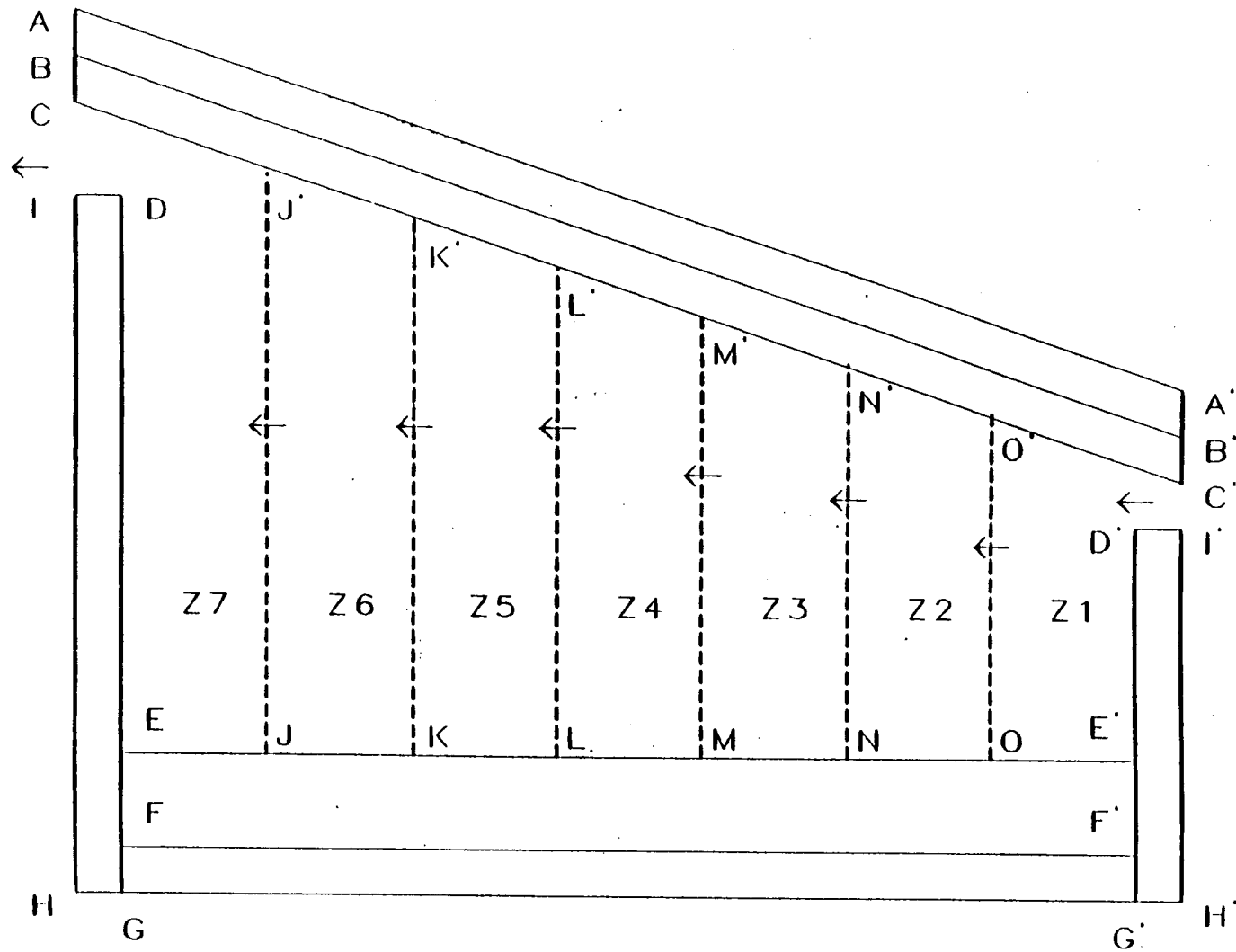


Figure I-16. Schematic Layout of the PCL Attic.

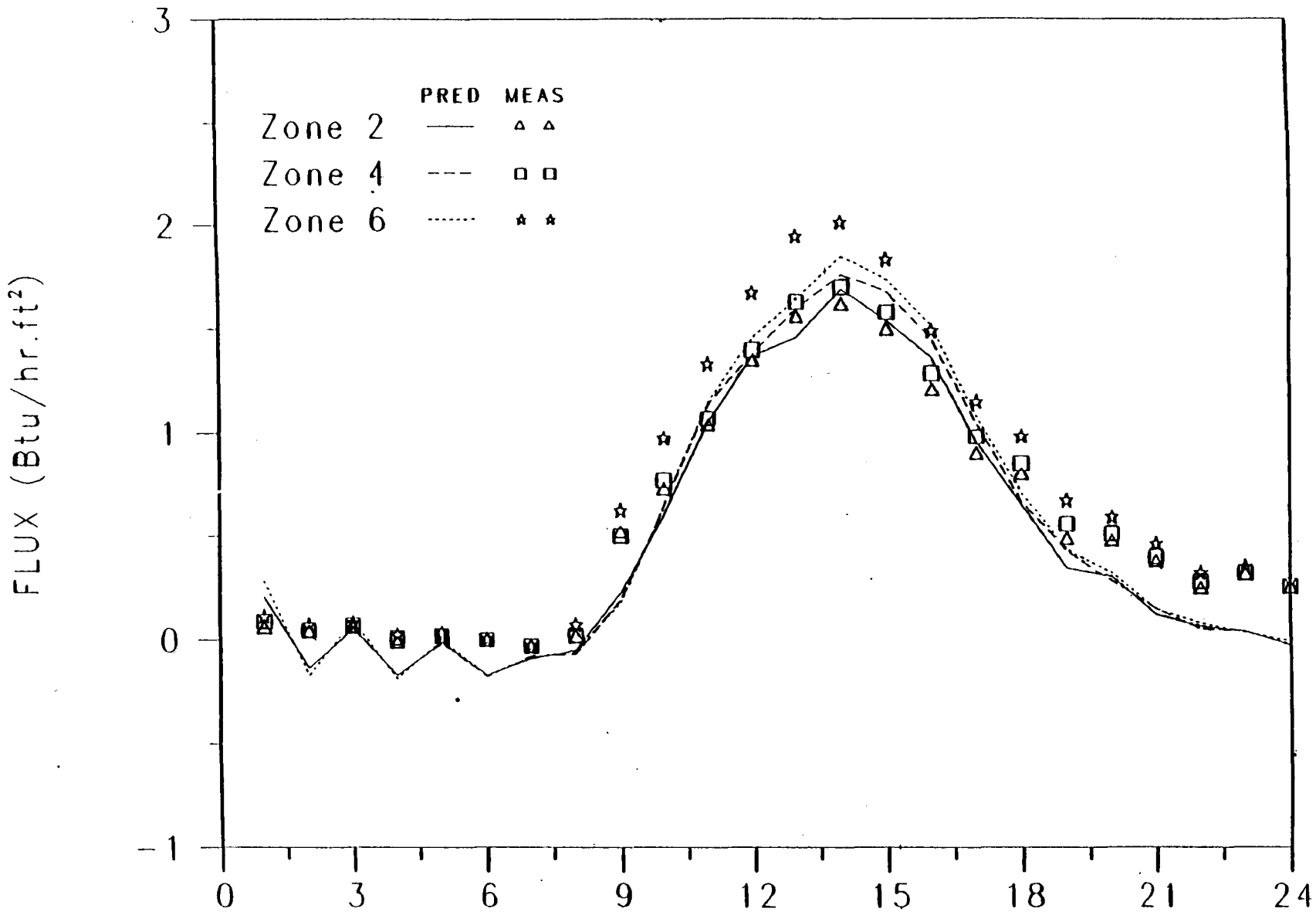


Figure I-12-(a).

EASTERN STANDARD TIME (22-SEP-1987)
 COMPARISON OF PREDICTED AND MEASURED CEILING HEAT FLUXES
 WITHOUT MOISTURE EFFECTS

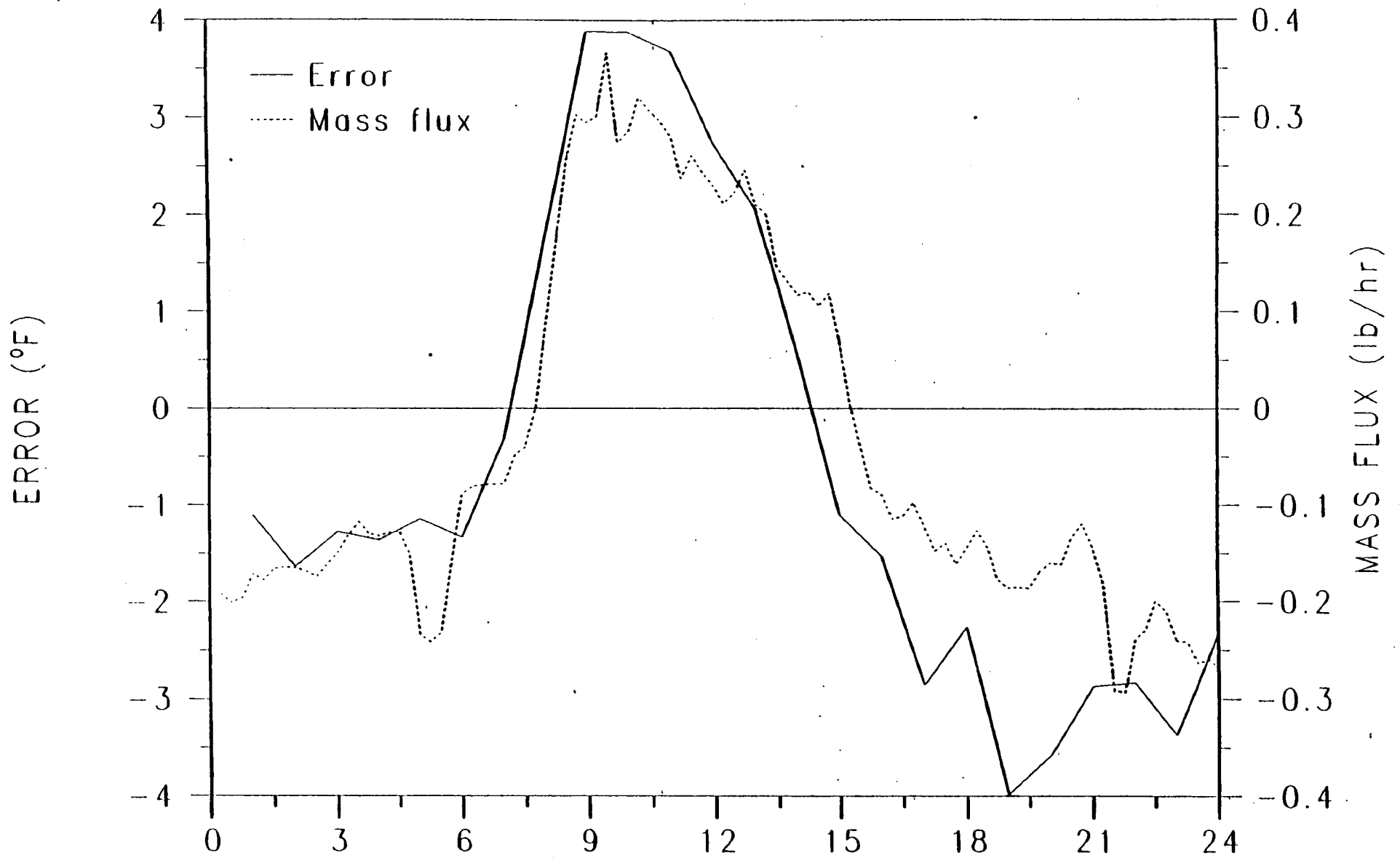


Figure I-12-(b).

EASTERN STANDARD TIME (22-SEP-1987)
Comparison of deck bottom temperature prediction error
and measured vent air moisture removal rate

NOMENCLATURE

A	Surface area [m^2]
b	Transfer function coefficient [dimensionless]
C_p	Specific heat [W.h/kg.K]
c	Transfer function coefficient [dimensionless]
d	Transfer function coefficient [dimensionless]
h_T	Convective heat transfer coefficient [$W/m^2.K$]
k_T	Thermal conductivity [W/m.K]
L	Length [m]
n	Summation index [dimensionless]
Q_T	Heat flow [W]
q_T	Imposed heat flux [W/m^2]
T	Temperature [K]
T_i	Initial temperature [K]
T_r	Room temperature temperature [K]
T_s	Sol-air temperature [K]
T_α	Ambient or surface temperature [K]
x	Coordinate [m]

GREEK LETTERS

α	Thermal diffusivity [m^2/h]
λ	Eigen value [dimensionless]
ρ	Density [kg/m^3]
τ	Time [h]

REFERENCES

ASHRAE 1976, Handbook of fundamentals, Chapter 22, Atlanta: American Society of Heating, Refrigerating and Air-conditioning Engineers.

ASHRAE 1985, Handbook of fundamentals, Chapter 23, Atlanta: American Society of Heating, Refrigerating and Air-conditioning Engineers.

Arpaci, V.S., Conduction Heat Transfer, Addison-Wesley Publishing Company, Massachusetts, 1966.

Judkoff, R., Wortman, D., O'Doherty, B. and Burch, J., A Methodology for Validating Building Energy Analysis Simulations, SERI/TR-254-1508, Solar Energy Research Institute, Golden, CO., 1983.

TARP 1983, Thermal Analysis Research Program, National Bureau of Standards, Washington, DC.

DOE AND MAJOR CONTRACTOR RECOMMENDATIONS FOR ANNOUNCEMENT AND DISTRIBUTION OF DOCUMENTS

See instructions on Reverse Side

1. DOE Report No. DOE/SF/16305-1
2. DOE Contract No. DE-FG03-86SF16305
3. Distribution Category No. UC-59

4. Title Theoretical and Computational Investigation of Algorithms for Simultaneous Heat and Moisture Transport in Buildings

5. Type of Document (x one)
a. Scientific and technical report
b. Conference paper: Title of conference _____ Date of conference _____

Exact location of conference _____ Sponsoring organization _____

c. Other (Specify) _____

6. Copies Transmitted (x one or more)
a. Copies being transmitted for unclassified standard distribution by OSTI/TIC.
b. Copies being transmitted for classified documents as contained in M-3679.
c. Copies being transmitted for special distribution.
d. Two completely legible, reproducible copies being transmitted to OSTI/TIC.
e. Thirty copies being transmitted to OSTI/TIC for OSTI processing and NTIS sales.

7. Recommended Distribution (x one)
a. Unrestricted, unlimited distribution.
Make available only
b. Classified—to M-3679 addressees only.
c. To U. S. Government agencies and their contractors.
d. To DOE offices only.
e. To DOE and WPAS contractors.
f. To DOE and any DOE contractor.
g. Within USA only.
h. Other—specify in item 14 below.
i. Refer all requests to _____

8. Recommended Announcement (x one)
a. Unrestricted, unlimited announcement.
b. Limit to U. S. Govt. agencies and contractors.
c. Limit to DOE and WPAS contractors.
d. Limit to applied technology contractors.
e. Limit to Unclassified Controlled Nuclear Information contractors.
f. Limit to authorized classified sites only.
g. Archives only—No announcement.

Future Handling of Limited Reports
After _____ (Date), this report may be reprocessed as item 7. _____ and 8. _____

Reason for Restriction Recommended in 7 or 8 above. (Explain fully) _____

Patent and Technology Transfer information
Does this information product disclose any new equipment, process, or material? x No
Has an invention disclosure been submitted to DOE covering any aspect of this information product?
If yes, identify the DOE disclosure number and to whom the disclosure was submitted.
Are there any patent-related objections to the release of this information product? x No

Does this information product contain? (Check all applicable boxes)
Copyrighted material (attach release)
Proprietary information (page numbers _____)
National security information
Restricted data
Formerly restricted data
Applied technology
Unclassified Controlled Nuclear Information
Other (explain) _____

Copy Reproduction and Distribution
Total number of copies reproduced _____ Number of copies distributed outside originator (exclude copies to OSTI/TIC) 4

Additional information or Remarks (Continue on separate sheet, if necessary)

Submitted by (Name and Position) (Please print or type) A. Alp Kerestecioglu
Organization Florida Solar Energy Center
Signature A. Kerestecioglu
Phone (407) 783-0300
Date 10/31/1988